Excerpts from

The NEURONS and NEURAL SYSTEM:
a 21st CENTURY PARADIGM

This material is excerpted from the full β-version of the text. The final printed version will be more concise due to further editing and economical constraints.

A Table of Contents and an index are located at the end of this paper.

A few citations have yet to be defined and are indicated by "xxx."

James T. Fulton
Neural Concepts

jtfulton@neuronresearch.net

January 15, 2018

[xxx clear remaining xxx's and [figure and [section editing markes

9 Stage 3, Signal Transmission Neurons [1]

9.1 Introduction

[xxx may want to pick up words from **old Chapter 10** about NoR. Search for 10.5 to highlight locations]

There are two distinct methods of signal transmission employed in the neural system, graded potential conduction or tonic signaling, and pulse propagation or phasic signaling. Graded potential and tonic signaling both refer to analog waveform signaling. Graded potential or tonic signaling is only employed within stages 1, 2, 4, 5 & 6 of neural signaling. Phasic (pulse) propagation is only used within stage 3 and stage 7 signaling.

> Propagation, as a technique, has not been discussed in the biophysical literature previously except indirectly. While the high transmission speed associated with phasic signaling (greater than 10 meters/sec) has been documented, the mechanism involved has not been elucidated. Attempts to explain axonal propagation by Lord Kelvin in the 19th Century and Rall in the 20th Century were exemplary failures (**Section 9.1.1.3**) .
>
> This work develops neural propagation as a mechanism based on Maxwells' General Wave Equations (GWE).
>
> This work will use the term signal transmission in the broad sense and differentiate between signal conduction, the slow flow of electrons in the orthodromic direction, ***and*** signal propagation, the rapid movement of electrons *perpendicular* to the orthodromic direction as a part of the wave projection mechanism used in both cables and broadcasting.

Juusola, et. al. have recently explored some aspects of graded-potential (i.e., analog) conduction along electrotonic signal paths, including electrotonic synapses[2]. Their figure 4C presents data on the various quiescent potentials (resting potentials) found by different investigators for both pre and post synaptic plasmas. Unfortunately, the different data points on the pre and post synaptic side are not paired.

This chapter will only address pulse propagation or phasic signaling as used in the neural system. Such neurons are found primarily in mammalian animals. This chapter will address the cytology, morphology, pathology and operation of the individual stage 3 neurons. The anatomy of the stage 3 neurons of the mammal was introduced in **Chapter 1** and is discussed in greater detail in **Chapter 10**.

A critical feature of the axons of stage 3 neurons is the periodic morphological constriction of the axons. The French pathologist Louis Antoine Ranvier first described this periodic constrictions

---

[1]Released: 15 January 2018

[2]Juusola, M. et. al. (1996) Op. Cit.

which interrupted the enshrouding of the axon by myelin. However, its functional significance has been obscure up to the present time. It has been described many times as a morphological oddity or a mere structural component. In fact, its physiological role is critical. These constrictions are now known as Nodes of Ranvier and to be the location of phasic signal regenerators critical to the operation of stage 3 neurons.

Zagoren & Fedoroff edited a volume on the Node of Ranvier in 1984[3]. It contains some useful electron-micrographs but is otherwise largely obsolete. All of their models employ simple RC circuits in electrical configurations while relying upon the chemical neuron concepts of sodium and potassium channels. Their "Current working model of the node of Ranvier" on page 319 is barely more than two dashed lines connecting two myelinated axon segments. Page 333 does show an excellent image of a stained axon of a pyramid cell reflecting the attraction of positive charges to the outside of the axon due to the presence of the high negative charge within it.

More recently, Fields introduced a paper by Tomassy et al. that reviewed the subject of stage 3 propagation based on their interpretation of the role of myelin in the cytology of the phasic neurons used therein.

The Fields paper made several open ended statements of interest but included no detailed models[4]. "Myelin is often compared to electrical insulation on nerve fibers. However, nerve impulses are not transmitted through neuronal axons the way electrons are conducted through a copper wire, and the myelin sheath is far more than an insulator. Meylin fundamentally changes the way neural impulses (information) are generated and transmitted, and its damage causes dysfunction in many nervous systems disorders including multiple sclerosis, cerebral palsy, stroke, spinal cord injury and cognitive impairments." While the above quotation is true, it offers no indication of how myelin is causal in these diseases. He then goes on, "A detailed understanding of myelin structure is therefore imperative, but is lacking." More is needed that an understanding of the structure of myelin; it is the functional role of myelin that is most critical. With an understanding of its functional role, abnormalities related to its structure expose the reasons for the diseases associated with myelin. Fields does note in closing, "Myelin ...facilitates modes of nervous system function beyond the Neuron Doctrine, . . ." This chapter will describe both the functional and structural role in much greater detail than the paper by Tomassy et al.

Tomassy et al[5]. address the gross structural details of myelin in a variety of situations but does not address the functional role of myelin directly. Nor does it address the fascinating structure of the myelin layers as they approach a specific Node of Ranvier (in order to form a functional "half-section" of electrical filter theory (**Section 9.1.2.4** in this work & in greater detail in **Sections 10.3.5** & **10.5.2** of "Processes in Biological Vision" (PBV)). In their discussion, they note, ". . .the thickness of the myelin sheath varies greatly, and it is a major determinant of the speed of impulse propagation." Contrary to the statement, "High resolution maps of myelin distribution along individual axons are not currently available," the geometry of the myelin forming two half-sections on either side of a Node of Ranvier is reproduced in figure 10.5.2-9 of PBV and originally presented by Rydmark & Berthold in 1983[6].

Tomassy et al. discussed a variety of neurons in the CNS without describing their individual functions, and thereby failing to differentiate the application of myelin in these different neuron types. They essentially treat all "pyramid" shaped neurons as equivalent, even though some are employed in the encoding of analog signals to generate action potential streams and others are used to decode action potential streams to recover analog information. Other smaller "pyramid" neurons in the CNS are actually stage4, 5 & 6 neurons handling only analog (tonic)

---

[3]Zagoren, J. & Fedoroff, S. *eds*. (1984) The Node of Ranvier. NY: Academic Press

[4]Fields, R. (2014) Myelin—More than insulation *Science* vol 344, pp 264-267

[5]Tomassy,G. Berger, D. Chen, H-H. et al. (2014) Distinct profiles of meylin distribution along single axons of pyramidal neurons in the neocortex *Science* vol 344, pp 319-324

[6]Rydmark, M. & Berthold, C. (1983) Electron microscopic serial section analysis of nodes of Ranvier in lumbar spinal roots of the cat *J. Neurocytol* vol. 12 pp. 475-505 and 537-565

signals. Tomassy et al. note, "It is interesting that these three profiles of myelination can be found in neurons located in immediately adjacent positions within the same cortical layer." They close their discussion with the assertion, "Our results suggest that different classes of pyramidal neurons are endowed with different abilities to affect OL (oligodendroctyes) distribution and myelination." This work suggests the neuron/OL relationship is quite different. The genetic code describes the form of both the neural cell and the application of OL to that neural cell in order to achieve the desired performance.

Tomassy et al. do identify premyelin axonal segments (PMAS) which are in fact portions of the neuron soma and not a separate axonal segment. These regions contain the axon hillock (the location of the Activa generating action potentials in stage 3 encoding neurons). Only the post Activa portion of the PMAS needs to be myelinated. However, if this portion is short, a Node of Ranvier may be inserted prior to the beginning of myelination on the first true axon segment.

Tomassy et al. close with a very insightful, although less than specific, comment, "Although the functional significance of these heterogeneous profiles of myelination awaits future elucidation, we propose that it may have served the evolutionary expansion and diversification of the neocortex by enabling the generation of different arrays of communication mechanisms and the emergence of highly complex neuronal behaviors." It did! The comment applies to the peripheral neural system as well as the neocortex.

This chapter will address the following;

Section 9.1.1, the topology of signal projection neurons,
Section 9.1.2, the physiology and propagation of neural signals,
Section 9.2, encoding of neural signals,
Section 9.3, actual codes used for neural signals,
Section 9.4, the functional role of the Node of Ranvier,
Section 9.5, the synapse in signal projection,
Section 9.6, the stellite neuron as a signal decoder,
Section 9.7, special topics related to signal projection.

9.1.1 The fundamental topology of the stage 3 signal projection circuit

While the neurons of stage 3 generating action potentials represent only a small number of the total number of neurons (about 5%), they play a major functional role and have been studied most closely (because of their ease of access and easily isolated signals).

Function is used here in the context of the underlying process of a given neural structure, and not as frequently found in neuroscience texts to describe the purpose of the structure.

Stage 3 neurons are found wherever signals are to be propagated more than a few millimeters. They appear to be an invention used primarily in and making possible the phylum of Chordata (colloquially the vertebrates).

9.1.1.1 A preview of neuron morphologies based on the electrolytic theory

One of the simplest forms of the neuron is that most studied, the morphologically bipolar but electrolytically three-terminal signal processing neuron. In its simplest form, it shows no arborization of the dendritic structure and no bifurcation of the axonal structure. It is shown in frames A and B of **Figure 9.1.1-1**. As noted earlier, each neuron is a three-terminal device. The dendritic terminal on the left and the axonal terminal on the right (the pedicle) are well defined in the literature. However, the podoplasm (shown as the white bar below the internal Activa) and its external poditic terminal, have been less well defined (even though it is well represented in the electron micrographs of cytology). Frames A & B stress the triviality of the difference between morphologically defined monopolar and bipolar neurons. The nucleus, and its location, play no functional role in neural signaling.

Frames C and D introduce the first order of elaboration found in neurons. In C, the poditic structure has been expanded into a recognizable external structure. This is a very valuable form found widely in neurobiology. As will be described in Chapter 4, [xxx check] this configuration provides a "noninverted" pedicle output signal compared to the input signal at the dendrite. However, it provides an "inverted" pedicle output signal compared to the input signal at the podite. This feature is the basis for the signal processing performed within the neurological system. Frame D shows the beginning of the further elaboration of the neuron. Both the dendritic and poditic structures are subject to very large degrees of elaboration beginning from simple dendritic and poditic stems. By selectively synapsing with multiple antidromic neurons, the neuron is able to perform significant feats of signal summation, differencing, correlation and thresholding.

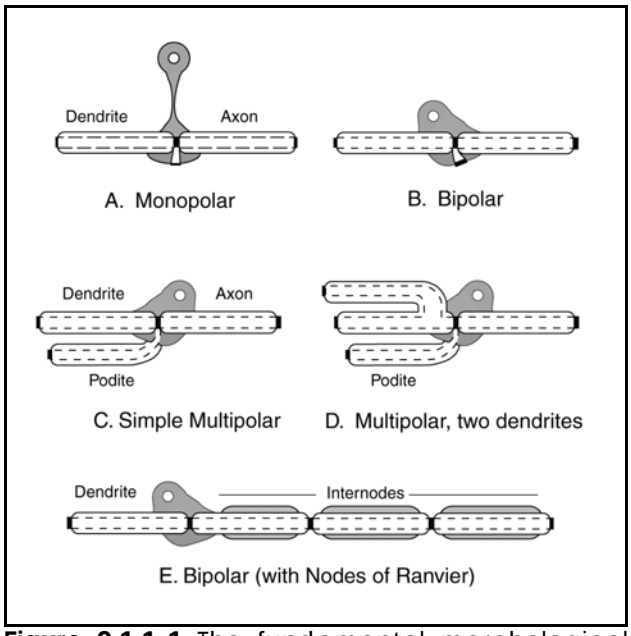

Figure 9.1.1-1 The fundamental morphological forms of neurons.

Frame E shows an additional degree of elaboration. In this case, the axon has been elaborated into a serial series of axon segments or internodes separated by Activa at each junction between the axon segments. The axon segments are shown by an outer myelin wrap. The active mechanism between each pair of conduits allows regeneration of the signal at intervals to compensate for the attenuation associated with the individual axon segment. While this process is noisy in analog circuits, it is an ideal method of noise-free regeneration in phasic circuits. If all of the axon segments shown are supported homoeostatically by the same soma and nucleus (as shown), the junctions between the axon segments are known as Nodes of Ranvier. If the segments are supported by different soma, the junctions are called synapses.

As noted as early as 1961 by Davis[7], Nodes of Ranvier can occur between any two conduit segments at locations before or after the soma.

9.1.1.1.1 The neuron as an electrolytic circuit

Figure 9.1.1-2 reproduces frame C of the above figure and shows the electrolytic representation of the same cell. The circuit (lower right) displays two distinct input terminals, $V_{in}(1)$ and $V_{in}(2)$ and a common output analogous to the pedicle of the axon. $V_{in}(1)$ represents the input to the circuit associated with the dendritic structure. The signal applied to this terminal is reproduced at the axon with the same polarity. The signal waveform is not inverted. $V_{in}(2)$ represents the input to the circuit associated with the poditic structure. The signal applied to this terminal is reproduced at the axon with the opposite polarity. The signal waveform is inverted. This circuit configuration is ideally suited for taking the mathematical difference between two analog signals.

[7]Davis, H. (1961) Some principles of sensory receptor action *Physiol Rev* vol 41(2), pp 391-416 fg 2

6 Neurons & the Nervous System

The simple circuit elements shown between each input and output terminal and the common ground symbol are more complex in the real case. They typically incorporate both an electrical impedance and a voltage source, although in some cases the voltage of the source may be zero. All of the circuit elements associated with a given Activa can be grouped into a single complete circuit (or a conexus). The designation AL refers to the type of Activa used in this lateral type neuron. Lateral neurons include both the horizontal neurons and the amercine neurons of the visual retina. They occur widely in the signal processing and signal manipulation circuits of all sensory modalities.

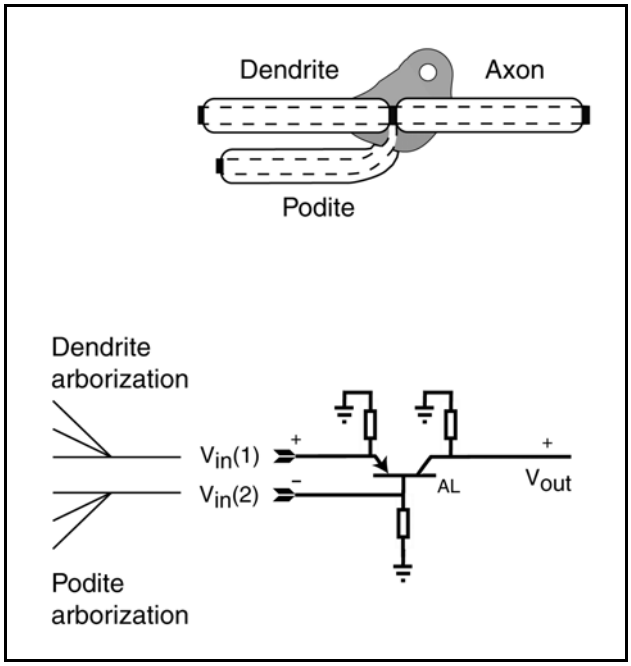

Figure 9.1.1-2 The electrolytic representation of a simple multipolar neuron. Top; generic cytology. Bottom right; basic electrolytic circuit. Bottom left; arborization of each neurite. See text.

The input structures are expanded at lower left to suggest the tree-like extensions of the basic dendritic and poditic inputs. This process is described as arborization. Dacey & Lee have provided excellent imagery of dual arborizations of the type described in this figure[8]. However, they did not recognize the physiological difference between these two input structures and described their figures as bi-stratified dendritic structures. They did recognize the capability of this neuron type to take signal differences, which they associated with "color opponency" in the visual system.

The two inputs to the same Activa indicate the availability of a differential input structure. A signal at $V_{in}(1)$ appears at V_{out} with the same polarity and this input is thereby labeled the non-inverting input. On the other hand, a signal at $V_{in}(2)$ appears at V_{out} with the opposite polarity and this input is thereby labeled the inverting input. These two inputs are available simultaneously and therefore the structure is described as a differential input structure. $V_{out} = a \cdot V_{in}(1) - b \cdot V_{in}(2)$.

Dacey & Lee observed an important point in their 1994 introduction. "The neural mechanisms producing colour opponency are not understood." The above figure and discussion resolves one aspect of their concern, how the signal value associated with observed opponency is created within the neural system.

The number of inputs to a specific dendritic or poditic tree is known to reach the thousands. Morphology has been unable to account for, or interpret the function of, such large numbers of inputs. The summation of such a large number of uncorrelated inputs, by either arborization, would typically lead to a constant amplitude signal as a function of time. However, physiology provides an answer. The arborizations reach out and contact antidromic neurons that are either correlated in time, in frequency, or space, depending on the sensory modality. Whenever correlated signals appear at the pedicles of these neurons, their signals sum to significant signal amplitudes in the orthodromic neurites for a nominal period of time. This correlation capability

---

[8]Dacey, D. & Lee, B. (1994) The 'blue-on' opponent pathway in primate retina originates from a distinct bistratified ganglion cell type *Nature* vol 367, pp 731-735

plays a major role in the information extraction functions of the neural system.

The dendritic and poditic input circuits exhibit another major difference beside signal inversion. The signal applied to the dendritic input is always reproduced at the pedicle at nominally the same amplitude. However, the signal applied to the poditic input is both inverted and amplified. Depending on the parameters of the Activa within the neuron and the circuit elements associated with that Activa, the circuit can exhibit amplification factors of from 1.0:1 to as much as 200:1. This feature is of fundamental importance to the sensory neuron circuits. While most of the neural system operates in a nominally constant signal amplitude environment, the sensory neurons are expected to amplify the very small signals at their input up to a nominal amplitude appropriate to the neural system.

The following material will address the operation of the stage 3A analog (tonic) signal to phasic signal encoding mechanism in greater detail along with a detailed discussion of the mechanism of signal propagation along an axon after that encoding.

The histological description of signal propagation neurons is straightforward. **Figure 9.1.1-3** describes the stage 3 signal propagation circuit conceptually. It includes an encoding neuron described functionally as a ganglion neuron and a decoding (or signal recovery) neuron described as a stellite neuron. Other investigators describe the ganglion neuron of the retina as a pyramid neuron in the cerebrum or a Purkinje neuron in the cerebellum. The ganglion neuron accepts analog signals and creates a phasic pulse train. The stellite neuron accepts a phasic pulse train and creates a copy of the original analog signal. To support signal propagation over long distances, the ganglion neuron incorporates signal regeneration circuits at intervals of about 2 mm. known as Nodes of Ranvier (NoR). The Nodes of Ranvier are functionally independent circuits incorporated morphologically into the ganglion neuron, and supported homeostatically by the soma of that neuron. Each internode of the ganglion neuron consist of regeneration circuit (NoR) coupled to a myelinated axon segment. Myelination is only used with stage 3 neurons. It is used to increase signal propagation efficiency from an energy conservation perspective. At the same time, myelination increases the speed of signal transmission. The dendrites shown in the figure are unmyelinated and generally much shorter than 2 mm.

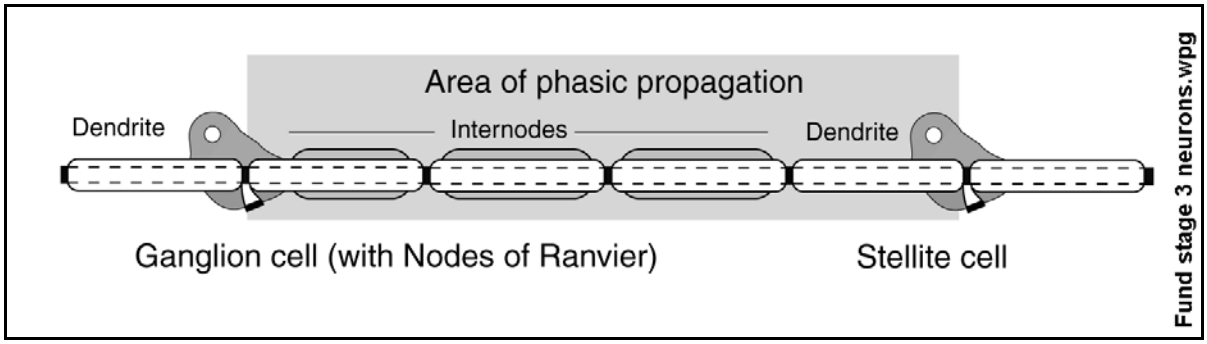

Figure 9.1.1-3 Conceptual stage 3 neural circuit. Each internode consists of an axon segment followed by a Node of Ranvier, or in the final internode a pedicle of the axon. The pedicle interacts with the dendrite of the stellite cell via a synapse.

The term stellite is used as the functional description of the decoding neurons of stage 3. It describes a large number of the morphologically defined stellate neurons and includes a majority of the large neurons of layer IV of the cerebral tissue.

> Functional is used here in the context of the underlying process of a given neural structure, and not as frequently found in neuroscience texts to describe the purpose of the structure

9.1.1.1.2 Equivalent circuit of the stage 3 signal projection circuit

The Electrolytic Theory of the Neuron can be used to represent the stage 3 signal propagation

circuit using standard electronic symbology. **Figure 9.1.1-4** shows such a stage 3 circuit using the circuits developed individually in **Chapter 2**. The circuit shows five active electrolytic devices (known as Activa) using the standard symbol for a PNP type transistor device. The active devices are shown incorporated in four different circuit configurations. It should be noted that all of the circuit configurations show the base, or poditic terminal of the Activa connected to the external neural matrix (generally through an impedance, P). This configuration is generally known as the common base or common ground configuration. This configuration appears to be used in all neural circuits, except for the second Activa in each receptor neuron.

1. The left-most Activa is shown connected as an active diode representing the synapse between the analog circuit and the encoding Activa of the ganglion neuron. A second synapse, represented by the fourth Activa connected as an active diode, is shown at the input to the stellite neuron.
2. The second Activa from the left is part of the circuit that accepts analog information and generates an action potential pulse stream at its output.
3. The third Activa from the left is embedded in a monopulse regenerator circuit that faithfully regenerates each individual action potential pulse, introducing a fixed delay in the timing between the pulses. As noted, this NoR circuit can be replicated as many times as necessary.
4. The last Activa on the right is embedded in a stellite circuit designed to output a signal indicating the arrival of the first pulse in a pulse train and to provide an analog output signal represented by the integral of the pulses in the pulse train.

The myelinated axon segments are shown as electrolytic elements exhibiting both capacitance and inductance distributed along their length. The presence of the inductance has been documented since the 1950's. This depiction replaces the conventional, and archaic, representation showing a capacitance and resistance distributed along the axon segment. The inductance of the axon segment is the key to the high efficiency of the propagation mechanism.

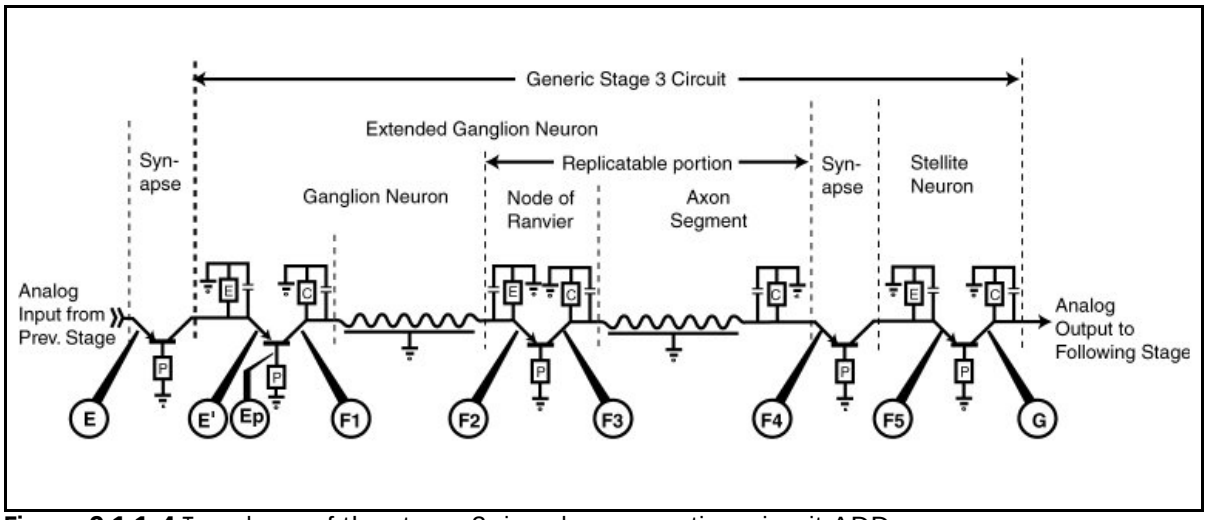

Figure 9.1.1-4 Topology of the stage 3 signal propagation circuit ADD.

Each of the Activa are shown connected to a local ground terminal represented by the local external neural matrix.

Below the graphic are shown a series of electrolytic test points where signals can be readily sensed. The electrical signals acquired at these points clearly characterize the electrolytic signals being passed through the stage 3 circuits.

- The signals at E and E' are demonstrably analog signals.

- The signals at each F# are demonstrably phasic signals (action potentials).
- The signal at F2 is an attenuated copy of F1.
- The sigal at F3 is a precise though delayed reproduction of the signal at F1.
- The signal at Ep generally shows a summation of the waveforms at E' and F1.
- The signal at F5 shows a delayed copy of the F1 waveform at a bias level.
- The signal at G shows a delayed replica of the signal at E'.

Berry & Pentreath have provided a set of waveforms that can be used to illustrate these signals[9]. Unfortunately, they;

- are from a giant dopamine neuron (GDN) of a mollusc
- required rebiasing during stimulation by up to 35 mV out of a total range of less than 140 mV.
- were stimulated parametrically using a double barrelled microelectrode filled with 0.6 M K_2SO_4
- are from different preparations and
- employ different clock rates during excitation.

Nevertheless, the waveforms can be rearranged in **Figure 9.1.1-5** to illustrate the waveforms associated with the stage 3 signal projection mechanism. The following figure shows waveforms from test point E', Ep, F1 & G in order beginning on the left. The waveform labeled Ep in the lower row will be discussed below.

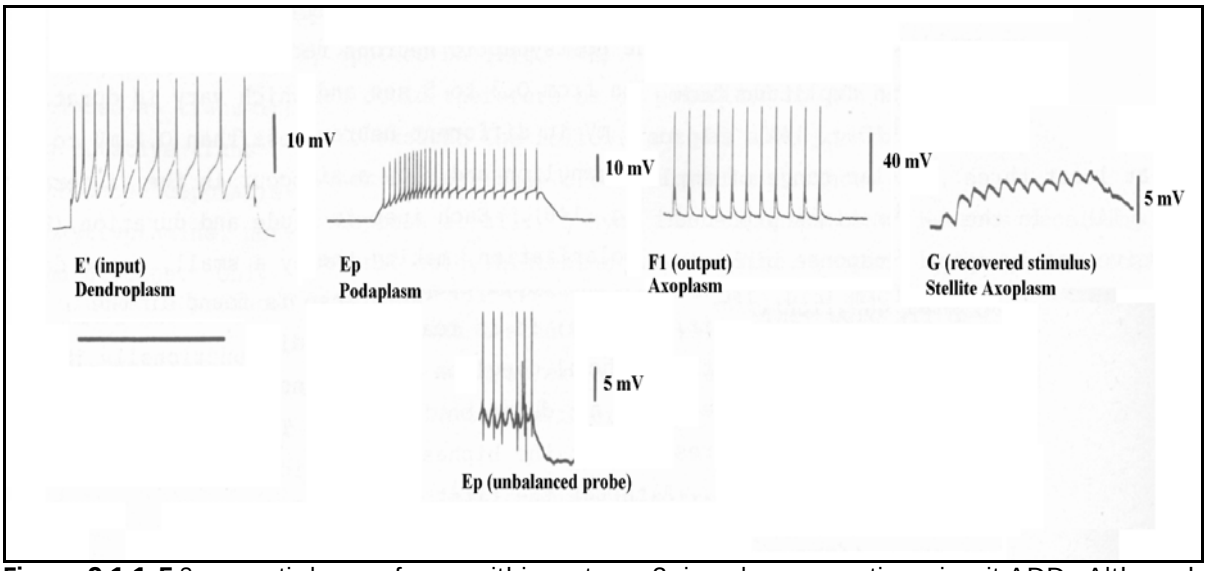

Figure 9.1.1-5 Sequential waveforms within a stage 3 signal propagation circuit ADD. Although not stated explicitly by the source, the Ep waveforms have been inverted for purposes of illustration. From Berry & Pentreath, 1978.

The time calibration bars are given as 2 sec for E', and 10 sec for Ep & F1. The voltage calibration bars are difficult to specify from the original citation.

Using the conventional wisdom of 1978, Berry & Pentreath asserted they probed "the soma" of their neuron. They did not seek to probe the electrolytically isolated dendroplasm, podaplasm or axoplasm (hillock) compartments within the soma of their neuron.

While no absolute voltages are given relative to the external neural matrix, the waveforms

---

[9]Berry, M. & Pentreath, V. (1978) The characterised dopamine neuron in *Planorbis corneus*. *In* Osborne, N. *ed*. Biochemistry of Characterised Neurons. NY: Pergamon Press pg 89

provide considerable information.

The E' (dendroplasm) waveform shows a step in the analog portion of the waveform followed by a series of ramps caused by integration in the dendrite circuit. Each ramp is reset by the spike coupled into the dendrite circuit from the axon circuit. The spikes are seen to be of constant amplitude. However, the amplitude of the root of each spike shows the waveform of the analog stimulus. The pulse rate is seen to decrease following the first pulse until a steady state is reached.

The Ep (podaplasm) waveform shows much smalleer action potentials riding on an analog waveform representing the stimulus. The attack time constant of the analog component is obvious. The decay time constant after cessation of stimulation is different.

The F1 (axoplasm) waveform is distinctly different. It shows no variation in the baseline prior to action potential generation (no analog stimulation component) and a distinct decay time constant as part of each action potential. The baseline has been truncated to the left of the first pulse and the pulses are equally spaced in this different preparation. The eleven-pulse pattern is compatible with the last 11 pulses of the Ep waveform.

The G waveform shows the recovery of the analog waveform expected from the analog component of the Ep waveform. Each pulse is integrated into the overall response during its duration and the overall response decays at the decay time constant of the stellite decoding circuit. Following the last action potential, the decay continues back to the baseline potential (not shown in entirety).
Additional details related to these waveforms will be provided in the next page of this set.

Berry described his test configuration only by "Conventional amplifying and stimulation equipment was used." A direct coupled oscilloscope is needed to show these waveforms properly. Otherwise, as here, their important DC bias level is lost and the AC waveforms generally exhibit misleading overshoot artifacts. Compare the waveform labeled Ep and the Ep waveform below it (at a differnt time scale) due to a poorly balanced probe. The negative spikes below the analog waveform are artifacts of the test configuration. Such artifacts are commonly found in the waveforms acquired in biological laboratories.

9.1.1.2 Equivalent circuit of the myelinated axon element

The electrical characteristics of the axon have been studied the most because of their presumed dominance in the historical common wisdom. It has been due primarily to the ease of access to axons. The dendrites are generally very small structures and the poditic structures have not generally been identifiable through morphology. These structures will be addressed independently in this section. **Figure 9.1.1-6** shows a spinal nerve root of the mouse from Deerinck & Ellisman[10]. As noted in the caption, the caption writers reference to a simple wire enclosed by insulation is not appropriate for this image. Each combination of axoplasm-myelin-matrix constitutes a coaxial cable with the matrix acting as the outside conductor and the axoplasm acting as the inside conductor. The myelin acts as the insulator down which the electromagnetic waves of Maxwell actually travel (See below). The axoplasm cavity is obviously filled with a mesh that would drastically slow any physical transport of ions along the length of the neuron. No details were provided as to how the nerve was cut and whether the asymmetrical shape of the individual neurons was present before cutting. While the diameter of the axoplasm varies significantly among the neurons, the thickness of the myelin wrap is surprisingly constant.

[10]Deerinck, T. & Ellisman, M. 2017) Bundled up *Discover* page 14

9.1.1.2.1 Historical Background

Over the years, a series of ever more complex two-terminal networks have been presented in the literature that purport to represent the active characteristics of "the axon" or of "the axon membrane." From an analyst's perspective, the proposed networks have gotten out of hand. The original two-terminal network of Huxley et. al. consisted of three current paths and one capacitive path in parallel, each connecting to the "inside" and the "outside" of the plasma membrane[11]. Shepherd shows a total of seven paths[12]. Demir et al. have recently shown eleven independent paths and introduced an unexplained symbol to represent some sort of resistance[13]. Each current path consisted of a battery and a "variable resistor" in series. Subsequent to Huxley et al., the polarity of the batteries frequently varied in subsequent transcriptions, analyses, and expansions of these simple circuits (example, Nickerson et al[14].). These networks have no significance in the world of electrical engineering and the symbol of a resistor with an arrow through it is not that adopted by the IEEE for a variable resistor. If in fact the symbol represents a resistor, all of the proposed circuits all reduce to a much simpler circuit. The symbol is more closely related to a diode in current circuit theory. These circuits appear to be strictly pedagogical or at best conceptual and requiring many words to elucidate the actual concept. The original network of Hodgkin & Huxley is shown in **Figure 9.1.1-7(A).** The circuit was highly conceptual at the time and no reason could be found in their papers for the battery in series with the load resistance, R_L. In the original paper, the authors were careful to specify that they were reporting on a membrane. They did not claim to be reporting on a functional neuron, a functional axon, or even an operating axon, in that paper. The variable resistor symbols were seldom discussed in detail. There has been no discussion of what is controlling their

Figure 9.1.1-6 Spinal nerve root of the mouse showing myelination ADD. Orange; axoplasm space. Yellow; the fatty substance, myelin. The space between myelin wraps is a water-based conductive medium. Each axoplasm-myelin-matrix combination constitutes a coaxial cable; not a simple wire protected by insulation as in the original caption. 10,000X From Deerinck & Ellisman, 2017.

---

[11]Hodgkin, A. (1951) The ionic basis of electrical activity in nerve and muscle Biol Rev vol. 26 pp 339-409

[12]Shepherd, G. (1988) Neurobiology, 2nd ed. NY: Oxford Press Pg. 114

[13]Demir, S. Clark, J. & Giles, W. (1999) Parasympathetic modulation of sinoatrial node pacemaker activity in rabbit heart: a unifying model *Am J Physiol Heart Circ Physiol* vol 276, pp H2221-H2224

[14]Nickerson, D. & Hunter, P. (2010) Cardiac Cellular Electrophysiological Modeling *Card Electrophysiol Meth & Models* pp 135-158

variation although Raymond & Lettvin[15] offer the important observation: "It is obvious that g_{Na} and g_K are not two-terminal elements but three-terminal elements; they are governable conductances in much the same way as is any junction transistor . . ." Their idea is correct, these proposed impedances are typically three-terminal impedances controlled dynamically by an unknown hand.

Figure 9.1.1-7(B) shows a more precise representation of a portion of neural membrane using the *style* of Huxley, et. al. The membrane is represented on the right as consisting of a single conductive path and a single capacitive path. The conductive path consists of a diode and a battery in series. The symbol, i_{diff} represents a conventional current entering the plasma through the membrane; the symbol, e_{diff}, represents the equivalent electron current flowing out of the membrane from the plasma. In this representation, the circuit on the left represents both the electrostenolytic source biasing the plasma to a negative potential and the load impedance. The load impedance is shown as external to the equivalent circuit of the membrane alone. There are problems with both of these representations. In (**A**), no means is provided to determining the value of the individual resistances although it is stated that they vary with time and the membrane potential. This statement implies that there must be other elements to the circuit.

(**B**) is more explicit in defining the membrane as an impedance, Zm – a diode, in series with a voltage, E_m., both shunted by the intrinsic capacitance of the lemma. These are intrinsic parameters of the bilayer membrane. There are no undefined variable impedances. However, it does not separately identify the different types of lemma present. The circuit on the left represents the electrostenolytic process biasing the axoplasm of the complete neuron. It includes both the load impedance and a battery. The battery potential, V_{sten}, is normally much higher than the intrinsic potential, E_m, of the membrane. The electrostenolytic source is the subject of **Chapter 3**.

The above representations are incomplete. The actual operation of the axon compartment can be understood using a more complete end view of an axon shown in (**C**). This frame segregates the membrane of an axon into four identifiable regions shown here as quadrants separated by the lines at 45 degrees.. Two of the regions are normally in contact with the extra-neural matrix. The other two are not. In the latter case, each of the regions is in intimate contact with another conduit of the neural path. When biased properly, these two conduits constitute an Activa and exhibit "transistor action." The emitter terminals on the left appear as diodes in series with an impedance, Z_P. Any change in current, I_{in} ,resulting from a potential, V_{in}, will result in an equal change in current to be injected into the axoplasm causing a depolarization. This depolarization of the axoplasm will cause a change in the current flowing out of the axoplasm through the right Activa. Simultaneously, the electrostenolytic supply will begin to cause current to flow out of that channel to restore the quiescent condition.

It is important to note the pure capacitance in the upper quadrant. A majority of the membrane of any conduit is type 1 lemma and not designed to pass any current. The lower region represents a key element of the overall axon. Like the lemma in the left and right quadrants, the lemma is type 2. Although the membrane itself appears much the same visually as the type 1 lemma, it is intrinsically and functionally different. The membrane exhibits a finite impedance and an intrinsic membrane potential as shown. This portion of the membrane, when coated with an electrostenolytic material, can introduce an electron flow into the axoplasm by electrostenolytic action. This current will generate a voltage across the combination of all of the current paths represented by the various lemma. There is a source impedance associated with this electrostenolytic source. This impedance is the load impedance of frames (**A**) and (**B**).

The relationship between the electrostenolytic source, the source impedance and the net impedance of the diodes in parallel determines the <u>quiescent potential</u>, or resting potential, of the axoplasm. To a large extent, it is this axoplasm potential that is measured in experiments.

---

[15]Raymond, S. & Lettvin, J. (1978) Aftereffects of activity in peripheral axons as a clue to nervous coding. *In* Physiology and Pathobiology of Axons, Waxman, S. *ed*. NY: Raven Press pp. 203-225

If the overall circuit in (C) is disturbed by connection to a test set, the quiescent potential and any changes in current flow must be evaluated by adding the test set equivalent circuit to the electrolytic configuration in frame (C). Hodgkin and Huxley reported that the impedances, which they showed as resistances in frame (**A**), varied with the potential of the plasma. It will be shown this is exactly what is expected of the network of frame (C). In their early papers, they did not address the question of whether their calculated impedances were due to the static or dynamic characteristics of the equivalent diode.

It becomes obvious from frame (C) that the method of sample preparation plays a large role in the measured characteristics of a single section of neural conduit, whether it is called an axon, a dendrite or a podite.

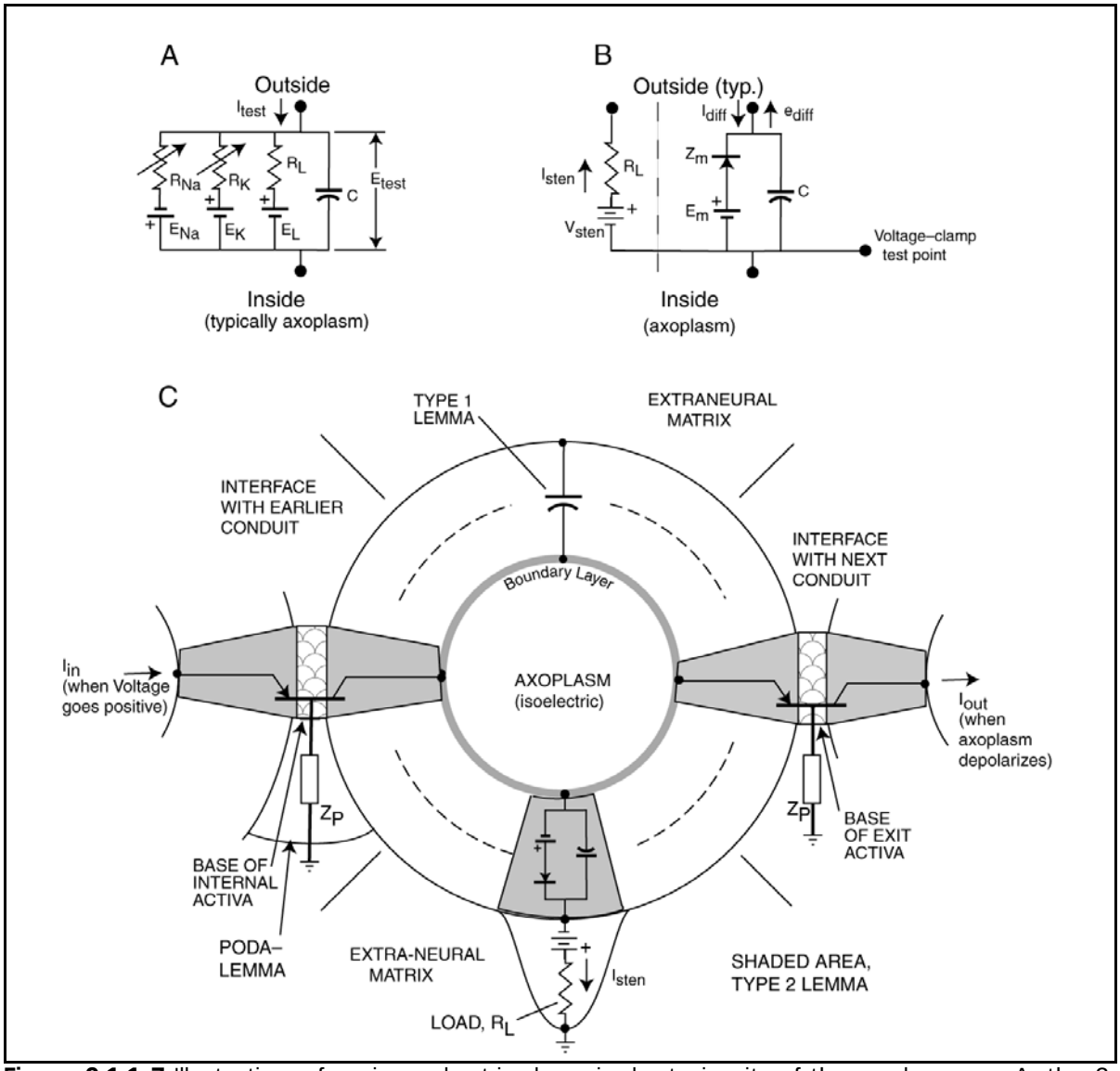

Figure 9.1.1-7 Illustration of various electrical equivalent circuits of the axolemma. A; the 2-terminal equivalent circuit of the isolated axolemma based on the constrained analysis of Hodgkin & Huxley and others. B; the more general network associated with the axolemma that can be used in several specific applications. C; a composite representing a longitudinal cross section of an axon before it has become extended horizontally. The boundary layer between the axolemma and the axoplasm is needed to properly understand the operation of the conduit. The Activa on the left represents the internal connection with a dendrite. This region of the axolemma is of type 2. Conventional current is injected into (electrons actually leave) the boundary layer by transistor action. [all arrows in frame C represent conventional currents]. The Activa on the right represents the synaptic connection with an orthodromic axon segment or dendrite. This region of the axolemma is of type 2. Conventional current leaves (electrons actually enter) the boundary layer by transistor action when the axoplasm depolarizes. The capacitance at the top represents the type 1 membrane used for a majority of the axolemma surface. The network at the bottom represents the type 2 membrane region used to polarize the axoplasm combined with the electrostenolytic source (battery). A conventional current leaves the boundary layer when the axoplasm becomes depolarized. The axoplasm remains iso-electric through out the process due to the mutual repulsion among the electrons within the axolemma.

9.1.1.2.2 The longitudinal cross-section of an axon with or without myelination)

The axon operates significantly differently as its length increases and whether or not it is myelinated.

> This section will focus on the topography and terminology associated with an ***unmyelinated*** axon. However, since the axon is only a conduit that is very similar in many ways to the conduits known as dendrites and podites, the discussion is easily generalized. The myelinated axon will be discussed in **Section 9.1.2**.

Figure 9.1.1-8 describes an axon from the perspective of electrolytic chemistry by combining the above material. Frame **A** is reproduced from **Chapter 8** primarily for orientation. Frame **B** provides an expansion of frame **A** to add additional details regarding the nature of the materials associated with the different functional elements. It is derived from the figure in **Section 10.1.2**. Within both the Activa and the synapse, the outer compartments consist of the bilayer membrane of the lemma facing the central compartment. This compartment contains a liquid crystalline "plug" of water that is the core element of the Activas within both the neuron and the synapse (through which all signal information is transmitted). The ionic conduits representing the axon and two dendrites are shown in block form.

Frame **C** shows the axon of **B** in greater detail. There is a region of the axoplasm, described by the Helmholtz Effect that is found everywhere along the inside of the axolemma when it is negatively biased with respect to the surrounding medium. Because of the mobility of the ions within the axoplasm, the axoplasm cannot support rapidly changing electrical fields more than 0.002 microns (2 nanometers or 20 Angstrom) from the lemma wall. Therefore, the bulk of the axoplasm within this Helmholtz Region (shown shaded) remains electrically isostatic during the operation of the neuron. The stream lines indicating electrons leaving the synapse and the electrostatic source and entering the Activa have been exaggerated for clarity. All moving charges remain within the nominal 0.002 microns of the inside wall of the lemma at all times. The significance of this fact is that the effective series resistance of the axoplasm is higher than expected from bulk measurements. In real situations, the effective series resistance should be calculated from the limited cross sectional area of the annulus formed by the Helmholtz region and the effective resistivity of the material within that region.

> It is important to note that the electrostenolytic site shown in the figure is a glutamic acid receptor site. However, like in other conduits, the site does not receive glutamic acid secreted in the synaptic gap as a putative neurotransmitter. It receives it from the IPM or INM as a routine source of electrical power (**See Chapter 3**).

When present, the myelination sheath, typical thickness ~2 microns, surrounds the lemma of the axon and the power source is pushed further toward end of the axon segment. The result is the formation of a coaxial cable consisting of the axoplasm, myelin sheath and surrounding conducting matrix.

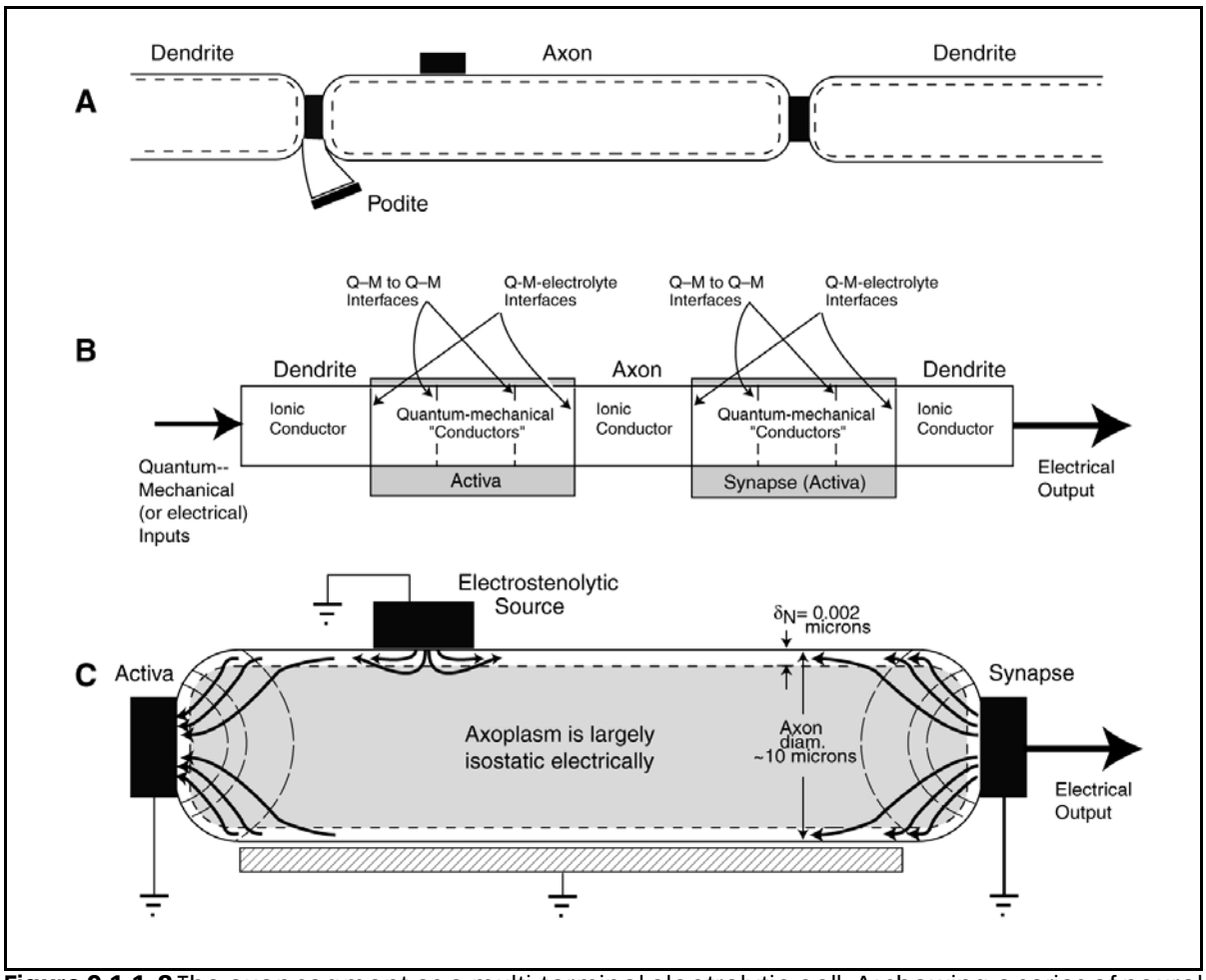

Figure 9.1.1-8 The axon segment as a multi-terminal electrolytic cell. A; showing a series of neural conduits for orientation. B; expansion of A to show the location of quantum-mechanical conductors (Activa and synapse) between conduits forming ionic conductors. C; expansion of part of B to show details of axon as an electrolytic conductor. Dashed field lines are exaggerated. Arrow flow lines show flow of electrons under various conditions. Hatched area represents the interneural matrix surrounding the axon. See text.

9.1.1.2.3 Methods of myelination in the neural system

The histological description of the myelination process has been awkward because the process is treated differently for individual and grouped propagation axons or alternately for neurons within the CNS and within the PNS. Fields has made this difference clear in **Figure 9.1.1-9**. The majority of the stage 3 neurons in the CNS are grouped into commissure and adjacent axon segments within these commissure are myelinated by specialized cells labeled oligodendrocytes. In the PNS, the majority of stge 3 neurons follow separate paths and their individual axon segments are myelinated by individual Schwann cells. The transition between these two methods of myelination is less clear. Further search of the literature would probably show how myelination is performed in the brain stem and spinal cord.

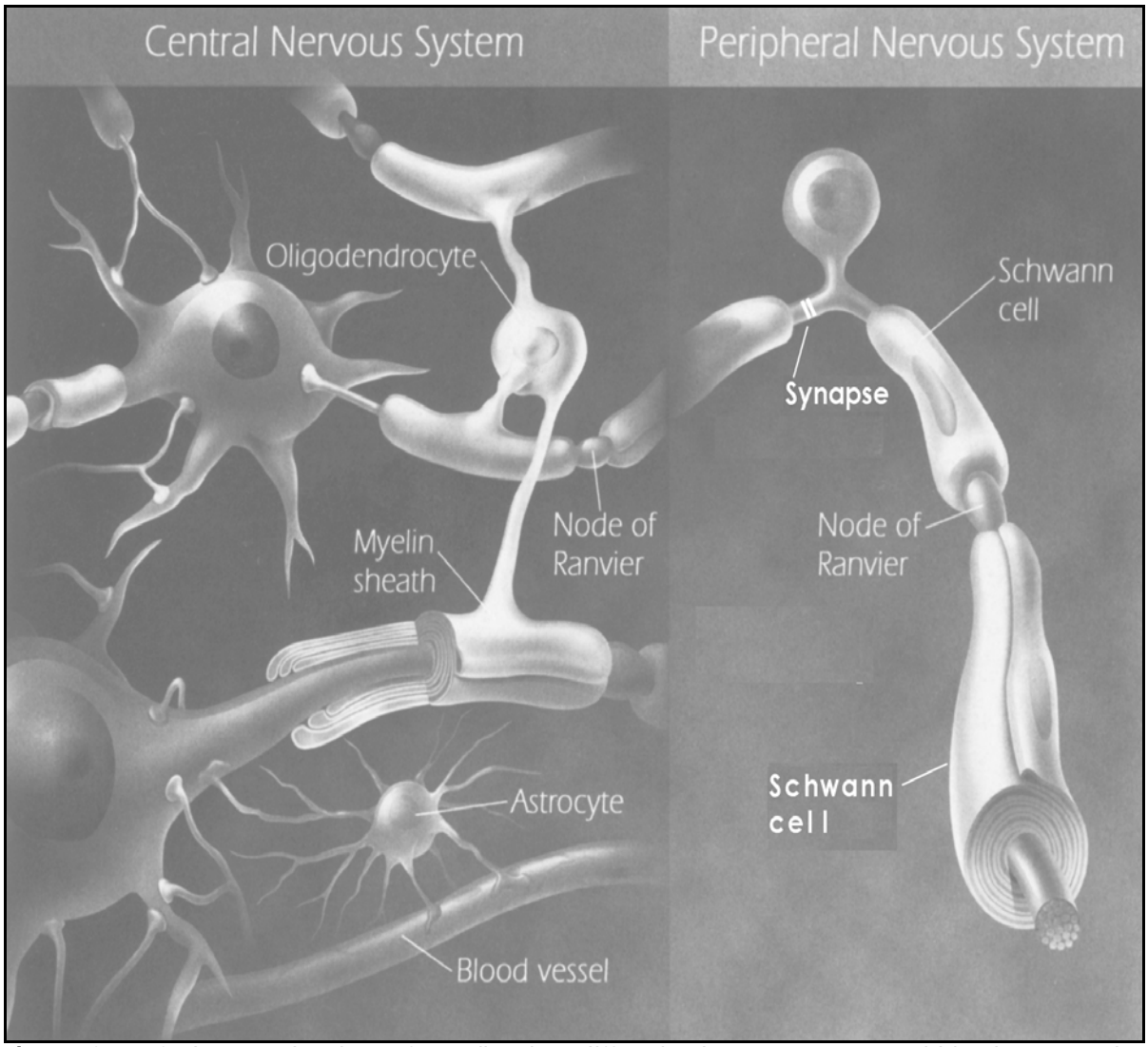

Figure 9.1.1-9 The mechanism of myelination differs in the CNS & PNS, Within the CNS, the majority of neurons are grouped into commissure where adjacent axon segments are myelinated as a group by individual oligodendrocyte cells. Where neurons follow individual paths (the predominant situation in the PNS, the axon segments are myelinated individually by separate Schwann cells. See text. From Fields, 2010.

Morrell et al. have provided a drawing showing their conception of the myelination of multiple neurons in greater detail[16]. Aggarwal et al. have recently discussed the histological structure of myelin generated by oligodendrocytes in considerable detail[17]. They noted the role of myelin as an insulator but did not address the electrical properties of the myelin specifically. They did note its role in preventing other chemical entities, particularly proteins, getting close to the

[16]Morrell, J. Schwanzel-Fukuda, M. Fahrbach, S. & Pfaff, D. (1984) Axonal projections and peptide content of steroid hormone concentrating neurons *Peptides* vol 5(Supp1), pp 227–239

[17]Aggarwal et al., (2011) A Size Barrier Limits Protein Diffusion at the Cell Surface to Generate Lipid-Rich Myelin-Membrane Sheets *Dev Cell* vol 21, pp 445+

axolemma, getting between the surface membranes of the myelin sheet or between the adjacent sheets of myelin. They report a sheet thickness of 44.0 ± 8.4 nm. From an electrolytic perspective, the myelin is used to increase the thickness of the dielectric formed by the combined axolemma and myelin sheath. It is critically important that an electrically conductive path not be allowed between the surface of the axolemma, or the surface of any intervening myelin layer and the surrounding extra-neural matrix, thereby reducing the effective capacitance of the combination.

9.1.1.2.4 Time of appearance of myelination

Brodal has provided a short discussion of the appearance of myelination in humans[18],

> "Myelination of axons starts in the *fourth month of gestation* and is *completed 2 to 3 years after birth*. Although many axons in the central nervous system remain unmyelinated, the process of myelination is clearly related to functional maturation of neuronal interconnections. Full functional capacity cannot be expected before myelination is completed. As for the individual neuron, myelination starts at the soma and proceeds distally. Different tracts are myelinated at different times. Overall, *tracts concerned with basic tasks, necessary for life, are the first to be myelinate* (such as sucking, swallowing, retraction from harmful stimuli, emptying of bowel and bladder, and so forth). Such connections are also phylogenetically the oldest.
>
> In the *spinal cord* myelination starts in the cervical region and proceeds in the caudal direction. First to be myelinate are the propriospinal fibers (interconnecting various spinal segments)." Ventral root motor fibers are myelinated earlier than the dorsal root sensory fibers. Myelination of ascending spinal tracts starts in the sixth fetal month, and tracts descending from the brain stem follow shortly after (reticulospinal and vestibuospinal tracts). These tracts need to be functioning at birth. In contrast, the *pyramidal tract*, which controls the most precise voluntary movements, is fully myelinated only about 2 years after birth. Connection from the cerebral cortex to the *cerebellum* are myelinated at the same time as the pyramidal tract, which seems logical since these connections are important for coordination of voluntary movements.
>
> Myelination of the *cranial nerves* starts in the sixth fetal month, except for the optic nerve (which is a central tract and not a peripheral nerve). Myelination starts shortly before birth in the optic nerve.
>
> In the *cerebral cortex*, myelination begins shortly before birth, first in motor and sensory areas. The association areas are mainly myelinated during the first 4 months after birth, although myelination continues after a period. The last regions to become fully myelinated are the association areas in the frontal lobe (prefrontal cortex).

9.1.1.3 The electrical circuit of the axon as a transmission line

Many authors have discussed the axon (and the axon segments in a long axon), such as found in a projection neuron, in the context of *charge diffusion along a transmission line* with minimal success. **Section 6.3.1.2** has presented the technical and historical reasons why the neurological literature has overlooked the propagation mode of signal transmission.

The equations of propagation, (also known as radiation in the unconstrained spatial environment) are not found in chemistry. The equations do not require the motion of charged particles to propagate energy, only to initiate propagation. Formally, the propagation equations are known as Maxwell's Equations or the General Wave Equations (GWE). To understand them requires a background in *complex algebra*, a subject foreign to most

---

[18]Brodal. P. (2004) The Central Nervous System: Structure and Function, 3rd Ed. NY: Oxford Univ. Press page 113

bioresearch students and therefore not addressed in most introductory biochemistry and biophysics texts.

As noted below, the prominent 19th century physicist, Thomson (Lord Kelvin) fought the Maxwellian concept of propagation in favor of his own diffusion theory until he passed from the scene (after apologizing for his failure to understand or appreciate the GWE in a large scientific forum, **Section 9.1.1.3.1**).

To completely understand the transmission of neural signals over distances of more than a few millimeters within the biological organism, several features of the myelinated axon must be recognized.

• It is necessary to recognize the term conduction, as typically used in neuroscience, actually refers to physical charge diffusion along a potential gradient; whereas the term propagation refers to the transmission of energy along a path through the interplay between the electronic and magnetic fields originating from a dynamic change in charge on a capacitor.

• It is necessary to recognize that any coaxial electrical transmission element incorporates an inductance, even when not physically recognizable by the investigator. The dominant electrical elements associated with an axon segment are its capacitance and inductance per unit length.

• It is necessary to discard the archaic concept of the axon as an electrical signal conductor as envisioned initially by Kelvin and later by Hermann. The axon actually involves transmission by propagation, an entirely different mechanism based on the General Wave equation of Maxwell.

• It is necessary to distinguish between the phase (or instantaneous local) velocity of a signal traveling along an axon segment and the much lower average velocity of a signal traveling along an axon consisting of alternating axon segments and Nodes of Ranvier.

• It is necessary to recognize that deterioration in the performance of a pulse propagation path may be due to either (or both) signal attenuation and signal distortion due to differential phase shift as a function of frequency.

The following discussions develop the concepts of *electro-magnetic propagation* along a contiguous series of alternating axon segments and NoR where differential phase shift is a major limitation in performance.

Figure 9.1.1-10 compares several axon configurations with a man-made coaxial cable.

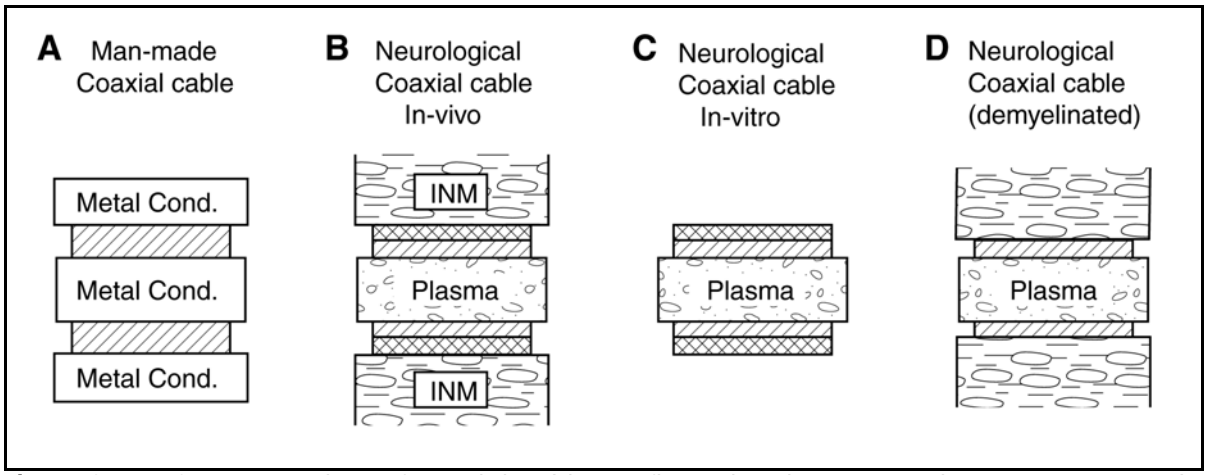

Figure 9.1.1-10 A comparison of coaxial cable configurations in cross-section. A; a man-made coaxial cable with metal conductors and a single dielectric between them. The outer conductors are part of a cylinder. B; an equivalent neurological coaxial cable showing liquid based conductors in the same configuration. The dielectric is composed of the inner layer (hatched) formed by the lemma and the outer layer (cross-hatched) of myelin. C; a neurological coaxial cable removed from its surrounding matrix and no longer functional as a coaxial cable. D; a neurological cable that has been de-myelinated in-vivo that no longer functions as an efficient coaxial cable. INM; inter neural matrix. See text.

While the man-made cables conventionally employ a metallic inner conductor surrounded by a metallic cylinder as an outer conductor, the neurological cable uses liquid based conductors for both the central plasma conductor and the outer conductor formed by the surrounding inter neural matrix (INM). Only a thin layer of the INM is needed surrounding the neuron to provide an electrical path for charge movement. However, the lack of such a continuous liquid path result in the situation in frame C that does not function as a coaxial cable. *The laws of electro-magnetism show that any coaxial structure exhibits an electrical inductance*. In an efficient coaxial cable, the thickness and dielectric constant of the dielectric is chosen to provide a capacitance per unit length matching the inductance per unit length of the cable. In frame D, the dielectric provided by the myelin wrap has deteriorated. As a result, the capacitance per unit length of the cable has been drastically increased and the cable is no longer an efficient one.

9.1.1.3.1 Failure of the archaic "Hermann Cable" concept

The Hermann cable derived from the earlier work of Thomson without significant change in concept. While the Thomson cable failed miserably when first put into real world application, Hermann continued to promote it in the biological field.

> The submarine cable placed between Ireland and Newfoundland in 1858, and designed to Thomson's specifications, required sixteen and one half HOURS to transmit the 99 word message of Queen Victoria to the New World[19]. The rate was six words per hour compared to the nominal rate of 15 words per minute of the first successful cable based on Maxwell's propagation concept. The Kelvin cable was slower than predicted by a factor of about 150:1 and clearly not commercially viable.

[19]Richet, P. (2007 in Eng, 1999 in French) A Natural History of Time. Chicago, Il: University of Chicago Press pg 198

> Interestingly, Richet documents a variety of other mis-characterizations and miscalculations made by Kelvin culminating in *Lord Kelvin's famous assertion of 1896* before the Scientific Jubilee. "One word characterizes the most strenuous efforts for the advancement of sciences I have made perseveringly during fifty-five years, and that word is **Failure**."

All subsequent coaxial cables were designed by electrical engineers in accordance with Maxwell's Laws (specifically the GWE described below). These have all performed as designed (beginning in 1863).

> While Thomson's accomplishments were many, he could not accept scientific defeat or the burgeoning work of others. His best remembered quotations from later in his life include: "Radio has no future" and "X-rays are a hoax." He obviously did not consider the general solution of Maxwell's Equations or the emerging understanding of the photon as too important. Thomson fought the Maxwellian concept of propagation until he passed from the scene.

- - - - -

Since 1850, the biological (including the medical) community has attempted to treat neural signal transmission as strictly concerned with charge diffusion (using the term conduction) as promoted by Kelvin. This treatment is incompatible with the operation of a wide temporal bandwidth transmission line. When examined from the perspective of an electrical transmission line, the axon is seen to be a coaxial cable in form. Such a structure of necessity exhibits both capacitance and inductance. It may or may not exhibit significant resistance, although it will always exhibit a resistive component in its input characteristic (that may not exist as a real resistance within the cable).

For some unknown reason, the biological community adopted the Hermann cable concept of conduction but never moved forward to accept the more complete Maxwellian Theory of Propagation.

- - - -

Hodgkin & Huxley (H&H) ran into complications in analyzing their data acquired on the basis of lumped parameter measurements. A similar problem was encountered by the competing Cole team. Their solution was to re-frame their operating concept and consider the axon a transmission line. They made this conversion relying upon the Hermann Cable approach involving only resistors and capacitors. Such a leaky transmission line does not describe the unmyelinated axon of *Loligo* or the mammalian myelinated axon.

In switching conceptual approaches, they introduced their equation 27 (pg 522) without providing any reference or discussion of its constraints. The equation is commonly known within biology as the cable equation as originally promoted by Hermann based on the earlier work of Lord Kelvin. The equation has a number of constraints that are addressed indirectly in both Cole (pages 60 and 212) and Taylor. H&H did not address the impact of their change in concept from a lumped constant axon to an axon supporting a traveling wave. It is difficult to follow the brief discussion in H&H related to their transition from a lumped constant model to the transition to a cable solution based on an action potential present as a traveling wave. Cole did address the change, at least in terms of its impact on the construction of his axial probe. The larger problem relates to the introduction of the "general wave equation" (GWE) and a propagation velocity, θ. They use the 1st order cable equation, that is lossy, as a baseline but substitute into it expressions from the 2nd order general wave equation that only applies to a loss-free line. They appear to have done this to keep θ a real number (as opposed to a complex number). It is not clear they were aware of this subtlety.

The above is typified by their use of the equation $V_m = f(x_0) = V_{m1} = f(x_1\text{-}vt)$ for a periodic traveling wave. If the line is loss free, this equation holds and the velocity of transmission, $v = (x_1 - x_0)/t$ where $x_1 - x_0 = \lambda$, the wavelength of propagation. However, the condition that the line is loss free prohibits the introduction of a series resistance, R, and a capacitance, C, into the cable equation. The presence of R requires the attenuation constant, α, not be identical to 1.00. The presence of R and C requires the phase constant, β, not be identical to 1.00. If α and β are not equal to 1.00, then amplitude of $f(x_0)$ cannot equal the amplitude of $f(x_1\text{-}vt)$ at any frequency. The correct

solution of the general wave equation to a lossy coaxial line was well known by the time of Cole and Hodgkin[20]. This author was exposed to it during sophomore year in 1955. Specifically, the dispersion in the signal is due to the difference in velocity of the signal components as given by the equation, velocity = $\omega/\beta(\omega)$.

Hodgkin and Huxley were aware of the complex plane plots of the impedance of the squid axon produced by Cole[21]. These plots clearly demonstrate that the squid axon involved a 2nd order differential equation with both inductive and capacitive components. An axon exhibiting both inductance and capacitance is not compatible with the 1st order differential equation they used. Nor is it compatible with the Hermann Cable. While Hodgkin & Huxley recognized the claim of Cole that an inductance was present, and they calculated a value for it from one of their relaxation curves, all of their equations and calculations involved real numbers. No imaginary terms appear anywhere in their equations. The phase shift associated with an inductance was never addressed (pg 540).

Taylor attempted to rationalize some of the many models of cables in the literature up through that of Hodgkin & Huxley. Taylor presented a thorough mathematical review of "Cable Theory," as restricted to an RC cable, in detail[22]. He includes a section on the giant axon with an axial wire introduced into it. Taylor does note the following crucial fact ten years after the work of Hodgkin & Huxley. "Since the 1939 papers of Tasaki, in which he demonstrated directly that only the nodes of Ranvier in mammalian myelinated nerve are excitable it has been abundantly shown and generally conceded that the 'salutatory' theory as propounded by Lillie is correct." This position may have been more controversial than he suggests. However, it remains correct today. He references Tasaki's 1953 paper and provides a caricature of the myelinated axon with Nodes of Ranvier. Why Taylor did not interpret the complex plane data of Cole as calling for a second order differential equation containing both inductance and capacitance is not clear.

Taylor then makes a set of assumptions. "We make the assumptions that the radial currents in the core and external region are to be ignored, that the myelin sheath between nodes has an infinite resistance and negligible capacitance and that the node width is negligibly small but with finite impedance." This statement defines a loss-free line and not the Hermann Cable he continued to use in his analyses.

While the review by Taylor in 1963 provided a more modern interpretation of the work of Hermann and Thomson, He chose to "consider only the steady state in time, and only the direct current resistance and conductance concepts." By also ignoring any radial electrical fields within the plasmas, he further restricted his analysis to the Equation of Heat Flow. He posited that if the membrane was represented by only a parallel combination of a resistance and a capacitance, his core conductor model represented an "ideal submarine cable," the differential equation for which has been derived a number of times since first treated by Thomson (Lord Kelvin). This approach essentially takes the field back in time to that of Kelvin and Hermann and ignores what was learned about a real submarine cable from the *in-place* test results.

At mid-20th Century, Cole discovered and documented the inductance associated with myelinated axons[23]. However, the biology community did not understand the terminology Cole used and rejected the idea that inductance played a role in axonal physiology.

Twenty years later, Rall provided a short mathematical rationale between signal propagation

---

[20]Albert, A. (1934) Electrical Communications. NY: J. Wiley & Sons. pp 192-214 in the 3rd edition of 1950

[21]Cole, K. (1968) Membranes, Ions & Impulses. Berkeley, CA: University of California Press pp 77-87

[22]Taylor, R. (1963) Cable Theory *in* Nastuk, W. *Ed*. Physical Techniques in Biological Research. NY: Academic Press

[23]Cole, K. (1941) Longitudinal impedance of the squid giant axon J Gen Physiol pp 771-788

by diffusion versus electromagnetic waves[24]. However, he did not differentiate between signal projection neurons involving action potentials and other types of neurons. The matter of myelination is a crucial factor in discussing these two major classes of neurons. Without recognizing the difference between these classes, it is unrealistic to draw conclusions as is done at the end of his rationale.

Rall was a prolific author with a formal background in physics and later training in many biology laboratories of his day. He apparently had no formal training in electrical circuit theory or engineering. An annotated summary of his life's work was published in 1995[25] by researchers that new him personally. A key paper that appeared in that summary listed his basic premises[26]. His work focused on highly simplified geometric structures with little reliance on empirical data obtained in a biophysical laboratory. As noted above, his work relied upon the "Heat Equation," a second order differential equation that relies upon the excitation applied at one end of a conduit to remain present until the signal it generated arrives at its terminal destination. While this is a plausible assumption within the dendritic and poditic trees of neurons, it is not compatible with the length of the axons of stage 3 signal propagation neurons.

Even in the above summary of Rall's writings, including the annotations of his successors, the subject of Maxwell and his General Wave Equation (GWE) are not addressed and do not appear in the Index. Thus, Rall and his successors do not consider the difference between conduction and propagation. They frequently appear to use the terms interchangeably. Rall's papers appear to only consider the flow of conventional electrical current through generalized resistive media enclosed by a membrane forming a capacitance between the media and the surrounding isoelectric matrix (a Hermann Cable). He generally relies upon lumped constant electrical parameters. No discussion of "hole" conduction is apparent in any of his writings.

Rall's lack of practical experience in electronics is exemplified by two specific items. First, although recognizing that the dendrites of a neuron are filled by and surrounded by a highly conductive fluid environment, he did not recognize the dendrites were coaxial cables that can be characterized by well developed and precise equations. These equations demonstrate significant differences in the capacitance of a cylindrical dendrite compared to a flat plate capacitor. Second, even though coached by his mentor, Cole, who had first discovered the presence of inductance within biological structures like the dendrites and axons (but did not realize the origin of that inductance), Rall described the product of "a negative inductance and a negative series resistance" as equaling a time constant (in analogy to the product of a positive capacitance and a positive resistance)[27]. There is no such passive component as a negative inductance. The cited discussion shows a naive understanding of the character of the reactance versus resistance relationship in electrical circuits.

Rall consistently assumes the interior of a neuron does *not* exhibit discrete compartment.

The premise of this work is that myelinated signal projection neurons employ electromagnetic wave propagation while the considerably shorter unmyelinated signal processing neurons employ a parabolic partial differential equation as found in mechanism employing diffusion. In the case of electromagnetic wave propagation, the partial differential equation is hyperbolic.

---

[24]Rall, W. (1977) Core conductor theory and cable properties of neurons. Chapter 3 *In* Handbook of Physiology, Section 1, Vol. I, Kandel, E. *ed*. pg. 60

[25]Segev, I. Rinzel, J. & Shepherd, G. (1995) The Theoretical Foundation of Dendritic Function. NY: MIT Press [xxx I own this volume]

[26]Rall, W. (1959) Branching Dendritic Trees and Motoneuron Membrane Resistivity *Exptl Neurol* vol 1, pp 491-527

[27]Rall, W. (1960) Membrane potential transients and membrane time constants of mononeurons *Exptl Neurol* vol 2, pp 503-532 *Last page*

Rall also provides a simple definition of the Neuron Doctrine, based on morphology, that dates from Cajol. Although accepting the part of the doctrine that suggests the signal path is not continuous but contiguous with interruptions at (at least) the synapses, it discounts the idea of the neuron as the basic building block in favor of the Activa-conduit pair. He also presents a brief definition of the core conductor concept of an axon which is considered too simple for purposes of this work. His table of parameters for different types of axons is useful.

Rall references Kaplan & Trujillo[28] who considered the transition between these two functional environments. They used the physical model of an axon found in Rall and the empirical differential equations of Hodgkin & Huxley. The physical model was a a simple core of axoplasm surrounded by an infinite volume of INM. Their computations involved numerical solution by digital computer. They adopted Hodgkin & Huxley's lossy axolemma in their analysis and assumed physical transport of charge along the axon in the form of ionic flow. They did not discuss how ionic flow was achieved in a viscous, possibly liquid crystalline material. They discuss a "left-over" term in their equation fitting their model and use an impulse function to simulate the leading edge of an action potential. Unfortunately, they adopt an average velocity of 12.3 m/sec as a reference value for the velocity of neural signals common to all neurons. This led to problems in their analyses. Instead, they should have introduced the much higher phase velocity, of 4400 m/sec within an axon segment and a nominally higher 44 m/sec for the average velocity associated with a NoR/axon combination when addressing projection neurons (**Section 9.1.2.3**).

Scott[29] reviewed the Kaplan & Trujillo paper but found it wanting in several respects while indicating his analysis was "a drastic simplifications of the properties of a real active membrane." Scott does not clearly establish whether the "action potential" of the squid giant axons is the result of diffusion of a signal or propagation of a signal. Its slow speed over a short distance that does not include a Node of Ranvier suggests, it is a pseudo action potential. He adopts the slow diffusion (conduction) velocity of 21.2 m/sec of Huxley and Hodgkin while he employs the propagation equations of Maxwell. His model of the axon is very simplified. He introduces the terms magnetic inductance and inertial inductance, computes the axon capacitance based on the properties of a flat sheet capacitor and proceeds to compute a negative inductance for a simple linear circuit. His one sentence conclusion is primarily political. However, he does suggest that the omission of any inductance by Hodgkin & Huxley in their equivalent circuit was based on "good intuition." In a later book[30], Scott is forced to introduce the analogy of "little green boys" (pages 45–46) to explain the variability in the membrane of Hodgkin & Huxley. Good intuition must continually be re-confirmed by up-to-date experiments.

- - - -

Rushton made a move away from the Hermann cable by proposing a "local circuit" showing energy in the form of charges moving along the axolemma in a periodic manner. It is unfortunate that other investigators did not challenge the work of Rushton. Replacing his essentially static "local circuit" by the dynamic "local interaction" of electromagnetic fields would have led to an entirely different perspective on neural signal transmission.

It is important to note that there is no requirement that a transmission line provide a conductive path for electrons or ions along its length. It is only necessary that electromagnetic energy can be continually shared between infinitesimal segments of a capacitor and an inductor. The process is similar to the propagation of radio signals through free space. No ether is required.

---

[28]Kaplan, S. & Trujillo, D. (1970) Numerical studies of the partial differential equations governing nerve impulse conduction: the effect of Lieberstein's inductance term. *Math. Biosci.* vol 7, pp. 379-401

[29]Scott, A. (1971) Effect of the series inductance of a nerve axon upon its conduction velocity *Math Biosci* vol 11, pp 277-290.

[30]Scott, A. (1977) Neurophysics NY: John Wiley & Sons

The phase velocity of signals along such a line is determined by the product of the inductance and the capacitance per unit length. It does not depend on the conductivity of any plasma within the conduit. This fact negates many of the conceptual models in the literature based on a current loop frequently conceptualized as involving a "local circuit" (discussed in **Section 6.3.1.2**).

9.1.1.4 Application of the GWE to the myelinated axon

As noted at the beginning of this chapter, to understand the operation of the neural system, it is necessary to move beyond a single concept applicable to all neurons. Different conditions related to unmyelinated, myelinated and pseudo-myelinated axons result in different underlying mechanisms. Different mathematical solutions describe these mechanisms. This chapter builds on the fundamental characteristics and features of the action potential generating pulse neuron of **Section 2.6** with specific attention to the role of myelination of the axon and its individual segments. the myelinated axon supports a mode of signal transmission, known as signal propagation in the electronics field that is critically important to the understanding of stage 3 neuron operation. Failure to appreciate the role of signal propagation, as opposed to signal diffusion along conductive paths, will prove a major barrier to understanding the physiology of the neural system.

A cursory scan of Physical Chemistry texts quickly confirms a relevant fact. The field of chemistry does not usually employ the complete version of the General Wave Equation (GWE). Only the simplified forms of Poisson's Equation and the Heat Equation are found. As a result, most of the investigators in neurological research have not been introduced to the GWE, the fundamental equation describing stage 3 signal projection.

The General Wave Equations (GWE) of Maxwell are required to understand the operation of a coaxial transmission line such as a myelinated axon or axon segment. These equations are second order differential equations that are deterministic and easily solvable in closed form. They are required when the coaxial transmission line includes an inductance component, and all coaxial lines include an inductance as a component. The neuroscience community has avoided the use of the GWE even after the presence of an inductance component was measured in detail by Cole during the 1940's. This has caused a serious impediment to the understanding of the neuron. If no inductance term is present, the second order differential equations of the GWE reduce to a single first order differential equation, known as the diffusion equation or the heat equation, of Thomson (Lord Kelvin). However, as noted above all coaxial cables exhibit an inductance component, even if the researcher does not recognize its physical presence. As noted in **Section 9.1.1.3.1**, Lord Kelvin made a fool of himself in the 19th Century denying the existence of the GWE even though he was Director of the Cavendish Laboratory when Hermann and Maxwell shared office space there during the 1830's.

Students and journeymen neuroscience investigators usually do not have the necessary mathematical background, including complex algebra, to understand the methods of GWE solution. However, the results described in this chapter are well supported and used universally. A critical factor is the axon is a cylindrical coaxial transmission line with the myelinated lemma acting as the insulator and the fluids of the axoplasm and the surrounding extracellular fluids acting as the inner and outer conductors respectively.

9.1.1.4.1 The fundamental GWE

Maxwell's equations have been expressed in integral, differential and matrix form. This makes their application easy in the hands of an experienced investigator. However, they are frequently daunting in the eyes of the uninitiated.

Maxwell's General Wave Equation, in its most compact matrix form, can be expressed as;

26 Neurons & the Nervous System

$$\nabla^2 V = \frac{1}{v^2} \cdot \frac{\partial^2 V}{\partial t^2}$$

where del, the inverted delta, is a vector operator but not technically a vector itself. Capital *V* is a vector and nu, ν, is a scalar (that may be a complex mathematical function). [Note the awkward display of the expression (δt^2) in this typography.] This equation applies to any problem involving up to the 2nd differential of the variable, *V*, with respect to any coordinate system required to adequately express the variable.

In differential form, it is usually expressed in Cartesian coordinates as;

$$\frac{\partial^2 V}{\partial x^2} + \frac{\partial^2 V}{\partial y^2} + \frac{\partial^2 V}{\partial z^2} = \frac{1}{v^2} \cdot \frac{\partial^2 V}{\partial t^2}$$

The equation describes the sum of the 2nd order differentials of the variable with respect to the three spatial coordinates as equal to the 2nd order differential of the variable with respect to time. In many applications, the equation simplifies significantly when some of the terms in the expanded form of the equation are equal to zero.

1. If the value of the right-hand term equals zero, the equation is known as *Laplace's Equation*. This form is important in the study of electrostatics and many other problems involving static fields.

2.If the value of the right-hand term is a constant, the equation is known as *Poisson's Equation*. It applies to more complex electrical field problems that contain a localized concentration of charge, and many other problems.

3. If the value of the right-hand term is proportional to the time and the left-hand term only involves the first order differential with respect to position, the equation is known as *Kelvin's Equation* or more often, *the Equation of Heat Flow*. The equation represents the transfer of heat between a stationary source and a sink *by conduction (diffusion)*.

4. The general condition applies when the right-hand term is a second derivative with respect to time. This is the form (the General Wave Equation or GWE) that introduces the dynamic interaction between the variable with respect to both distance and time. This is the form that predicted the propagation of radio and light waves through free space (independent of any aether or other medium) and describes the travel of electromagnetic and acoustic waves through, or along the surface of, a variety of materials.

The GWE is also the form used to describe the operation of electrical filters of arbitrary complexity. Filter theory is a very specialized discipline even within electrical engineering and not widely taught except at the graduate level.

Transmission lines are a special class of electrical filters. The coaxial cable is a specific type of transmission line that is of particular interest here.

The filigreed terminations of the myelination on axons and axon segments at NoR are also specialized applications of the GWE in filter theory. These areas constitute "half-section" filters.

The operation of the cochlea of hearing is an even more specialized filtering application of the GWE involving a cylindrical coordinate system. The specific form of the cochlea is an exponential helix where the dispersion of acoustic energy is controlled by the curvature of the helix in space.
http://neuronresearch.net/hearing/pdf/4Physiology.pdf beginning with Section 4.4 and
http://neuronresearch.net/hearing/pdf/5Generation.pdf

9.1.1.4.2 General & Particular Solutions to The fundamental GWE

The following quotations are abstracted from Reddick & Miller[31] but similar statements will appear in any more recent text on differential equations used to solve physical problems.

The GWE is a "linear partial differential equation of the second order." By a solution of a differential equation we mean any functional relation among the variables, free of derivatives and reducing the given equation to an identity. For example, the relation $y = e^{2x}$."

"A solution containing the maximum number of constants is called *the general solution*; for instance. . . " Any solution obtainable from the general solution by giving specific values to one or more of the arbitrary constants is call *a particular solution*, for instance. . . " Note the use of "the" in front of "the general solution" and the use of "a" in front of "a particular solution."

"In a physical problem, the differential equation involved is usually accompanied by certain auxiliary conditions on the variables." This is the key area where Thomson (Lord Kelvin) stumbled during the 19th Century, and Herman and then Roll failed to realize this failing in promoting Kelvins Heat Equation as the solution to the coaxial cable problem (**Section 9.1.1.3**).

Chapter IV of Reddick & Miller addresses solutions of more difficult practical problems not solvable in closed form. It addresses the use of a Power Series. Chapter V addresses solution of more difficult practical problems by using a Fourier Series, consisting of an infinite series of trigonometric functions. These techniques are generally required to solve problems involving non repetitive functions, particularly non repetitive (transients) as a function of time.

Chapter VII addresses the solutions to a series of simple real problems. As part of that discussion they point out (page 275), "Consequently the complete formulation of our problem is comprised of the differential equation (1), the boundary values (2), and the initial conditions (3)."

In Article 71, Reddick & Miller address the Heat Equation of Thomson (Lord Kelvin). They separate the solution from that for the vibrating string, because the boundary values for the Heat Equation are not both zero. They therefore divide the solution into a *steady state* part and a t*ransient* part.

In Article 74, Reddick & Miller address the "Flow of electricity in a cable." Their attack is to consider the unbalanced cable, a wire above a ground plane. It applies equally well to a coaxial cable if the GWE is expanded in cylindrical coordinates and the capacitance and inductance is calculated from the appropriate cylindrical equations. See Kraus[32] or other texts on electromagnetics.

Their equations (5) & (6) on page 301 are the equations of signal *propagation* in a real cable (or in free space when the voltage and current variables are changed to the electrical field and the magnetic field). They are also the equations of signal propagation within a myelinated axon segment (**Section 9.1.1.5**). Propagation is a "term of art" in signal transmission, to borrow a phrase used mostly in the legal profession. These equations show that if either the *inductance* OR *capacitance* are reduced to zero, the equations reduce to the Heat Equation of Article 71. Under these conditions the flow of current is by *diffusion* through a physical medium. This diffusion is traditionally called *conduction* by biochemist.

9.1.1.4.3 Discussion of the Lieberstein & Mahrous (1970) papers

---

[31]Reddick, H. & Miller, F. (1955) Advanced Mathematics for Engineers, 3rd Ed. NY: John Wiley & Sons.

[32]Kraus, J. (1953) Electromagnetics. NY: McGraw-Hill Book Company section 4.16, page 167

Lieberstein & Mahrous published two papers in 1970 relating to modeling the axon segment[33,34]. The Abstract of the first paper opens, "Recent efforts of one of us (HML) have been directed toward demonstrating that line inductance must be included in any mathematical formulation of the electrical properties of axons, for nerve and muscle as well as pacemaker and receptor cells." They go on, "These efforts have yielded unquestionable, if somewhat indirect, evidence of the occurrence of magnetic fields that accompany every action potential, and of surprisingly large inductance characteristics for any axon which is thin enough to be regarded as a transmission line." Unfortunately, these mathematically oriented papers treating the radial passage of currents through an axon segment, do not provide any values for the inductances they assert are large, even though the words large inductance appear in the title of one paper. While Maxwell's Equations are used extensively, they do not include any significant models of their concepts, much less any relevant data.

These two apparent mathematicians cite a variety of psychology-based and mathematics-based papers but do not cite any of the papers by Cole and colleagues[35]. Cole and colleagues are the only people who have published laboratory data related to the inductance associated with neuron axons.

They do cite a value of 1.2 cm/sec for the rate of travel, θ, of their currents "are moving to the right at the same rate as the rate of propagation of an action potential." This is an absurdly slow rate for an axon. It suggests a neural signal associated with a six foot (1.8 meters) sciatic nerve would require 150 seconds to reach the brain from the toe. They cite the rate as provided by Hodgkin & Huxley for a wave moving along their nerve at 6.3° C. Unfortunately, the Hodgkin & Huxley nerve was not propagating an action potential, but a set of swim generating waveforms. Much better data has been provided by Smith et al. (**Section 9.1.1.5.4**). It shows a *phase velocity*, θ, between Nodes of Ranvier in a rat spinal root neuron of 4,400 m/sec This phase velocity is slowed to an average velocity of 44 m/sec by the delays of 0.019 msec at the Nodes of Ranvier occurring ever 2 mm along the neuron. A *phase velocity* of 4400 m/sec is *3.6 million times faster* than the 1.2 cm/sec value of Lieberstein & Mahrous. The *average velocity* of 44 m/sec (which is only achieved occasionally in the neural system) is *3,600 times faster* than the 1.2 cm/sec value. These grossly different values explain why Lieberstein & Mahrous calculated such large inductances using their model. Lieberstein & Mahrous note in a footnote on page 53 of their paper,

> "For a chain-of-cells transmission line described in Lieberstein (1969) (and taken from the work of Lowenstein and Kanno (1965) where current travels along the interior and on the outside of a chain (not through the exterior membranes), the coaxial model for inductance is probably the correct one." For a an axon described by **Figure 9.1.1-11** in **Section 9.1.1.5.1**, **Figure 9.1.2-1** in **Section 9.1.2** shows values calculated for a coaxial cable form of myelinated axons segment should exhibit an inductance per unit length of typically 1 to 10 nano-Henries per meter for an axon lemma with a radius of 1 micron. The *phase velocity* of such an axon is calculate at between 300 and 3000 meters/sec depending on other relevant factors.

On page 271 of their paper, they note a delay in the firing of a nondescript action-potential-generating neuron of 27 msec. This is an order of magnitude longer than portrayed in the full equation for action potential generation in this work (Section xxx) and supported by laboratory results (again in **Figure 9.1.1-12** in **Section 9.1.1.5.4**). The total delay in a Node of Ranvier at exothermic temperatures is only 0.019 msec.

---

[33]Lieberstein, H. & Mahrous, M. (1970) A Source of Large Inductance and Concentrated Moving Magnetic Fields on Axons *Math Biosci* vol 7, pp 41-60

[34] Lieberstein, H. & Mahrous, M. (1970) A Formulation Concerning the Electrical Effects of Axon Variations from Cylindrical Shape: Spindle Cells and Bulbous Synapses *Math Biosci* vol 7, pp 259-272

[35]Cole, K. (1968) Membranes, Ions and Impulses: A Chapter of Classical Biophysics. Los Angeles, CA: University of California Press

The Lieberstein & Mahrous papers can not be taken seriously until they adopt a more reasonable phase velocity in their calculations.

9.1.1.5 Application of the GWE to neuron operations

To understand the operation of the neural system, it is necessary to move beyond a single concept applicable to all neurons. Different conditions, related to unmyelinated, myelinated and pseudo-myelinated axons, result in different underlying mechanisms. Different mathematical solutions describe these mechanisms.

By closely examining the operation of neurons, in the context of the GWE, it is possible to define two fundamentally different operating modes. One deals with the *conduction* (diffusion) of electrotonic signals (energy) through a bulk medium in the presence of a resistive element and a lumped-constant reactance that is dominated by capacitance. The second mode deals with the *propagation* of phasic signals (energy) largely independent of the medium present (except it may be guided by major discontinuities in the electrical properties of the medium or the surroundings). In this case, the electrical elements (R, L & C) of the cable are distributed. In a well-designed system, the reactances of the capacitive and inductive components of the coaxial cable tend to cancel each other.

The first mode corresponds to conduction in the unmyelinated axon, and in the neurites. When expressed in mathematical form, this mode corresponds to a first order differential equation such as the Heat Equation. The solutions of these equations are represented by "real" mathematical expressions. The second mode is more complex. When expressed in mathematical form, the mode corresponds to a second order differential equation satisfying the GWE. The solutions of these equations are represented by "complex" mathematical expressions. These expressions introduce the new mechanism of propagation.

The solution for the one-dimensional transmission of energy over an axon is well known and is given as; [xxx see page 328 in Chapter 7 of hearing book, section 7.4.3.2]

Demyelination results in yet another situation related to myelination that is clearly pathological and will be addressed briefly in the context of a medical condition in **Section 9.1.2.5** and more completely in the Chapter on disorders affecting the neural system. xxx

9.1.1.5.1 The cylindrical transmission line EDIT

The axon segment of a stage 3 signal projection neuron is a cylindrical transmission line. Its performance is significantly increased if it is myelinated to reduce the effective capacitance of the axon segment per unit length. In this case, the input impedance of the axon segment is reduced considerably and the propagation velocity is increase significantly (to the values measured in the laboratory).

The biological community has generally calculated the capacitance of an axon by calculating the apparent area of the axon and considering it equivalent to a flat plate capacitor. For precise work, it is necessary to recognize and use the correct formula for the capacitance of a concentric cylindrical structure. This structure exhibits both a capacitive and an inductive electrical component. The formulas are given in the previous reference to Kraus. The result is that any axon transmitting a waveform of complicated shape with respect to time consists of all of the circuit elements discussed below.

As noted by Schwan, the *in-vivo* capacitance of an axon may differ from its value in air due to the absence of the higher dielectric material that normally surrounds it[36]. If the *in-vivo* material has a complex dielectric constant, the effective capacitance *in-vivo* must be divided by the square root of that value. This variation may aid in rationalizing some of the capacitance values

---

[36]Schwan, H. (1963) Determination of biological impedances *In* Physical Techniques in Biological Research NY: Academic Press pp 323-406

found in the literature.

- - - -

By closely examining the operation of neurons, in the context of the General Wave Equation (GWE) of Maxwell, it is possible to define two fundamentally different operating modes. One deals with the *conduction* of electrotonic signals (energy) through a bulk medium. The second deals with the *propagation* of phasic signals (energy) largely independent of the medium present (except it may be guided by major discontinuities in the electrical properties of the medium or the surroundings).

Only the un-myelinated neuron is properly represented by a first order differential equation such as the Heat Equation (also known as the diffusion equation).

> Scott[37,38,39] tried to calculate the exact transmission characteristics of an unmyelinated axon in 1971 through 1975. His first examination showed, "A recently developed exact transmission line equivalent circuit is then used to estimate the series inductance for a squid axon. It is found to be about five orders of magnitude too small to influence the conduction velocity." In the second paper, he performed extensive mathematical manipulations, and incorporated a variety of assumptions, but failed to determine that the inductance per unit length of a coaxial transmission line was a logarithmic function of the thickness of the lemma/myelin combination. By 1975, Scott had reverted to a "derivation of the nonlinear diffusion equation." Scott's approach has not been pursued effectively in recent times. His difficulty arose in two areas. He was mistaken in confusing the actual propagation velocity of the axon segments with the apparent (average) propagation velocity of the combined axon segment and slow signal regenerator within the Node of Ranvier. He was also in error when he tried to apply coaxial cable theory to the unmyelinated axon.

When Maxwell's equations are applied to the myelinated axon situation, they call for the interaction of electrical and magnetic fields. These fields can be related to two primary parameters, a resistive component and a reactive component(s). The reactive component(s) is represented by the imaginary terms in the equations (see **Section 9.1.2.2**). This component is present in two forms. In physical systems, the positive imaginary component is associated with the inductance of the system. The negative imaginary component is associated with the capacitance of the system. In transitioning from a heat flow analog to an actual electromagnetic application, the inductance of the axon measured by Cole (in cited section) becomes quite understandable.

9.1.1.5.2 Physiological model for a signal projection neuron

Figure 9.1.1-11 presents the electrical circuit of the typical axon within the larger context of the neural system. The figure is meant to be generic and apply to both the simple neuron and the more physically extended neuron consisting of one or more Nodes of Ranvier. In this context, the two titles above the figure are dual and the last Activa on the right may be either a Node of Ranvier or a generic synapse. By referring to the individual zones of the axon, it is possible to avoid confusion. For compatibility with other figures, the Activa on the left is shown being driven by a voltage source, V_e. The conduit in the center of the figure is the transmission line of interest. It is partially myelinated. The electrostenolytic voltage sources are shown as V_{cc} and V_{ee}. The

---

[37]Scott, A. (1971) Effect of the series inductance of a nerve axon upon its conduction velocity *Math Biosci* vol 11(3-4), pp 277-290

[38]Scott, A. (1972) Transmission line equivalent for an unmyelinated nerve axon *Math Biosci* vol 13(1-2), pp 47-54

[39]Scott, A. (1975) The electrophysics of a nerve fiber *Rev Modern Phys* vol 47(2), pp.487-533

dashed line within the conduit represents the reticulum of the axon (or axon segment). The solid lines from the Activas to the reticulum are shown symbolically for convenience. In fact these conductors are formed by the physical concentration of the reticulum as it approaches the Activas. The region labeled x constitutes a lumped constant capacitance associated with the collector circuit of the first Activa. This capacitance is large due to the extremely short distance between the reticulum and the electrolyte surrounding the axon. Within the area labeled y, the capacitance of the transmission line is distributed and much smaller due to the increased distance between the inner and outer electrolytes. The area labeled z constitutes the lumped capacitance of the unmyelinated part of the conduit in the vicinity of the input to the second Activa.

A coaxial transmission line is an *unbalanced* transmission line. Such a line does not require a conductive path between its two terminals. However, if energy is extracted from the terminal, a conductive path back to the source must generally be provided. In man-made circuits, this is typically through a "ground" connection which is independent of the actual transmission line. In many high performance transmission lines, the conductive path associated with at least one of the conductors is intentionally broken to avoid undesirable extraneous loop currents.

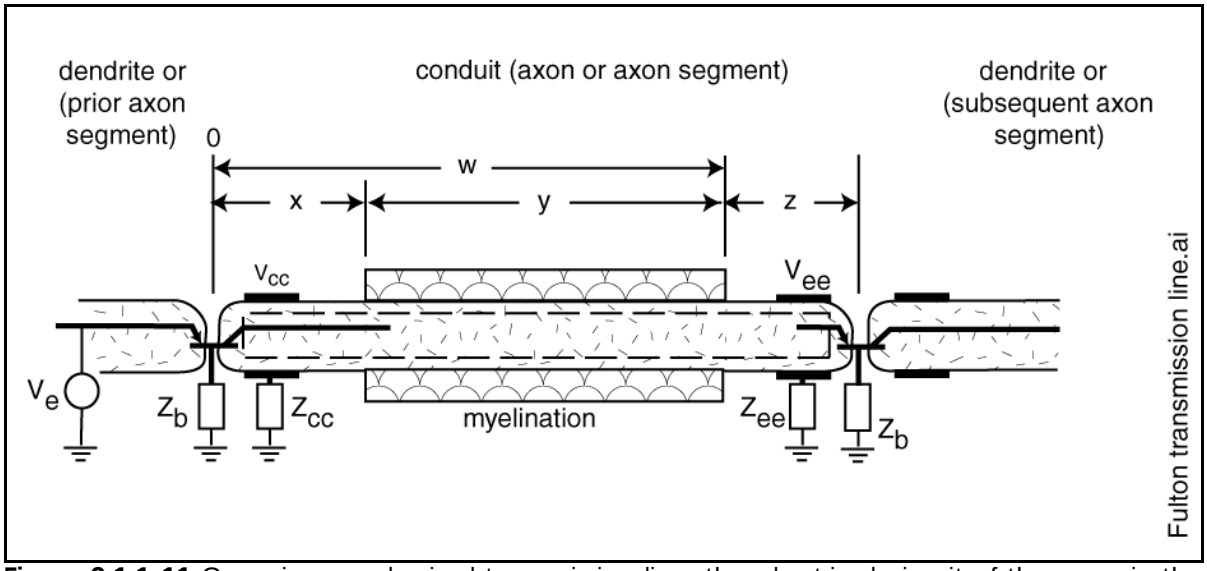

Figure 9.1.1-11 Generic neurological transmission line; the electrical circuit of the axon in the context of the overall neural system. X; the postsynaptic transition (matching) section. Z; the presynaptic transition (matching) section. Y; the distributed parameter transmission section.

Little is known about the detailed electrical properties of the individual membranes and electrolytes forming the conduit. This is partly due to the oversimplified model of the conduit used previously. Stampfli says the specific resistance of the INM is similar to that of Ringer's solution (90 ohm-cm at 20 Celsius)[40]. However, because of the high quality of the insulator represented by the axolemma and the myelination, little error is introduced by making the above assumption. Under this assumption, the capacitance and inductance of the transmission line and the two lumped capacitors can be calculated and compared to the measured values in the literature. In general, only lumped capacitance values are found in the literature.

9.1.1.5.3 The electrical transmission line model of a signal projection neuron EDIT

There has been a general misconception in the biological literature, dating from Hermann in the

[40]Stampfli, R. (1981) Overview of studies on the physiology of conduction in myelinated nerve fibers. *In* Demyelinating disease: basic and clinical electrophysiology. Waxman, S. & Ritchie, J. *ed*. NY: Raven Press pg. 16

late 1800's[41], that an electrical transmission line of adequate bandwidth can be composed of only resistors and capacitors. This position is not founded on electrical engineering principles[42] nor supported by subsequent physiological experiments. **The axon of a neuron can not be properly modeled as a Hermann Cable.** Cole discussed this fact extensively in 1968[43] based on his paper of 1939[44] that relied upon Hermann's RC cable. The opening of his section labeled Discussion asserted, "The concept of an inductance in a cell membrane is so foreign to our past experience and so difficult to grasp that we must inquire closely into each of the steps which has led to it before we can resign ourselves to the necessity of accepting and using it." Cole & Curtis[45] described the test set used by Cole.

He showed that the typical axon exhibited a large inductive component through measurement. While he did not provide a satisfactory explanation for this inductance, it was clearly present, and is well documented. As Cole describes it, "The suggestion of an inductive reactance anywhere in the (neural) system was shocking to the point of being unbelievable." To this day, the fact that the axon of a projection neuron exhibits considerable inductance has not been accepted in academia and pedagogy. However, the tide was turning at the research level even then. Schwan also began discussing the inductance of axon in 1963[46]. As seen in this work, it is the combination of inductance and capacitance that determines the very high signal propagation velocity of the individual axon segment when operating in the signal propagation mode (where it is usually myelinated). This velocity is much higher than the velocity achieved by diffusion in axons associated with stage 1, 2 and 4 neural operations.

Hermann adopted a simple RC network to represent what he understood to be "a leaky telegraph cable." It must also have been a short leaky telegraph cable. This configuration suffers from significant temporal dispersion in the frequency components of the signal with distance. A transmission line always consists of capacitors, inductors and resistors. Technically, the resistor is optional. A transmission line is an electrical circuit designed to emulate free space but to direct the signal energy to a more limited target location. Free space has a resistive characteristic impedance of 376.7 Ohms although it is completely empty and exhibits no resistive element. An electromagnetic wave travels through free space at the speed of light. Except in a few novel situations, a passive transmission line always exhibits a characteristic impedance less than that of free space. The velocity of energy propagation along a transmission line is always lower than the speed of light.

[**Figure 10.3.4-4**] illustrates the equivalent circuits representing a coaxial axon. (A) shows the typical lumped-parameter representation. In the ideal case, and within the operating range of the axon, the values of the resistive elements are such that the currents through them can be ignored. The dominant currents are reactive currents associated with the inductive and capacitive elements. The resulting lumped constant network is show by the heavier lines. To more accurately represent the physical length of a real axon, it is more appropriate to describe it by using the heavier network on the left replicated on an incremental basis. The resulting distributed model is shown in (C) This simple network describes the electrical performance of the real axon over the distance between its terminal components.

---

[41]Hermann, L. (1905) Lehrbuch der Physiologie, 13th ed. Berlin. See also Hille, pg. 27

[42]Kraus, J. (1953) Electromagnetics. NY: McGraw-Hill pp. 417-444

[43]Cole, K. (1968) Membranes, Ions and Impulses: A Chapter of Classical Biophysics. Los Angeles, CA: University of California Press, pp 77-103

[44]Cole, K. (1941) Longitudinal impedance of the squid giant axon *J Gen Physiol* pp 771-788

[45]Cole, K. & Curtis, H. (1939) Electric Impedance of the Squid Giant Axon during activity *J Gen Physiol* pp 649-670

[46]Schwan, H. (1963) Determination of biological impedances *In* Physical Techniques in Biological Research NY: Academic Press pp 323-406

The network in (C) has a characteristic impedance that is seldom well matched to the driving source. This leads to electrical in-efficiency. To avoid this problem, good design practice calls for the introduction of a "matching filter" section between the transmission line and the source and between the transmission line and the following sink. These matching sections are lumped parameter networks similar to that in (D). These filters are similar to one half of the filter shown in (A) but with slightly different parameter values.

Several significant features should be noted for such an ideal circuit.

1. No resistive elements appear in the distributed equivalent circuit of the axon. The circuit is not dissipative of electrical power.

2. An actual axon consists of two portions, the extended middle section described by the distributed equivalent circuit, and the "matching" end segments which are best modeled using a circuit similar to the lumped constant model.

3. The signal propagation velocity along the axon is determined entirely by the ratio of the inductive to capacitive components per unit length.

4. The loss in signal amplitude along the axon is very low in the ideal case.

In a real myelinated stage 3 signal propagation axon. The shunt conductance is negligible but the series resistance (representing the conductivity of the plasmas on each side of the myelinated axolemma, is not. It is the primary parameter limiting the propagation velocity of the axon. It also dissipates some power. This resistance introduces both attenuation and phase distortion into the transmission line. As will be discussed in the data section below, it appears phase distortion is a greater problem in real axons than is attenuation.

These features of a real axon differ considerably from the Hermann Cable model.

A transmission line exhibits a series of important parameters. Four of these parameters are basic;

+ the series inductance per unit length of the line, L/m

+ the series resistance per unit length of the line, R/m

+ the shunt capacitance per unit length of the line, C/m

+ the shunt conductance per unit length of the line, G/m

The series impedance of the line is given by Z/m = L/m + R/m. The shunt admittance is given by G/m + C/m.

Three additional parameters are calculated from the above;

+ a characteristic impedance--it is important in how a separate circuit drives and how a receiving circuit terminates the transmission line.

+ the velocity of signal propagation along the transmission line

+ the propagation constant of the transmission line. It is a measure of the quality of a transmission line.

To understand, derive, and evaluate expressions for these parameters, it is necessary that the investigator be familiar and comfortable with complex algebra. The characteristic impedance, Z_0, is defined as the square root of the series impedance divided by the shunt admittance determined from the four basic parameters. The propagation constant, γ, is defined as the square root of the product of the series impedance and the shunt admittance. These two quantities are usually defined using complex algebra, where they are the real and imaginary parts. The real part of the propagation constant describes the attenuation constant, α. The attenuation factor for a line is given by the expression $e^{-\alpha x}$, the decrease in signal amplitude with distance along the line. The imaginary part describes the phase constant, β. The propagation velocity is given by the frequency of the signal divided by the phase constant. In transmitting a pulse waveform

over a transmission line, it is important that all Fourier components of the pulse travel at the same velocity. Otherwise, the line is considered dispersive and the pulse is distorted as it travels along the line. If β is a not a linear function of frequency, the velocity of propagation of the transmission line will be a function of frequency and the pulse will become distorted as it travels along the line.

There are only a few special cases among these equations. A *lossless* line does exhibit a characteristic impedance given by a pure resistance, as does the lossy line where G/C = R/L. In general, a lossy line does not satisfy this ratio. Any other lossy transmission line exhibits a complex characteristic impedance and all lossy transmission lines exhibit a phase constant that is a function of frequency--resulting in waveform distortion. The phase constant associated with *a transmission line lacking in inductance, i. e. made up of only resistors and capacitors, is highly dispersive and such a line is not appropriate for pulse transmission.* Fortunately, all coaxial transmission lines, such as used in neurons, exhibit considerable inductance.

9.1.1.5.4 Recent modeling of axons based on passive models EDIT

[xxx copied in bulk from a section in Chapter 19 on pain]
McNeal et al. introduced a passive model of the axon in 1976 based roughly on the much earlier conceptual work of Huxley and Hodgkin. During the 1990's, several authors discussed a variety of passive axon models. They discussed both the pros and cons of these models. In 2002, McIntyre et al. provided an extensive paper that actually used the term "active" to describe the operation of a neuron and proposed conceptually an active component to their model[47].

Rattay & Aberham provided their interpretation of four different models of the axon[48]. They noted, "Up to now, most results were obtained with the Frankenhaeuser-Huxley model, but nearly all of them are wrong in time scale and the cathodic block phenomenon was not observable because the temperature dependence of the gating mechanism has been neglected." They provide an analysis of the McNeal model but they provide no schematic to support their modeling.

McIntyre et al. also introduced the physical description of a Node of Ranvier from Berthold and associates of the 1980's (see footnotes to their Table I). As they note, "Unfortunately, geometric representations of the internodal sections in nerve fiber models have not been stricly based on experimental morphology. Instead generically sized sections of two layers of components representing the axolemma and myelin sheath have been used, and as a result, the fine geometrical properties of the paranode could not be accurately represented." This situation is easily corrected by referring to Chapter 9 of this work and the more extensive description of stage 3 neuron operation provided in Chapter 7 of "Hearing: A 21st Century Paradigm[49]." It is shown there that the operation of the stage 3 myelinated neuron and its Nodes of Ranvier is much different from that predicted in the conventional literature. The sections of the axon adjacent to the Node of Ranvier identified by the Berthold group are easily shown to be "end sections" within the conventional academic specialty of electrical filter design. The Node of Ranvier is easily shown to consist of an Activa, an active liquid crystalline semiconductor device analogous to the transistor of the man-made solid state semiconductor world.

Unfortunately, McIntyre et al. adopt the unsolved partial differential equations of Hodgkin and Huxley (1952) as their baseline in their Appendix. In their figure 1, their circuit models have been limited to RC networks employing variable resistors where the mechanism of changing their resistance is unspecified. With the increased capacity of desktop computers, their approach has been widely employed in spite of the availability of closed

---

[47]McIntyre, C. Richardson, A. & Grill, W. (2002) Modeling the Excitability of Mammalian Nerve Fibers: Influence of After potentials on the Recovery Cycle *J Neurophysiol* vol 87, pp 995-1006

[48]Rattay, F. & Aberham, M. (1993) Modeling axon membranes for Functional Electrical Stimulation *IEEE Trans Biomed Eng* vol 40(12), pp 1201-1209

[49]Fulton, J. (2008) Hearing" A 21st Century Paradigm. Bloomington, IN: Trafford. Chapter 7 *also* http://neuronresearch.net/hearing/pdf/7Projection.pdf

form equations describing the operation of the stage 3 neuron much more precisely.

Most of the computer aided modeling of neurons beginning in the late 1980's and continuing to date is best described as pedagogical procedures, rather than an actual investigation related to the neural system. They have frequently been reported by undergraduates[50] or post docs still learning their craft. Warman et al. assert that McNeal first introduced the methodology they employ when McNeal (1976) attributes the methodology to Hodgkin & Huxley (1952). Warman et al. limit their cable model to the RC networks of Hodgkin & Huxley with the undefined hand controlling the variable resistive impedances.

In Figure 1, McIntyre et al. also introduce their concept of a double cable model which they attribute to Halter & Clark[51]. While Halter & Clark adopt the model of the myelinated neuron of Berthold and associates, they do not describe a double cable model. In fact, the concept of a double cable model is faulty. The myelination is functionally integral with the lemma of the axon segment. The result is a simple coaxial cable with the fluid within the axon segment and the matrix outside of the neuron forming the electrically conducting structures surrounding a very high quality insulator formed by the lemma and the myelination. Halter & Clark do note the choice of Hodgkin and Huxley to ignore the effect of nodal constriction on conduction velocity to be significant due to the relatively short distance of the constriction. None of these parties recognized the very significant delay introduced by the Node of Ranvier into their average conduction velocity calculations (see the next figure and discussion).

A second source from McIntyre et al. is Zhou et al[52]. Zhou et al. also rely upon the graphics and designations of the Berthold group, although they attribute them to Halter & Clark. However, they focus entirely on the Node of Ranvier and do not document the propagation velocity of the axon segment. Their interests involve the effect of genetic mutations. They make an assertion that indicates their failure to understand the fillagree region of the myelination on each side of the Node of Ranvier, "The transition zone between the myelinated and the nonmyelinated segment near the nerve terminal is a site of impedance mismatch that is particularly vulnerable to excitability perturbation, both physiologically and pathologically." In fact, this region is a "matching section" of filter theory designed to specifically avoid their assertion of mismatch.

A second paper by Zhou and Chiu provide their model of a branch point at a Node of Ranvier supporting two subsequent axon segments[53]. [xxx need to study this paper] Their failure to recognize the transimpedance properties of the Activa within the Node of Ranvier, and their subsequent use of linear matrix algebra, limits the value of this paper.

Figure 8A of the 2002 McIntyre paper has been simplified from Text-fig 6 in a paper by Boyd & Kalu[54] in order to make their results appear more relevant to empirical measurements. There is no operational rational for subdividing a data set, calculating individual linear regression lines for each portion and taking the regression lines as the actual data. The dashed higher order regression line of the original figure is just as valid.

---

[50]Warman, E. Grill, W. & Durand, D. (1992) Modeling the effects of electric fields on nerve Fibers: determination of excitation thresholds IEEE Trans Biomed Eng vol 39(12), pp 1244-1254

[51]Halter, J. & Clark, J. (1993) The influence of nodal constriction on conduction velocity in myelinated neerve fibers *NeuroReport* vol 4, pp 89-92 *Also* Houston, TX: Rice University; Center for Research on Parallel Computation CRPC-TR93309

[52]Zhou, L. Messing, A. & Chiu, S. (1999) Determinants of Excitability at Transition Zones in Kv1.1-Deficient Myelinated Nerves *J. Neurosci* vol 19(14), pp 5768–5781

[53]Zhou, L. & Chiu, S. (2001) Computer model for action potential propagation through branch point in myelinated nerves *J Neurophysiol* vol 85, pp 197-210

[54]Boyd, I. & Kalu, K. (1979) Scaling factor relating conduction velocity and diameter for myelinated afferent nerve fibres in the cat hind limb *J Physiol* vol 289, pp 277-297

Boyd & Kalu provide considerable data on the average velocity of neural signals in various types of neurons using cats. They attempted to correlate these average velocities to the total diameter of the associated neuron. They did not comment on the dimensions or degree of myelination of these neurons.

In 2013, Capogrosso et al. provided an extensive 3D computational model of the motor neurons involved in epidural stimulation of spinal neurons. They used FEM techniques. Their paper is discussed in **Section 19.11.8.4**. They continued to use a conceptual model based on the archaic Hodgkin and Huxley model of the 1940's (although they did not cite this source).. That model assumed the outer membrane of a axon segment was the functional element of the neuron. They offered similar but statistically different conductivity values from those of Struijk based on Geddes & Baker. While their graphics are colorful, their schematics do not provide any insight as to the operation of the axon segment and Node of Ranvier beyond the conceptual circuits of Hodgkin & Huxley.

The modeling activities since the 1980's have also described conduction velocities for their neurons that are misrepresented. Their velocities in the order of 30-60 meters/sec actually apply to the combination of an axon segment and a Node of Ranvier, where the delay associated with the regeneration of the action potential is actually dominant. The propagation velocity along an axon segment is very well documented to fall in the 4400 meters/sec range (nominally 100 times faster than typically reported in these pedagogical studies). **Figure 9.1.1-8** is an annotated figure from Figure 7.4.5-1 in "Hearing: A 21st Century Paradigm[55]," using the data from Smith et al[56].

[55] http://neuronresearch.net/hearing/pdf/7Projection.pdf#page=46

[56] Smith, K. Bostock, H. & Hall, S. (1982) Saltatory conduction precedes remyelination in axons demyelinated with lysophophatidyl choline *J Neurol* Sci vol. 54, pp 13+

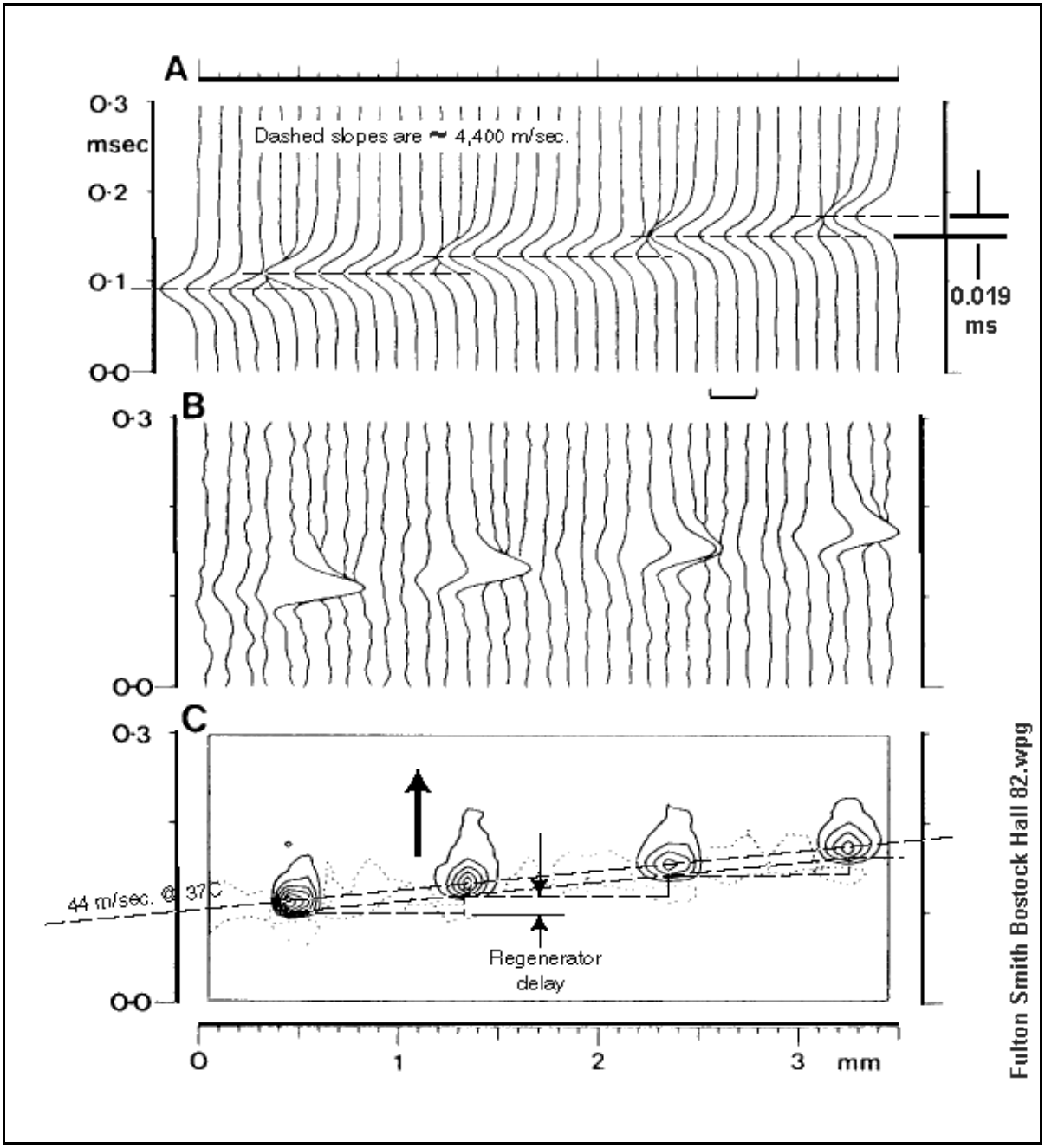

Figure 9.1.1-12 Saltatory conduction in a normal rat ventral root fiber. Frame A shows the propagation velocity for the axon segment extending between Nodes of Ranvier. Frame B & C show different presentations of the same data clearly showing the average propagation velocity between nodes of Ranvier and dominated by the regenerator delay (0.019 msec) of the Node. Modified from Smith et al., 1982.

This figure clearly shows the propagation velocity of an individual axon segment is approximately 4400 meters/sec while the average transmission velocity between equivalent points separated by a Node of Ranvier is on the order of 44 meters/sec, a reduction of a factor of 100 due to the significant delay introduced by the regeneration of the action potential within the Node of Ranvier.

9.1.1.6 The relaxation oscillator of stage 3A and Nodes of Ranvier

The relaxation type oscillator is a rare form of oscillator that provides an output pulse of the same polarity as its stimulating pulse but only involves a single active device (one Activa in biological circuits or one transistor in man-made circuits). See **Section 7.3.4 in PBH**. The active device relies upon internal feedback via the impedance attached to its base terminal (poditic terminal of the neuron) to mediate oscillation..

9.1.2 The propagation of action potentials–the dynamic situation

To completely understand the transmission of neural signals over distances of more than a few millimeters within the biological organism, several features of the axon developed in **Section 9.1.1** must be recognized.

The following discussions rely upon the concepts of electro-magnetic propagation along a contiguous series of alternating axon segments and NoR where differential phase shift is a major limitation in performance.

9.1.2.1 Background

Because the concept of signal propagation within the myelinated axon of a neuron is new to most readers of this work, a comparison between the conceptual, and cartoon dominated, discussions of signal *conduction* versus the more fundamentally founded discussions of signal *propagation* is appropriated and probably mandatory.

The key fundamental differences are two;

• Signal propagation along a myelinated axon or axon segment does not involve the movement of charged particles. It involves the coupling between *changing* electric and magnetic fields.

- The phase relationship between these fields determines the direction of propagation.
- No electrical field parallel to the direction of propagation is required.
- The velocity of the propagation is determined exclusively by the permittivity and permeability of the medium through which the propagation occurs, and the ratio of the outer to inner radii of the combined lemma and myelin sheath.

• Signal conduction along any neurite or axon element requires an electrical potential gradient parallel to the direction of charge (ion or hole) flow.

- The electrical potential gradient must be maintained for the duration of the conduction process.
- The biological medium is generally in the liquid crystalline state.
- There are many parameters associated with charge transport through a liquid crystalline substrate.

Propagation is entirely defined by the General Wave Equations of Maxwell. Conduction within a solvent medium is controlled by a host of generally nonlinear and concentration dependent mechanisms.

Donders made extensive, although primitive by modern standards, investigations of the velocity

of neurons related to stage 3 propagation[57]. However, he did not differentiate between conduction velocity and electromagnetic propagation velocity in his non-invasive experiments. His measurements show a "ballpark" similarity to modern measurements.

Newman has provided early data on signal transmission without discriminating between propagation and conduction (and using the later term exclusively) from a clinical perspective[58]. The distances in his chapter XIX require signal projection by myelinated neurons.

9.1.2.2 Ionic velocity in solvents EDIT

The discussion of charge flow along the structures of neurons has long been dominated by cartoons rather than more formal diagrams and detailed discussions. The few measured values reported in the biological literature frequently involve indirect measurement over poorly defined paths. Even in the more fundamental physical chemistry literature, the values are frequently extrapolated to infinite dilutions to obtain limiting values. As Barrow has noted[59], "At higher concentrations, the law of independent migration of the ions fails, and the conductance is really a property of the electrolyte rather than of the individual ions of the electrolyte (page 677)."

Discussions of the velocity of ions in solvents is very complicated. The velocity of ions within gels is even more complicated, and to a large extent does not exist. What little charge transfer occurs within a gel, or even a high concentration solution, is frequently by "hole transfer." Hole transfer is the movement of electrons in a retrograde path where an electron moves from a neutral atom to a nearby ion. The nearby ion thereby becomes a neutral species and the previously neutral atom is now ionic.

Since individual ions do not often exist in solutions, even dilute solutions, the motion of ions along an electrical potential gradient is complicated and frequently a function of multiple nonlinear parameters.

Even determining the electromotive potential (the electrical potential gradient) within an electrolyte is difficult because of the interaction between man-made electrodes and the solutions. It is complicated further by the rapid establishment of boundary layers and conditions near those electrodes. These boundary layers distort the assumed electromotive potentials very significantly.

As a result of the above considerations and other factors, Barrow noted, without addressing gels (page 680), "the path of an ion under the influence of an electric field is a slow, devious trek of a cumbersome solvated ion through the interfering solvent molecules. This would be explained also by saying that the electric field that is conveniently applied to a solution is not an overwhelming factor in the affairs of ions. The ions are to be though of as having only a slight directional component imposed on their random motions."

What can be said is that the transfer of a charge from one electrode to another by ionic conduction does require the presence of the electromotive potential between the two electrodes during the entire interval of charge transit.

> [xxx Based on Thomson's (Lord Kelvin's) assertion that signals would pass along a submarine cable by his law of diffusion (ionic conduction) and their velocity was a function of the applied potential, the first cable failed when the operators attempted to increase the signal velocity by increasing the applied voltage (to the point the insulation used in the cable failed). See **Section 9.1.1.3.1**.

---

[57]Donders, F. (1969) On the speed of mental processes *Acta Psychologica* vol 30, pp 412-431 The Koster translation of the original German text of 1868

[58]Newman, P. (1980) Neurophysiology. NY: SP Medical & Scientific Books pp 52-53 & Chapter XIX

[59]Barrow, G. (1966) Physical Chemistry, 2nd Ed. NY: McGraw-Hill Chapters 21,22 & 23

9.1.2.3 Ionic velocity in gels

The interior of most axons and axon segments are gels. The parallel homeostatic channels supporting the axons and axon segments are also generally gel filled. As a result of the zero to very low velocity of ionic flow within gels, axons and axon segments do not employ ionic transport between junction devices (Activa within the neuron, NoR or Synapse) in signal transport. In some cases, the gels are extruded near one junction device and are absorbed near a second junction device. As a result, any ionic elements within the gel may be transported along the axon at velocities measured in millimeters per hour or millimeters per day. Such ionic transport is not related to signaling.

9.1.2.4 Energy propagation along a coaxial cable EMPTY

9.1.2.4.1 The capacitance of the axon segment

The biology community has long calculated the capacitance of a section of BLM in an overly simplistic manner. They have assumed the capacitance can be calculated using the area of a flat plat having the "nominally" equivalent area as the conduit. The best available data is actually from bilayers formed on the surface of a liquid. These bilayers generally exhibit a capacitance of nominally 6 nanofarads/mm^2 (6 x 10^{-9} farads/mm^2) based on Alexander & Fuchs[60]. However, the purpose of these experiments is to determine the precise permittivity of the dielectric, not the capacitance of a specific flat plate capacitor.

This procedure has obscured a feature of a conduit that will become critically important later in this chapter. The cylindrical form of the conduit results in a capacitance that is not given correctly by the above approximation.

The correct formula for the capacitance of a cylindrical dielectric is given by (Kraus, page 75):

Capacitance(in farads/unit length) = $2\pi\varepsilon / \ln(R_o/R_i) = 2\pi\varepsilon / \ln(1 + (R_o - R_i)/R_i)$

If ε is in farads/meter, the capacitance is also in farads/meter.

The basic form of the equation is shown as (**A**) in the following set of equations. For convenience, the above equation can be written as $24.2\ \varepsilon_r / \log(R_o/R_i)$ in $\mu\mu$f/meter

where ε_r is the relative permittivity of the medium (lemma and myelin combined) and logarithms to the base 10 are used.

While the thickness of the dielectric ($R_0 - R_i$ in the second expression) is intrinsic to the equation so is the interior diameter (R_i) of the dielectric. The latter relationship is lost when using the flat plate approximation. This later relationship is critically important when dealing with "giant axons" as will be seen later.

The calculation of the capacitance associated with the spherical endcaps of the sausage shaped axon segment in the above figure is usually ignored because of the small area involved compared to the area of the cylindrical portion.

The intrinsic collector capacitances of an Activa depends on the size of the Activa. They are very small and difficult to measure. The collector to base and collector to INM capacitances are most important. The bulk of the capacitance associated with the collector is due to the extended area of the unmyelinated portion of the axolemma.

It appears the collector-to-base capacitance has played an important role in the parametric stimulation of the neuron employed by Hodgkin & Huxley. Under some circumstances, it

---

[60]Anderson, O. & Fuchs, M. (1975) Potential energy barriers to ion transport within lipid bilayers. *Biophysic J* vol. 15, pp 795-829

appears the collector-to-emitter capacitance played a significant role in the Hodgkin & Huxley experiments.

It is generally necessary to make a distinction between the capacitances associated with the collector alone and with the overall axon.

9.1.2.4.2 The inductance of the axon segment

While little known and poorly understood within biophysics, the cylindrical form of the typical axon conduit always exhibits an inductance. The purpose and/or importance of this element has been bewildering to electrophysiologists since at least the 1930's. They were able to measure the inductance of a portion of a conduit but were not able to determine its origin. The origin appears clearly in electromagnetic theory. As noted above, any cylindrical structure consisting of an insulator between two conductors, will exhibit an inductance per unit length–just as it does a capacitance per unit length.

The inductance of a neural conduit is given by the similar equation (Kraus, pg 167):

Inductance(in Henries/unit length) = $(\mu/2\pi)\bullet \ln(R_0/R_i) = (\mu/2\pi)\bullet \ln(1 + (R_0-R_i)/R_i)$

If μ is in Henries/meter, the inductance is also in Henries/meter. The permeability of a vacuum is $4\pi\bullet 10^{-7}$ Henry/meter. The permeability of water and other biological materials is nominally equal to the permeability of vacuum and the relative permeability of biological materials, μ_r is equal to 1.0.

As in the capacitance of a coaxial line, the thickness of the lemma plus the myelination is given by R_0-R_i and the inner radius, R_i, of the axoplasm) is significant.

This inductance plays a critical role in the propagation of signals over what will be defined as stage 3 neurons, those transmitting action potentials over distances greater than two millimeters.

The role of the inductance and capacitance in the typical axon segment of stage 3 is so important, the segment even exhibits secondary features to optimize the inductance per unit length in accordance with good electrical filter design.

- - - -

The axon, like the real submarine cable is not represented by only resistive and capacitive elements. Any coaxial transmission line exhibits an inductance under transient conditions. The value of this inductance per unit length is a function of the geometry of the cable and the permeability of the dielectric medium. The equation for this inductance is (**B**) in the following set where r_o is the outside radius and r_i is the inside radius of the dielectric.

The equation in (**B**) is also known as the external inductance of a coaxial cable to differentiate it from the internal inductance that is related to the inductance of a straight solid conductor. The total inductance of a cable is the sum of the external (or mutual) inductance and the internal (or self inductance) of the cable. The internal inductance of an axon could be very large because of its small diameter if the axoplasm was a good conductor like copper. However, the resistivity of the axoplasm is many orders of magnitude higher than that of copper. It may be several orders higher than that of sea water due to its liquid crystalline (gel-like) character. The total inductance of the axon appears to be dominated by the external inductance.

The presence of an inductance associated with the giant axon of *Loligo* was extensively documented by Cole. However, he did not associate that inductance with a cable. Instead, he associated two inductances with the *h* and *n* parameters and an additional capacitance with the *m* parameter of the equations and equivalent circuit of Hodgkin & Huxley. He diagramed them as parallel circuits in their shunt circuit diagram (pg 299). Cole notes that: “Every element of the circuit, except the membrane capacity C, changes with the potential difference across the membrane.” As a result, the symbols used should not be interpreted as

associated with fixed circuit elements.

Any coaxial transmission line also exhibits a capacitance under transient conditions. The value of this capacitance per unit length is a function of the geometry of the cable and the permeability of the dielectric medium. It is **not** found by using the flat plat equivalent area of the dielectric. The equation for the capacitance per unit length of an axon is (**A**) in the following set of equations where ε is the permittivity of the dielectric.

$$C = \frac{2\pi\varepsilon}{\ln\left(\frac{r_o}{r_i}\right)} \qquad (A)$$

$$L = \frac{\mu}{2\pi}\ln\left(\frac{r_o}{r_i}\right) \qquad (B)$$

$$v_p = \frac{1}{\pm\sqrt{L \cdot C}} = \pm\frac{1}{\sqrt{\mu \cdot \varepsilon}} = \pm\frac{c}{\sqrt{\varepsilon_r}} \qquad (C)$$

$$Z_o = \pm\sqrt{\frac{L}{C}} = \pm\ln\frac{r_o}{r_i} \cdot \sqrt{\frac{\mu}{4 \cdot \pi^2 \cdot \varepsilon}} \qquad (D)$$

(3) Impedances of an ideal axon based on its outer and inner radii.

Figure 9.1.2-1 presents the calculated value for these impedances for various size axons. The values are for both unmyelinated and myelinated neurons based on the membrane dimensions and for a permittivity assumed to be equal to 3.0 for discussion. As calculated, 100 layers of membrane causes a change in capacitance of about 12:1. Note the significant change in these values as a function of axon radius. The unmyelinated values shown intersecting the gray bar are typical of the values to be expected in the experiments of Hodgkin & Huxley. These values are clearly not typical of the 1-5 micron radius applicable to stage 3 projection neurons in *Chordata*.

Chiu & Ritchie measured the capacitance of normal and unmyelinated axonal segments in mammals (rabbits)[61]. Although they did not provide the radius or length of their segments, they described an increase of 20 +/– 2.6 times in the capacitance after demyelination from an initial total value of 3 +/– 1.2 pF. The capacitance ratio of 20:1 would suggest a myelination consisting of about 150–200 BLM layers in their specimen.

[61]Chie, S. & Ritchie, J. (1980) Potassium channels in nodal and internodal axonal membrane of mammalian myelinated fibers *Nature* vol. 284, pp 170-171

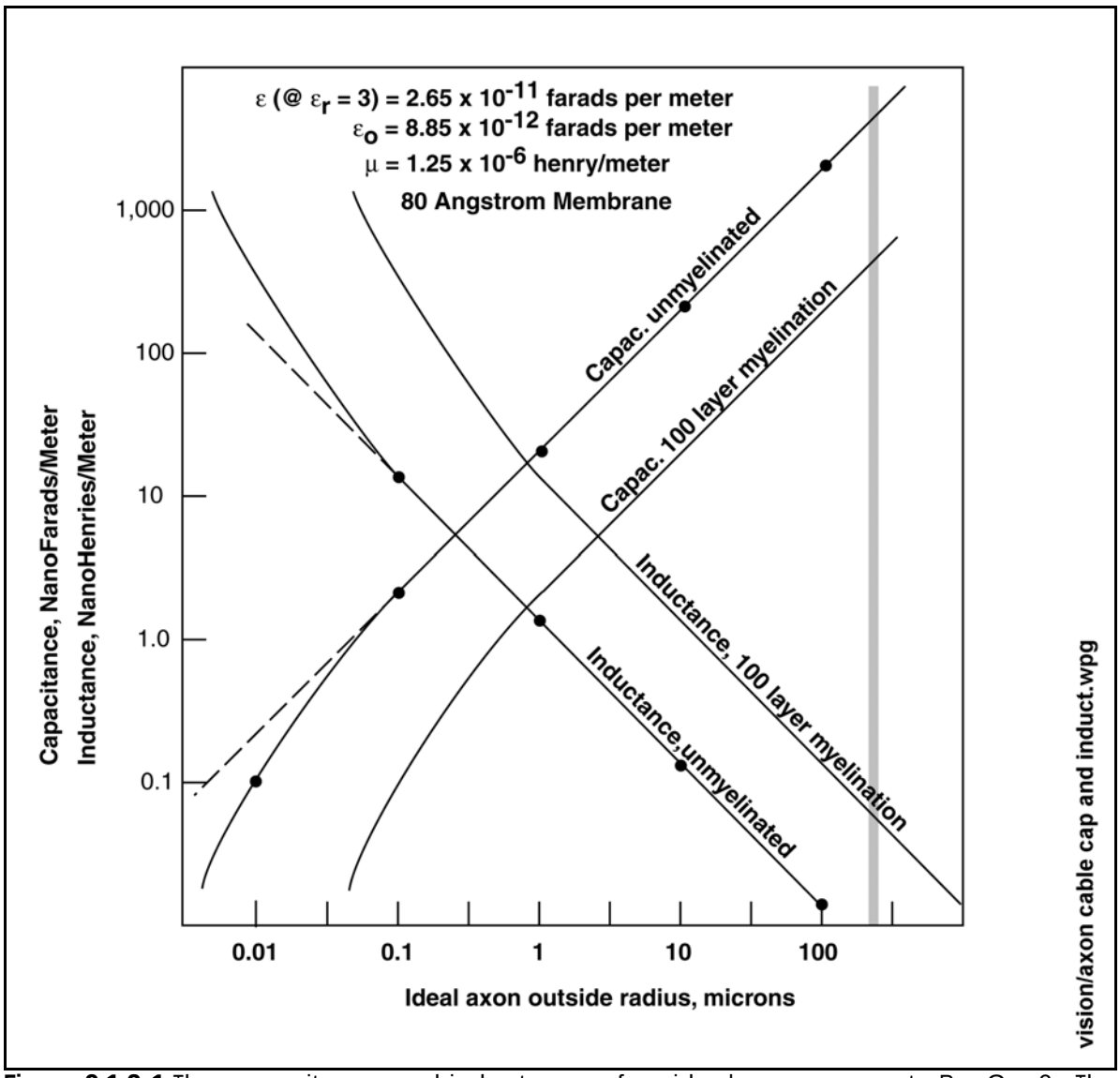

Figure 9.1.2-1 The capacitance and inductance of an ideal axon segment. R = G = 0. The vertical gray bar represents the radius of the typical *Loligo* axon without surrounding tissue.

9.1.2.5 The impedance & phase velocity of the ideal coaxial cable EDIT

Figure 9.1.2-2 shows the characteristic impedance, Z_0, of an ideal axon segment based on equation (D). A major problem with using the giant axon of *Loligo* is seen immediately. The characteristic impedance of that size axon is very low. As a result, it is extremely difficult for the conexus of the neuron to excite it. While it can support the transmission of a signal by diffusion, it may not be able to support it by propagation. While the giant neuron of Loligo makes a good signal processing (stage 2) neuron, it makes a very poor stage 3 signal propagation neuron. **The giant axon of *Loligo* is not analogous to the stage 3 propagation neurons found in *Chordata*.** The propagation velocities shown in the figure represent ideal transmission lines with various values of dielectric constant at the top and estimates associated with lossy lines such as a real axon. The latter will be discussed in greater detail below.

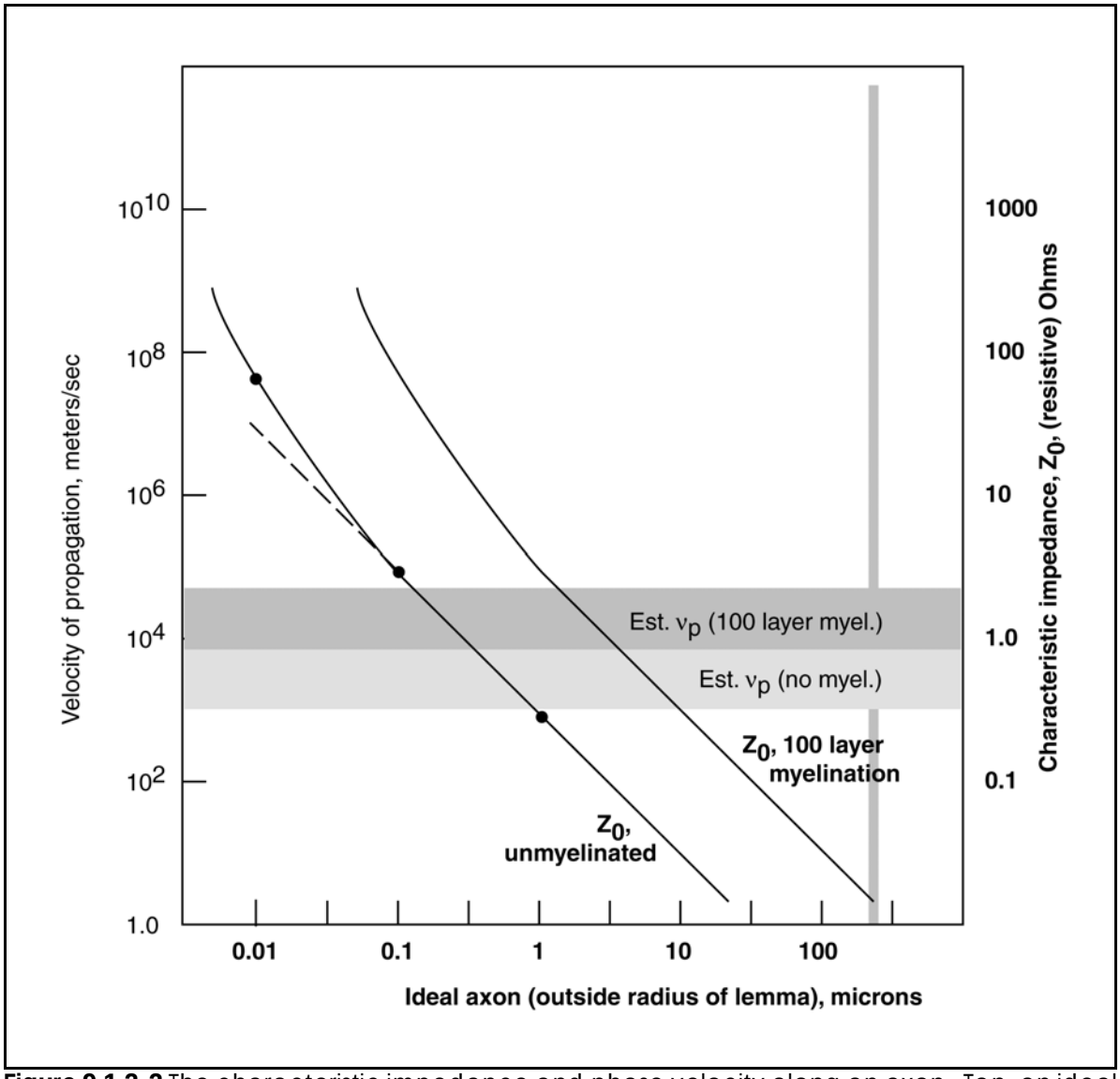

Figure 9.1.2-2 The characteristic impedance and phase velocity along an axon. Top, an ideal axon segment. R = G = 0. The phase velocity does not vary significantly for typical biological dielectrics. The estimated values are for a real axon where R is finite but G = 0. The vertical gray bar represents the radius of the typical axon of *Loligo*.

Equation 2(C) shows that an ideal axon with a dielectric constant of 3.00 has a transmission velocity of $(1/3)^{0.5}$ that of the speed of light or about 17×10^8 meters/sec. This extremely high value is not compatible with the values found in the literature for signals flowing from one end of a neuron to the other, or even along a single axon segment. This fact suggests that the axon segment is not an ideal axon and that its series resistance and shunt conductance must be considered more carefully. However, the form of equation 2(C) explains why a signal impressed in the middle of an axon segment is propagated in both the positive and negative directions along the segment. There are two values for the function. One travels to the right and one travels to the left. It also shows a significant variation in the velocity of propagation as a function of frequency. Like a simple RC filter network, the ideal axon exhibits a significant variation in the velocity of a sine wave traveling along an axon as a function of frequency.

The equations for the velocity of a wave traveling through a lossy axon segment (coaxial cable) are quite complex but readily available in text books[62]. They show that the velocity is slowed considerably as a function of the frequency and of the series resistance and shunt conductance. In the case of the real axon, the specific resistance, e.g. resistivity, of both the axoplasm and the INM are reported to be on the order of 110 Ohm-cm. This compares with a value of 1.7×10^{-6} Ohm-sm for copper wire. Such a high resistivity has a significant effect on the movement of charge within the electrolyte adjacent to the dielectric. **Figure 9.1.2-3** shows the typical situation for both an ideal axon (left) and a real axon (right). The left figures are similar to those found in many biology texts, except they have been expanded. They now show the electric field lines between the charges and the magnetic field lines surrounding the fields due to the charge on the inner and outer conductors. With conductor resistivities very small relative to the inductances, all charge is located very close to the walls of the dielectric and it can move along these walls very rapidly. As a result, the propagation velocity of a wave along this cable is a fraction of the speed of light. For a real axon as shown on the right, the situation is different. The resistivity of the plasmas is now far from zero and significant when compared to the inductance of the structure. The electric field lines now enter the plasmas a significant distance and the speed of electrons along these field lines is considerably reduced. As a result, the position of the electrons at any instant is hard to define and the propagation velocity of the wave is considerably reduced. Note the electrical field lines are closed in both the ideal and real axons. There is no net current flow in the direction of propagation. As shown in **Section 9.4.2**, the nominal propagation (phase) velocity for the wave traveling along an axon segment is 4400 meters/sec (~1.5×10^{-5} times the speed of light).

---

[62]Ramo, S. & Whinnery, J. (1953) Op. Cit. pg 41

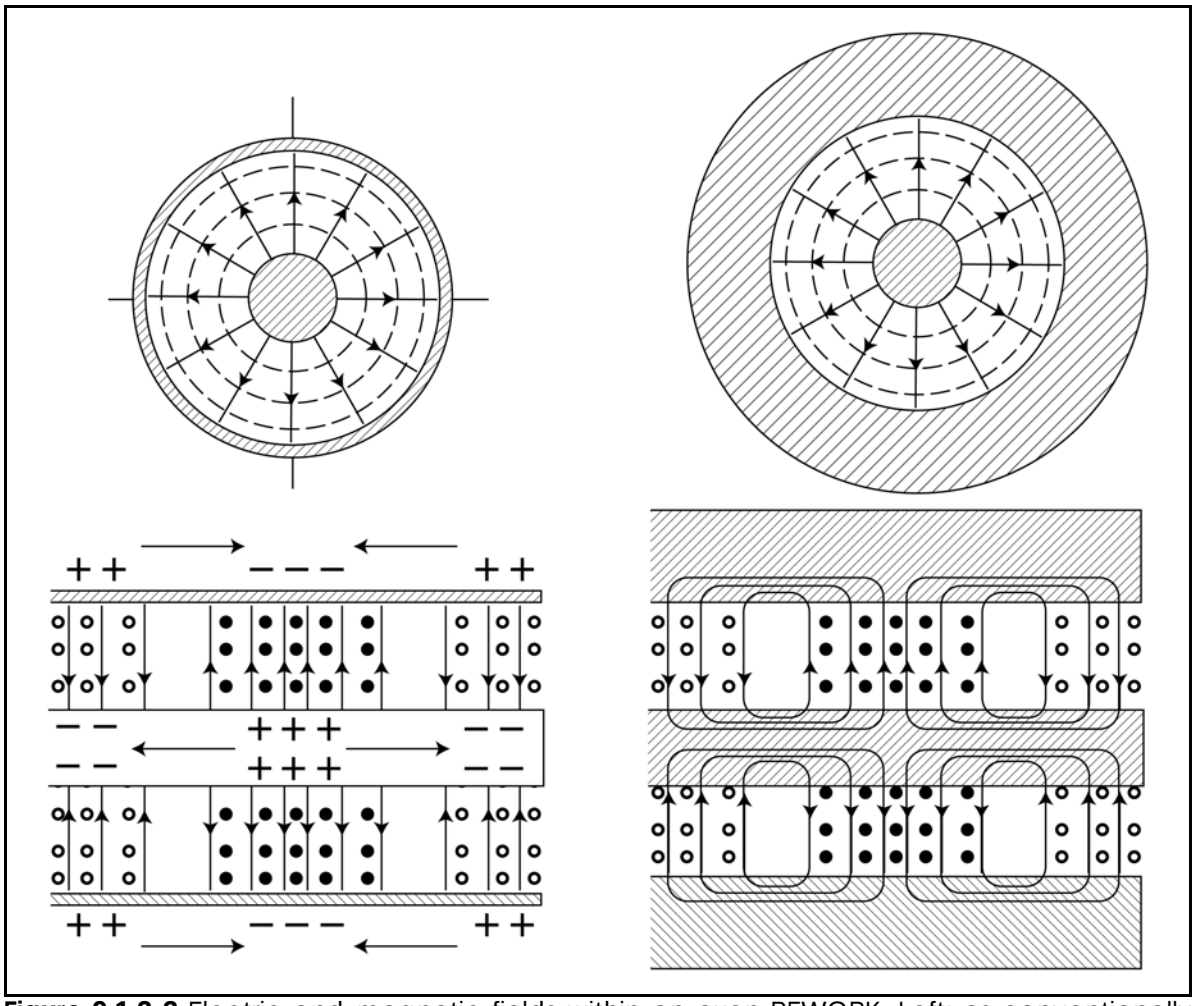

Figure 9.1.2-3 Electric and magnetic fields within an axon REWORK. Left; as conventionally described in the biological literature, the magnetic lines (solid and hollow circles) are omitted and the conductors are considered ideal. The plus and minus symbols represent charges that are only notional. Right, the real case of an axon with a nearly ideal dielectric but a lossy axoplasm and surrounding inter neural matrix. The loops describe the magnetic fields associated with the electrostatic fields that combine in Maxwellian energy propagation.

A phase velocity of 4400 meters/sec is 300 to 1000 times faster than the speeds calculated by Taylor and Hodgkin. For they were trying to make their Kelvin—>Hermann based approach agree with the average velocity of a neural signal traveling between two identical points in a Node of Ranvier and axon unit, instead of the phase velocity of an axon segment. **The modern models of Taylor and of Hodgkin do not predict the actual phase velocity of an axon segment**.

The presence of the inductance requires the adoption of a model of a coaxial cable including this inductance. Such a model is given in **Figure 9.1.2-4**. (A) is such a model in an unbalanced form, the usual form for discussing a coaxial cable. (C) is the balanced form often found in the biological literature (without the inductances). (C) shows the unbalanced form in its distributed form. To properly connect to the form in (C), a half-section matching filter is used of the type shown in (D). A uniform distributed line terminated at both ends with the appropriate matching section can achieve 98% transfer efficiency over considerable distances if the required bandwidth is not to great.

The introduction of an inductance into the model negates all of the equations found in the

biological literature for the coaxial cable representing the biological axon in a stage 3 projection neuron. The mathematical description of a real axon requires solution of the General Wave Equation of Maxwell. The solution of this equation also introduces a concept not found in the lower order Laplace and Poisson equations, the characteristic impedance of the axon (or coaxial line). The value of this impedance plays a crucial role in the efficiency of the axon as a transmission line.

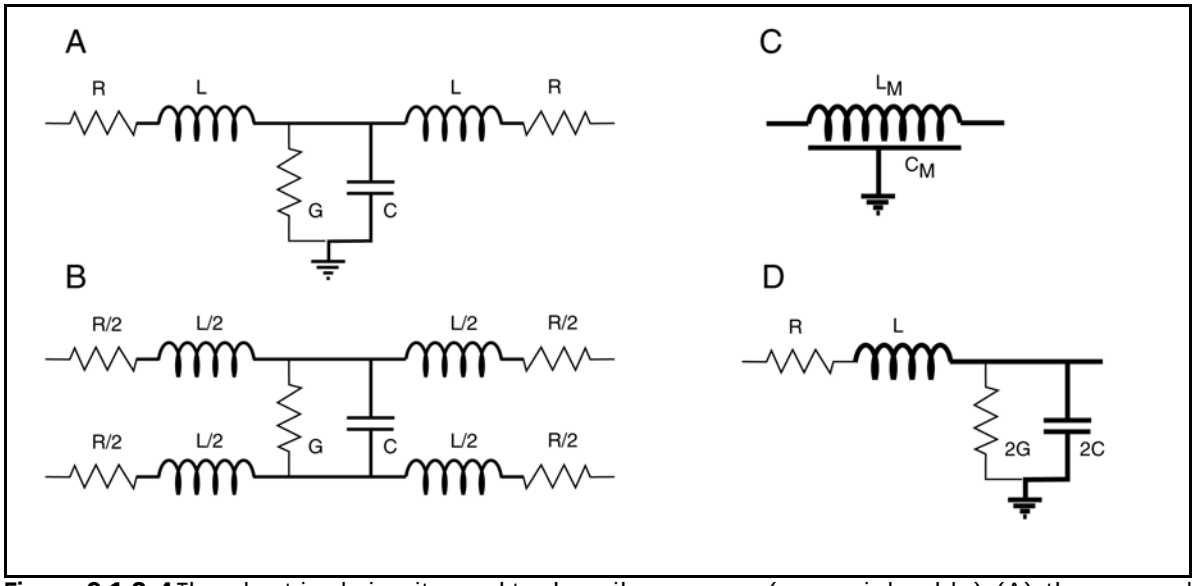

Figure 9.1.2-4 The electrical circuits used to describe an axon (a coaxial cable). (A); the general circuit in unbalanced lumped-parameter form. (B); the same circuit drawn in balanced lumped-parameter form. In efficient cables, the conductive currents passing through the resistive elements are negligible compared to the displacement currents through the inductive and capacitive elements. As a result, a simpler notation is available. (C); the simplified distributed network based on the dominant displacement currents. It forms an efficient propagation medium. (D); the half-section used to terminate either end of the line in (C) based on the component values in (A).

9.1.2.6 Propagation over a lossy coaxial cable–real axon

Cole was the first to report impedance measurements on a variety of neural and muscular tissue. **Figure 9.1.2-5** shows actual impedance measurements by Cole on the squid axon after undefined preparation procedures. Caution should be observed here. It is likely that the preparation changed the effective conductance of the fluid within the axon. The plasma was frequently replaced by sea water to simplify the instrumentation procedure. Such a change would have a significant change in the conductance of the internal fluid. He describes the empirical derivation of the expected impedance on pages 36-37 (without considering any potential inductance) and then notes the considerable consternation in the community when the axon was found to exhibit considerable net positive reactance at low frequencies. Pages 78-79 describe conceptual discussions aimed at avoiding the obvious. The coaxial axon exhibits significant inductance.

Cole presented the data in a non-standard form in his original work. By using conventional filter theory and complex plane plotting conventions (positive reactance at the top), the revised figure can be used to evaluate the nature of the impedance measured on a lossy axon based on conventional filter theory.

The following equations replace equations (C) and (D) in the previous set when the values of the resistance and conductance associated with the coaxial cable or axon are not negligible compared to the inductance and capacitance. Two new equations have been added in this set. An approximate equation for the attenuation along the line and an approximate equation for the phase constant along the line. The exact equations are much more complicated and are not needed here.

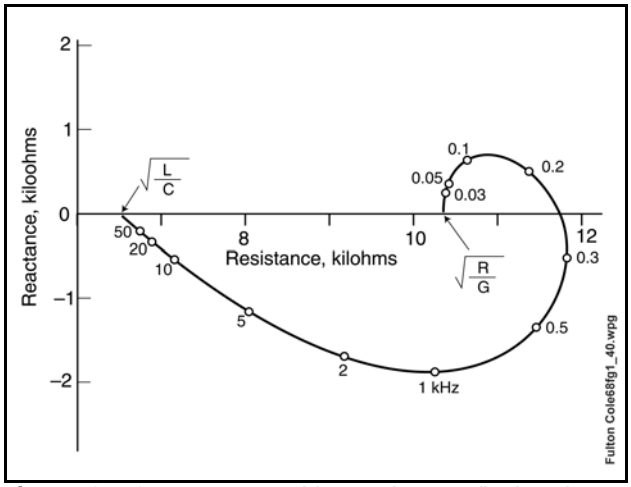

Figure 9.1.2-5 Measured impedance (inductive & capacitive) of a real axon after unspecified preparation procedures. Replotted from Cole, 1968, and annotated.

$$v_p = \frac{1}{\pm\sqrt{(R + j\omega L)\cdot(G + j\omega C)}} \qquad (A)$$

$$Z_0 = \sqrt{\frac{R + j\omega L}{G + j\omega C}} \qquad (B)$$

$$\alpha \approx \frac{R}{2Z_0} + \frac{G\cdot Z_0}{2} \qquad (C)$$

$$\beta \approx \omega\sqrt{LC}\cdot\left[1 - \frac{RG}{4\omega^2 LC} + \frac{G^2}{8\omega^2 C^2} + \frac{R^2}{8\omega^2 L^2}\right] \qquad (D)$$

(4) Equations of a lossy coaxial cable applicable to an axon

The interpretation of these equations in a specific application is aided by experience. As a general rule, equation (A) is not used. It is re-written in the form of equations (C) and (D) which are easier to interpret. (C) describes the attenuation constant applicable to the cable. (D) describes the phase shift constant applicable to the cable. A brief theoretical interpretation is provided below. The comparison of the theoretical and measured values for the axon will be presented in **Section 10.3.5.4**.

9.1.2.6.1 Theoretical <u>intrinsic/phase velocity</u> and attenuation on a lossy line

Equation (A) gives the phase velocity of the signal when the coaxial line exhibits significant Resistivity and conductivity. The propagation velocity is dependent on four parameters in a very complex manner. In cases where the resistivity and conductivity dominate, propagation is slowed considerably below the value for the ideal cable. The velocity is given by $\nu_p = (R\bullet G)^{-0.5}$ for this case (which always occurs at low frequencies). At high frequencies, the velocity is usually given by $\nu_p = (L\bullet C)^{-0.5}$. At intermediate frequencies, equation (A) is generally written in a different form that allows the separation of the attenuation constant for the cable (C) and the phase constant for the cable (D). The phase constant describes the velocity of propagation as a function of wavelength or frequency. This velocity varies with the wavelength (or frequency) of each Fourier component in the signal. The variation leads to the dispersion of the energy in the original signal with distance along the cable. Dispersion appears to be the principle cause of deterioration in the shape of the action potentials in the neural system. It generally limits the distance between Nodes of Ranvier or other regenerating features to less than two millimeters.

The intrinsic phase velocity of even a lossy axon is much higher than the average velocity of propagation. The average velocity is limited by the significant delay associated with the periodic signal regeneration process (involving Nodes of Ranvier, see **Section 9.4**).

9.1.2.6.2 The theoretical impedance of a lossy cable

Equation (B) in this set of equations describes the characteristic impedance, Z_0, of a lossy coaxial cable. This equation can be useful in interpreting the complex impedance plane measurements of Cole. However, it must be noted first that the equation only applies to a transmission line that is terminated at each of its ends using an impedance equal to this characteristic impedance. If the cable is not properly terminated, measurements such as Cole made will depend on the precise position along the axon where they are made. The measured values will reflect this inadequate termination by exhibiting a voltage standing wave ratio, VSWR, along the line. This parameter is an indicator of the error in termination.

In the case of a real axon, the adequacy of the termination is currently unknown. However, a matching filter is usually required between the myelinated portion of the axon and the conexuses at each end of each axon segment. Such a matching filter is usually formed by the unmyelinated section of the axon segment.

The above Cole figure can be annotated using equation (B). At zero angular frequency, the value of the impedance is given by the square root of the ratio of R divided by G. This impedance is purely resistive and is about 10.4 kilohms in the figure. Conversely, at very high frequencies, the value of the impedance is given by the square root of the ratio of L divided by C. This impedance is also purely resistive and is about 6.6 kilohms in the figure. The value of 11.7 kilohms at 260 Hertz is also descriptive of the cable. It is a purely resistive impedance. This resistive value will move toward the characteristic impedance as the terminations are adjusted to optimum. At frequencies below 260 Hz, the cable exhibits a positive reactance. It can be considered to be inductively loaded at this location. At frequencies above 260 Hz, the cable exhibits a negative reactance. It can be considered capacitively loaded at

this location.

9.1.2.6.3 Intrinsic pulse dispersion along a lossy line

Equations (C) and (D) of the above set are also instructive. They are approximations of the attenuation constant, α, and the phase constant, β, of a lossy cable. The describe the distortions in a pulse transmitted along a lossy cable. For the distances of interest in neuroscience, it will be shown that the attenuation constant is not significant. The amplitude of the energy in the Fourier components of the pulse does not diminish significantly over distances of a few millimeters. However, the phase constant is a direct function of the frequency of the Fourier component. This term causes each Fourier component to exhibit a different phase velocity when propagating over a lossy cable. The effect is to smear the shape of the action potential pulse, eventually to the point of unrecognizability. To effect useful signal propagation, the pulse shape must be restored before it reaches this point. This restoration through regeneration is the precise role of the Nodes of Ranvier. They must be placed at sufficiently frequent intervals along an axon to sense the signal accurately and reliably before it falls below the threshold amplitude of the conexus within the Node of Ranvier.

The phase constant, β, associated with a real axon, and represented by a lossy cable, makes one of the several assumptions of Taylor in his analysis of a cable untenable. He made the following assumption (page 226). "If the open circuit potential V_0 does not vary with position on the membrane, we may use as our variable of voltage $V_m - V_0 = V(t)$." This is clearly not the case within the individual groups of measurements by Smith, et. al. Taylor assumed that the velocity of all components of a pulse waveform traveled at the same velocity in a lossy line. This was also the failing in the original analysis of the undersea cable by Lord Kelvin.

9.1.3 Modeling stage 3 myelinated neuron branch points

Several models of branching neurons have appeared with the advent of inexpensive computational modeling via desktop computers. No realistic models have yet appeared. The past models have been indirectly based on the proposed and unsolved partial differential equations of Hodgkin & Huxley (1948-1952) for a simple giant axon (unmyelinated) of a mollusc (no known stage 3 neurons propagating action potentials). Although not stated explicitly with the set of their equations, their solution also included a set of switching points at which the various differential equations were phased into and out of their conceptual solution. Relying upon this set of unsolved partial differential equations with boundary conditions is unfortunate, since a closed form equation for the operation of the active mechanism associated with every Node of Ranvier (including the one typically embedded in the soma of a stage 3 neuron is readily available (Section 9.xxx).

Zhou et al. and Zhou & Chiu have provided the most explicit description of their model of a branching stage 3 (myelinated) neuron. They followed the interpretation of the Hodgkin & Huxley equations by Halter & Clark of 1991[63] and 1993[64]. Their figure 1 on the 2001 paper exhibits a number of serious problems with their physiological model (including its tendency to exhibit Amyotrophic Lateral Sclerosis (ALS, Lou Gehrig's Disease). Their figures 4 and 6 through 9 show an even more serious shortcoming, the failure of their model to maintain pulse train integrity (the very hallmark of, and most needed feature of a pulse encoded signaling system). They show a significant loss of pulse train integrity using their model under a variety of conditions, including very small differences in temperature that could not be avoided in cold-blooded animals and even warm-blooded animals running a significant fever.

The 1991 paper of Halter & Clark speaks of the extent of the axoplasm of an axon segment, "Sealed-end conditions are assumed." This presents no (conventional) current flow through the terminal longitudinal elements of the end segments. In fact, this work shows the semiconducting properties of the terminal zones of the axon segments allow the transfer of electrical charges but not ionic charges through these terminals. Halter & Clark illustrate and

---

[63]Halter, J. & Clark, J. (1991)

[64]Halter, J. & Clark, J. (1993) The influence of nodal constriction on conduction velocity in myelinated nerve fibers *NeuroReport* vol 4, pp 89-92

speak of the coaxial cylinders forming the axon segments (figure 2b) but fail to associated an inductance with such structures. Thus, they only calculate the distributed resistance and capacitance components of their axon segments. They fail to correctly calculate the capacitance per unit length of a cylindrical capacitor. The correct calculation involves the logarithm of the ratio of the outside radius of the insulator to the inside radius of the insulator (see any electrical engineering handbook). Their resulting RC model does not adequately describe the propagation properties of the axons. Interestingly, they note the use of double precision arithmetic in their computations to insure accuracy when the precision of their input parameters and the accuracy of their formulas do not support using double precision arithmetic.

Figure 1A of Zhou & Chiu illustrates a continuous axoplasm passing through a number of axon segments and Nodes of Ranvier before bifurcating into two branch channels. Their figure 1B shows the assumed space between the axolemma of the neuron and the myelin sheath (where the axoplasm appears closed off by the Nodes of Ranvier). The dimensions of their representation are available in the 1993 Halter & Clark paper. No electrical schematic of the combined axon segment and Node of Ranvier is provided in the Zhou & Chiu paper. The equations provided appear to be linear, and directionally symmetrical interpretations of RC networks derived using Kirchoff's Laws. No inductive terms are included as always required when transmitting alternating current signals along coaxial cables. While their model includes the geometric features of the myelin sheath and the axon segment developed by Rydmark & Berthold in the 1980's, they do not attempt to interpret these features as constituting a "matching section" of a typical electrical filter based on the filter theory of electrical engineering.

Implementation of a dynamic Node of Ranvier as developed in this work leads to a significantly different model that avoids the problems stated in the previous paragraphs.

9.1.3.1 Comparison of branching models

Figure 9.1.3-1 compares Figure 1A of Zhou & Chiu with an alternate configuration developed based on the above portions of this work. The original variant follows that of Rydmark & Berthold from the 1980's. It reflects the predominant view from before the days of the electron microscope that the axolemma and axoplasm of a single neuron extended the length of the neuron. This position is not affirmed by modern electron microscopy. The individual axon segments involve fully enclosed axolemma and thereby individual chambers of electrically isolated axoplasm. The areas of closest approach of adjacent axolemma are formed of special semiconducting lipids. They thereby support the formation of an Activa with its base terminal provided access to the surrounding matrix as indicated by the open path at the bottom of each Node of Ranvier. The top of each Node of Ranvier is shown as contiguous between axon segments (but separate from the neural signaling function) in order to support the transfer of nutrients along the length of the axon.

The diameters and lengths of the closed axolemma of each daughter axon segment of frame B need not have any relationship to the dimensions of the parent branch.

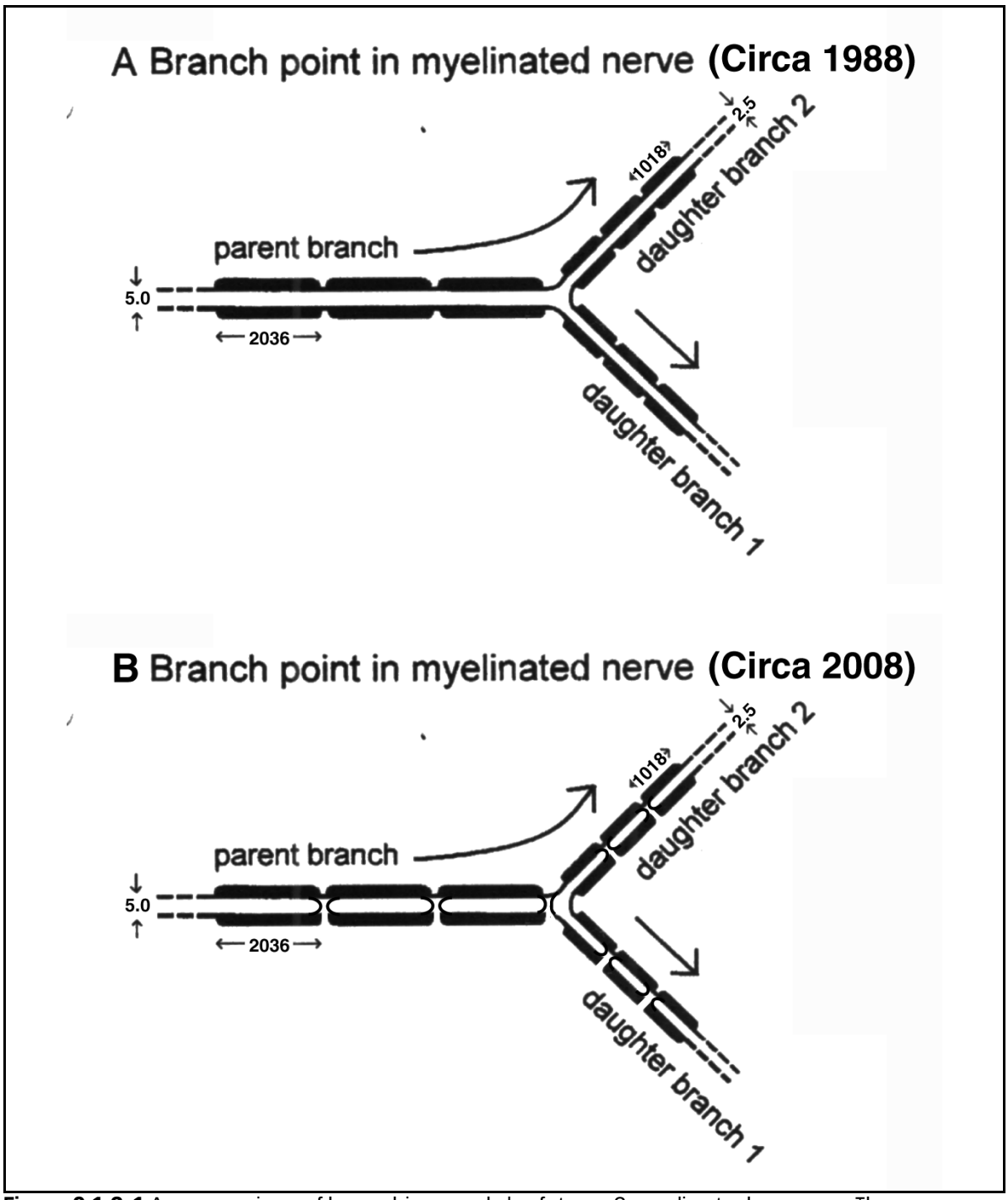

Figure 9.1.3-1 A comparison of branching models of stage 3 myelinated neurons. These neurons support the propagation, not just conduction, of neural signals over long distances. A; the model of Zhou & Chiu (2001) based on an archaic description of the physiology of a stage 3 neuron. B; an alternate model assuming an active semiconductor device (an Activa) present at each Node of Ranvier. Note closed axolemma for each axon segment separated from the adjacent axolemma by an open space with access to the surrounding matrix. Note also the closed axolemma to the right of the branch point. The dimensions of the elements to the right of the branch are inconsequential in the updated variant of frame B. See text.

Figure 9.1.3-2 expands on an earlier figure above to show the branched axon in greater detail. Zhou & Chui modeled their segments at a branch point based on Kircholff's Laws for a linear RC network where the sum of the currents at the node equals zero. The resultant model is electrically bidirectional. The current work models the branch point as occurring at a Node of Ranvier containing an Activa (an active semiconductor device that is not electrically bidirectional). The input to the Node is characterized as a voltage and the output of the Activa is also a voltage that can be used to excite any number of subsequent axon segments. The impedance of the collector terminal of the Activa is sufficiently below the impedance of the individual orthodromic axon segments that there is very little electrical cross talk between the orthodromic segments.

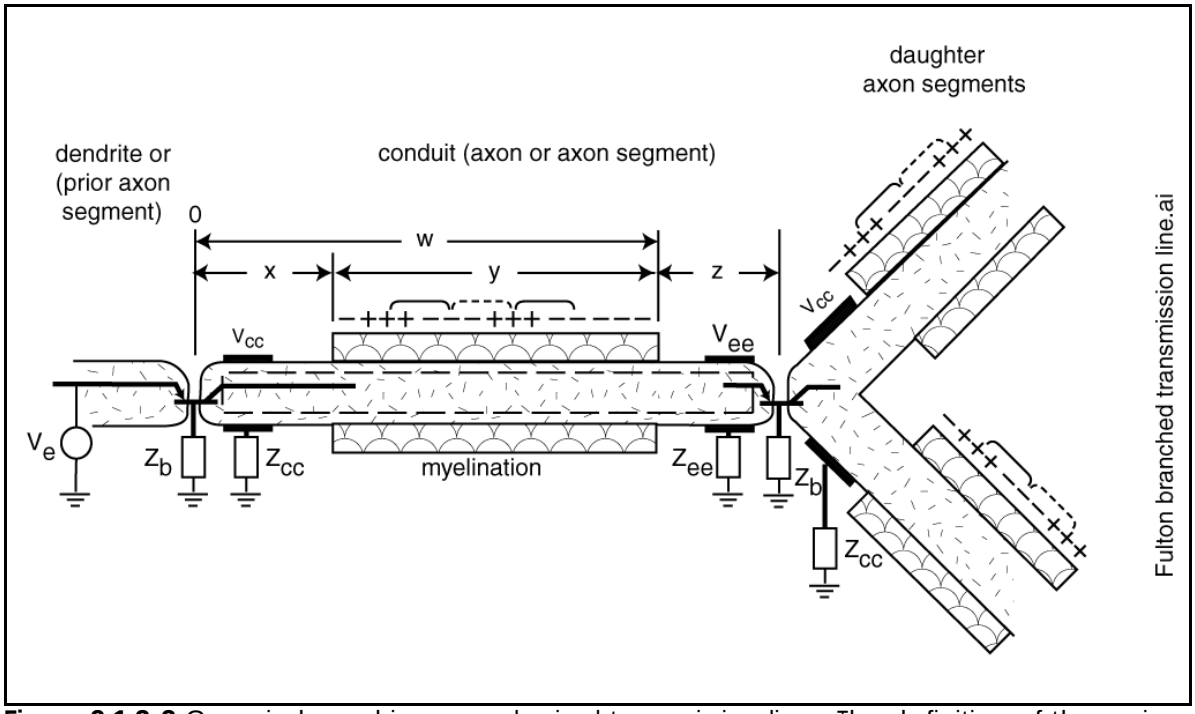

Figure 9.1.3-2 Generic branching neurological transmission line. The definition of the various signals is the same as in the earlier figure of a non-branching generic transmission line. The spreading of charge at the output of the Activa within the Node of Ranvier is also as shown in an earlier figure. See text.

> The overall circuit is very similar to an active coaxial cable signal splitter of the type frequently used in home TV antenna systems. The splitter box provides one input jack for receiving one input cable, provides a "matching section" for optimizing the voltage level delivered to the amplifier, provides a very low impedance output voltage, and then shares that voltage among multiple "matching section" feeding each of the output cable jacks.

In the immediate vicinity of the terminals of the Node of Ranvier, the circuit operates in the analog mode. The areas marked Z and X (not shown but repeated on each of the daughter axon segments) constitute the matching sections corresponding to the regions labeled MYSA by Rydmark & Berthold (See also **Section 9.4**). These sections mediate the conversion of the signal to a propagating electro-magnetic wave in the regions labeled Y. It is in these regions that the propagation velocity is on the order of 4400 meters/sec depending on the specific level of myelination described in earlier figures. The propagating signals are shown by the alternating groups of plus and minus signs along the outside of the upper axon segments as discussed earlier. The same patterns have been omitted for convenience on the lower surfaces of the myelinations.

As long as the voltage of a pulse delivered to the input of the Activa exceeds the threshold level for the Node of Ranvier to act as a pulse signal regenerator, a new pulse will be generated (following a finite delay) that will be shared by the daughter axon segments. There is no chance for the introduction of spurious pulses or the absence of pulses (for pulse rates below a nominal 1000 pps as encountered in the computed results for the computational models of Zhou & Chiu.

As noted earlier, the role of the myelination is to decrease the capacitance per unit length and increase the inductance per unit length of each axon segment in order to achieve a unique electrical condition. If the myelination is not wrapped tightly around the axolemma to prevent any fluid from the external matrix enterring the space between these two elements, the impedances seen by the axoplasm will not be modified, an electro-magnetic wave will not be propagated along the myelination and the neuron will fail to operate properly. When observed in the clinic, such a nerve will be described as exhibiting ALS (Lou Gehrig's disease).

The above network can be shown in a more condensed form using **Figure 9.1.1-2** as a template. The distributed character of the parameters associated with the myelination is stressed in this notation.

9.2 The fundamental encoding neuron, the pyramid or ganglion neuron

Figure 9.2.1-1 shows the morphology of a nominal stage 3 encoding neuron as found in mammals; in the cortex incorporated into either an association neuron or a commissure, or in the PNS as a projection neuron. The stage 3 portion of the neuron extends from the Activa within the hillock of the soma to the extreme of the axon segments and the last Node of Ranvier. It operates in the phasic mode. The analog portion of the neuron (technically part of either stage 2, 4, 5 or 6) includes the extensively arborized dendritic structure and potentially the similarly arborized podite structure. If both neurites are arborized, the neuron is labeled bi-stratified.

Morphologically, the stage 3 ganglion neuron is frequently labeled a pyramid cell, particularly when it is found in the receptive layers (laminae 5 & 6) of the CNS tissue. In the retina, the encoding neuron has traditionally been described as a ganglion neuron. Occasinally, the literature has used the label, hemi-node.

The figure is not to scale, the total length of the axon can vary from about 2 mm to a maximum approaching the longest dimension of the limbs or spinal chord of the host animal.. Lengths of two meters are not uncommon in the larger animals. These figures are typically prepared using a camera lucida and the details recorded depend on the artist, or their instructions. In this figure, the spines covering the dendrites are clearly shown, those of the podite arborization less clearly. No effort has been made to document the location and/or size of the soma containing the active Activa. Similarly, the artists has stressed the axolets at the end of the axon but has omitted showing the Nodes of Ranvier located periodically along the length of the axon, alternating with myelinated axon segments. The axolets are typically found beyond the last Node of Ranvier and the associated impedance converting the axon current to a pedicle voltage. The axolets all exhibit a similar, if not identical, voltages that are applied to the various synapses with other neurons.

The journal literature and the internet contain an endless range of discussions concerning the decoding of the neural code. Many of these are based more on philosophy than neuroscience. They are seldom accompanied by a definition of the term code. It is frequently used by psychologists in a totally abstract sense. Many of these papers are introductory presentations by lower level academicians to naive students. Assertions are frequently made that the neural code is probabilistic, is Bayesian, or involves a "rate" code. None of these assertions is factual.

It is important to recognize neural signaling occurs in both the analog and pulse domains. Both the analog and pulse neural codes are totally deterministic. The neural code used in pulse domain signaling has already been decoded and described in significant detail (**Section 9.3**).

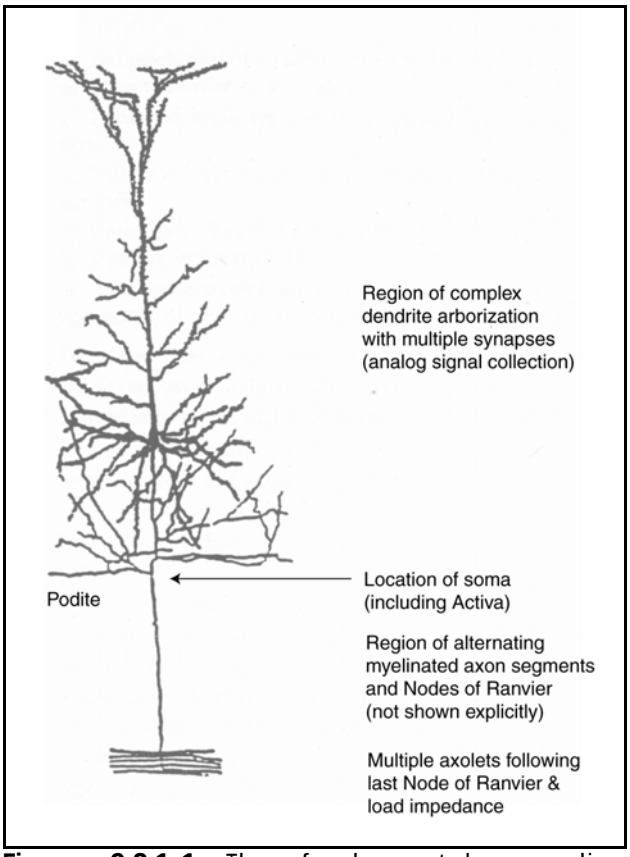

Figure 9.2.1-1 The fundamental encoding (pyramid or ganglion) neuron NOT A GOOD EXAMPLE. SOMA IS HIGHER IN PIX. Not to scale, see text. Modified from Taylor, 1999.

The pulse neural code is more sophisticated than a simple rate code. A rate code requires multiple pulses to establish a rate (a frequency in pulses per second). The pulse neural code is a place code. The first pulse (action potential) carries information on the time of initial stimulation in the place code used in the neural system. In electrical engineering terminology, the place code is a phase code and not a frequency or rate code). The phase code used in the neural system is well known and has been used in telemetry systems for many decades (beginning in the late 1940's (See IRIG code in **Section 9.3.1**). It is also described as a time-delay type of pulse position code. This time-delay code is particularly easy to generate and decode by simple neural circuits.

As will be introduced in **Section 9.3.1** and discussed in **Section 15.6.8.3**, the "neural code" of biology is actually used in two distinct formats, a word serial/bit serial format primarily in the PNS and a word serial/bit parallel format primarily among the cognitive engines of the CNS. The physiological circuits employed are the same in each but the architecture of those circuits is different.

The literal neural code used in the PNS is directly relatable to the physical parameters of the stimulus. In the case of the visual modality, the code is primarily associated with the intensity of a specific sensory neuron, or the difference between two types of sensory neurons at a similar location in the field of view.

The operation of the literal neural code of the PNS is well understood and will be discussed in this chapter. The operation of the symbolic neural code of the CNS is currently a total mystery and will only be discussed in **Section 15.6.8.3** at this time.

The following material related to the literal neural code is broken into five sections:

Background required to understand the origin of the place code

The Operation of the coding ganglion neurons
The neural place code used in monopolar amplitude encoding pathways
The neural code used in bipolar amplitude encoding pathways
The Transfer function of ganglion neurons used in these pathways

9.2.1 Background

Discovering and elucidating the literal neural code of biology requires;

- a clear understanding of the physiology of the nervous system
- attention to the definition of the terms involved
- familiarity with the encoding approaches used in man-made telemetry and communications systems.

Based on these requirements, it can be shown that;

- the desire for linear encoding within the neural system is operationally unjustified
- both analog and phasic signal coding are used within the neural system
- the neural code of the literature usually refers to the phasic coding (action potentials)
- the analog coding prior to encoding of the analog information is critically important and usually ignored
- failure to recognize the analog coding prevents precise interpretation of the phasic coding
- the phasic neural code occurs in two distinct forms.
    - that associated with unidirectional analog signals
    - that associated with bidirectional analog signals

9.2.1.1 The Visual Modality as an exemplar of the neural system

The visual modality provides a comprehensive, and well understood, exemplar of the neural system. The modality makes effective use of analog signal processing between the stimulus and the phasic encoding circuits and additional signal manipulation following phasic signal decoding. **Figure 9.2.1-2** shows a generic neural system in the PNS labeled to represent the visual modality. The operation of this portion of the visual modality is well described in the author's work, "Processes in Biological Vision" and will not be repeated here except in overview.

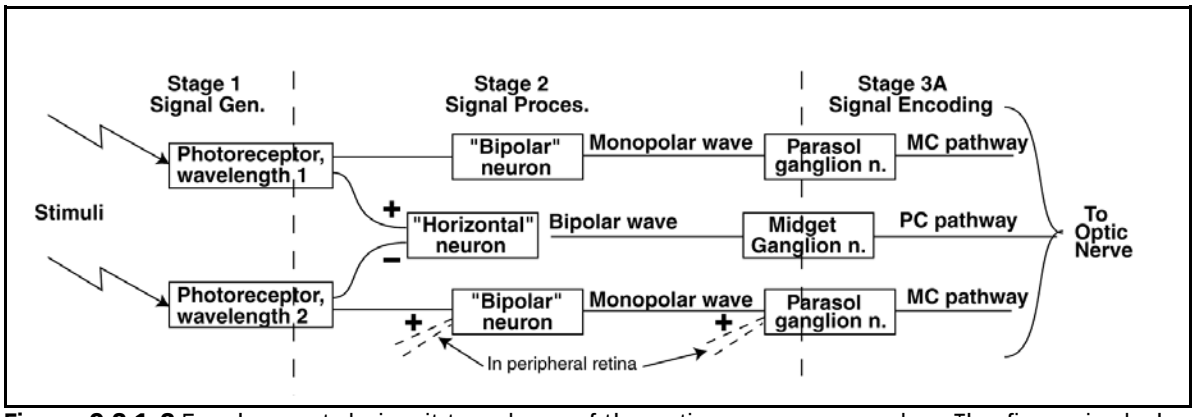

Figure 9.2.1-2 Fundamental circuit topology of the retina as an exemplar. The figure includes the stage 1 sensory receptors (accessing information at different wavelengths), multiple stage 2 signal processing paths (including the convergence of many stage 1 paths on stage 2 circuits associated with the peripheral retina, and similar stage 2 signal convergence at the ganglion neurons. In both converging situations, bandwidth shaping of the analog communications channel may also occur prior to encoding of the signals by the stage 3A encoding neurons..

The figure shows the unique elements in the two types of fundamental paths through the

foveola of the retina. The path through the morphologically labeled bipolar neuron is a non inverting signal path leading directly to the optic nerve. The signal is monopolar in the sense it never reverses polarity relative to the quiescent potential of the axon. The path through the morphologically labeled horizontal neuron is a differencing signal path wherein one of the signals is inverted while the other is not. The resulting signal at the axon is bipolar with respect to the quiescent value of the axon potential.

The paths through the peripheral retina generally involve additional summations as shown by the dashed lines in the figure. Such signals frequently lead to a discussion of converging signal paths within the neural system. While important, this additional processing tends to complicate the operation of the system and reduce the spatial resolution of the retina (essentially tracking the reduced spatial resolution of the optical system.

9.2.2 Historical nomenclature problems

The historical nomenclature based on morphology is awkward. The morphological bipolar neuron has an output (and input) that are electrolytically monopolar. Conversely, the morphological horizontal neurons have multiple inputs that are individually monopolar but an output that is electrolytically bipolar. In both cases, the neurons are in fact three-terminal circuits incorporating a three-terminal Activa.

The historically labeled parasol neurons (frequently labeled pc for parasol cell) connect to the magnacellular pathway (frequently labeled mc), while the midget neurons (frequently labeled mc for midget cells) connect to the parvocellular pathway (frequently labeled pc). The terms magnocellular and parvocellular are morphological labels associated with the size of the neurons targeted within the lateral geniculate nucleus (LGN). The abbreviation PC is also used for the Pacinian corpuscle of the somatosensory modality.

It has also been found that some stage 3 auditory neurons have their soma displaced to a less crowded area of the cochlea than their analog to pulse encoding mechanism. The result is a stage 3A encoding mechanism separating an unmyelinated neurite feature from the myelinated ason feature. This configuration has been labeled a hemi-node in the morphology of the somatosensory neurons where the configuration is also found (**Sections 8.8.4** & **8.8.5**). Thus, the stage 3A encoding function typically found within the soma of a ganglion neuron or *some* pyramid neurons may be found as a stand alone feature in other applications.

9.2.3 The neural coding ganglion neurons

The encoding neurons of biology are described here functionally (and electrolytically) as ganglion neurons. These neurons all exhibit a common internal electrolytic circuit that can be biased into either of two conditions. Those ganglion neurons processing monopolar signals are biased to operate as driven monopulse oscillators. Those ganglion neurons processing bipolar signals are biased to operate as free-running monopulse oscillators. Both types of oscillators generate a phasic pulse exhibiting only one stable (rest state). They do not exhibit two stable states as in binary encoding circuits. As a result, their output is optimized for signal propagation. Their output is not suitable for shift register operations or other binary pulse signal processing. **Figure 9.2.3-1** shows the operation of the generic stage 3A encoding neuron as it generates a single action potential.

Frame (a) of the following figure illustrates the electrolytic circuitry of the ganglion neuron using standard electronic symbology. It is an expansion of the circuitry shown in the previous page of this subject set. Every ganglion neuron contains an active electrolytic device (within the circle) known as an Activa.

As indicated, the ganglion neuron operates with a negative voltage (V_{cc}, nominally –154 mV) applied to the axon terminal of the Activa. The Activa is a three terminal PNP type junction device in electrical engineering terminology. The dendritic terminal of the Activa is known as the emitter (***E***), the poditic terminal is known as the base (***B***), and the axon terminal is known as the collector (***C***). In electrical terminology, a conventional signal current flows from the emitter (more positive relative to the base) terminal to the collector (more negative relative to the base) terminal of the Activa when the device is in its active mode.

Notice the serial combination of the two parallel circuits, Z & C_z of the preceding synapse and R_s & C of the dendritic circuit. These elements form a lead-lag network in electrical engineering terminology. Their precise values can significantly affect the shape of the leading edge of the voltage pulse supplied to the emitter terminal of the Activa.

The operation of the ganglion neuron is critically dependent on the feedback impedance (R_b) connected between the base terminal of the Activa and the external poditic terminal of the neuron. This impedance provides internal positive feedback between the axon circuit and the dendritic circuit. This feedback causes the emitter circuit to exhibit a negative impedance characteristic (a region of the curve slopes downward to the right) as shown in frame (b). As a result, the overall circuit can be made to oscillate in a variety of ways.

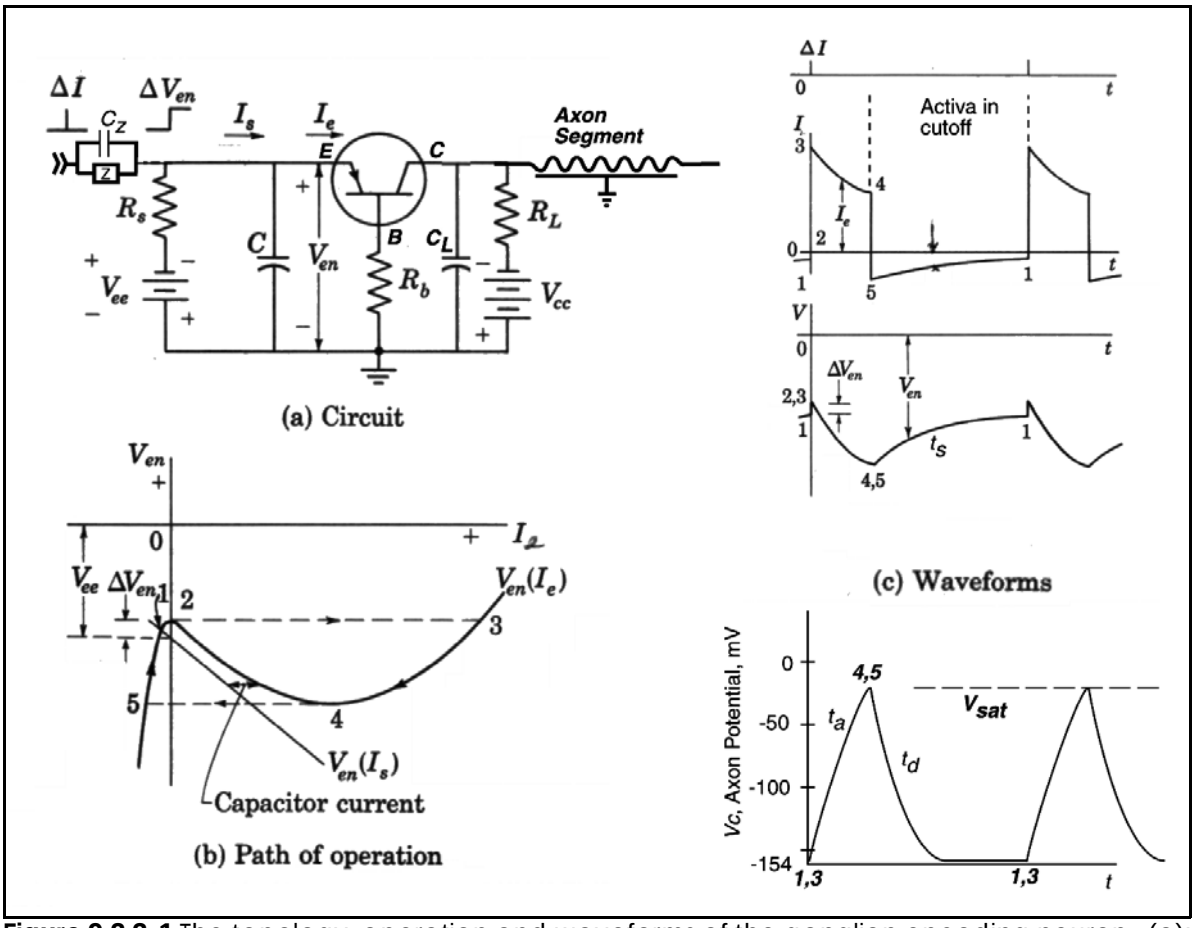

Figure 9.2.3-1 The topology, operation and waveforms of the ganglion encoding neuron. (a); the nominal stage 3A encoding circuit with the first myelinated axon segment shown. (b); the operating characteristic of the input circuit (V_{en} vs I_e). (c); the middle waveform shows the input circuit potential waveform (V vs t). The upper waveform shows the resulting current through the Activa as a function of time (I_e vs t). The lower waveform shows the resulting voltage on the collector of the Activa (the action potential associated with the axoplasm). Segment 3-4 represents the depolarization of the axoplasm via the Activa. Segment 5-1 represents the repolarization of the axoplasm via the power supply, V_{cc}, and the load impedance, R_L. t_a represents the attack time for the action potential. t_d represents the decay time of the action potential.

In the case of the monostable parasol ganglion neuron, the method of choice is for the oscillation to be controlled by the dendrite capacitance, C and for the dendrite bias voltage

(V_{ee}) to be only slightly more negative than the voltage across the feedback resistance, R_b. In the absence of any stimulus via the synapse, the circuit is quiescent at point 5. Making the emitter more positive by ΔV_{en} causes the circuit to be unstable and the current, I_e, to immediately increase to its saturation value as shown in both frames (b) and (c). I_e decreases along the transfer function to point 4 where it immediately jumps to point 5. It then proceeds slowly back to the quiescent level at point 1 (or point 2 if the stimulus from the synapse is still present).

The upper graph of frame (c) shows the current flow into (I_s) and out (I_e) of capacitor C. The middle graph of frame (c) shows complete waveform of Ven The lower graph shows the voltage (V_c) at the collector, or axon terminal. The rising portion of the collector voltage is due to the current through the Activa ($I_c = I_e$) charging the capacitor, C_L. The precise shape of this current is controlled by the lead-lag network described above. To the extent the collector current, I_c is of constant amplitude, the slope of the collector voltage waveform is a straight line between points 3 and 4. In general, it is not an exponential waveform and the time constant, t_a, is only an approximation. However, the time constant, t_d is a proper parameter of the collector voltage decay characteristic.

During the interval from point 5 to point 1, the neuron is in the refractory state. It takes a larger stimulus to raise the voltage V_{en} to the threshold voltage value of point 2.

The action potentials generated by the ganglion neuron are highly asymmetrical and their time constants are very temperature sensitive. **Section 7.3.2** of "Processes in Biological Hearing" illustrate these sensitivities using excellent data from Schwarz & Eikhof[65]. It is important to note that Schwarz & Eikhof did not model the entire signal at the output of the stage 3 neurons (see caption to their figure 2). They only modeled the portion in the "phasic range," the range from 2 to 5, in the previous and following figure, based on the chemical neuron hypothesis. The complete range from 1 to 5 and back to 1 has never been modeled in its entirety using the chemical neuron hypothesis. Their figure 3 is almost identical to frame (b) of the above figure, except for their extrapolated "leakage current" that does not exist under the electrolytic hypothesis. Their sodium current is the conventional euphemism for the discharge (electron) current through the Activa during the attack portion of the action potential waveform. Note their equation used to fit their measured data did not include temperature as a parameter. Thus, they had to develop different values for each parameter to satisfy the data sets at different temperatures. Calculating and compensating for these variations in parameters occupied a majority of their paper. Such calculations are not required using the more complete equations of the electrolytic theory that include temperature as a extrinsic variable. Those equations show the temperature effect is different for the attack and recovery portions of the action potential waveform (**Sections 2.8.4** & **2.9.2**).

The ganglion neuron is a switching-type oscillator. The currents and equations leading to the attack portion of the output circuit waveform are different from those leading to the decay portion of the circuit. The basic assumption by Hodgkin & Huxley that the waveform is based on a single set of equations between point 3 and point 1 is in error.

An increasing positive potential to the dendritic terminal relative to the poditic terminal, or to the external neural environment (or matrix), constitutes a larger stimulus to such a device. **Figure 9.2.3-2** from Berry & Pentreath shows the result of stimulating the dendroplasm with a large step function. The numbers correlate with those in the figure above.

---

[65]Schwarz, J. & Eikhof, G. (1987) Na currents and action potentials in rat myelinated nerve fibres at 20 and 37 Celsius. Pflugers Arch. vol. 409, pp. 569-577

The excitation was a square wave beginning at a very negative artificial bias level. The voltage of the dendroplasm rises vertically in the high impedance region below cutoff. Upon reaching cutoff, the dendroplasm potential rises rapidly, due to the lower impedance of the Activa in the active regime, until it reaches the phasic threshold. Above the threshold, the circuit enters the phasic or oscillatory regime. An action potential is immediately generated, and the dendroplasm is discharged back to the cutoff potential. If the stimulus remains above cutoff, the cycle repeats itself and another action potential is generated. The time between the stimulus driving the dendroplasm potential above cutoff and the time threshold is reached is indicative of the strength of the stimulus. The closeness of the early action potentials suggests the input circuit incorporates a lead-lag network arranged as a pre-emphasis circuit.

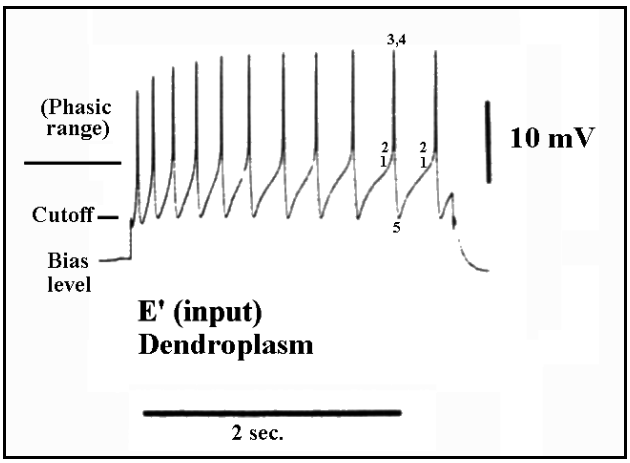

Figure 9.2.3-2 Measured dendrite waveform under parametric conditions. Stimulation of the dendritic structure at a potential below axon cutoff has no effect. Stimulation in the range between cutoff and threshold (region 5 to 1) results in analog copying of the stimulant waveform. Stimulation exceeding threshold causes monopulse oscillation followed by a refractory level relating to further stimulation. From Berry & Pentreath, 1978.

If the bias of the dendroplasm of the ganglion neuron is at the cutoff level, the circuit will be much more sensitive to small stimuli. The first action potential will be generated as soon as the dendroplasm potential (the integral of the stimulus above the cutoff level) reaches the threshold value. Subsequent pulses will be generated at time intervals determined by the integral of the stimulus following the first pulse. Thus, the pulse interval will shrink for higher stimulus levels and expand for lower stimulus levels. See the following section on the transfer function of the ganglion neuron.

The output signal of such a device, in response to a positive going stimulus, is a positive going waveform of about 100 mV amplitude, relative to the quiescent axon potential of about -154 mV.

It is clearly seen that the output of the ganglion neurons is totally deterministic. They represent a state-variable circuit, whose output is totally defined relative to their input signal. They exhibit a refractory period that is typically unimportant in their *in-vivo* application since the input signal is typically band limited by the preceding circuitry.

Crill has provided excellent waveforms, both static and dynamic, showing the generation of action potentials by the mechanism described above[66]. He employs TTX to destroy the feedback necessary to create action potentials by neural circuits. He used layer V pyramidal cells from rat. While employing the euphemism "sodium currents," his instrumentation reports voltages and currents.

9.2.4 The SERAPE representation of nonlinear circuits

It is difficult to describe the operation of a complete nonlinear circuit using a simple schematic, particularly if it is important to interpret both the normal (*in-vivo*) and frequently abnormal (*in-vitro*) operation of the circuit. The stimulation applied *in-vitro* is not only abnormal in stimulation characteristics but frequently in point of application. An alternate representation, christened

[66]Crill, W. (1996) The functional role of a noninactivating sodium current in neocortical neurons *In* Franzen, O. Johansson, R. & Terenius, L. *eds*. Somesthesis and the Neurobiology of the Somatosensory Cortex. Boston, MA: Birkhauser pp 41-47

a Serape, is often used in engineering to combine the basic schematic with a set of waveforms keyed to specific nodes within the schematic. It can be used to describe both of the above situations; the *in-vivo* and necessarily orthodromic stimulation, and the in-vitro (and frequently parametric stimulation) in detail..

While presenting considerable information in a single figure, use of the serape format as shown in **Figure 9.2.4-1**, unifies our understanding of a neuron under either orthodromic or parametric stimulation via the axoplasm.

> **The serape–** This figure introduces a graphic approach much used in describing non-linear and switching type circuits in electrical engineering, the circuit serape. The approach allows discussing features of circuit operation unexplainable using linear circuit techniques, except through division of the circuit operation into separate and distinct time intervals. It combines a circuit diagram on the left with a set of waveforms on the right as a function of time. The thin dashed lines are used to interconnect features of the two frames, nodes on the left and individual node waveforms on the right.
>
> The circuit portion of the figure is drawn with an unconventional orientation to allow a positive potential at the top in the waveform portion of the figure. The resulting action potentials appear conventional in this graphic.
>
> The serape approach is particularly appropriate for any multiple-probe patch clamp oriented electrophysiology laboratory investigations, such as those of Tolias at Baylor College of Medicine (atolias@cns.bcm.edu). Each of the waveforms can be associated with a specific probe.

If needed, a second orthodromic stimulation could be introduced into the podite circuit without difficulty. A key feature of this circuit diagram is the axoplasm-to-dendroplasm capacitance, C_{AD}, shown to the immediate right of the neuron for clarity but actually an integral portion of the neuron. The operation of the circuit is *critically* dependent on the values of the podoplasm and dendroplasm impedances, the quiescent dendrite to podite potential, and the load line of the overall circuit (See **Section 2.2.4**).

As shown on the right, the circuit is in its quiescent state prior to the injection of a long current pulse into the axoplasm parametrically at time zero.

> It is important to distinguish between an *impulse*, a stimulus that lasts for an interval shorter than any time constant in the circuit under evaluation, and a *pulse* that lasts significantly longer than any time constant in the circuit. Impulse stimulation allows characterization of the circuit elements (only in the absence of any active amplifier elements). Pulse stimulation allows characterization of the circuit elements, whether it includes active amplifier elements or not.

The circuit is not biased as a typical stage 3 signal encoding neuron, of either the midget or parasol ganglion type. It is biased as a typical stage 2 or stage 4 neuron, with an electron current passing from the axoplasm to the podoplasm, through the Activa, continuously. The conventional current, consisting of imaginary positive charges, passes from the podaplasm through the Activa and into the axoplasm. This imaginary current is the one Hodgkin & Huxley associated with the “inward current” that was later described by the euphemistic term “sodium current.”

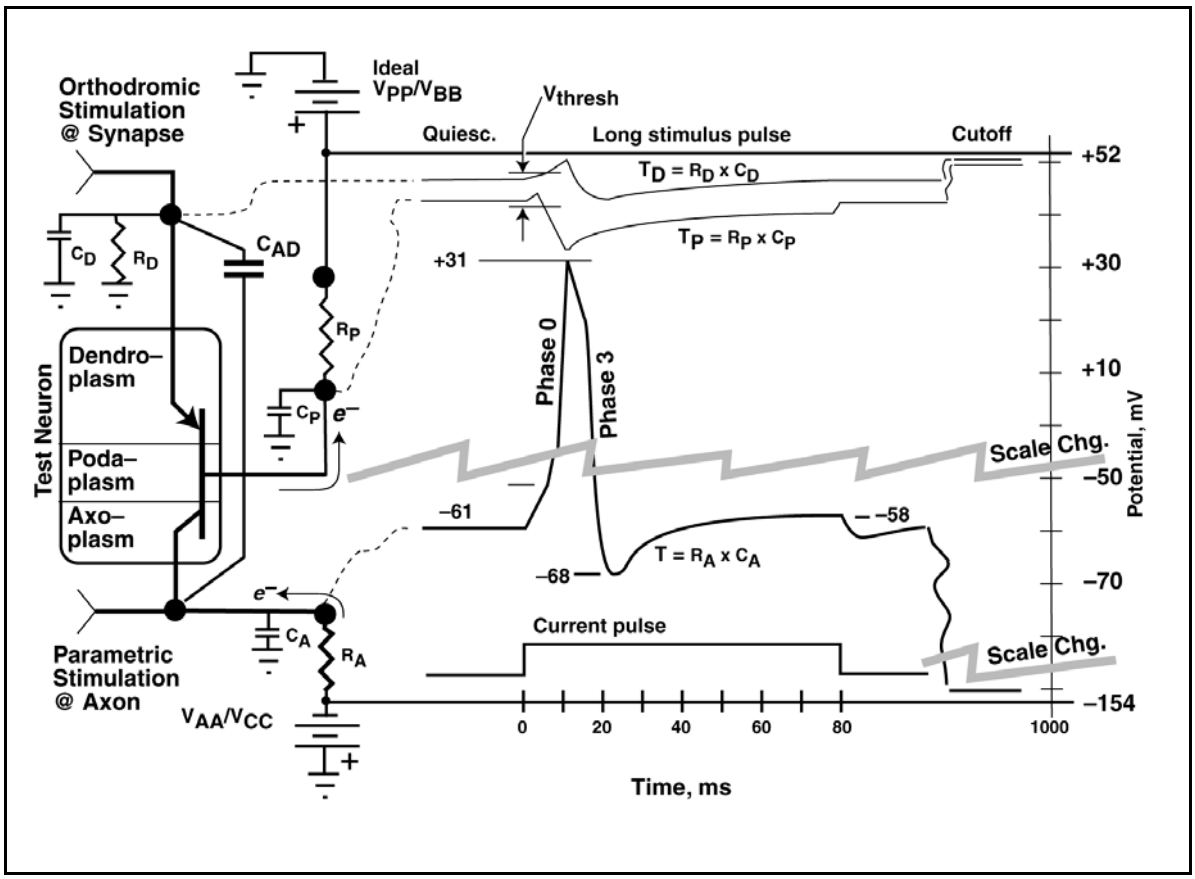

Figure 9.2.4-1 Waveforms on parametric stimulation of a pathologically modified neuron. The current pulse shown along the bottom was injected into the axoplasm via the parametric stimulation port at lower left. No stimulation was introduced into the dendroplasm via the synapse at upper left. The inter-electrode capacitance, C_{AD} (alternately, C_{CE}) plays a key role in parametric stimulation of the axoplasm of a neuron. Data values from Armstrong 2008. See text..

Upon application of a conventional step current pulse at time zero (electrons are actually withdrawn from the axoplasm), the axoplasm potential becomes more positive. If the pulse is large enough, it dominates any current flowing from the battery V_{AA}, and the compensating electron current flowing into the Activa. If the pulse is of constant amplitude, the potential on the axolemma capacitor, C_A, increases linearly as shown. Because of the Capacitances C_{AD} and C_D in series, the potential of the dendrite increase proportionately. When the dendrite to podite potential exceeds the circuit threshold, the internal feedback gain exceeds 1.00 and the circuit begins monopulse generation. The potential of the axoplasm becomes more positive and the potential of the podaplasm becomes more negative very rapidly. The dendroplasm becomes more positive as well due to the above capacitive coupling. The rise in axoplasm potential is virtually linear until the axoplasm to podaplasm potential approaches Activa saturation at about 20 mV. This linear rise is labeled phase 0 by a clinical electro-physiologist. During phase 0, the electron current flowing into the Activa is limited by the current capacity of the Activa. The differential equation describing the axoplasm potential during this phase is dominated by this maximum capacity Activa collector current and is particularly simple. It is the integral of the maximum current capacity of the Activa times *dt* divided by the axolemma capacitance. The resulting axoplasm potential departs from the quiescent level abruptly, although a second order departure is usually reported because of the bandwidth limitation of the potential recording test instrumentation.

At saturation, the axoplasm potential plateaus at +31 mV, the current through the Activa falls to zero, the podaplasm potential falls toward the original quiescent condition the internal feedback gain falls to near zero, and the circuit switches to the axoplasm discharge mode. When the dendrite to podite potential falls below the threshold value, due to the time constant T_D, the circuit enters phase 3. Phase 3 is dominated by the electrostenolytic power supply circuit which is actually a second order filter in most cases. As a result a negative going overshoot is encountered extending to –68 mV before settling to the new stable value of –58 mV during the remainder of the stimulus pulse. During much of this terminal period, the potential difference between the dendroplasm and the podoplasm is held below the original quiescent difference, resulting in what is generally described as the refractory period (a period during which a larger than normal change in stimulus height is needed to initiate another monopulse.

It is important to note the duration of the monopulse formed by the circuit investigated by Armstrong and by Hodgkin & Huxley much earlier, is much longer than that normally recorded for *in-vivo* action potentials (on the order of 10 to 15 ms compared to real action potentials of 1–2 ms). This is partly due to the low fixed temperature of a given experiment (temperature of 6–8 Celsius maintained to an accuracy of ±0.1 Celsius in the case of Armstrong). It is also partly due to the fact the neurons they tested were not stage 3 neurons of class 1 or class 2 as defined by Hodgkin and reiterated above by Clay and this work. As noted above the squid *Loligo* giant axon is basically a specialized locomotion muscle timing generator neuron.

The delay prior to the beginning of the monopulse response, and the time to reach peak response after the start of the parametric stimulus, are obvious.

The potentials given in the above figure are not typical of stage 3 action potential generators (encoding ganglia) or regenerators (Nodes of Ranvier). These circuits do not use a poda supply and are normally biased to cutoff (~ –154 mV) during quiescence. The pulse peaks at about ~ –30 mV in these circuits *in vivo*.

The voltage waveform at the base (poditic) terminal measured across the impedance, R_P, is the S potential of Bishop and colleagues discussed in **Section 2.6.2**. The waveform is described in greater detail in that section. In Armstrong's 2008 paper, the waveform labeled $I_g + I_{Na}$ is clearly the S potential measured across an unspecified resistance. His waveform labeled I_{Na} and reduced by a factor of 20, is clearly the action potential generated at the pedicle of his neuron.

9.2.4.1 Refractory period–theory vs measured data.

The above serape representation can be validated using data for the refractory period of a real neuron using abnormal stimulation. Newman[67] has provided the relevant data from the sciatic nerve of a frog in **Figure 9.2.4-2** using a stimulation described as a compound action potential test (stimulation by two pulses at less than *in-vivo* separation). The resulting waveforms clearly support the refractory period described in the above figure. As E_b-E_c (approximately E_p - E_d) decays toward the threshold value, the amplitude of the stimulus required decreases and the amplitude of the second action potential increases. Unfortunately, the temperature at which the data was collected was not specified. By the length of the time intervals, it appears the temperature was quite low, probably near 20C.

[67]Newman, P. (1980) Neurophysiology. NY: SP Medical & Scientific Books page 50

- - - -

[xxx edit the following]
The waveforms shown in the literature are inconsistent with regard to the pulse polarity that must be applied to the axoplasm to cause the illustrated response. [xxx provide references to H&H and to Cole–possibly starzak figure also] This difference strongly suggests a difference in the prepared specimens. Looking at the circuit of the Activa along with the capacitances between the collector and the emitter and base, these differences can be understood. If the dominant circuit involves the capacitance associated with the emitter terminal, an excitation with the same polarity as the response would be expected. However, if the dominant circuit involves the capacitance associated with the base, an excitation with a polarity opposite to the response is to be expected. Both of these parasitic circuits have a time constant.

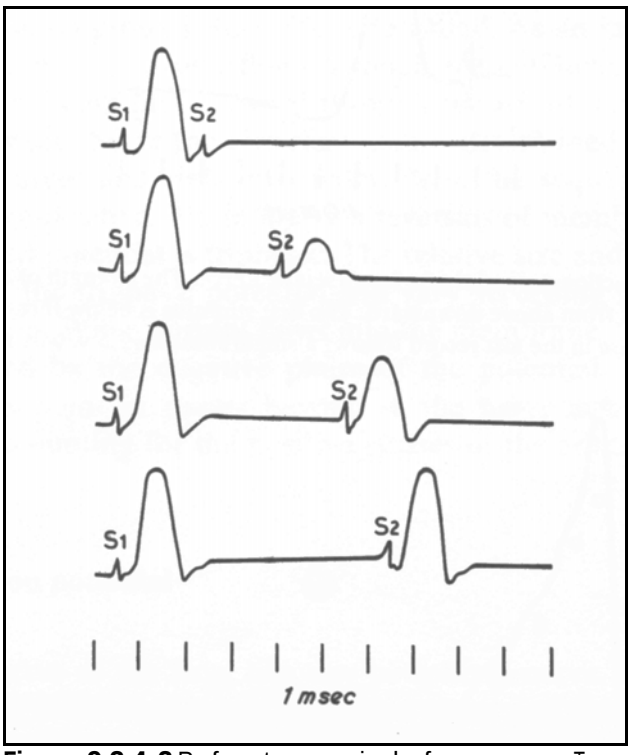

Figure 9.2.4-2 Refractory period of a neuron. Top; the second stimulus (S2) is applied during the absolute refractory period when it fails to give a response. As the interval between S1 and S2 is increased, the second response increases in amplitude until both responses are the same size. Time between stimuli; 2.0, 3.5, 5.0 and 6.0 msec at an unspecified temperature.. From Newman, 1980.

Armstrong (2008) has provided new waveforms that appear to describe his results clearly[68]. Unfortunately, he tries to interpret them in terms of a chemical theory of the neuron. As a result, he includes a long section on "Research Questions" not answered within his discussion. After more than 60 years of investigation, he includes the following statement in 2008, "Much remains unknown about the Na^+ channel" required by his chemical analogy to neuron operation.

Armstrong's results appear to be compatible with the operation of the switching type monopulse oscillator as described in **Section 2.6.2** of "The Neuron & Neural System: A 21st Century Paradigm."

9.2.5 The action potential waveform in closed form

[xxx does the following duplicate the previous section 9.2.4?]

The previous investigation by this author of the physiology of the visual system documented the role of the Node of Ranvier as a regenerative repeater typically found orthodromic to the soma of its neuron[69]. The physiology of the hearing modality supports an expanded role for the Node of Ranvier. As noted earlier, it appears that within the cochlea, a conexus equivalent to a Node of Ranvier can occur before the soma of the neuron. It also appears that the first of these equivalent NoRs can act as an encoding

[68]Armstrong, C. (2008) Gating currents *Scholarpedia* vol 3(10), pp 3482+

[69]Fulton, J. (2004) Biological Vision: A 21st Century Tutorial. Victoria, BC, Canada: Trafford pp 65-70

conexus instead of a regenerative repeater. While more experimental verification is warranted, these findings are consistent with the generic form of the neuron presented in Chapter 2.

Like the excitation/de-excitation equation of stage 1 neurons, the equation of the action potential generators of stage 3 can be given in closed form. However, the closed form is not contiguous. The relaxation oscillator used to form the action potential is a switching type oscillator. The action potential generator operates in three distinct modes. It operates as a Class A amplifier for stimulation levels below a threshold voltage level. If the stimulation level exceeds the threshold potential, The action potential generator goes into a positive feedback mode that generates a rapid rise in polarization associated with the collector circuit of the Activa, the axoplasm of the neuron. Upon the Activa reaching maximum polarization, which occurs due to saturation of the Activa, During this interval, the rising portion of the action potential is generated based on one set of parameters within the oscillator circuit. Following saturation, the falling portion of the waveform is generated based on a second set of parameters (with the Activa in cut-off until its emitter-base, dendritic-poditic, circuit completes its refractory period). During Activa cutoff, the collector (axon) circuit relaxes according to a simple RC circuit decay function. As in the case of the excitation/de-excitation equation, the action potential generator equation is temperature sensitive as developed below.

9.2.5.1 The interneuron and Node of Ranvier as regenerators

This section will focus on the forms of the regenerative repeater most easily identified morphologically. In their most common form, these circuits generate a single positive-going monopulse waveform in response to a positive-going monopulse stimulus exceeding a threshold level.

The physiology of the Node of Ranvier, the synapse and any fully embedded conexus are nearly the same. The difference between them is primarily in their morphological association with the adjacent neurons. The synapse forms a distinct demarcation between the morphology of two neurons while the Node of Ranvier is largely encapsulated within one neuron (except for electrolytic access to the surrounding extra-neural matrix). The fully embedded conexus cannot be recognized morphologically. Only electron microscopy can identify its cytological organization and biasing.

Figure 9.2.5-1 provides a more detailed look at a single generic junction between two neural conduits. For purposes of this section, the nucleus and soma of the interneuron will be ignored. They are shown only to supply context. As shown, the figure represents the Node of Ranvier between two axon segments. By changing the axon segment on the left to a dendrite, and adjusting the biases, the same configuration can be considered a monopolar neuron.

Frame A shows the basic conexus associated with any junction in the neural system in circuit diagram form. It consists of a single Activa and its supporting electrolytic circuit elements, connected into the pre and post junction conduits and the surrounding electrolytic environment.

Frame B provides a composite caricature of both the morphological and electrolytic features of the typical conexus amid the pre and post junction conduits and the environment. The shaded areas represent molecularly asymmetrical, Type 2, plasmalemma. The unshaded areas of the lemma are of Type 1. The small electrical networks represent the fundamental electrical properties of the Type 2 lemma in the respective shaded areas.

Frame C provides a more integrated view of the generic stage 3 neural junction. The nomenclature has been generalized from that used earlier to more appropriately describe the stage 3 neuron. The small circuit diagrams of the asymmetrical lemmas forming junctions with adjacent conduits have been replaced with their more concise form, an active electrolytic semiconductor device, the Activa. This notation highlights the functional nature of the typical junction. It is to provide unidirectional transfer (with or without amplification) of the electrical signal propagating along the neural path. This unidirectional feature is established by the electrical biases applied to the otherwise bidirectional Activa.

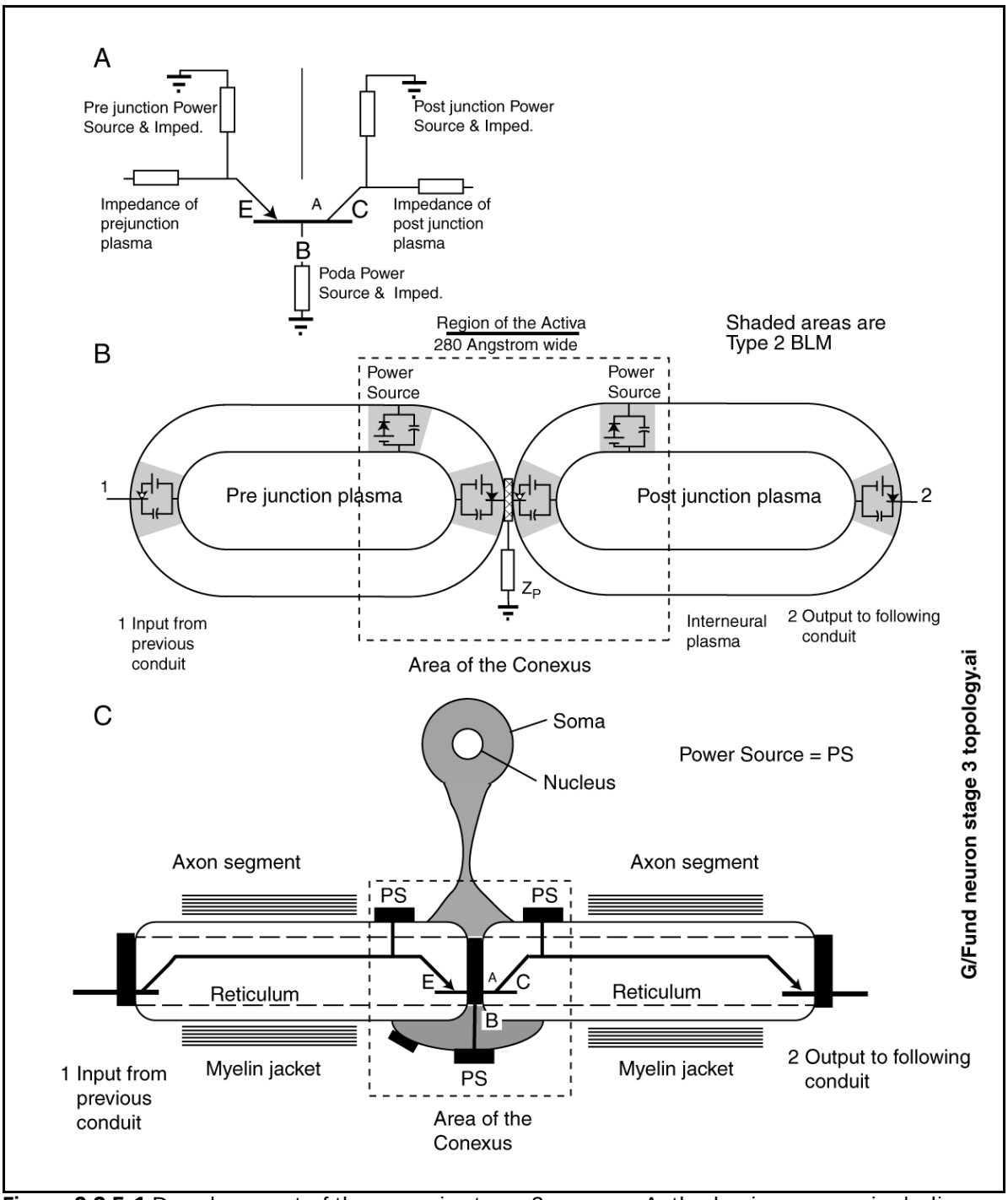

Figure 9.2.5-1 Development of the generic stage 3 neuron. A; the basic conexus including an Activa. B; the graphic representation of a typical stage 3 junction between two conduits. C; a more schematic description of a typical stage 3 conexus between two conduits. If the nucleus and soma are ignored, the circuit is typical of a Node of Ranvier. Note the diode symbology at the two extreme ends of the figure. The input diode on the left (half of the Activa symbol) typically forms the collector portion of the preceding junction. The output diode on the right (half of the Activa symbol) typically forms the emitter portion of the orthodromic junction. See text.

Several critical features of the stage 3 conexus are shown in frame C. The regions of the axon segment immediately adjacent to the conexus are not covered by myelin. These regions support the electrostenolytic processes providing power to the conexus (and labeled PS). They also form large value capacitances, due to the extreme thinness of the lemma, when needed to support relaxation oscillation by the conexus. Farther from the conexus, the myelin encloses the axon segment and prevents any of the external matrix fluids from contacting the lemma. This action insures the capacitance per unit distance is orders of magnitude lower than it would be for the unwrapped lemma. This major reduction in the capacitance per unit length is critical to the propagation of the action potentials of stage 3 along the conduit (See **Section 7.4.5**).

The symbols at the extreme ends of the two conduits represent the "functional diodes" associated with the synaptic junctions at those locations. The diode symbol on the left represents the post junction diode (associated with the collector of the conexus at that location). This diode is typically part of the Activa forming the synapse and is reverse biased. The diode symbol on the right represents the pre junction diode normally associated with the synapse at that location. This diode is typically forward biased. In patch-clamp experiments, it frequently acts as a nonlinear resistance in shunt with the other impedances associated with the plasma of the axon segment. This shunt element frequently degrades the electrical performance of the post junction circuitry, resulting in a voltage-current characteristic that approaches a straight line instead of the ideal exponential curve. Both diodes are morphological parts of either another regenerative NoR or of a synapse.

9.2.5.2 The detailed circuitry and operation of the Node of Ranvier

The circuitry of the conexus within the Node of Ranvier is typical of any man-made common-base semiconductor (transistor) circuit. Such circuits have been used commercially for many years[70]. The only difference is that the neural circuit is formed of liquid-crystalline-state semiconductor materials instead of solid-state semiconductor materials. The common-base circuit is particularly subject to oscillation and this susceptibility has been widely used in practice. The susceptibility arises if the impedance of the base (or poda) circuit is high and a significant reactive impedance is found at one of several potential locations in the circuit. The following paragraphs will explore these situations using **Figure 9.2.5-2**.

[70]Gray, T. (1954) Applied Electronics. NY: John Wiley & Sons pp 819-825

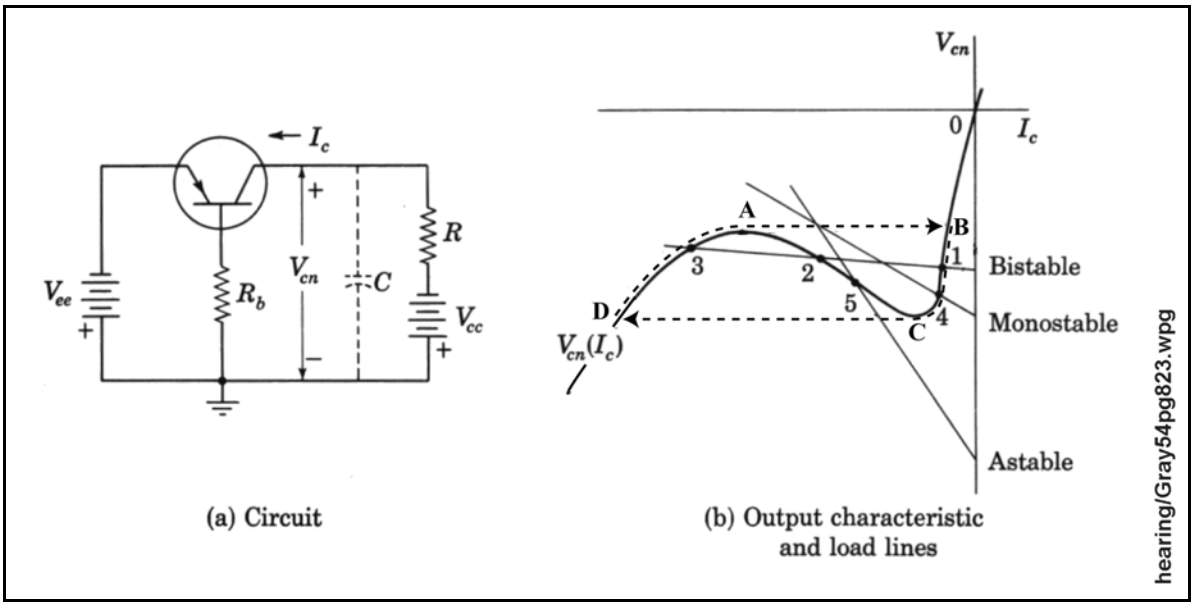

Figure 9.2.5-2 The electrolytic circuit of the generic stage 3 encoding neuron. Ignoring the capacitance, C, all of the dashed lines and the letters in frame (b), the circuit shows the nominal circuit with feedback between the input and output circuits provided by the common-base resistance, R_b. As shown, the circuit can operate bistatically, monostatically or astably depending on the load impedance, R, and the bias potential V_{ee}. The circuit can change its operating point along the curve $V_{cn}(I_c)$ very rapidly (limited only by the current capacity and stray capacitance of the circuit elements). If a capacitor, C, is added to the collector circuit, the switching performance of the circuit is controlled by that capacitor. See text. Adapted from Gray, 1954.

The following discussion is brief and purely pedagogical. For more details concerning the potential oscillation of common-base active circuits, a more specific text should be consulted. These circuits, consisting of only resistive and capacitive impedances and an active device exhibiting positive internal feedback, are usually described as relaxation oscillators. At a more fundamental level, they are described as switching oscillators as shown in frame (b). This switching character is key to understanding the action potential generated by a neuron (**Section 7.3.1**).

If the conexus in the above figure contains a resistive impedance, R_b, between its base connection and the surrounding medium (electrical ground), the overall device will exhibit a degree of positive *internal* feedback which is controlled by the value of that impedance. This internal feedback will introduce a unique characteristic into the *input impedance*, the *output impedance* and the *transfer impedance* of the neuron. Frame (b) illustrates this feature. The voltage-current characteristic of the output (collector) circuit, $V_{cn}(I_c)$, exhibits a significant deviation from a straight line. It is important to note the unusual impedance in the region of the deviation. The portion of this curve sloping down and to the right can be defined as a region of negative (dynamic) impedance--a clear indication of the presence of an active electronic device since no conventional passive impedance can exhibit such a characteristic.

Three load lines are shown representing different values of the resistance, R, and different values of the supply voltage, V_{cc}. If the load resistance, R, and the collector supply voltage, V_{cc}, are selected appropriately, the circuit can be made to operate monostably (operating about a stable quiescent point, 4), bistably (switching between two fixed operating points, 1 & 3, when stimulated) or astably (continuously switching between two operating points, A & C) as shown.

Only one voltage-current characteristic is shown. However, this characteristic is also a function

of the bias applied to the emitter circuit. Changing the net potential at the emitter has the effect of changing the effective collector supply potential, V_{cc}. This results in the intersection of the load lines with the ordinate moving up or down but the slope of the load lines remaining fixed.

The above circuit with the load line labeled monostable is conditionally stable. The axoplasm will remain at a specific voltage with a small current passing through the collector of the Activa as described by point 4 indefinitely. However, if the load line should be momentarily moved down to where the load line intersects the voltage-current characteristic in the negative region, the circuit will become unstable. The locus of operation will move from point C to point D very rapidly and then proceed to point A before jumping to point B and then returning to the stable point at 4. This behavior is due to the capacitance between the collector and the local ground of the collector circuit. The potential across a capacitor cannot change instantly. However, the current flowing into or out of a capacitor can change instantly. As a result, the horizontal dashed lines indicate changes in current flow that can occur without any voltage change. On the other hand, the voltage can change between points D & A and B & 4 as the current discharges or charges the capacitor potential. During interval D to A, the rate of voltage change is controlled by the size of the capacitance and the current capability of the Activa. During the interval B to 4, the rate of voltage change is controlled by the size of the capacitance, the resistance *R* and the current capability of the voltage source V_{cc}. For a given circuit, the time for the operating point to traverse the locus one time is equal to the time interval between D & A plus the time interval from B to 4. The primary factor controlling this interval is the capacitance, C.

The above circuit with the load line labeled Astable is unstable. If any small perturbation of the nominal voltage across the capacitance, C, at point 5 occurs (even due to Brownian motion), the current will proceed to point C, jump to point D, proceed to point A, jump to point B, proceed back to point C and repeat the sequence indefinitely. Here again the time for the operating point to traverse the entire locus is given by the time interval required to travel from D to A plus the time interval required to travel from B to C. The primary factor controlling this interval is again the capacitance, C.

9.2.6 The Action Potential (AP) vs pseudo action potentials

The concept of an action potential arose from the observation that the axon of many easily accessed neurons exhibited a uniquely shaped output pulse. While these pulses frequently occurred in groups, the structure of the groupings were difficult to interpret.

> It is important to differentiate between the waveform recorded at the pedicle of a sensory neuron, and called the generator potential and the pulse waveform known as the action potential. While the generator potential may be pulse-shaped, that characteristic is a result of the stimulus used.

The action potential is intimately associated with the stage 3 projection neurons of *Chordata* and is generally assumed to be unique to *Chordata*. It is closely associated with the long neurons forming the neural chord within the backbone, and other long neural pathways, in those species. It can be considered necessary in any large animal with a central nervous system.

The occurrence, but not the unique shape of the action potential has been extensively investigated. The individual action potential contains very little information. However, groups of these pulses *represent* the fundamentally analog information projected between engines of the neural system. These groups are generated by ganglion neurons typically near the output of a given engine and decoded by stellite neurons typically near the input region of a second engine. Action potentials are the temporal responses of the encoding neurons of stage 3.

The true action potential consists of a pulse with distinctly different leading and trailing edges. The leading edge is straighter than an exponential response because it is formed by an active circuit including feedback. The majority of the leading edge is a straight line when voltage is plotted versus time. This is because the circuit forming it acts as a constant current source charging a capacitor. The trailing edge of the true action potential is fundamentally an

exponential curve since it is formed by the charge stored on a capacitor leaking off through a nominally resistive impedance. Variations occur among these waveform elements in practical situations.

A pulse, believed to be similar to an action potential in the 1940's, had been observed in several cephalopods of the Order *Mollusca*. Based on this observation, Hodgkin & Huxley investigated the source of the assumed action potential associated with the giant axon of the squid *Loligo*. Following their work, Mueller & Rudin attempted to fabricate synthetic (symmetrical!) bilayer membranes exhibiting the same properties as those described for the axolemma of Loligo[71]. While the work of this team is exemplary, their activities were premature. They did not recognize the different forms of lemma that are known today and most of their advertised action potentials were products of their test set and protocols (their fig. 1). When they explored more complex membranes formed of natural biological material[72], they obtained more interesting results, including the natural breakdown potential of biological bilayers (sphingomyelin), the effect of doping these bilayers and apparently monostable and bistable oscillations.

9.2.6.1 Details of the generic action potential waveform

There is considerable difference between the *in-vivo* chordate action potentials and the waveforms measured and interpreted by Hodgkin & Huxley, Mueller & Rudin and others. While Hodgkin & Huxley based their analysis on the difference between two currents that existed for the entire duration of their pseudo-action potential, a true action potential is formed by currents that are switched on and off at the peak of the pulse.

Figure 9.2.6-1 shows the features of the action potential generated at a Node of Ranvier. The left and right scales of the figure are not directly related. Schwarz & Eikhof[73] have presented a similar figure recorded from a single myelinated rat nerve fiber. Action potential generators are typically biased so that they are in the cutoff condition under quiescent conditions. The axoplasm-to-ground potential is near –155 mV, and the dendrite-to-podite potential is typically near –10 mV. [An axoplasm potential of –140 mV is shown to agree with the reported measurements.] For dendrite-to-podite potentials of between –10 and 0 mV, the circuit operates in a linear amplifier mode. The axoplasm potential will vary by small amounts in direct response to changes in the dendrite to podite potential. However, if the dendrite-to-podite potential becomes positive, the gain of the circuit becomes greater than one and the circuit goes into an oscillatory mode. Current will begin to flow from the axoplasm through the Activa. This current will cause the axon potential to become more positive and the podite potential to become more negative. The more negative podite potential reinforces the dendrite-to-podite potential difference and causes still more current to flow out of the axoplasm. During the resulting rapid positive-going change in the axoplasm potential, the Activa acts like a constant current drain that discharges the axoplasm capacitance. The leading edge of the output waveform rises nearly linearly until the axoplasm potential approaches the saturation level of the device (axoplasm potential of about –10 mV). Upon reaching saturation, the current through the Activa collector circuit goes to zero. Meanwhile, the stimulus has already declined. As a result, the quiescent dendrite-to-podite potential becomes reestablished and the Activa goes into cutoff. The axoplasm capacitance is now recharged from the electrical power supply acting as a constant potential source in series with a resistance.

The axoplasm potential follows an exponential curve during this recharging cycle. Depending on the temperature of the specimen, the axoplasm potential follows the curve marked T_0 or T_1. The shape of the axoplasm potential as a function of time has been given the name action

---

[71]Mueller, P. & Rudin, D. (1968) Resting and action potentials in experimental bimolecular lipid membranes *J Theor Biol* vol 18, pp 222-258

[72]Mueller, P. & Rudin, D. (1968) Action potentials induced in biomolecular lipid membranes *Nature* vol 217, pp 713-719

[73]Schwarz, J. & Eikhof, G. (1987) Na currents and action potentials in rat myelinated nerve fibres at 20 and 37C. *Pflugers Archives-European Journal of Physiology,* vol. 409, pp. 569-577

potential. Good instrumentation is required to record the detailed shapes of its rise and fall and the discontinuity near its positive peak. The recording problem is exacerbated if the electrical probe used to record the waveforms is not properly compensated to insure a flat frequency response. If the probe is not compensated, an overshoot (where the apparent potential of the axoplasm becomes positive) is frequently recorded. This condition is pathological due to the protocol.

9.2.6.2 The effect of temperature on the action potential

Temperature has a very distinct impact on the shape of the action potential. The effect on the leading and trailing edges are distinctly different. They both are based on a common capacitance that does not change significantly with temperature. The leading edge time constant is also determined by the collector-to-base resistance of the Activa within the neuron when conducting. This value is virtually independent of temperature. As a result, the leading edge of the action potential does not change significantly for temperatures within the biological range. The trailing edge time constant is determined by the load impedance of the collector (axon) circuit. This impedance is dominated by the impedance of the electrostenolytic power source and the impedance of the associated vascular supply system. These components are highly dependent on the temperature of the organism. As a result, the trailing edge time constant is strongly affected by the temperature. **Figure 9.2.6-2** shows the effect of temperature on the action potential of the rat from figure 1 of Schwarz & Eikhof[74]. While not shown in detail, note the slower rise of the voltage prior to the beginning of the action potential at 20C. This suggests the time constant of the dendrite-to-base circuit was also temperature dependent. The time constant of this dendritic circuit is also dominated by the parameters of its electrostenolytic source and the vascular supply.

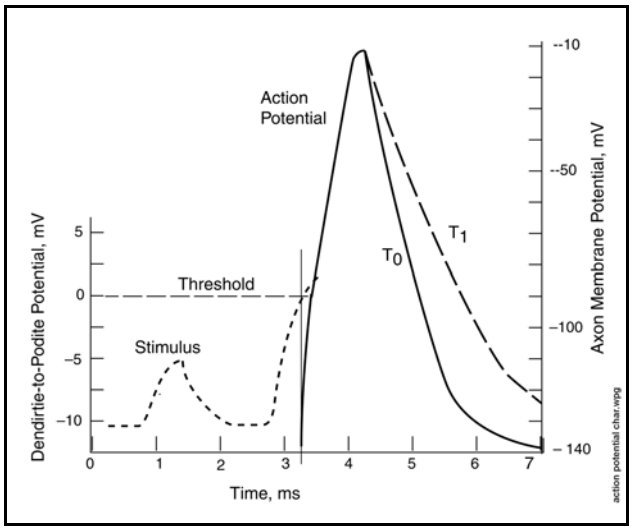

Figure 9.2.6-1 The features of the action potential at a Node of Ranvier. The stimulus is shown dotted and uses the scale on the left. The first stimulus pulse does not cause the generation of an action potential. The second stimulus exceeds the amplitude threshold and does cause an action potential to be generated. There is a significant delay between the peak of the stimulus and the peak of the action potential.

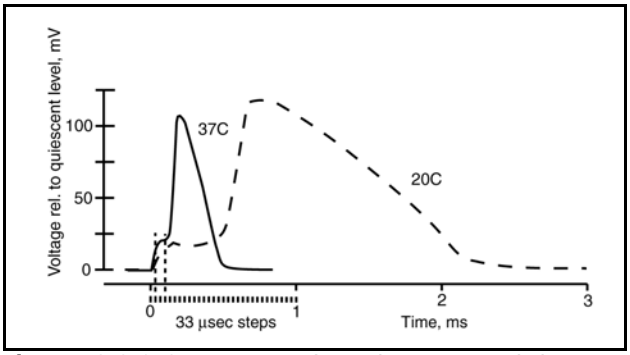

Figure 9.2.6-2 Measured action potentials as a function of temperature for rat motor neurons. The 37C response was elicited by a 30 µsec current pulse. The 20C response was elicited by a 100 µsec current pulse. From Schwarz & Eikhof, 1987

> The effects of temperature on the action potential reported by Schwarz & Eikhof provide strong support for the switching current mechanism proposed here and strong repudiation (falsification) of the current difference theory of Hodgkin & Huxley.
>
> A variety of pseudo action potentials

[74]Schwarz, J. & Eikhof, G. (1987) Na currents and action potentials in rat myelinated nerve fibres at 20 and 37 Celsius. *Pflugers Arch*. vol. 409, pp. 569-577

appear in various conceptual papers in the hearing literature. The most famous of these was proposed by Huxley & Hodgkin and discussed above[75]. Another example is the activating function defined by Rattay and discussed in considerable detail in Zeng, Popper & Fay[76]. The continuous mathematical form of this activating function is significantly different from that of the actual, switching-generated, action potential.

Mueller & Rudin, working in the 1960's, used the generic term action potential to describe virtually any pulse response, whether driven or not and whether related to the nervous system or not[77, 78]. They were working to emulate a biological membrane through reconstitution from recovered biological material or synthesis from stock materials. They proposed that the action potential was generated by a two-terminal neuron employing a "tunnel diode" mechanism (a popular newly discovered electronic device during that period). While this approach cannot be ruled out a priori, it involves an asymmetrical membrane that has been "heavily doped" in the semiconductor sense of the term. The literature of the biological membrane has not previously or subsequently reported such heavy doping. The use of the tunnel diode concept also requires the presence of resonant circuits, in addition to the diode, to shape the resulting voltage profile to resemble an action potential. No such resonant circuits have been identified in real biological membranes.

None of the above approaches defined any role for the neurites of the neuron, although Hodgkin & Huxley reported considerable experimental difficulty unless all vestiges of the neurites were removed from the soma of their neuron. Such "spontaneous activity" related to the presence of the neurites clearly indicated their importance in the overall operation of the neuron.

9.2.7 Electrical operating conditions in the absence of feedback

The description of the switching regenerative repeaters provides a baseline for describing all action potential pulse generating neurons. Assuming the internal Activa is biased into the active state, the critical parameter is the emitter to base potential, $V_E - V_B$. If the emitter-to-base potential is significantly negative, the device is in cutoff, no current flows through the collector circuit and the axoplasm potential will be at its supply potential, nominally –154 mV. As $V_E - V_B$ becomes positive, current will begin to flow through the collector circuit and the axoplasm potential will begin to move toward zero potential. As the $V_E - V_B$ potential becomes more positive, the current through the collector circuit will increase and the axoplasm potential will continue to become more positive until a saturation condition is reached (maximum collector current and minimum axoplasm potential). Saturation occurs when the collector-to-ground potential reaches the base-to-ground potential. This condition occurs when both potentials are approximately –20 mV in observed neurons. Under this condition, the $V_E - V_B$ potential is typically +30 mV and the emitter-to-ground potential is about +10 mV.

Stage 3 neurons operate under large signal conditions and the pulse generation circuits spend a majority of their time in the cutoff condition. Thus, thermal noise at their input terminals is not normally a significant consideration. Noise in the emitter circuit rising to the threshold potential for the circuit can cause the generation of action potentials. The Poisson statistics of the noise stimuli recorded by Kiang (1965, pp 93) suggest these signals were generated in just this way. Below-threshold noise in the emitter circuit can add to the applied excitation and thereby cause a marginal advancement or delay in when the emitter-to-base potential reaches threshold. This can cause a similar marginal advance or delay in when the action potential is

---

[75]Hodgkin, A. & Huxley, A. (1952) A quantitative description of membrane current and its application to conduction and excitation in nerve *J Physiol* vol 117, pp 500-544

0. Abas, P. & Miller, C. (2004) Biophysics and physiology *In* Zeng, F-G. Popper, A. & Fay, R. *eds*. Cochlear Implants: Auditory Prostheses and Electric Hearing NY: Springer pp 161-164

[77]Mueller, P. & Rudin, D. (1968) Op. Cit. *Nature* vol. 217, pg 714

[78]Mueller, P. & Rudin, D. (1968) Op. Cit. *J Theor Biol* vol. 18, pg 237

generated.

9.2.8 The encoding (ganglion) neurons

The physically dominant neurons of stage 3, signal projection, are those used to generate and regenerate action potentials. These neurons are known as ganglion cells in the neural systems of both vision and hearing. Ganglion neurons, by whatever name, are introduced as a matter of power efficiency at the expense of some time delay. In the auditory system, they are typically found at the output of the OHC and IHC neurons and at the output of every signal processing and signal manipulation engine of the system.

9.2.8.1 Operation of the ganglion neuron

The Node of Ranvier is typically used to regenerate at full amplitude the phasic waveform of a reduced-amplitude action potential applied to its input. It accomplishes this on an individual pulse basis. The same circuit can be used in an alternate mode; the generation of one or more phasic pulses in response to the application of a sustained electrotonic (analog) waveform at its input. This is the role of the ganglion neuron.

Consider the circuit for a Node of Ranvier described in **Figure 7.3.1-2** under different operating conditions. Let the circuit be incorporated into a neuron and let a constant voltage be applied to the dendrite of the neuron. If this voltage is slightly higher than the threshold for the neuron, the neuron will be unstable and generate a single action potential followed by a refractory period while the emitter-to-base voltage, V_E - V_B, is more negative than its quiescent value. However, because of the potential applied to the dendrite, the emitter-to-base voltage will attempt to return to a voltage slightly higher than its quiescent voltage. When it exceeds its threshold value, another single action potential will be generated. This cycle will be repeated as long as the voltage at the dendrite is above the threshold value. Under this condition, the stream of action potentials will be continuous and exhibit a uniform pulse-to-pulse interval characteristic of the circuit elements associated with the Activa within the neuron.

Now consider the same circuit within a neuron but apply a slowly rising ramp voltage to its dendrite. The circuit will operate as above only every time it attempts to return to its quiescent value, that value will be incrementally higher than on the previous cycle due to the voltage applied to the dendrite. As a result, the threshold voltage of the circuit will be achieved incrementally sooner and the pulse-to-pulse interval will be incrementally shorter. The result will be an initial pulse followed by a series of pulses of incrementally shorter pulse-to-pulse interval. This is the fundamental operating mode of the electrotonic signal encoding neurons of the neurological system. These neurons have been defined functionally as ganglion neurons in this work.

The ganglion neurons can encode any electrotonic waveform having frequency components below the maximum action potential pulse frequency that it can generate. This maximum frequency is on the order of 200-500 Hz but can be as high as 1000 Hz for certain ganglion neurons associated with the source location circuits of hearing.

The data of Golding & Oertel recorded using a current-type axonal patch-clamp shows the operation of the encoding ganglion neuron in considerable detail when interpreted in the context of the Electrolytic Theory of the Neuron[79]. Their waveforms support the theory presented in **Section 7.3** very well.

9.2.8.2 Characteristics of ganglion neurons

Since the performance of the ganglion neuron is a function of the emitter-to-base potential, this neuron can be driven by potentials applied to either its dendritic or poditic terminals. The combinations of circuit elements associated with the synapse and dendrite, and the synapse and podite, can be complex circuits. These circuits may act as differentiators or integrators.

---

[79]Golding, N. & Oertel, D. (1996) Context-dependent synaptic action of glycinergic and GABAergic inputs in the dorsal cochlear nucleus *J Neurosci* vol 16(7), pp 2208-2219

In some cases, the dendritic input is known to combine these mechanisms to form complicated lead-lag networks. For consistency, this work considers such networks as stage 2 networks at the input to stage 3 encoders.

Ganglion neurons exhibit several time delays. Each of the input circuits exhibits a delay due to the diffusion time of current along the length of the neurite. Upon reaching the capacitance associated with each Activa emitter and base, there is a time required to charge the RC network to the threshold potential associated with that terminal. The total time required for the circuit to reach threshold is the intrinsic latency of the ganglion neuron. After achieving threshold, there is a finite time required for the action potential of the collector circuit to reach peak amplitude. The intrinsic latency plus this additional delay equals the clinical latency of the circuit at the collector terminal.

To provide the necessary capacitance to achieve the unstable condition required to create action potentials, the cytological area associated with the collector of the neuron is typically enlarged. This area is normally described as the hillock region.

Although the above discussion brings to mind the conventional ganglion neuron where the encoding circuit is found with the soma, this is not a requirement. In the case of ganglion neurons of the spiral ganglia, it appears that the encoding circuit is in the first "bead" associated with the input to the soma of the neuron. This is confirmed by the artifacts of the encoding process that have been measured at the synapse with the sensory neuron. The first bead acts as an analog-to-phasic encoder while subsequent beads operate as Nodes of Ranvier, whether they precede, are within, or follow the soma.

In the typical ganglion neuron, the axon is formed as a long thin tube that is tightly wrapped with an electrically insulating material, myelin. The fact that the axon is a long coaxial tube introduces electrical inductance into the circuit. This inductance per unit length complements the capacitance per unit length resulting from the lemma and myelin wrap. When these two parameters are approximately equal, the mode of signal transmission along the axon changes from diffusion to propagation as described in **Section 7.3.5**. This is a fundamental change of immense importance. Of crucial importance, the action potential continues to propagate along the axon without regard to the electrical potential at the collector terminal of the Activa. Such a condition cannot be achieved by diffusion. Diffusion requires the electrical source to remain at the signal level until the diffusion packet reporting the signal reaches the termination of the circuit.

The action potential propagated by a myelinated axon travels much faster than it would by diffusion (an instantaneous velocity of approximately 4400 meters/sec). However, the amplitude of this signal does dissipate with distance and regeneration is required. At each Node of Ranvier, the signal is regenerated to its maximum value and an additional delay is introduced into the overall delay. This situation makes the total delay, measured along the axon, increase by a significant increment at each Node of Ranvier. The average propagation velocity of the ganglion neuron is dominated by this incremental delay. As a result, the average propagation velocity is reduced to a value near 40 meters/sec.

Figure 7.3.2-1 suggests three different potential definitions of latency. The simplest concept measures the latency as the time from some arbitrary event until the peak of an action potential occurs. The peak of an action potential is most easily measured in a clinical environment. However, not all action potentials exhibit the same width and their peak does not represent a significant functional event.

From an engineering perspective, two other latencies can be defined. A simple application-oriented concept measures the latency as the time from some arbitrary event until a level is reached following the start of the action potential. This level is frequently taken as the level defined as 10 percent of the rise of the action potential from its baseline to its peak. This level is easy to determine graphically. However, it also lacks any functional significance.

The most functionally important and reproducible concept of latency measures the time from some arbitrary event until the action potential initially deviates significantly from the baseline. This condition can be defined at either the axon, dendrite or podite of any phasic conexus

(neuron or Node of Ranvier). It signifies the change from a feedback condition with a gain of less than 1.0 to the regenerative condition with a feedback gain of greater than 1.0. For the feedback gain of less than 1.0, the axon segment waveform generally looks like an amplified copy of the stimulus to that conexus. For the feedback gain of greater than 1.0, the conexus axon segment waveform is an action potential regardless of the stimulus waveform.

Figure 9.2.8-1 describes the components of latency as measured at the auditory nerve as presented by Young et al. It shows data representing the mean latency of assorted neurons as a function of their best frequency at a stimulus intensity of 25-35 dB above threshold. They defined the acoustic delay of their test set as 0.55 ms. They drew a freehand curve below the high spontaneous rate data points. This curve has been replaced by a more informative estimate of the delay based on the mean velocity of the Rayleigh wave within the cochlear partition of an endothermic animal (dashed line). The curve can be moved without rotation on this linear plot with respect to position on the cochlear partition. However, there is more scatter in the other data sets.

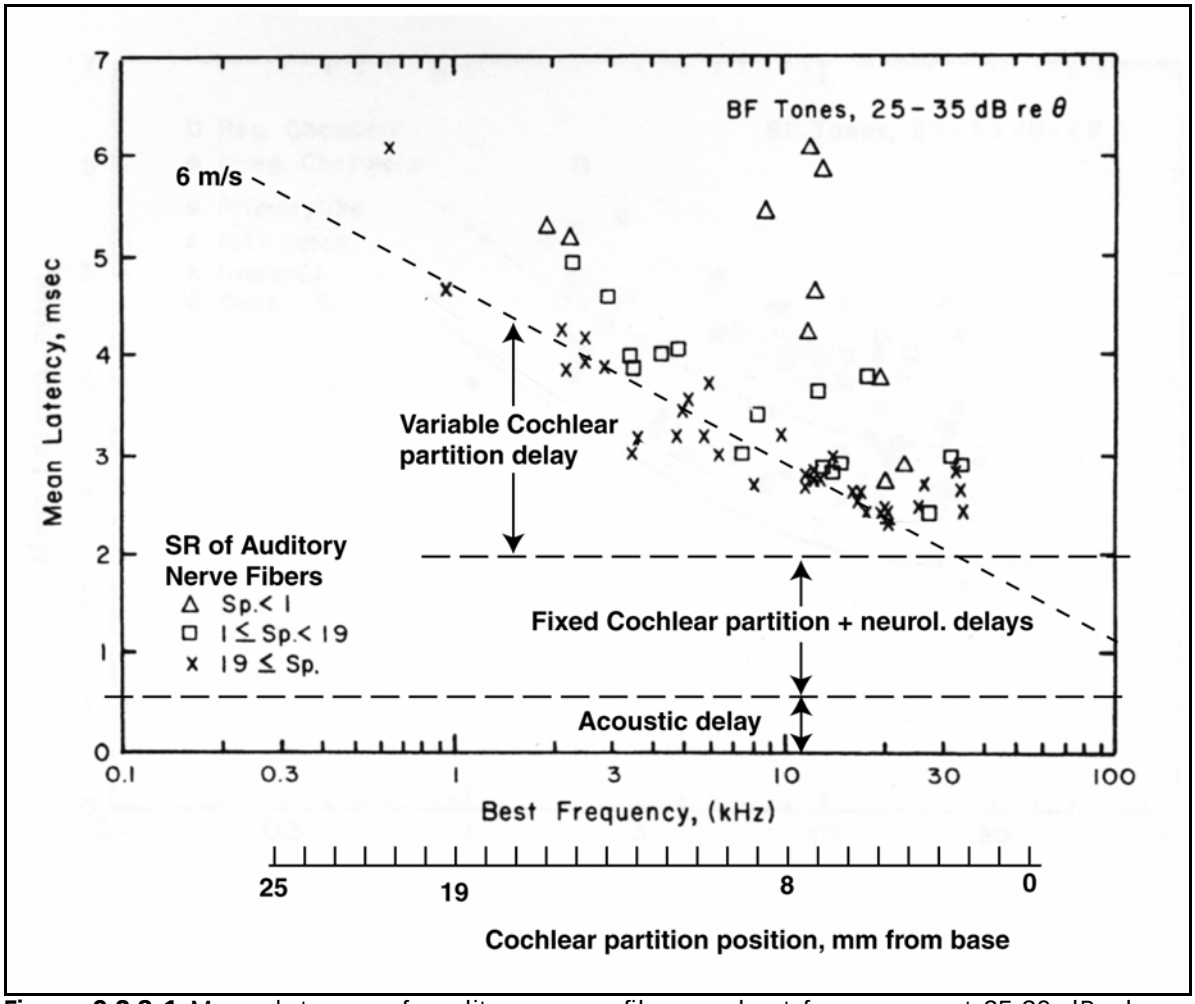

Figure 9.2.8-1 Mean latency of auditory nerve fibers vs best frequency at 25-30 dB above reference level for decerebrate cats. The legend at lower left defines the spontaneous (uncontrolled) rate of neuron firing. The acoustic delay was defined by Young et al. The other delays, and the proposed Rayleigh wave velocity within the cochlear partition are from this work. Modified from Young et al., 1988.

Many authors have described a phase shift in the action potentials collected at the auditory nerve as a function of stimulus frequency without considering the character of that phase shift.

A time delay is frequently interpreted as a phase shift. Smolders & Klinke have provided good data and a discussion describing the two components of such phase shifts[80]. However, they did not de-convolve the time delay into acoustic (in air), mechanical (primarily in the tectorial membrane) and neural components. In the crocodile, the delay component of the phase shift came to 1.49 ms.

Figure 9A in Smolders & Klinke shows a possible second group of delays approximately one millisecond above the main distribution. This delay could be caused by probing a ganglion neuron at a point beyond a Node of Ranvier. Each Node typically introduces a one millisecond delay in the signal stream.

Synchronization and the synchronization index are not clearly defined concepts in hearing. While various mathematical definitions have been offered, they are based on totally empirical interpretations of laboratory data. Synchronization generally refers to arranging some rate associated with one independent source to equal a similar rate associated with a second independent source. The phase-locking of a local oscillator with an incoming signal from an independent distant source is a typical example.

In hearing, phase-locking is used in a narrower sense. It describes the timing of a driven action potential pulse with respect to the generator waveform at an axon causing that pulse. The most frequent concept is to compare the time of the peak in the action potential waveform with the zero crossing of the generator waveform resulting from sinusoidal acoustic stimulation. Less frequently, the time of the peak in the action potential waveform is compared with the zero crossing of the sinusoidal acoustic stimulation. The time of the peak is expressed in angular measure with respect to the generator or stimulation waveform. The time of occurrence of the peak is a function of the intensity of the stimulus and the state of adaptation of the hearing system.

The concept of synchronization is generally used when speaking of generator waveform frequencies below 3000 Hz and most often for frequencies below 600 Hz. For higher frequencies, the synchronization index goes to zero. At higher frequencies a different synchronization index can be defined based on the envelope of the stimulus. Rose illustrates this situation in a montage[81]. Goldberg & Brown provided an early description of a synchronization index in a specific context[82]. Delgutte provided a textual definition in 1980 based on data from acoustic tests that are of limited utility[83]. Javel described two or more different definitions in 1988 based on external electrical stimuli[84].

The low frequency synchronization index is difficult to define for three reasons. First, it involves a variety of mechanisms. Second, it frequently involves artificial external stimulation of a neuron. Third, it only applies to certain types of phasic neurons. **Figure 9.2.8-2** from Javel provides the necessary data from a cat auditory fiber responding to a sinusoidal stimulus. Javel provided definitions of synchronization indices based on detailed mathematical manipulations

---

[80]Smolders, J. & Klinke, R. (1986) synchronized responses of primary auditory fibre-populations in *Caiman crocodilus* (L.) to single tones and clicks *Hear Res* vol. 24, pp 89-103

[81]Rose, J. (1959) (1959) Organization of frequency sensitive neurons in the cochlear nuclear complex of the cat *In* Rasmussen, G. & Windle, W. *eds*. Neural Mechanisms of the Auditory and Vestibular Systems. Springfield Il: Charles C. Thomas Chap 9 pg 123

[82]Goldberg, J. & Brown, J. (1969) Response of binaural neurons of dog superior olivary complex to dichotic tonal stimuli: some physiological mechanisms of sound localization *J Neurophysiol* vol 32, pp 613-636

[83]Delgutte, B. (1980) Representation of speech-like sounds in the discharge patterns of auditory-nerve fibers *J Acoust Soc Am* vol 68(3), pp 843-857

[84]Javel, E. (1988) Acoustic and electrical encoding of temporal information *In* Miller, J. &. Spelman, F. *eds*. Cochlear Implants: Models of the Electrically Stimulated Ear. Englewood Cliffs, NJ: Prentice Hall pg 285

but did not describe the range limits on the definitions. It can be inferred that his definition related to sinusoidal stimulation was restricted to the range of zero to 90 degrees. These definitions are not mutually compatible. Javel did note the theoretical maximum of his synchronization index was pi/4 = 0.78 for a sinusoidal stimulus (p. 250) but 1.0 for a square wave stimulus (p. 275).

Frame A shows a 200 Hz sinusoidal stimulus and an overlaid oscilloscope presentation showing multiple traces of the generated action potentials over an extended period of time. Unfortunately, the individual action potentials are not numbered to show their sequence. They are clearly unstable with reference to a given phase angle of the stimulus. At a 200-Hz stimulus frequency (period of 5.0 ms), the fiber can be expected to show some degree of refractiveness following the generation of each pulse. The effect of this refractiveness will be discussed in conjunction with frame C.

Frame B shows the synchronization index calculated by Javel for the data in frame A. It also shows a moving window average through the data points (solid line). Equally interesting, a dashed line has been added showing the data points support a theoretical description of the synchronization index based on an exponential expression. This is the expected expression for a relaxation oscillator with a recharging interval controlled by an RC network.

In natural situations, regenerative pulse repeaters called Nodes of Ranvier (monopulse oscillators) achieve "synchronization" indices that are nominally 1.0. They generate one output action potential for every input action potential received (with a constant phase angle and a very high degree of reliability). In natural situations, encoding neurons (astable oscillators) can produce more than one action potential per applied stimulus (synchronization indices above 1.0) if the applied stimulus is of sufficiently low frequency (typically below 50 Hz). This condition appears to be outside the range of frequencies that Javel considered in his definitions. In the region of 100 to 500 Hz, encoding neurons typically achieve synchronization indices near unity (or pi/4 depending on the mathematical definition). Above 500 Hz, the output of the encoding neuron depends on the combination of the height of the excitation pedestal (due to integration) and the height of the AC component (reduced by the integrator) applied to it.

Frame C shows how an initial action potential is generated when the stimulus amplitude exceeds the stimulus threshold of that neuron. The static threshold of the neuron is shown as the dotted line labeled T_S. The dynamic threshold of that same circuit is shown by the dashed line, T_D. The dynamic threshold is the result of internal changes in the potentials applied to the Activa as part of the monopulse oscillation process. It is not the actual action potential generated but it is similar in form to the action potential. Note that after a period of time, the dynamic threshold decreases to the value of the still present stimulus. The result is the generation of a second action potential (not shown). This second pulse may exhibit a lower peak amplitude at the axon because the recharging process may not be complete. However, the result is clear. The positive going stimulus of sufficiently low frequency can cause the generation of more than one action potential during a given cycle. The vector diagram for this situation shows the first pulse occurring the first 90 degrees of the circle but the second pulse occurring much later and frequently in the second quadrant of the circle. The presence of a pulse occurring in the second quadrant causes great difficulty for the definition of synchronization index proposed by Javel for sinusoidal excitation.

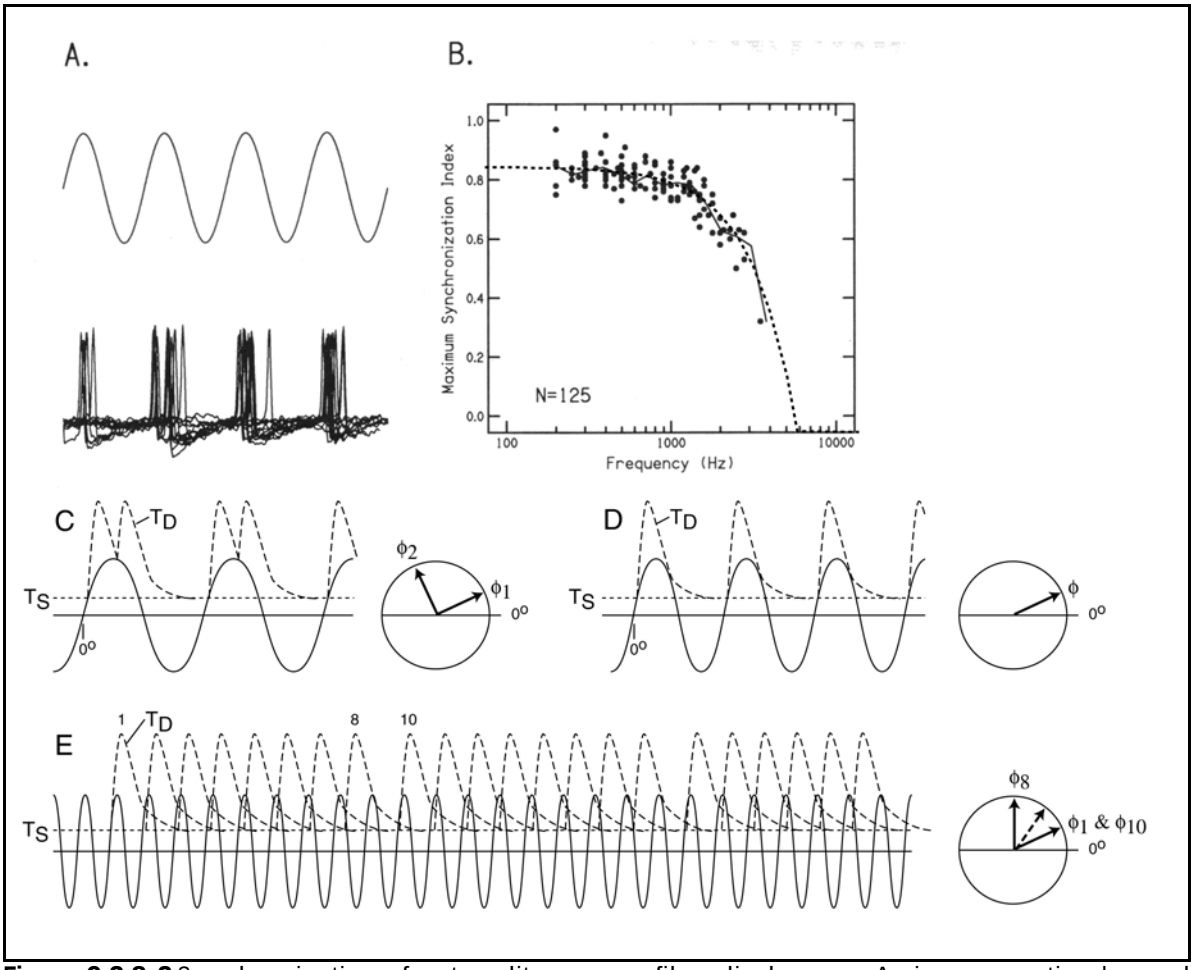

Figure 9.2.8-2 Synchronization of cat auditory nerve fiber discharges. A; sine wave stimulus and overlay of action potentials generated in response to a to a 200 Hz tone stimulus. B; synchronization index as a function of stimulus frequency. Solid line is a moving window average computed by Javel. Dashed line is theoretical exponential curve through data points. C; response of a driven reflex oscillator to a sine wave of frequency far below its refractory frequency limit. D; response of driven reflex oscillator by a sine wave stimulus larger than the static threshold amplitude, T_S, but at less than one half the refractory frequency limit. Dashed lines are the instantaneous threshold of the emitter-to-base circuit. The action potential is generated at a constant phase angle relative to the excitation as shown by the vector diagram at right. E; response of same oscillator to a sine wave stimulus of same amplitude but at twice the refractory frequency limit. Each stimulus pulse after the first encounters a higher instantaneous threshold. Note missing 9th and 18th pulses. The stimulus amplitude did not exceed the dynamic threshold during this interval. The phase diagram shows the variation in angle with pulse number during one set of stimuli. See text. Data from Javel, 1988.

Frame D shows the case more commonly found in the literature, whether due to natural or unnatural stimulation. The stimulus frequency, although higher than in frame C, remains below the refractory frequency limit of the neuron. As a result, each positive going half cycle of the stimulus causes the generation of an action potential. The threshold of the circuit rises abruptly during generation of the action potential but does not fall to a potential lower than the stimulus during the remainder of the half cycle. Prior to the start of the next half cycle, the dynamic threshold has returned to the level of the static threshold. The result is a synchronization index of nominally unity. One action potential is generated for each positive half cycle of the

stimulus. As shown by the vector diagram on the right, the phase angle of each action potential relative to the stimulus is nominally constant at $\phi = K$.

Frame E shows the case where the stimulus frequency exceeds the refractory frequency limit. In this case, the dynamic threshold of the neuron does not return to the static threshold before the next positive going half-cycle of the stimulus. As a result, the action potentials are generated at slightly different times, as shown by the increase in the phase angle, ϕ. The phase angle of the first pulse occurs at angle, ϕ_1. The phase angles of pulses two through eight increase gradually until a pulse is actually omitted. Pulse ten then occurs at the same phase angle as ϕ_1. This process repeats indefinitely until the amplitude of the stimulus fails to exceed the dynamic threshold during the positive half cycle.

As shown in frame E, the interval between pulses varies incrementally at this stimulus level and there is the potential for missing pulses. Such a pulse train will generate a PST histogram with pulses grouped around an average pulse-to-pulse interval. If the stimulus frequency is varied in amplitude incrementally, a point will be reached where the synchronization index will be precisely 1.0. At that stimulus value, the pulse-to-pulse groupings will become narrower and the histogram will frequently present a chopped appearance with the pulse-to-pulse spacing equal to the period of the stimulus.

Under clinical conditions, any pharmacological agent that causes the neuron to recharge more slowly than normal will likely result in lowering the synchronization index. Similarly, in the electrophysiology laboratory, any probe adding significant capacitance to the recharging circuit of the neuron will tend to reduce the synchronization index.

If the amplitude of the stimulus in the above figure is significantly reduced, the synchronization index may be impacted drastically.

Figure 9.2.8-3 shows the range of discharge rates achievable in a driven encoding neuron for very small changes in excitation intensity[85]. The sinusoidal stimulus was externally generated and each neuron exhibited a negligible spontaneous firing rate following destruction of the associated sensory neurons. As a result, each neuron exhibited a static action potential threshold of approximately 52 dB relative to the test set reference. For the lowest two stimulus frequencies, the action potential rate reached the stimulus rate within less than 2 dB. The synchronization index went from zero to a nominal 100% for a change of only 2 dB. At 600 Hz, the index went from zero to 100% for a change of only 6dB. The curve for 800 Hz, which is well outside the expected operating range for an encoding neuron, is incomplete. However, the index went from zero to a value near unity for a change of less than 8 dB.

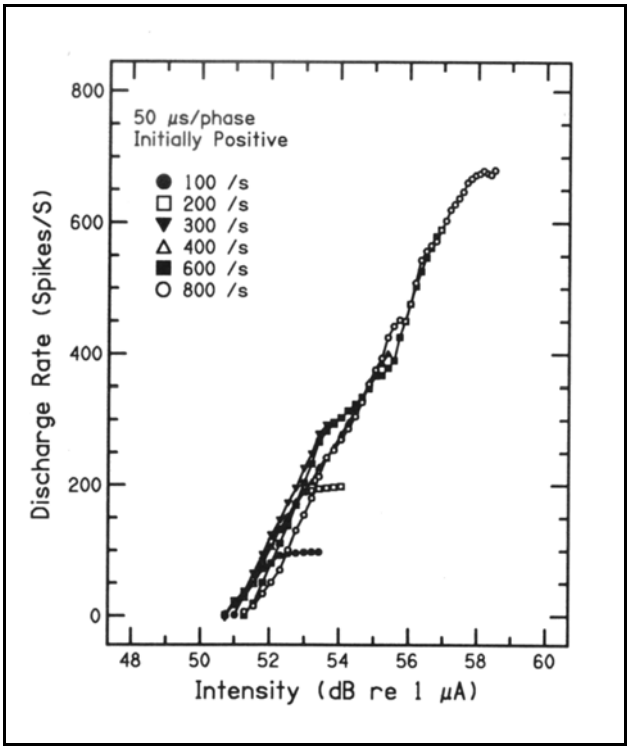

Figure 9.2.8-3 Action potential discharge rate as a function of intensity. The nerve fiber was responding to biphasic electrical pulse trains presented at rates ranging from 100 to 800 pulses/second. From Javel, 1988.

If this figure applied to free running

[85]Javel, E. (1988) Basic response properties of auditory nerve fibers *In* Altschuler, R. Hoffman, D. & Bobbin, R. *eds*. Neurobiology of Hearing: The Cochlea NY: Raven Press. Chapter 13, pg 284

encoder neurons, the illustrated performance would be suggestive of a modulation index on the order of 75% of the carrier frequency near 375 Hz. This is a very high index that would suggest nonlinear encoder performance and the generation of significantly more sidebands. While this nonlinearity may make interpretation of histograms relating to action potentials more difficult, the original modulation is fully recoverable without distortion by a properly implemented phase modulation decoder.

Javel provided another discussion related to pulse, as opposed to sinusoidal, stimuli (pages 273-6). While his figure 17.15 shows a constant synchronization index, the raw data in figure 17.14 does not support that position. The histograms for stimuli below 47.4 dB show distinctly different discharge phase angles. Even at 51 dB the distribution of phase angles is finite whereas his definition of the synchronization index requires the phase angle to be a constant for an index of 1.0.

9.2.8.3 The introduction of myelin in connection with the axon

As indicated above, a lengthening of the axon of the ganglion neuron relative to the bipolar neuron can introduce capacitance in shunt with the other impedance elements of the output circuit and lead to oscillation in the ganglion circuit. However once a critical level of capacitance is reached, additional capacitance is not desirable. It requires the Activa to switch more current between the input and output circuit to achieve the same level of action potential amplitude. To avoid this problem while achieving maximum axon length, a portion of the axon is wrapped in myelin. This process has the effect of thickening the dielectric between the axoplasm and the surrounding plasma and thereby lowering the effective capacitance per unit length of the axon.

9.2.8.4 The introduction of the Node of Ranvier in connection with the axon

Wrapping a significant part of the axolemma in myelin is an effective way of allowing the axolemma to be increased in length. However, it is not an adequate modification if the action potential is to be projected over distances beyond a few millimeters. In that case, active signal amplification is necessary. This can be provided by analog amplifiers while accepting the degradation of the signal waveform implicit in transmitting a pulse waveform over a relatively simple electronic transmission line, e.g., one without equalization stages to compensate for the normal phase distortion per unit length. The alternate approach is to regenerate the waveform. This actually involves replacing the received signal waveform with an alternate waveform, typically of similar waveshape. This regeneration of the waveform is the purpose of the Node of Ranvier. The process can be repeated indefinitely along the neuron since there is no cumulative waveform distortion in this approach.

9.2.8.5 Signal input via the poditic conduit

Although not a well-developed situation in the hearing literature, there are examples in the broader literature of ganglion cells exhibiting both dendritic and poditic arborizations. Such poditic arborizations suggest the poditic conduit accepts signals. These signals would be treated as out-of-phase with respect to the dendritic inputs. They could therefore subtract from the critical signal amplitude needed to initiate generation of an action potential. Such signal subtraction would normally be considered a stage 2 operation at the input to a stage 3 encoding neuron. If an exceptionally large signal was applied to the poditic terminal, it could be considered inhibitory.

9.2.8.6 Transfer function of the stage 3 encoding circuits

Figure 9.2.8-4 shows an ideal overall transfer function of a stage 3 projection circuit. The left half of the figure describes the transfer function of the encoding circuit. The input excitation can be of either the monopolar or bipolar type. However, the intrinsic absolute bias point is set differently in the two situations. The vertical scales shown in the figure are nominal. The important feature is they are linear with respect to time but not with respect to frequency.

The labels at the lower left refer to the typical parasol ganglion neuron, a neuron optimized for

monopolar signal processing. In the absence of any input, the quiescent point of the parasol neuron is near the negative most extent of its operating range. Its action potential generation rate will be near zero under this condition. Upon excitation, it will generate action potentials with a time period between pulses inversely proportional to the excitation potential. The label between the two frames defines the operating point of a midget ganglion neuron, a neuron optimized for bipolar signal processing. In the absence of any input, the quiescent point of the midget ganglion neuron is near the middle of its operating range. If biased near –16 mV, it will generate about fourteen action potentials per second on average (one pulse every 0.07 sec). Upon application of a signal, the action potential discharge rate can be driven up to about 200 pulses per second (one pulse every 0.005 sec) or down to only a few pps (one every 0.14 sec).

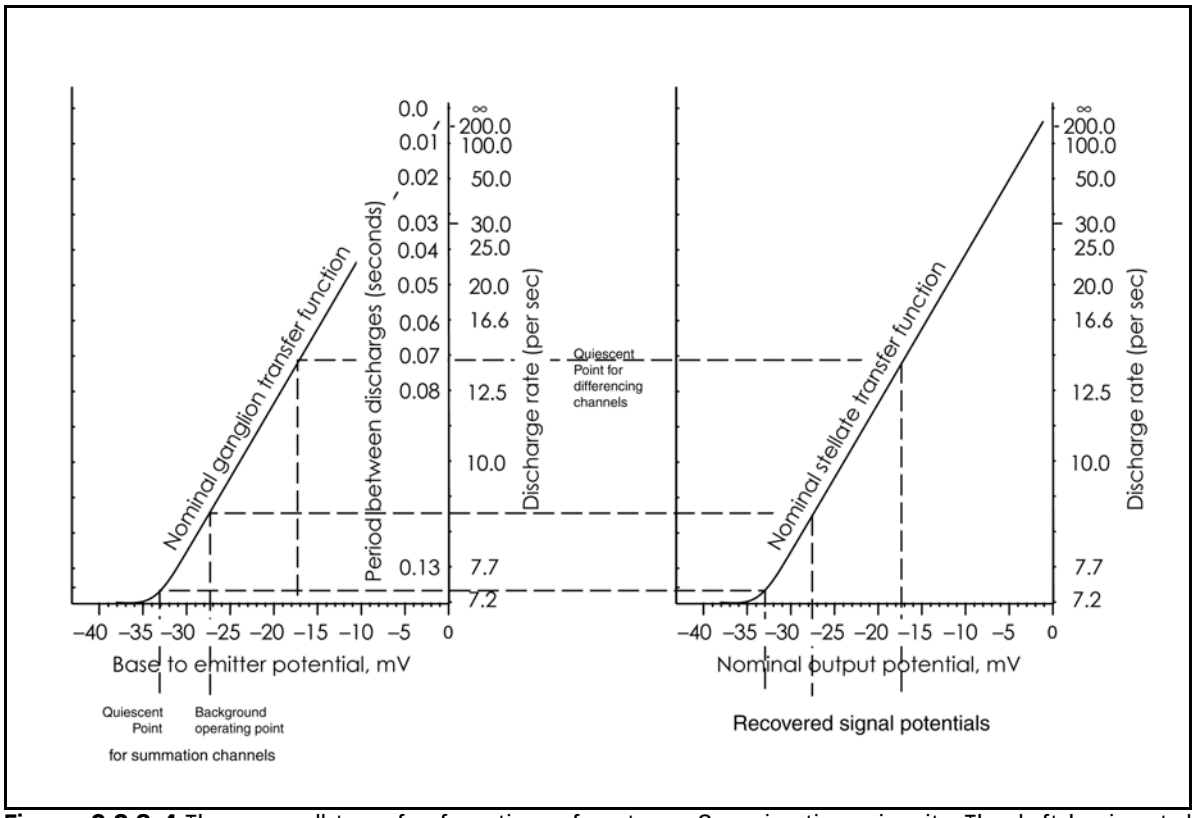

Figure 9.2.8-4 The overall transfer function of a stage 3 projection circuit. The left horizontal scale represents the absolute emitter to base (dendrite to podite) potential of the ganglion encoder circuit. The right horizontal scale represents the equivalent (but relative) voltage scale for the output of a stellite decoder circuit. The entry points for a monopolar input signal are shown at lower left. In the absence of any signal, the quiescent operating point of the parasol type ganglion neuron is shown as –33 mV. The nominal background operating point is shown as –27 mV. Under large signal conditions, the signal extends from near –33 mV to near zero mV. Under ideal conditions, one form of the stellite decoding circuit will reproduce these voltages perfectly as shown by the dashed lines proceeding to the lower right. For a bipolar input signal, the midget ganglion neuron is typically biased to – 17 mV. The excitation can drive this potential over the range of –32 mV to about –2 mV. Under ideal conditions, the pulse rate generated is shown by the vertical scales. These scales can be multiplied by a constant to cover different operating ranges. The pulse interval is linearly related to the excitation potential. The actual pulse frequency is reciprocally related to the excitation. As for the monopolar signal, an ideal bipolar stellite decoder will generate an output potential that is a faithful replica of the input excitation. See text.

9.2.8.7 Correlation with the literature

Tasaki presented an early "Two Stable State Theory" in 1968[86]. His discussion and theoretical foundation did not recognize the negative impedance characteristic of an Activa with a podal impedance. Absent the concepts of an Activa and internal feedback, his electrical circuit, with arbitrary variable resistors, and his explanation of the measured I-V characteristic (figure 7) is less than satisfying. His description of what constitutes an action potential apparently includes any square wave.

As expected from the earlier discussion, the majority of the ganglion neurons of stage 3 are rate-limited to less than 300 action potential pulses per second. This is true of both the auditory and visual systems. This limitation on the maximum acceptable rate of about 300 Hz has been discussed frequently in the literature[87]. However, the discussion has been largely anecdotal and the constellation of neurons examined has been far from comprehensive. On the other hand, special stage 3 neurons associated with the source location subsystems of hearing and the ocular pointing functions of vision are known to operate at up to 550 pps. Johnson and others have recorded pulse rates of up to at least 550 pps in cats[88].

Inoue et al[89]. presented additional data, compatible with the theory presented here, on how the neural response is affected by pharmacological and temperature changes.

Miller et al. have provided recent data on the refractory characteristics of stage 3 neurons in cats[90]. They recorded intercellular signals of low amplitude (a few millivolts) from the auditory nerve following electrical stimulation of the basal turn of the scala tympani. The deviation of their data from a Gaussian distribution in figure 5 shows the limited extent of their data set. Their figure 10 shows the exponential character of the refractory interval clearly. Their introductory discussion notes the variation in the refractory interval among different neurons before settling on a mean value of 330 microseconds. They made an interesting observation that the spontaneous rate of action potential generation was zero in their chemically deafened cats (p. 217). This would confirm the typical spontaneous rate was a result of uncontrolled external noise detected by the sensory neurons.

Pfeiffer & Kim provided very early data on the auditory nerve of the cat following a long experimental period (five years)[91].

Palmer & Evans have provided good data that can be used to quantify the performance of the stage 3 projection neurons in the cat[92]. The data was recorded at either the auditory nerve

---

[86]Tasaki, I. (1968) Nerve excitation: A macromolecular approach. Springfield, Ill: Charles C. Thomas also in Tower, D. (1975) The basic neurosciences, vol. 1 NY: Raven Press pg. 177-195

[87]Carlyon, R. & Deeks, J. (2002) Limitations on rate discrimination *J Acoust Soc Am* vol. 112(3), pt 1, pp 1009-1014

[88]Johnson, D. (1980) Op. Cit. pg 1116

[89]Inoue, I. Kobatake, Y. & Tasaki, I. (1973) Excitability instability and phase transitions in squid membrane under internal perfusion with dilute salt solutions. Biochem. Biophys. Acta. vol. 307, pp. 371-377

[90]Miller, C. Abbas, P. & Robinson, B. (2001) Response properties of the refractory auditory nerve fiber *JARO* vol 2, pp 216-232

[91]Pfeiffer, R. & Kim, D. (1972) Response patterns of single cochlear nerve fibers to click stimuli: descriptions for cat *J Acoust Soc Am* vol. 52(6) pt 2, pp 1669-1677

[92]Palmer, A. & Evans, E. (1982) Intensity coding in the auditory periphery of the cat: responses of cochlear nerve and cochlear nucleus neurons to signals in the presence of bandstop masking noise *Hear Res* vol. 7, pp 305-323

or the cochlear nucleus in response to a node A stimulus. While they did not specify whether their data applied to the stage 3 neurons at the input or the output of the cochlear nucleus, it can be assumed it applied to the input because of its simple relationship to the stimulus.

Javel and his coworkers have provided very valuable data on the operation of the encoding neurons under a variety of natural and unnatural stimulus conditions. Lacking a theoretical model, their test signals have taken on unusual characteristics and their empirical results have not always been analyzed optimally. Javel has provided a complex probability histogram for the response of a single cell to a biphasic pulse train introduced electrically into the cochlear fluids[93]. The key to interpreting this histogram is to recognize the sub-harmonic relationship between the stimulus frequency and the action pulse frequency.

Delgutte[94] has provided a set of histograms of unique precision that can help define the two classes of signals defined by Liberman in 1978. These histograms tell a much larger story than they were designed to tell. The waveforms shown represent the output of stage 3 ganglion neurons responding to the output from the stage 1 sensory neurons. The acoustic stimuli were synthetic vowels and other complex signals. The material in Delgutte provides a good introduction to the relationship between the vocalization of sound and the action potential pulse frequencies involved. He makes an important observation when speaking of synthetic stimuli. "Unlike natural vowels, the stimuli have only one peak in their spectrum and cannot, in general, be identified by listeners as a specific vowel."

9.3 The actual codes used in signal propagation

There has long been a debate as to whether the action potential pulses are deterministic or probabilistic in character. As van Drongelen noted, the electrophysiologist easily demonstrates the action potentials are deterministic following their stimulation[95]. However, the neurophysioloogists have routinely asserted the action potentials are probabilistic because they can not achieve repeatable results in their experiments. The difference is clearly due to their inadequate understanding of the circuits within a stage 3 neuron. The stage 3 neuron is completely capable of incorporating a lead lag network of sufficient complexity prior to the pulse generating Activa to cause the problems encountered by the neurophysioloogist.

> As an aside, the conceptual sketch of a nerve fiber in figure 14.1 of van Drongelen shows he does not appreciated that there is no "vertical" membrane current through the axon segment of a stage 3 myelinated neuron.

Bershadskii has recently provided a series of papers describing the *in-vitro* operation of selected neurons operate in a chaotic (deterministic via a complex function) model[96,97]. He suggests his neurons are excited by random noise. He did not show the actual output waveforms of any neuron but made computations based on a correlation function ostensibly representing a series of action potentials recorded *in-vitro*. Although noting the nominally equal height of the action potentials from a single neuron *in-vivo*, he did not indicate the amplitude for his action potentials. Specifying this height is critically important in determining whether a pulse stream is a real set of action potentials from a stage 3 neuron or merely the result of forced oscillation

---

[93]Javel, E. (1988) Acoustic and electrical encoding of temporal information *In* Miller, J. &. Spelman, F. *eds*. Cochlear Implants" Models of the Electrically Stimulated Ear. Englewood Cliffs, NJ: Prentice Hall Chapter 17

[94]Delgutte, B. (1980) Representation of speech-like sounds in the discharge patterns of auditory-nerve fibers *J Acous Soc Am* vol. 68(3), pp 843-857

[95]van Drongelen, W. (2007) Signal Processing for Neuroscientists. NY: Elsevier pg 220

[96]Bershadskii, A. (2011) Prime numbers and spontaneous neuron activity http://arxiv.org/abs/1103.1167v1

[97]Bershadskii A. (2010 Broken chaotic clocks of brain neurons and depression http://arxiv.org/abs/1012.1611v2

in a neuron due to an intentional or incidental bias change associated with the probe protocol.

> Wikipedia provides a nice brief overview of the correlation function and its variants. Although unsigned, the material does reference a recent text[98]. It does develop the inconsistency of notation among scientific disciplines at even this late date. "Different fields of study define autocorrelation differently, and not all of these definitions are equivalent. In some fields, the term is used interchangeably with autocovariance."

Much of what Bershadskii asserts is correct from a mathematical perspective. However, he is unable to show that his responses are valid under *in-vivo* situations or to describe the actual limitations on the application of his findings. He did not address the actual encoding algorithm of the neural system although his results are compatible with the neural algorithm. This algorithm is developed below. His correlation function suggests his neuron was synchronously excited rather than by a random input. It exhibits an initial pulse followed by a long tail with a ripple suggestive of the presence of a harmonic component (probably due to the nonlinear mechanisms present).

As recently as 2005, Ventriglia & Di Maio[99] have asserted the neural code presumably associated with the peripheral neural system was unknown. "The problem of the code used by brain to transmit information along the different cortical stages is yet unsolved. Two main hypotheses named the rate code and the temporal code have had more attention, even though the highly irregular firing of the cortical pyramidal neurons seems to be more consistent with the first hypothesis." Their discussion does not address the details and options utilized in stage 3 signal projection. They do not identify the requirement of any useful (intensity–related stimulus) code to identify clearly the time of the initial event.

This section will describe the phasic code actually used in the stage 3 neural system and how the information encoded by the ganglion neuron can be recovered by a stellate neuron, including a series of examples demonstrating the solution to the above neurophysiologists' problems.

9.3.1 The Neural Code used in the magnacellular (brightness) and other monopolar pathways

The optimum parasol type (monopolar input) ganglion neuron should show maximum sensitivity to stimuli without introducing significant noise into the neural pathway. This condition calls for the quiescent emitter (dendrite) voltage, Ven(quiescent), to be more negative than but as close as practical to the cutoff voltage labeled point 2. This maximizes the dynamic range available for the signal, between cutoff and saturation and accepts the generation of an occasional extraneous action potential due to analog noise.

The pulse train(s) generated by parasol type (monopolar input) ganglion neurons are described in the engineering literature as representing time-delay encoding or modulation. This type of modulation is characterized by packing more information into a given signal space than nearly any other form of modulation. Time-delay encoding is a more sophisticated form than a simple rate-based code. It is a place code. Time-delay encoding generates an initial pulse that occurs earlier the more intense the stimulus. Subsequent pulses occur closer together for higher intensity stimuli, as in rate-based coding.

The time-delay code used in the neural system is a (temporal) place code and not a rate code. The time of occurrence of the first pulse is relevant and provides important information related to the intensity of the stimulus. The time interval before the next pulse is linearly proportional to

---

[98]Dunn, P. (2005) Measurement and Data Analysis for Engineering and Science, New York: McGraw–Hill, ISBN 0-07-282538-3

[99]Ventriglia F., Di Maio V. (2005) Neural Code and Irregular Spike Trains. In: De Gregorio M., Di Maio V., Frucci M., Musio C. (eds) Brain, Vision, and Artificial Intelligence. BVAI 2005. Lecture Notes in Computer Science, vol 3704. Springer, Berlin, Heidelberg

the stimulus amplitude during the that interval. The reciprocal of this interval, the pulse rate, is not linearly related to the stimulus and is in fact asymptotic.

If the lead-lag network of a ganglion neuron creates a flat frequency pass band from the sensory neuron to the ganglion Activa, the first action potential departs from its quiescent level immediately upon the input exceeding the threshold level of the circuit. This initial pulse is used as an alarm mode signal in the subsequent circuits of stage 4. Subsequent pulses occur with a decrease in time delay that is linearly proportional to the amplitude of the stimulus above threshold.

In typical laboratory experiments, the probe impedance is usually many megohms (compared to the synapse impedance of about 0.25 megohms (**Hearing, figure 3.6.2-1**). As a result, parametric excitation of a ganglion neurons usually employs a constant current source that charges the input capacitor, C. The result is an emitter to ground voltage that is a linear ramp up to the threshold level. The capacitor is discharged during the pulse interval and the ramp begins again. This is the condition seen between points 5 and 2 in the above dendrite potential waveforms.

More details related to time-delay modulation in monopolar neural circuits can be found in Section 14.2.2 of "Processes in Biological Vision[100]."

If care is taken in experiment design, it is possible to ensure a simple bandlimited step input to the encoding portion of the stage 3 ganglion neuron(s) associated with monopolar signals (such as brightness). The absolute voltage levels relative to the neural matrix and the polarity of the step are significant. The transient performance will vary with this polarity.

9.3.1.1 The IRIG description of the code

The code used in monopolar neural signaling was categorized by the Inter Range Instrumentation Group (IRIG, a for-runner of NASA) during the 1950's in Standard 106-96. The monostable pulse stream is described as a return-to-zero (RZ) type of code. It is described as an analog representation in the pulse domain of an analog signal. The actual time-delay code is described as a pulse position modulation (PPM) code.

> In the IRIG and in the neural PPM code, the time of the first pulse is associated with when the event took place and the interval between subsequent pulses describes the intensity of the stimulus at the start of that interval. This type of code is also known as a "phase code" or a "place code."

The instrumentation industry has moved on with the advent of the digital computer and the emphasis of the IRIG today is totally on pulse code (rather than pulse position) modulation. All of the files of the IRIG are in a repository at the University of Arizona Libraries.

9.3.1.1.1 An IRIG encoder compatible with a stage 3A neuron

Figure 9.3.1-1 illustrates a circuit used in a typical IRIG encoder of 1965[101]. The circuit configuration within the dashed line is the fundamental oscillator, based on a commercial NPN transistor, 2N3553. The circuit is essentially identical to that in the figure of Section 9.xxx. Only the polarity of the power supply is reversed to accommodate conventional telemetry practice. This requires use of an NPN transistor instead of its PNP equivalent.

---

[100] Fulton, J. (2004) Processes in Biological Vision http://neuronresearch.net/vision/pdf/14Tertiary.pdf

[101] D'Elio, C. & Poole, J., [RCA] (1965) Single-Transistor, L-Band Telemetering Transmitter. University of Arizona Libraries http://hdl.handle.net/10150/578467

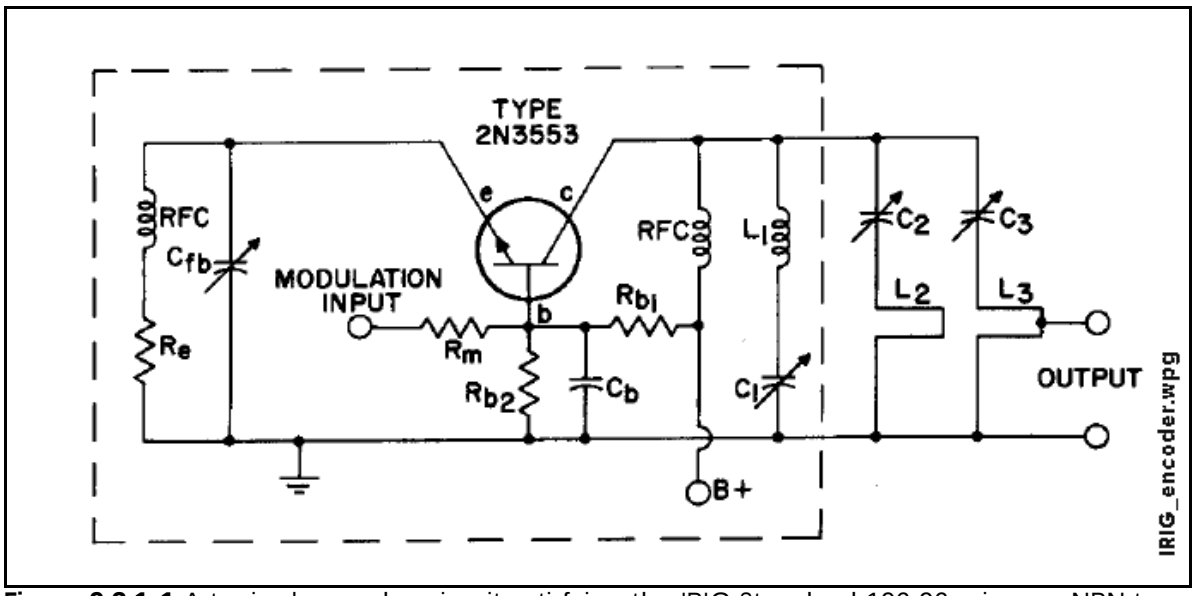

Figure 9.3.1-1 A typical encoder circuit satisfying the IRIG Standard 106-96 using an NPN type instead of a PNP type semiconductor device. The circuit outside of the dashed box is used to raise the frequency of the output pulse train. It is not needed in the neural application of this circuit. It can be replaced by a coaxial cable or in the neural case, by a myelinated axon. RFC; radio frequency choke. See text. From D'Elio & Poole of RCA, 1965.

In this example of a commercial encoding circuit, the analog signal is introduced at the base (b) or inverting terminal of the transistor. It could just as easily be introduced at the emitter (e) terminal.

The RFC employed on the right in the figure is used to prevent pulses formed in the collector circuit from leaking back into the base circuit. This RFC will prevent the analog waveform from being contaminated by the pulses in the collector circuit. In neural circuits, whether such an RFC is present is important. When a oscilloscope probe is attached intra-cellularly to the soma with the RFC present, the recorded waveform will be pure analog. If it is attached in the absence of the RFC, the recorded waveform may show the summation of the analog driving waveform and the pulse output waveform. It is up to the investigator to understand this choice and take it into account when discussing his data.

The complimentary, PNP, type to be used in emulating a biological neuron or Node of Ranvier consists of the 2N2904 series of discrete devices.

As discussed in the earlier subsection, this circuit can be made to generate pulses continuous, modulated by the analog signal input OR made to only generate pulses in response to the analog input by varying the values of R_{b1} and R_{b2}.

9.3.2 The Neural Code used in the parvocellular (chrominance) and other bipolar pathways

The optimum midget type (bipolar input) ganglion neuron should accomodate the largest amplitude bipolar signal without causing significant distortion. This condition calls for the quiescent emitter (dendrite) voltage, Ven(quiescent), to be in the middle of the dynamic range between the emitter cutoff and saturation voltages. As a result, the same ganglion circuit as used for the magnocellular pathways is biased to provide a continuous series of action potentials that can be phase modulated to encode the amplitude information associated with the bipolar analog stimulus.

Being a place code, the action potential stream generated by the ganglion neuron will exhibit a discontinuity very near the time of any major change in the stimulus. However the value of that change may not be apparent until the next clearly defined time-delay interval (between the subsequent two pulses). This fact has long been recognized in the electrical engineering community and it is memoriallized in both the NTSC and PAL analog color television standards. As in these systems, the neural system uses the positive region of the bipolar signal to encode "green" information and the negative region to encode either "blue" or "red" information (there are two chrominance channels in the large mammals).

If care is taken in experiment design, it is possible to ensure a simple bandlimited step input to the encoding portion of the stage 3 ganglion neuron(s) associated with bipolar signals (such as chrominance). Being a bipolar channel, the absolute starting and ending voltage levels of the step relevant to the neural matrix are significant. It is frequently desirable to generate a monopolar stimulus starting from the nominal quiesecent level of the input circuit.

9.3.3 The Transfer Functions for the Sum & Difference Neural Codes

The following figure shows the nominal transfer function for the ganglion neuron; biased for monopolar operation on the left and for bipolar operation on the right. Note the linearity of the transfer function with respect to time delay interval. Conversely, the transfer function is highly nonlinear (in fact assymptotic) with respect to the rate of action potential generation.

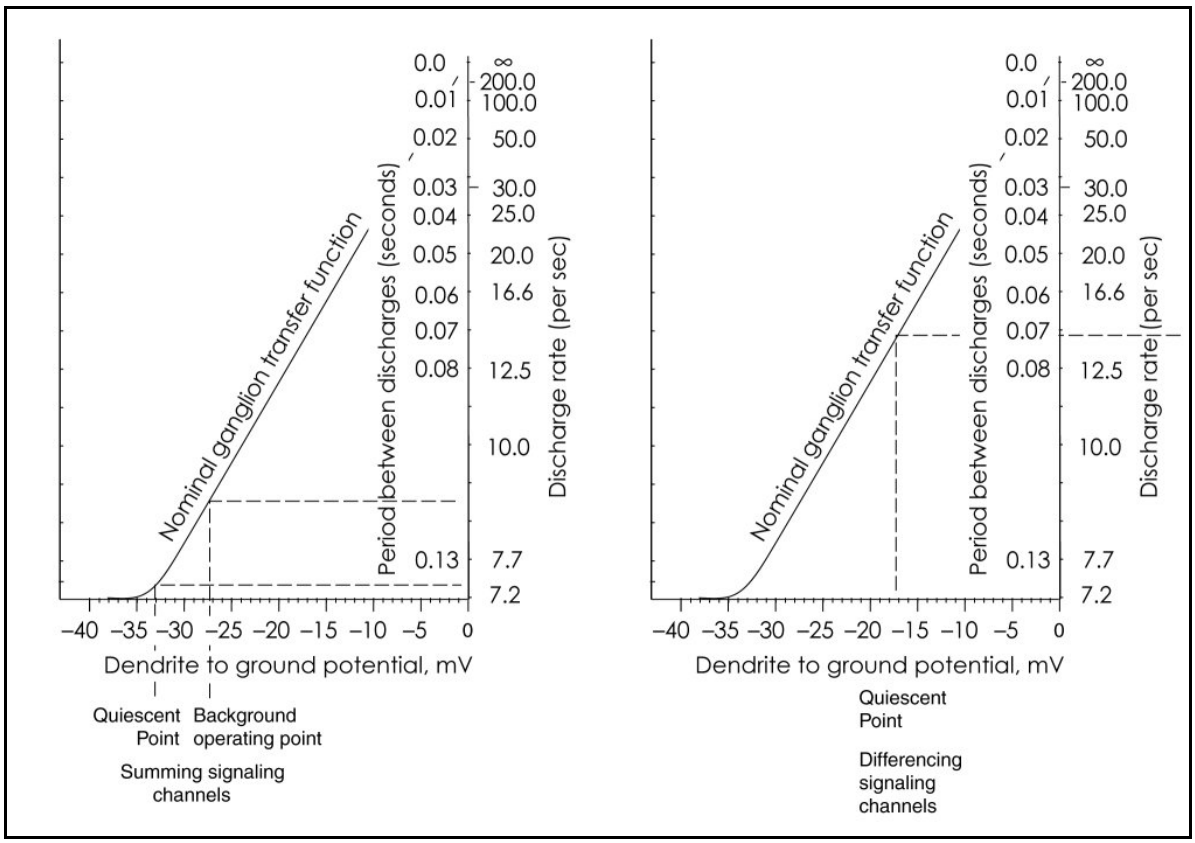

Figure 9.3.3-1 The steady state transfer functions of the stage 3A encoding neurons. Left; the steady state transfer function of the monopolar (summing channel) encoding neurons. The neuron is biased to generate less than 8 pulses per second in the absence of stimulation. The generated pulses are frequently irregular when measured *in-vitro* due to extraneous signals. Right; the steady state transfer function of the bipolar (differencing channel) encoding neurons. The circuit is typically biased to generate about 15 pulses per second in the absence of stimulation. The pulses are equally spaced under *in-vivo* conditions. Note the linear vertical scales for intervals between pulses as opposed to the logarithmic vertical scales for the frequency generated for a static dendrite to ground potential. Cutoff typically occurs near –32 mV dendrite to ground potential.

9.3.4 Examples of sound encoding

The following figure provides simple examples of signal encoding. The left frames show the typical quiescent condition at the top (output above the related input), a phasic signal resulting from stimulus by a constant amplitude analog signal, and a phhasic signal resulting from a higher amplitude analog signal. In both cases, both analog signals cause a first phasic action potential very near the start of the analog signal.

The right frames show a more complex situation. The top frame shows a constant phasic signal in the absence of any analog input stimulus. The middle frame shows the phasic response to a two-step positive-going analog stimulus, while the lower frame shows the response to a two-step negative-going analog stimulus. In both cases, a change in the pulse spacing occurs with the start of the analog waveform. Note that large negative going analog signals can drive the resulting phasic signal to very long pulse-to-pulse spacings. These long intervals greatly restrict the transfer of information by the system.

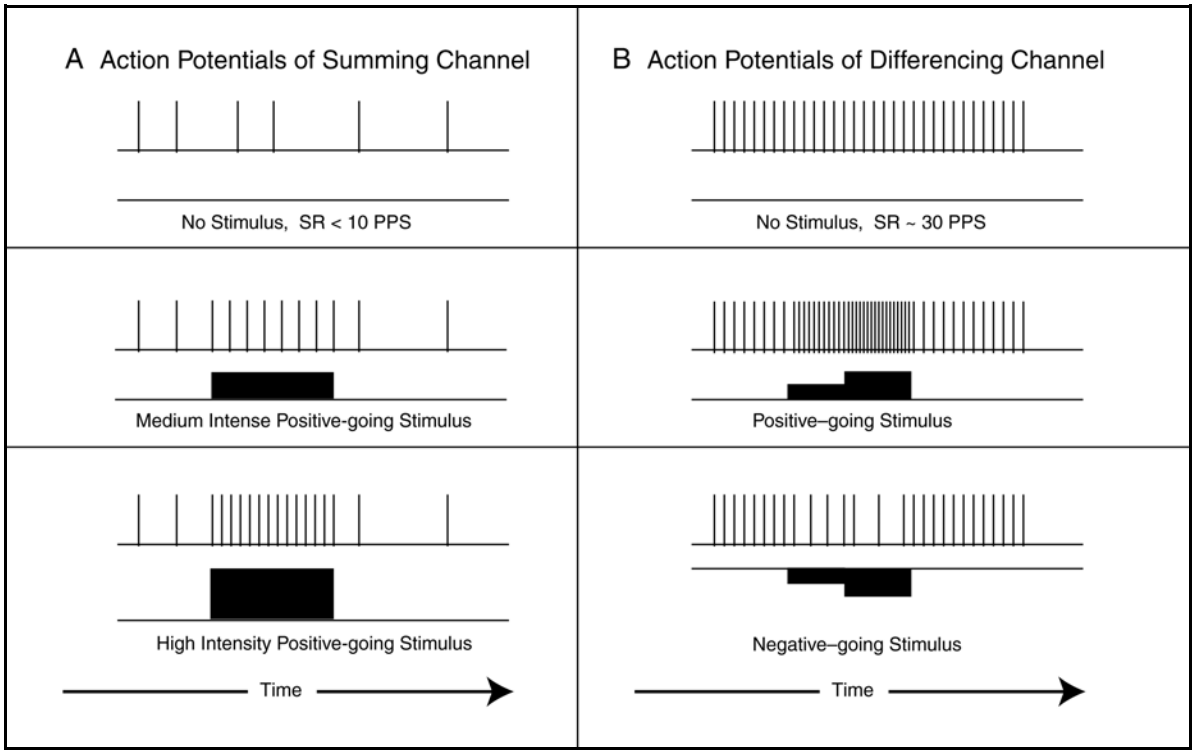

Figure 9.3.3-2 Examples of the place code used in the neural system. The code is the same but its application to the summing (A) and differencing (B) channels is fundamentally different. In A (top) only random noise spikes occur in the absence of stimulation. Stimulation causes the generation of an organized set of spikes with their spacing indicative of the intensity of the stimulation. In B (top), a set of equally spaced spikes are created in the absence of stimulation. Upon stimulation by positive-going stimuli, the interval between spikes decreases in proportion to the amplitude of the stimulus. Conversely, negative-going stimulation causes a proportionate increase in the interval between spikes in proportion to the intensity of the stimulus.

The maximum action potential pulse rate is difficult to specify. Under *in-vivo* conditions, the maximum rate reported in the literature is typically above 200 but less than 500 pulses per second. Under *in-vitro* conditions, and particularly parametric excitation conditions, rates up to 900 pps have been reported. However, it is not clear that these high rates are significant and can be decoded without distortion by the stellite neurons discussed in the following pages of this subject set.

9.4 A functional Node of Ranvier as an exemplar of a *type 2* (phasic) conexus

The geometry and material properties of the Node of Ranvier have been studied in great detail within the cytology community. However, these studies have not led to an understanding of how the Node operates.

This section will develop in detail the morphological and electrophysiological aspects of a Node of Ranvier in its role as a type 2 conexus in a stage 3 neuron. This role requires the conexus to regenerate action potentials received from a previous conexus associated with the signal projection (stage 3) function. A complete understanding of the operation of the conexus within a Node of Ranvier leads directly to understanding the signal encoding function performed by a similar conexus in the ganglion cells of the visual system. It also explains the operation of a variety of similar encoding cells, such as the Purkinje cells of the cerebellum.

The Node of Ranvier consists of two parallel paths between contiguous axon segments. The

primary signaling path is discontinuous with respect to the axoplasm of the pre-NoR terminal and the dendro/axoplasm of the post NoR segment. Simultaneously, there is a continuous chemical path paralleling the signaling path and responsible for the homeostasis of the complete stage 3A neuron. The chemical path is considerably larger than the signaling path and much easier to photograph, particularly when using light microscopy. When using electron microscopy, it is extremely difficult to orient the axon of the neuron to differentiate between these two paths.

From the signaling perspective, the Node of Ranvier forms the simplest, and most accessible, amplifier in the neural system. It exhibits an axial symmetry and is recognized to be a region of action potential regeneration based on its description as being a site in the salutatory transmission of the neural signal. In this context, there are no analog signaling circuit element related to the NoR. Its sole purpose is to generate an action potential at the collector terminal of its Activa any time a monopulse of sufficient amplitude is received at its input terminal (the emitter of the Activa).
If the functional operation of these features of the NoR of a projection neuron can be understood in detail, it becomes much easier to understand the operation of other active locations.

9.4.1 Merging morphology and electrolytic topology

While the functional performance of the NoR is very simple, the pre-NoR and post NoR regions of the associated axon segment (particularly with regard to their myelinated sheaths) are not.

The Electrolytic Theory of the Neuron provides the first detailed interpretation of the complex morphology of the Node of Ranvier. It shows that the various paranodal areas are in fact electrical matching filters between the lumped parameter circuit of the node and the distributed parameter character of the remainder of the axon segments (internodes). These regions are responsible for;

• receiving a propagating energy signal and changing it back to an electrical charge signal diffusing into the emitter area of the NoR, and

• accepting a higher amplitude regenerated action potential, converting it into a propagating energy signal and launching it along the next axon segment.

Berthold provide a thorough geometric analysis of a typical Node of Ranvier, exterior to the axon itself. However, the analysis was based on low magnification imagery that does not support discussions at the molecular and membrane level. There is considerable imagery available at higher magnifications. This imagery provides much of the foundation for the following discussion. **Figure 9.4.1-1(A)** provides a composite schematic of the Node of Ranvier at a detailed level. The principal modification is to show the reticulum, the area within the dashed lines and also called the smooth-surfaced endo-plasmic reticulum (SER), of each axon segment branching to contact the specialized bilayer membrane on each side of the Activa within the node[102]. These specialized areas occupy regions of the nodal gap usually labeled recesses. The specialized areas need not extend around the entire circumference of the lemma at each location[103]. This reticulum branching arrangement is analogous to the arciform structure seen in pedicle micrographs. An additional reticulum area, shown in (B), is found within the poditic area and extending from the base of the Activa to the specialized area of the nodal lemma. An additional modification expands the area of electrostenolytic activity to show two zones. The first zone is shown by heavy solid lines at three points of the plasma lemma. This zone consists of the specialized membrane and its electrostenolytic coating. The

---

[102]Berthold, C. (1978) Morphology of normal peripheral axons. *In* Physiology and Pathobiology of axons, Waxman, S. Ed. NY: Raven Press pp. 42, plate 17. This theory calls for a third area of SER at or beyond the left edge of this figure.

[103]Berthold, C. (1995) Morphology of normal peripheral axons. *In* The Axon, Waxman, S. Kocsis, J. & Stys, P. Ed. NY: Oxford University Press pg. 36

second zone is shown crosshatched and is next to the exterior surface of each specialized membrane. It is the site of local bioenergetic material storage (and/or recycling).

The electrical modifications consist of showing the input current, I_{in}, arriving at the node from the pre-nodal axon segment, the output current, I_{out}, going from the node into the post nodal axon segment and the three principal currents passing through the nodal gap in support of the active circuit within the node. These currents will be discussed in detail below.

The diffusion modifications consist of showing a manifold, M, within the nodal gap where bioenergetic material can be exchanged among the three bioenergetic material storage areas (adjacent to the exterior plasma membrane of the axon) and with the vascular system outside the nodal gap. This exchange is shown by the darker gray areas in the figure. The details of the overall circulation of the bioenergetic materials will not be discussed in detail.

In the past, the electrical characteristics of the node have always been discussed using simple circuit diagrams based on direct currents flowing through linear networks, consisting of lumped constant[104],[105],[106]. Leakage through the wall of the axon segment has usually played a significant role in these equivalent circuits. Only a conceptual discussion of the actual current flow has been offered. To understand the actual situation, and the importance of distinguishing between the use of probes penetrating the axolemma versus those sensing the electrical field within the nodal gap, exploring the electrical model under dynamic conditions is necessary.

Figure 9.4.1-1(B) expands on (A). For simplicity, it only shows an expanded view of the upper half of that figure, which is assumed to be axially symmetrical for this discussion. The three specialized regions are shown separated by 7-layer membranes where the axseglemmas merge with the nodal lemma. These 7-layer, sometimes called 5-layer, structures form tight junctions. They are not electrically active. The membranes need not be asymmetrical individually. The regions associated with the specialized membrane areas are shown in additional detail. Note that three open boxes have been shown on the inside of the plasma membrane, one associated with each specialized lemma. These boxes represent the internal coating of the lemma in these areas frequently discussed in the literature. Most current literature does not subdivide this undercoating into three separate regions. However, assuming this coating is subdivided to match the subdivision of the SER into three regions is reasonable. See Berthold reference above. The important point is that these internal coatings are not in intimate contact with the membranes[107]. They may or may not be important from an electrical perspective.

---

[104]Ritchie, J. (1995) Physiology of the axon. *In* The Axon Op. Cit. pg. 69

[105]Stys, P. & Kocsis, S. (1995) Electrophysiological approaches to the study of axons. *In* The Axon Op. Cit. pg. 330

[106]Zagoren, J. & Fedoroff, S. (1984) The Node of Ranvier NY: Academic Press pg. 111

[107]Pannese, E. (1994) Neurocytology NY: Thieme Medical Publishers pg. 148

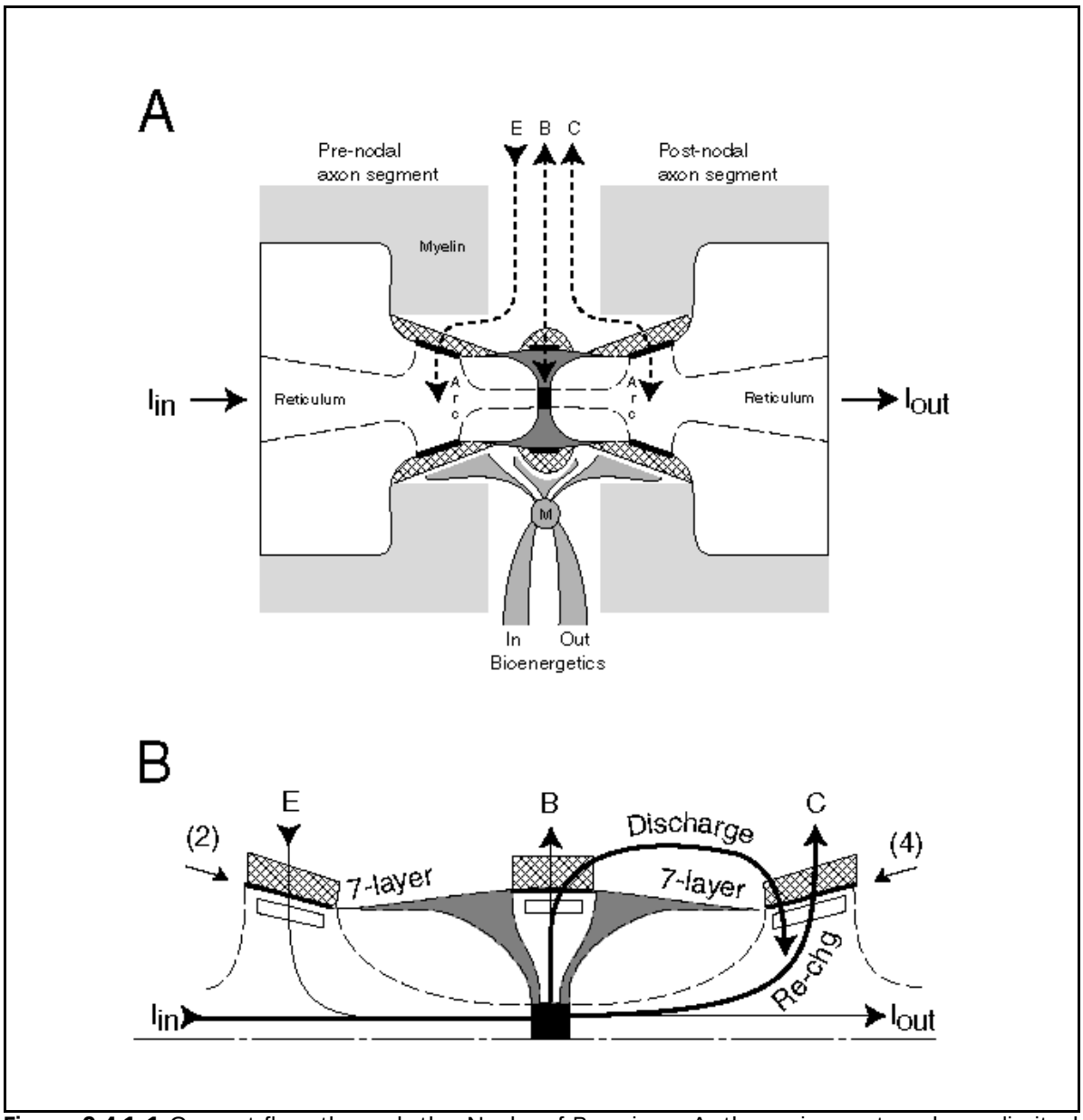

Figure 9.4.1-1 Current flow through the Node of Ranvier . A; the quiescent node. a limited current may flow from the emitter to the base as shown by arrows. Virtually no current flows in or out of the collector. B; during stimulation, the currents are complex because of the currents flowing through the Activa (active device) constituting the regeneration amplifier of the NoR. In the region between the two sections of myelination, the propagating signal is transferred back to a diffusing signal. The diffusing signal is funneled into the emitter area of the Activa as I_{in}. If it creates a potential that raises the emitter/base potential to exceed threshold, the axon potential will be discharged through the base terminal as shown. Once started, this discharge is independent of the emitter/base potential and is represented by the output current, I_{out}.. Iout stimulates a new propagating signal within the myelinated portion of the next axon segment. When the amplification factor of the Activa is reduced sufficiently, the discharge phase terminates and the recharging of the axoplasm chamber begins via the collector bias terminal labeled C. Until the collector (axoplasm) is restored to its resting potential, the Activa is in a refractory condition and cannot be stimulated to generate a second action potential. See text.

The weight of the lines indicating the direction of the current flow suggests the general amplitude of the current at that location. However, the actual flows are functions of time that will be discussed below. There is a bias potential introduced at (2) due to the electrostenolytic process occurring at the surface of the specialized lemma. There is little current flow at E due to this bias potential. The purpose of the bias is to maintain a stable voltage on the emitter of the Activa within the node. The primary input current is that shown as I_{in}. This current passes between the emitter and the base of the Activa. Following paragraphs will separate the electrical operation of the node into three time intervals;

+ the initial period when the Activa is operating in a linear mode,

+ the discharge period when the leading edge of the action potential is being generated, and

+ the recharge period when the trailing edge of the action potential is being generated.

During the initial period, the current I_{in} causes an equal current to flow from the base to the collector of the Activa. Because of this action, the net current through the base, labeled B, is essentially zero. When the voltage between the emitter and the base reaches a threshold value, the circuit begins to do a one pulse oscillation. This causes a large additional current to flow through the Activa thereby discharging the capacitor in the collector circuit. However, this current flows out of terminal C and back into terminal B. There is no appreciable current flow through the nodal gap during this interval. After discharge of the capacitor in the collector circuit, the Activa becomes cutoff and the capacitor recharges through the power supply impedance (4). As this process proceeds, current emanates from terminal C and passes through the nodal gap. This is the current usually sensed by a non-penetrating probe introduced into the nodal gap.

9.4.1.1 Detailed operation

The exact function of the so-called nodal apparatus, within the nodal gap, has been sought a long time. Its complexity at first glance appears excessive for the function required--which has also been poorly understood. This section will describe in detail the functions carried out by the active portion of this apparatus. The sophistication of the Node of Ranvier exceeds that of almost any man made electrical circuit--and it is clearly an electrical circuit. No hint of any so-called chemical neurotransmitters has been found, although many materials enumerated as neurotransmitters are employed in the electrostenolytic processes powering the electrical circuits. **[xxx move part of this up to old 10.5.4]** It has been optimized from perspectives man seldom considers. The following discussion will probably overlook some of these perspectives.

+ Although the active circuit operates at a relatively low impedance during regeneration in order to drive the following transmission line properly, it exhibits a high input impedance while operating in the initial linear mode. This high input impedance lowers the requirements on the preceding transmission line segment.

+ To increase the input impedance of the active circuit further, the diode associated with V_{ee} exhibits a very high impedance at low input signal levels.

+ To reduce the demands on the impedance of the input transmission line during signal regeneration, the active circuit employs two separate capacitors and exchanges charge between them. Using this technique, there is no requirement for the input transmission line to provide a significant amount of power to the emitter circuit of the Activa.

+ To reduce overall power consumption, a significant part of the power drawn from power source V_{cc} is returned to the power source V_{ee} during the recharging phase of regeneration. This can reverse part of the normal electrostenolytic process at E. The reconstituted bioenergetic materials can be reused later or transferred to the power supplies at B or C by diffusion within the nodal gap (near the recesses).

+ To reduce interference between adjacent neurons, essentially all of the current flow associated with regeneration occurs within the cylindrical region formed by the narrowest

passage of the nodal gap (dimension G_2 in Berthold). Only the return current paths associated with the input and output signal actually pass through the nodal gap.

+ To avoid low reliability or premature failure, the threshold of the regenerator circuit is relatively low compared with the received signal amplitude. Some estimates have this safety margin at 5:1, a ratio supported by the analysis of this work.

Analyzing the overall circuit within the node by time interval is necessary to understand the operation of the node. **Figure 9.4.1-2** presents the full circuit diagram of the Node of Ranvier (A), a set of waveforms describing the operation of this circuit (B), and a very simplified model (C) suitable for overview discussions. Note the three individual power supplies consisting of a battery and a diode in series in (A). The complete circuit diagram of each electrostenolytic process, and the associated diffusion processes supporting it, are omitted for simplicity. Since the operation of the circuit involves several different modes involving significant shifts in current direction, care must be exercised in applying Kirchoff's Laws. Both the laws relating to the sum of the currents at a node and the continuity of the currents in a branch must be met. These laws must be used in the differential calculus form to accommodate the transfer of currents between resistive and capacitive circuit elements in transient circuits. Caution must also be observed with respect to the batteries in these circuits. These are rechargeable batteries and the circuit is configured to recharge some of them during operation. The form of the waveforms shown in (B) is freehand. However, they represent the actual exponential waveforms based on conventional circuit time constants. In some actual cases, the exponentials exhibit the effect of the variable impedance of the power supply diode. This variable impedance causes the time constant to be a variable during the recharging cycle. The resulting action potential waveforms are distinctly different from both conventional RC circuits and the so-called generator waveform of the P/D process and photoreceptor cell. For further details of the oscillatory process, see **Section 9.2.4**.

Initially, the emitter is biased so that the Activa is cutoff. No current flows through the collector and the collector voltage (the resting axoplasm potential) is at the intrinsic membrane potential, V_{cc}. With no current through the collector, there is no current through the emitter. The emitter voltage source, V_{ee}, holds the voltage of the emitter fixed but does not provide significant power to the circuit. When a signal, usually labeled an action potential, arrives from the previous active circuit, it charges the capacitance associated with the emitter circuit and injects current into the emitter. The circuit branch through the battery V_{ee} is open because of the diode. The current into the emitter generates an equal current emanating from the collector. The impedance of the diode and the capacitor cause the collector voltage, V_c, to become incrementally more positive. During this interval, V_c mimics the emitter to base voltage. This change in voltage occurs in time phase with the input signal as shown in the initial portion of (B). If the voltage at the emitter is not great enough to reach the threshold value, shown as 10 mV, the circuit operates as a simple amplifier. The threshold value is determined primarily by the impedance of the circuit between the base of the Activa and the point B. Since both the emitter current and the collector current flows through this element, its impedance causes the transfer impedance of the overall circuit to exhibit an incremental region of negative attenuation, i. e. amplification. Any incremental increase in emitter voltage above this critical voltage causes a significant increase in collector current. The circuit enters the discharge mode at time T_{in}. The Activa becomes equivalent to a closed switch between the emitter and collector terminals. The collector power supply and diode in series cannot sustain the collector voltage. A large current passes through the Activa from the output capacitor to the input capacitor, with a return path back to the output capacitor through E to C. This causes V_c (the axoplasm potential) to proceed to V_{sat} (about 120 mV more positive than the quiescent collector voltage), the intrinsic membrane potential established by the specialized membrane at C, as quickly as the circuit parameters will permit. As V_c moves toward V_{sat}, it reaches a point where the negative incremental transfer impedance of the Activa can not be sustained. This is the switching point at time, T_S. The Activa now looks like an open switch. At this point, the circuit changes from the discharge mode and begins the recharge mode. Note, there is no requirement for the discharge current to go to zero before the switching event. However, it does go to zero during the switching event.

After T_S, the Activa is an open circuit, and the overall circuit is now passive. The two capacitors return to their quiescent voltages independently. This independence is a factor in determining the refractory period of a Node of Ranvier. The precise values of the capacitors and diodes involved are not available from the literature. It can be assumed for the moment that the capacitors are of equal value. If so the final voltage across each capacitor will be approximately equal to about 50% of V_{cc}. The collector capacitor will begin to recharge and proceed toward V_{cc}. However, the emitter capacitor is already at a voltage greater than V_{ee}. This capacitor will proceed to redistribute charge between its plates by sending a current through V_{ee} in the direction to *recharge* this battery. Battery V_{ee} is in a unique situation. It is not required to furnish power to the emitter circuit when the Activa is cutoff. It does not provide power during the discharge portion of the operating cycle and it receives power from the emitter capacitor during the recharging portion of the cycle.

The time interval, T_r, is defined as the regenerator time delay. This interval is more easy to define mathematically than the time between T_{in} and the median time of the regenerated action potential. However, the interval between the median times of the input action potential and the output action potential is easier to estimate from experimental data.

Note the two dashed lines during the recharging interval of (B). One corresponds to the charge transfer versus time for each capacitor. Since the Activa acts as an open switch during recharging, the collector potential (the axoplasm potential) returns to the intrinsic membrane potential without regard to the recharging taking place in the emitter circuit. Thus the initial portion of the action potential in (B), prior to T_S, is formed by the combined discharge process involving both capacitors. However, the recharge cycle occurs separately in the emitter and collector circuits. The falling portion of the action potential, as normally recorded, is only dependent on the collector circuit parameters and the transmission line of the subsequent axon segment.

If the power supply impedance of the collector circuit is higher than normal or the collector capacitor is larger than proper, the recharging interval will be extended. This will lengthen the refractory interval of the axon and may lead to pathological conditions. A loss of myelination is the primary cause of excess capacitance in the collector circuit. Such loss is a primary cause of multiple sclerosis. An alternate cause is a lack of adequate bioenergetic material for the electrostenolytic processes. Inadequate performance of the similar elements in the emitter circuit can affect the overall refractory period but the shape of the action potential will not be impacted.

Both of the recharging circuits lie completely within the area of the specialized lemmas and the associated bioenergetic materials participating in the electrostenolytic process. During the recharging interval, the voltages across the two capacitors are returned to their quiescent values as quickly as permitted by the time constants of the respective circuit parameters. Very little current associated with the recharging process passes through the nodal gap. However, since the recharging process does complete the voltage profile of the axoplasm known as the action potential, a voltage signal is applied to the output transmission line of the axon segment. A current travels down the axon and a return current travels back from the next node via the interneural matrix. This current does pass through the nodal gap and point C. Since the transmission line of the next axon segment exhibits a nearly pure resistive characteristic impedance (see **Section 9.1.2**), the current traveling down that line is directly proportional to the voltage waveform of (B). This includes the small step on the leading edge of the waveform. Under normal conditions, this step is sufficiently attenuated before reaching the next node or synapse that it does not initiate signal regeneration.

Two points must be noted. The current passing into the post nodal axon segment occurs at a time later than the time of the current arriving from the pre nodal axon segment by the regenerator delay interval, T_R, see (B). This time interval between waveforms play a significant role in the calculation of the group delay and the average velocity associated with an axon. The overall average velocity, also known imprecisely as the conductance velocity of the neuron in the biological literature, is given by the physical length of the axon segment divided by this delay. This calculated and frequently quoted average velocity is 20-50 meters/second depending on temperature. Second, the phase velocity of the signal along the axon segment, between regenerators, is at least 4000 meters/second. This is much faster than the average velocity. See The Nominal Neuron in appendices.

There are a variety of simple circuits sketched in the literature attempting to describe the flow of electricity within and around neural conduits generally described as axon segments. All of those found by the author attempted to describe these currents using simple direct current practice, as opposed to pulse transmission practice. There is a great deal of difference between the two. As in radio transmission or light waves, having a literal return path carrying a current identically equal to the transmitted signal is not necessary in pulse transmission. Part (C) of the figure attempts to define the actual conditions found along a series of neural conduits as a function of time and to develop a convention regarding the charge flow conditions. The primary concern is the definition of inward and outward currents. Do the terms apply to the currents where measured external to the axon? Or, should they be associated with the actual regenerator circuit? In the latter case, the inward current contains three components. First, the current arriving at the regenerator circuit from the previous axon segment as shown in the 1st (upper) caricature. Second, the current arriving at the regenerator circuit from the INM as shown in the 2nd caricature. Third, a small component of current that generates the rising waveform of the action potential in the following axoplasm. The total outward current also contains three components. First, the recharging current shown in the 3rd caricature. Second, a component that drives the following axoplasm toward the quiescent axoplasm voltage. Third, an inconsequential and normally overlooked portion that is impressed on the previous axon segment as part of the emitter recharging process.

The role of each of these current components can be seen more clearly by considering the time interval when they occur. Prior to T_{in}, the only inward current of interest is that approaching from the previous axon segment. After T_{in} and before T_s, there is a large inward current from the INM due to the discharge of the capacitor associated with the following axon segment. Following T_s, there is a large outward current to the INM associated with the recharging of the two capacitors of the regenerator circuit. The currents affecting the following axon segment, and shown oversimplified in the 4th caricature, occur for the most part after T_{in}. A small part of the inward current from the INM drives the rising portion of the action potential and a small part of the outward current to the INM drives the falling portion of the action potential of the axoplasm.

It is a mistake to interpret the loops with arrows as indicating the direction of current flow in a neuron. They indicate the direction of energy flow, and information flow. They correspond to a Poynting Vector.

The currents flowing through the nodal gap are limited to the return current paths for the two axon segments involved. All other current flow, which is significant, is constrained to within the constriction of the nodal gap mentioned above. The current flowing through the nodal gap is readily sensed by a field probe that does not penetrate the axon. (C) shows a greatly simplified electrophysiological model overlaid on the morphological model of a Node of Ranvier. Compare this concept of two current pulses of opposite polarity and separated in time passing through the nodal gap with the interpretation of probe data from a toad presented by Tasaki[108] and republished widely[109]. The analysis in Zagoren & Fedoroff will not be used here because of several conditions and definitions they adopt. In the experiment of Tasaki using only one field probe outside of a single nodal gap, in the perinode and labeled N_1, the recorded waveform is bipolar as expected. By employing air gaps, the probe acted as a Faraday cage, capturing all of the current passing in or out of the nodal gap. The return lead is in contact with the remainder of the fluid surrounding the entire specimen. The peaks are separated by a period equal to the regenerator delay. The interval, T_R, is approximately 0.06 msec. The peak amplitudes of the two phases are in the ratio of 0.6:1. This ratio is very close to the relative amplitude of the nominal pulse arriving at a node at time T_{in} compared to the regenerated pulse leaving the node at time T_S and calculated in **Section 10.5.3.4.**

> When Tasaki summed the signals from two adjacent nodes, his test set inverted the polarity of the results and the return circuit is less defined compared with the desired signals. When measuring only one node, the signal was applied to the grid of an amplifier. When measuring two nodes simultaneously, the combined signal was applied to the cathode of the same amplifier. He did not isolate the currents through the nodes from the remaining fluid around the specimen except for the fluid next to the axolemma and myelin of the axon segment. Thus, his only Faraday cage collected signal current passing through a very high quality insulator. The result was an amplifier operating with an open grid (or an unspecified grid leak). Such a circuit is subject to unexpected signal rectification and poor DC response. The poor DC response is recognizable in the tail following the waveforms. The waveforms are clearly different from those in the one probe experiment and rectification must be considered. The probes at N_1 and N_2 were sensitive to any and all currents flowing in the surrounding fluids, including the desired currents through the nodal gaps. These conditions make unambiguous interpretation of the data difficult. The two recorded peaks are separated by about 0.106 msec. This interval corresponds roughly to twice the regenerator delay measured above as expected.

It should be noted that, to the extent that the inward and outward currents shown are created as part of the electrostenolytic process associated with the three batteries , the actual amplitude of the currents measured as flowing into or out of the INM will be reduced. To be complete, the inward and outward "energy flows" between each Node and the INM should be represented by both an electrical and a chemical component.

---

[108]Tasaki, I (1959) Conduction of the nerve impulse. In Handbook of Physiology, Wash. DC: American Physical Society vol. 1, Chap. III

[109]Zagoren, J. & Fedoroff, S. (1984) The Node of Ranvier NY: Academic Press pg. 114

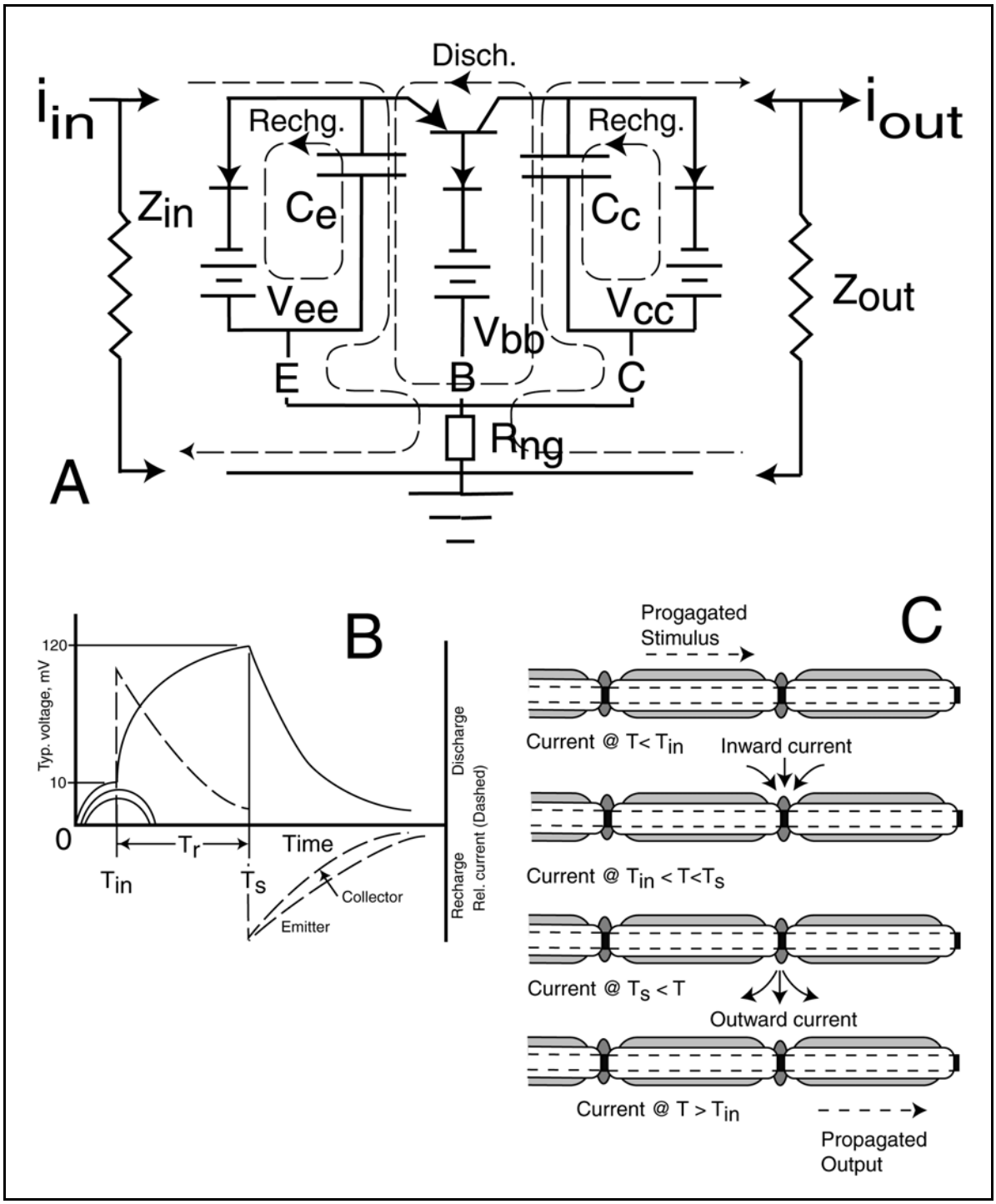

Figure 9.4.1-2 Operation of the Node of Ranvier BREAK OUT. (A) The detailed schematic. (B) The principle voltages and currents. (C) Additional details of current flow along the axon of a projection neuron.

The above putative waveforms agree well with those presented by Frankenhaeuser & Huxley[110], taken at the post-junction side of a hillock (**Section 10.10.1**) [or Bennett, Nakajima & Pappas 67] and provide an alternate explanation for the counter-flowing waveforms attributed to Na+ and K+ in Waxman & Wood[111]. **Waxman & Wood data is all computer simulations.**

9.4.1.2 The introduction of myelin in connection with the axon

As indicated above, a lengthening of the axon of the ganglion neuron relative to the bipolar neuron can introduce capacitance in shunt with the other impedance elements of the output circuit and lead to oscillation in the ganglion circuit. However once a critical level of capacitance is reached, additional capacitance is not desirable. This lumped capacitance requires the Activa to switch more current between the input and output circuit to achieve the same level of action potential amplitude. To avoid this problem while achieving maximum axon length, a portion of the axon is wrapped in myelin. This process has the effect of thickening the dielectric between the axoplasm and the surrounding plasma and thereby lowering the effective capacitance per unit length of the axon.

As the axolemma necessarily becomes a cylinder as it lengthens, another electrical phenomenon is introduced. An insulating cylinder surrounded by conductors introduces an inductance per unit length of the cylinder.

As a result, an extended axolemma contributes two electrical elements that profoundly affect the performance of a given Activa. The lumped capacitance near the unmyelinated ends of the axon, in combination with the resistive elements of the collector (axon) circuit directly control the temporal performance of the axon. The distributed capacitance, in combination with the distributed inductance, both on a per unit length basis, control the propagation velocity of signals along an extended axon. The propagation of neural signals is a phenomenon not previously described in neuroscience. The term propagation is introduced here to differentiate stage 3 neuron signal distribution from the concept of signal conduction (by chemical diffusion) which is not employed within a long axon. Propagation is a distinctly different mechanism. It is a key to understanding the operation of the stage 3 neurons.

There is a large community of physiologists and histologists attempting to explain the role of myelin and changes in myelination, without understanding the basic mechanisms associated with stage 3 signal propagation[112,113]. Without recognizing the role of inductance in stage 3 axon signal propagation, the actual mechanism of signal projection can not be discussed rationally. The history of signal transmission associated with myelinated neurons has been summarized in Fulton[114].

> ***Calculations of the capacitance of an axon per unit length found in the electrophysiological literature, based on a flat plate capacitor, are in error.*** As shown below, it is not the thickness of the dielectric that is important but the *ratio* of the thickness of the dielectric to the inner diameter of the dielectric.

---

[110]Frankenhaeuser, B. & Huxley, A. (1964) The action potential in the myelinated nerve fibre of *Xenopus Laevis* as computed on the basis of voltage clamp data. J. Physiol. (London) vol. 171, pp. 302-315

[111]Waxman, S. & Wood S. (1984) Impulse conduction in inhomogeneous axons. Brain Res. Vol. 294, pp. 111-123 [or Zagoren & Fedoroff pg. 339]

[112]Gibson, E. Purger, D. Mount, C. et al. (2014) Neuronal Activity Promotes Oligodendrogenesis and Adaptive Myelination in the Mammalian Brain *Science* vol 344, pp 487+ http://dx.doi.org/10.1126/science.1252304

[113]Betcher, M. & ffrench-Constant, C. (2014) M. E. Bechler, C., A new wrap for neuronal activity? *Science* 344, 480–481 (2014). DOI: 10.1126/science.1254446

[114]Fulton, J. (2008) Hearing: A 21st Century Paradigm. Bloomington, IN: Trafford pp 323-325

Similarly, ***the square root relationship between signal velocity along a stage 3 axon and the outer diameter of the myelinated axon found in the literature is also in error***. This *average* velocity relationship was developed by Rushton based on dimensional analysis, rather than rigorous mathematical investigation, using only a limited range of data[115]. Granit has provided a much larger data base to consider[116]. But neither investigator was aware of the importance of the radius of the inner conductor. Man-made coaxial cables with the same signal velocity and input impedance vary over a factor of ten in the diameter of their dielectric layer (ex., RG 19 versus RG 122). All 50 Ohm input impedance cables exhibit the same capacitance of 29.5 μμf/foot and exhibit the same signal phase velocity as computed below regardless of their outer diameter.

The physiology and mathematics supporting these statements were introduced in **Section 9.1.2**.

9.4.1.3 Voltage and Current waveforms associated with a Node of Ranvier

[xxx Schrager, writing in Waxman, et. al. provides the best set of action potentials acquired *in-vivo*[117]. While involving artificial stimulation at an earlier location in the signal chain, they do not suffer from any artifacts due to artificial stimulation (like those of Hodgkin & Huxley and of Cole).]

[show simplified waveforms and waveforms showing recharging during discharging in a switching context. Then compare with those of Hodgkin & Huxley.

[xxx separate propagation from conduction. Conduction is used in pedagogy for simplicity (and some ignorance of propagation). Note that the time delay between here and Mars is about 8 minutes. There is no external return path in propagation. The magnetic aspect of propagation shows through.]

It is important to differentiate between the transmission of signals within a neuron by ionic conduction, as typically encountered in the neurites of neurons, and by propagation as typically encountered within the myelinated portions stage 3 axons and axon segments. Ionic conductivity is associated with an electrical gradient within a solution. It is commonly associated with chemical diffusion within a solution exhibiting a chemical gradient.

Recently, Lemont Kier and his associates[118] have presented an article describing the movement of "protons" through the Node of Ranvier. They only conceptually describe a process of proton hopping. In their conclusion, they asserted in 2015, "No model for the inter-nodal jumping of the action potential has ever been postulated." This author would refer them to Fulton (2004, chapter 4) and Fulton (2009, chapter 7) for complete descriptions of the propagation of neural signals through myelinated axon segments. Online versions of these materials are cited above.

The next section will establish that protons do not move through the tissue or fluids of the neuron as described. Their protons are known in electronics and electrolytics as holes. Holes exhibit the charge of a proton but actually consist of the absence of an electron in a lattice. Through repeated movement of an electron from an occupied location in a lattice to an unoccupied

---

[115]Ritchie, J. (1995) Physiology of axons In Waxman, S. Kocsis, J. & Stys, P. The Axon. NY: Oxford University Press pp 68-73

[116]Granit, R. (1962) The Visual Pathway: a confrontation of physiology with anatomy *In* Davson, H. *ed.* The Eye, Volume 2: The Visual Process. NY: Academic Press pp 563-565

[117]Schrager, P. (1995) Action potential conduction recorded optically in normal, demyelinated, and remyelinating axons. *Chapter 18 in* Waxman, S. Kocsis, J. & Stys, P. The Axon. NY: Oxford Press pp 341-354

[118]Kier, L. Hall, L. & Tombes, R. (2015) Enhanced Action Potential Passage Through the Node of Ranvier of Myelinated Axons via Proton Hopping *Cur Comp - Aided Drug Des* vol 11(1), pp. 5-7(3)

location (a hole), a relatively slow movement of what appears to be a positive charge through a lattice can be observed. This mechanism is a keystone of modern electronics and is described in detail in any introductory text in semiconductor physics.

9.4.1.3.1 Proton hopping (ala Kier et al.) remains inadequately characterized

Kier and several associates have presented a number of papers describing their concepts of charge movement through an aqueous environment. Their basic proposal is that within "bulk water," a proton can move from one molecule of water to the next by utilizing a hydrogen bond with individual water molecules. Their first paper of 2013[119] was at best conceptual and primarily involved a simple computer model conforming to a set of probability rules. No forcing function was included to drive their mechanism. No time intervals between transfers of a proton between water molecules is provided. The modeling time is only related to the cycle times of their cellular automata (CA) model and the associated computer program.

> A cellular automaton is a collection of "colored" cells on a grid of specified shape that evolves through a number of discrete time steps according to a set of rules based on the states of neighboring cells.

The second paper of 2013 continues their investigations while relating their concept to myelinated axon nerve impulses[120]. Their abstract describes their approach,

> "We have used modeling approaches to simulate a role for proton hopping in the space between the plasma membrane and myelin sheath as the mechanism of nerve action-potential flow."
>
> They expand on the sentence in their abstract to assert, "It has been proposed that the action potential developed in these nodes passes along the axon by a jump, hop , or saltatory movement between nodes Myelinated axon nerve impulses travel 100 times more rapidly than impulses in non-myelinated axons. Increased speed is currently believed to be due to hopping or saltatory propagation along the axon, but the mechanism of this flow has never been adequately explained." See **Section 9.4.1.3**. for a refutation of this statement. It is worth noting their 2015 paper cited above uses the value of 300-fold rather than 100 for the increase in proton travel through their "bulk water" to what is apparently bulk charge transport by electrolytic means through water without offering any data to support either value. Their assertion of "300-fold appears only in their Abstract and is not supported in the body of their paper.
>
> See **Section 9.1.1** and **Section 9.1.2** for a full discussion of the propagation mechanism responsible for the putative saltatory mechanism. The concept is archaic, saltatory transmission was a concept developed when the available instrumentation was primitive.
>
> They offer no graphic describing the morphology, cytology or electro-physiology of the processes they discuss. They do note, "Myelin is a protein-lipid membrane that surrounds the axon between each node of Ranvier. The spaces between the laminar layers of myelin, and the myelin and axon, called the periaxonal space, is filled with water." This work depends on other data to show there is no water between the layers of the myelin or between the inner myelin layer and the lemma of the neuron. ***Their hypothesis is dependent on water existing between the inner myelin layer and the lemma of the axon***, their periaxonal space. This water is described as a "water wire" in their text. It supports the motion of protons along this periaxonal space. "This water wire is initiated by an action potential at the post-synaptic terminus of the axon, resulting in impulse propagation along a series of nodes and internode axons."

---

[119]Kier, L. Tombes, R. Hall, L. & Cheng, C-K. (2013) A Cellular Automata Model of Proton Hopping Down a Channel *Chem Biodivers* vol 10, pp 338-342

[120]Kier, L. Tombes, R. (2013) Proton Hopping: A Proposed Mechanism for Myelinated Axon Nerve Impulses *Chem Biodivers* vol 10, pp 596-599

The intimate relationship between the myelin and the outer lemma of the stage 3 axon has been explored extensively using electron-microscopy (**Section 9.1.2.5** & in greater detail in **Sections 10.3.5** & **10.5.2** of "Processes in Biological Vision" (PBV)). This includes the filagree structure of the myelin where it terminates at a Node of Ranvier. This filagree at the cytological level represents an "half-section" of an impedance matching element at the electro-physiological level based on conventional filter theory. ***The electron-microscopy illustrated and cited in*** **Sections 10.3.5** & **10.5.2** ***clearly demonstrate there is no water layer separating the inner myelin layer and the outer lemma of the axon***. The presence of such a water layer would be disruptive of the capacitance contributed by the myelin between the axolemma and the surrounding fluid matrix.

Their discussion includes,
• "On the basis of earlier modeling results and this study, we propose that axon action potentials arise from proton hopping through the periaxonal space separating the axon surface from the myelin sheath. This extracellular gap contains H2O in a narrow space that is ideal for rapid passage of proton-hopping information between nodes of Ranvier."

They do stress the H^+ does not move or diffuse, but the hydronium ion (H_3O^+) state shuttles along the path in bulk water. They make inadequate distinction between "bulk water" molecules in a fluid state and those in a liquid-crystalline state. In a fluid state, charge transfer along a linear path is extremely slow in the absence of a polarizing field. They note it is about 0.0001 m/s. It can be argued in the absence of a polarizing electric field, the net motion is zero. They also assert that action potentials travel at 0.5 to 10 m/s along unmyelinated axons (in the presence of an unspecified electrical field potential) and at about 150 m/s in myelinated axons (being higher in larger diameter axons). These velocities are not supported by any test data but are consistent with the values in various text books.

Kier & Hall offered an additional paper in 2013[121]. It relies upon the above concepts and will not be discussed further here. ***A range of 3:1 in a velocity measurement is unacceptable in engineering fields. The measurements of Kier need to be repeated using a better protocol accepting the reality of the GWE of Maxwell in signal propagation in stage 3 neurons.***

The Kier papers offer little insight into the operation of the neural system. Kier et al. offer no mathematics, no graphics or other justification in support of their assertions that charge can move along their periaxonal space at velocities of 150 m/s. The actual signal propagating along the myelination/lemma boundary is by electromagnetic field propagation that does not involve the net flow of any charged particle. The precise situation is explained in detail using the General Wave Equation (GWE) of Maxwell's Equations (**Section 9.1.2**). The biological community has had difficulty adapting the GWE because of its mathematical character and the communities earlier reliance on the erroneous proposals of Lord Kelvin during the 19th Century (**Section 9.1.1.3**).

9.4.1.4 Ionic velocity versus energy propagation in neurons EDIT

Figure 9.4.1-3 presents the currents in the above circuit in graphical form. Xxx These waveforms can be compared with the textual and graphical discussions of Hodgkin & Huxley. [conclude there is no need for ionic currents, the potassium current is identical to the current through the switching Activa, and the early and late sodium currents are due to the operation of the electrostenolytic process. xxx]

Note the decoupling between diffusion as a function of the linear bias potential versus the independence of propagation from any associated electrical bias potential.

---

[121]Kier, L. & Hall, L. (2013) The Creation of Proton Hopping from a Drug Receptor Encounter *Chem Biodivers* vol 10, pp 2221-2225

Figure 9.4.1-3 EMPTY REWORK this to show propagation separate from conduction. The currents related to a Node of Ranvier compared with the idealized currents of Hodgkin & Huxley.

9.4.1.5 Impedance matching between the lumped and distributed circuits EMPTY

The above figure from Pannese provides a very clear representation of both the morphological and electrophysiological features of the Node of Ranvier. Starting from the bottom of the figure, the myelination is shown at its fullest, thereby minimizing the capacitance of the prenodal axon segment. As the nodal area is approached, the number of myelin layers is reduced and their orientation changes. These actions raise the capacitance per unit length in this region. As a result, the characteristic impedance of this region changes. The region becomes a matching section between the distributed parameters of the axon segment and the lumped parameters of the Node of Ranvier. The Pannese figure does not show the fluting found in the earlier figure from Rydmark & Berthold. Such fluting can provide a similar change in the electrical parameters of the paranodal portion of the axon segment. The result is again a matching section between the distributed parameters of the axon segment and the lumped parameters of the Node of Ranvier.

9.4.2 Description of a node and an axon segment as a functional unit

[add a new overview sentence xxx, reword introduction to differentiate between functional unit and unit plus a second Node in the following figure]

An early work recognizing the saltatory form of the action potentials along a signal path was that of Huxley & Stampfli[122] exploring *Rana temporaria*. In that work, the position of the Nodes of Ranvier are shown explicitly.

Describing the functional characteristics and elements of the region consisting of a Node of Ranvier and its associated orthodromic axon segment is now possible. **Figure 9.4.2-1** presents a caricature of the region accompanied by a functional description using its electrical circuit diagram. Two basic features should be noted. The internode, excluding the conseg portion, is an essentially passive circuit element while the conseg portion is an active circuit. The data in the literature makes it difficult to describe the exact nature of the passive portion of the internode. Much of the experimental data is clinical in nature and involves a determination of the temporal distribution of conduction (group) velocities for aggregates of nerve fibers[123]. Data on the voltage profile of an action potential as it travels along an internode has been

[122]Huxley, A. & Stampfli, R. (1949) Saltatory transmission of the nervous impulse. Arch. Sci. Physiol., III, pp. 435-448

[123]Dorfman, L. Cummins, K. & Leifer, L. (1981) Conduction velocity distributions: a population approach to electrophysiology of nerve. NY: Alan R. Liss, Inc.

available since the 1940's. It is the variation in the amplitude profile with time as it propagates along the neuron that would allow a determination of the detailed electrical nature of the propagation environment.

The bulk of the axon segment can be described as a transmission (or delay) line as shown here. The terminology used should be relevant to the purpose at hand. However, it is not clear whether the series elements in the line should be shown as resistors or some other circuit element. If the material within the microtubules of the reticulum is liquid crystalline, it is possible for charges to be transferred by loss free mechanisms. Under these conditions, there is no need for energy to be dissipated as part of the charge transfer process. In this case, the series element could be considered a zero loss element and not a conventional resistor. The exact definition of this element is not required here. It could be a simple inductor. Only the recognition that the charge transport velocity in a typical axon segment is more than 4,400 meters/sec. for an 8-micron diameter neuron is important here. Whatever the nature of the series element, the shunt element is a simple distributed capacitor. The value of this capacitance is greatly affected by the thickness and dielectric constant of the myelination of the axon segment. This capacitance is greatly influenced by the quality of the myelin, axolemma contact. If fluid from the interneural matrix can enter the space between these two materials, the capacitance between the axoplasm and the interneural matrix is greatly increased. The myelin layers are arranged to provide a labyrinth type of seal to insure maximum integrity in this respect. Rasminsky & Sears[124] found that removing the myelin from a rat ventral root neuron slowed the internodal signal conduction time from 26 microseconds to more than 600 microseconds at 293 Kelvin.

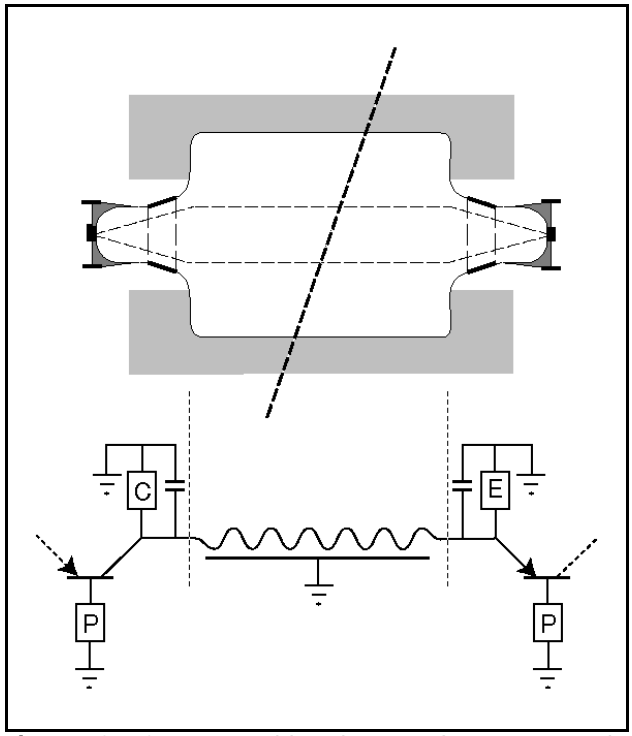

Figure 9.4.2-1 Repetitive internode segment in caricature and electrical circuit diagram. Top; the complete segment includes one Node of Ranvier and one axon segment surrounded by myelin. Bottom; the circuit diagram shows both the lumped parameter matching sections and the distributed parameter transmission cable. See text for details.

The signal being applied to the internode at the Node of Ranvier is shown on the left. The small area of the active device, the Activa, is shown as the vertical bar on the horizontal axis of the upper figure. In electron micrographs, this area is described as electron opaque. In the circuit diagram, it is shown as the base region of the Activa, using conventional solid state semiconductor notation.

Figure 9.4.2-2 shows a series of axon segments separated by Nodes of Ranvier. The bulk currents flowing in and out of the Nodes of Ranvier are illustrated as a function of time. These currents correspond to the inward and outward currents defined by Hodgkin & Huxley. However, the currents consist of electrons and do not involve any ionic flow across any

[124]Rasminsky, M. & Sears, T. (1972) Internodal conduction in undissected demyelinated nerve fibres. J. Physiol. (London), vol. 227, pg. 323

membranes. The relationship of these currents to the INM are exaggerated because of the presence of the electrostenolytic sources within the nodal areas. To a large extent, the inward and outward currents only exist in and very near the nodal gaps. The long term average of the sum of the inward and outward currents is zero. Also shown are the action potentials propagating along the axon. While these signals involve small physical displacements of charge traveling along the axons segment (a "local electromagnetic circuit"), they do not involve any long term average displacement (and there is no "return current" associated with propagation). As a result, there are no current loops (all components of which exist at a common time) related to the operation of the axon as a whole.

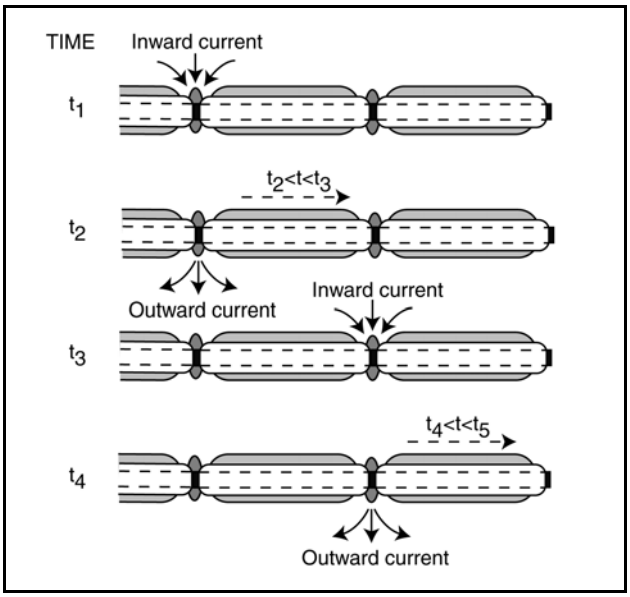

Figure 9.4.2-2 Currents along a myelinated stage 3 neuron with multiple Nodes of Ranvier. Bulk currents flowing in and out of the nodes are shown solid. The outward currents overlap the inward currents only slightly. Propagating action potential are shown by dashed lines. The bulk currents and propagating signals do not form current loops. There is no return signal related to the propagating signals. See text.

9.4.2.1 Determining the electrical performance of a node and internode region as a unit

It is difficult to measure the electrical performance of a projection neuron for several reasons. The size is the major difficulty. The typical axon is only 10-15 microns in diameter, including the myelin sheath. The typical Node of Ranvier is only 10 microns wide. The second problem is the lack of a good common electrical reference point, generally called a "ground" terminal. The interneural matrix consists of a relatively poorly conducting fluid. It is similar in concept to the atmosphere (or free space) when discussing antennas in that it exhibits a relatively constant impedance in Ohms per square (no other unit is needed) but does not provide a good ground terminal. In electromagnetic radiation at longer than a millimeter wavelength, defining a theoretical ground to occur at an infinite distance from the radiator is customary. This definition also supports the definition of the impedance of free space. In practice, the impedance is usually given with reference to a specific resonant dipole antenna. This antenna has a purely resistive impedance at the frequency of interest of 376.7 Ohms, although it is a highly conducting piece of metal with an ohmic resistance of less than 0.001 Ohms. A similar situation is assumed when recording electroretinographs. In that case, a location on the outer surface of the head is usually used as a reference potential. However, no impedance is assigned to the body plasma. Only an integrated electrical potential is recorded in response to an unknown current flowing through an unknown impedance.

The size problem is compounded by the difficulty of creating an electrical probe that is smaller than 100 microns in diameter, exhibits a serial impedance of greater than 100 megohms, and introduces a shunt capacitance of less than one picofarad at its tip.

The difficulty in making meaningful measurements in an environment containing active electrolytic semiconductor devices cannot be overemphasized. Because the probability of making a meaningful resistance measurement, without the aid of a detailed circuit diagram, is ludicrously small, none of the measurements in the literature will be references or vouched for in this work. **Section 10.10.x** will address this problem in detail.

In spite of the above difficulties, extensive effort has been expended over the years to understand the operation of the Node of Ranvier. The work can be separated into two main

tracks, that involving the voltage clamp technique and the other more general work.

The voltage clamp technique originated with the work of Cole and of Marmont in 1949[125]. It was adopted and effectively exploited by Hodgkin & Huxley and has been widely used since then. A major improvement in the test instrumentation occurred in the late 1960's with the introduction of more sophisticated transistorized test instrumentation[126]. This was followed by the work of Hille in the 1970's. In 1982, Tasaki provided a broad review of the field starting in the 1930's[127]. However, his review omitted much of the above work of the 1960's and 1970's. The most recent work has been by Schwarz, et. al. in the 1990's.

All of this work has been exploratory in nature and virtually no model of the actual mechanisms associated with the Node have been offered. All of the calculations have been based on the Hodgkin-Huxley equations. The simple model generally used is that of a continuous axon containing an excitable region in the area where it is unmyelinated. Many of the authors in the 1960's and 1970's provided no electrical model of the Node at all. When addressed, this excitable region has been represented by ever more complex variants of the original Hodgkin-Huxley model of the axolemma. Barrett & Barrett presented a simple model recognizing the difference between the myelinated and unmyelinated regions[128]. The model presented by XXX[129] figure 4-15 in Waxman, Kocsis & Stys is probably the ultimate in the extension of a simple linear circuit to a point of absurdity in order to model an unknown non-linear mechanism.

Because of the need for a very detailed discussion of the technique, the application of the voltage clamp technique to the Node of Ranvier will be addressed in **Chapter 2**.

9.4.2.1.1 A coaxial axon is not a Herman Cable

The biological community has long discussed signal transmission within the neural system based on the simple concept of a continuous series of resistor-capacitor networks as defined by Herman in the mid 1800's. This was shortly after the invention of the telegraph and before the invention of the telephone. Soon after the invention of the telephone, it was discovered that wide bandwidth signals could not be sent any appreciable distance over a telephone line consisting of only resistors and capacitors. The phase distortion was so high, the voice signal could not be understood. Furthermore, the attenuation was excessive. Two solutions were devised. The earliest solution was to introduce large inductors periodically along the line to compensate for the effect of capacitance. A more satisfactory solution came later. It was found that coaxial cables did not suffer from the same phase distortion.

Any coaxial cable exhibits an intrinsic inductance plus an intrinsic capacitance. In fact, the intrinsic capacitance and inductance of a coaxial cable are far more important than the resistance of the cable. They determine two properties of the cable, the input impedance and the propagation velocity of the circuit. A theoretical coaxial cable containing no resistance will still exhibit an input impedance that is resistive. It will also exhibit a propagation velocity given by the square root of the inductance per unit length divided by the capacitance per unit length (and independent of the resistance per unit length). These are the properties of importance in propagation of action potentials within neurons.

---

[125]Piccolino, M. (1998) Op. Cit. pg 399

[126]Nonner, W. & Stampfli, R. (1969) A new voltage clamp method. In, Laboratory techniques in membrane piophysics, Passow, H. & Stampfli, R. ed. NY: Springer-Verlag pp.171-180

[127]Tasaki, I. (1982) Physiology and electrochemistry of nerve fibers. NY: Academic Press.

[128]Barrett, E. & Barrett, J. (1982) Intracellular recording from vertebrate meylinated axons: mechanism of the depolarizing afterpotential *J. Physiol*. vol 323, pp. 117-144

[129]Xxx or Berthold, C. (1995) Morphology of normal peripheral axons. *In* The Axon, Waxman, S. Kocsis, J. & Stys, P. Ed. NY: Oxford University Press

To understand the electromagnetic propagation of action potentials, recognizing and understanding the electrical characteristics of an axon are important. Electrically, an axon is a coaxial cable. It consists of a conducting material, the plasma surrounded by a cylindrical insulating material, the lemma. The lemma is in turn surrounded by a second conducting material, the interneuron matrix. The fact that the interneuron matrix may be of great extent outside the axon is largely irrelevant. However, whether the axon is myelinated or not is highly relevant. The myelin exhibits a very low dielectric constant. Its presence greatly reduces the capacitance per unit length of the axon. This change increases the propagation velocity of the axon greatly.

The Herman Cable has been an archaic concept since 1890 or earlier. More recent discussions based on the Herman Cable are largely irrelevant to the propagation of action potentials. Their only relevance is to the diffusion of electrotonic signals over distances of less than a few millimeters.

9.4.2.1.2 Understanding the group velocity, and other signal velocities within a neuron

The literature frequently discusses the velocity of neural signals without clear definition of the velocities involved. The easiest velocity to define is the group velocity of a signal (an action potential) propagating within a stage 3 neuron. This is the average velocity of the signal measured by the time for it to travel between two points separated by at least one cm. The longer the separation distance, the more accurate the measurement. Such a measurement will include multiple axon segments and multiple Nodes of Ranvier. A mixture of ion transport and electromagnetic propagation modes will also be involved. The resulting group velocity can be dissected into its components. These include the diffusion velocity of the signal during ion transport, the phase velocity of the signal during electromagnetic propagation and a fixed time delay during the regeneration cycle at each Activa.

The easiest way to calculate the group velocity is to calculate the time delay associated with each segment of the propagation path. The group velocity is then given by the total distance divided by the total time delay. This allows the time delay associated with the regeneration process to fit seamlessly into the calculation.

The phase velocity of a signal within a conduit is a function of the dimensions of the conduit. Because of their complex shape, computing the precise phase velocity within a neurite is difficult (even as a function of position along the dendritic tree). In addition, the high capacitance per unit length of the neurolemma reduces the achievable velocity. Values of 0.01 meters per second down to 4.6×10^{-6} meters per second appear in the literature. A typical diffusion velocity is near 7×10^{-3} meters per second based on ERG data (**Section xxx**).

The task is much easier for an axon or interaxon. These have relatively constant diameters over significant distances. The phase velocity for the typical myelinated neuron is about 4400 meters per second. While this velocity cannot be sustained over a long distance, it is much faster than any potential diffusion velocity.

The time delay associated with regenerating an action potential is typically 0.6 ms in endothermic animals. The delay is much higher in exothermic animals. It can be as large as 500 ms at 20 degrees centigrade. Such a value explains the lethargy of many terrestrial exothermic animals before the sun warms them.

After combining the above delays and velocities, a typical group velocity for the propagation of action potentials is between one and 120 meters per second. Values above five meters per second are only found in specialized circuits (mostly within the POS of the CNS). Even at an average group velocity of five meters per second, electromagnetic propagation is 1000 times faster than ion diffusion transport.

The electrolyte within an axon plays no role in electromagnetic signal propagation. Any conductive electrolyte will serve as the inner conductor of the coaxial cable. The signal involves only electrical charges constrained to the surfaces of the lemma.

9.4.2.1.3 The marriage of the Node of Ranvier, electrostenolysis and the coaxial axon

Figure 9.4.2-3 combines all of the principles discussed earlier into the morphological and electrolytic description of an axon. The signal, V_e is delivered to the Activa within the soma of the neuron by diffusion. The signal is used to cause the generation of an action potential at the output terminal of the Activa. The Activa circuit consists of a group of morphological and electrical components extending over a distance shown by the dimension x. These are called lumped components. Signals are transported by diffusion in this area at a velocity of less than 0.01 meters per second. Within the myelinated portion of the axon (labeled y), the electrical properties of the axon are described using distributed components described by their inductance, capacitance, etc. per unit length. The myelination of the axon greatly reduces its capacitance per unit length. As a result the propagation velocity is

greatly increased. The signal is propagated by electromagnetic means at a nominal 4400 meters per sec. Attenuation of the signal is quite low in this region. The signal can be transmitted centimeters without being reduced below 10% of its original amplitude. At the termination of the myelination, the signal is returned to transport by diffusion. When it reaches the Node of Ranvier, it causes the Node to regenerate the action potential to its nominal amplitude. The process is repeated. The signal is returned to electromagnetic propagation until it approaches the next Node or a synapse.

The drawback to the mixed mode of operation just described is the finite delay (0.6 ms for endothermic animals) introduced at each regeneration point. This delay becomes the tradeoff point between diffusion and electromagnetic propagation of neural signals.

Once the electromagnetic propagation mode is adopted, it becomes important to minimize the distance related to the diffusion mode within the overall neuron. This is the reason why the myelination extends into the Node of Ranvier space so significantly. Any electrostenolytic and metabolic activity must occur as close to the junction of the Node as possible to minimize overall circuit delay.

9.4.2.2 Signal propagation over the Node of Ranvier and an axon segment as a unit

Huxley & Stampfli[130] presented a figure in 1949 that described both the phase velocity and the average velocity of the signal traveling along an axon *in vitro*. The data was limited by the instrumentation of the day. Although not as accurately calculable as in the next figure, the curves are consistent with the phase velocity of 4,400 m/sec and the regenerator delay of 0.019 msec found there. The signal waveforms are all monophasic.

Smith et al. have provided some data that updates the Huxley and Stampfli results[131]. The first three figures of Smith et al. describe real test configurations and real results. However, the mathematical models used to create figures 5-4 and beyond do not represent the propagation of a real signal along a real axon.

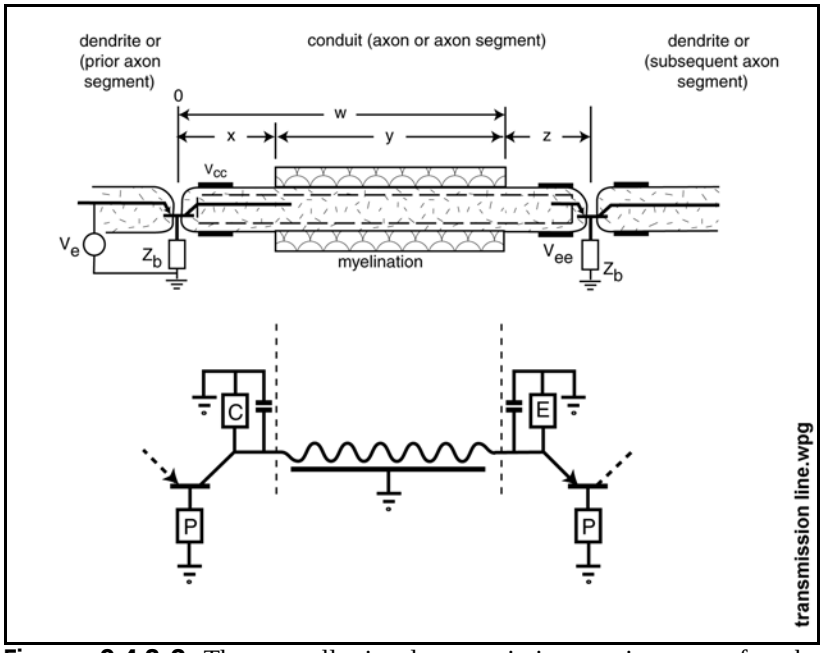

Figure 9.4.2-3 The overall signal transmission environment for the propagation of action potentials. Top; the morphological situation with electrolytic symbols as an overlay. Bottom; the electrolytic situation stressing the relevant lumped components and the distributed nature of the myelinated portion of the axon. Resistance plays no role in the operation of the interaxon (over the distance y). The letters in the boxes refer to the complex impedances of the electrostenolytic supplies. P = podite or base. C = collector. E = emitter.

---

[130]Huxley, A. & Stampfli, R. (1949) Evidence for saltatory conduction in peripheral myelinated nerve fibres. *J Physiol* Vol. 108, pp. 315-339. [Also at Stampfli, R. (1981) Overview of studies on the physiology of conduction in myelinated nerve fibers. *In* Demyelinating Disease: basic and clinical electrophysiology, Waxman, S. & Ritchie, J. *ed*. NY: Raven Press pp. 11-23]

[131]Smith, K. Bostock, H. & Hall, S. (1982) Saltatory conduction precedes remyelination in axons demyelinated with lysophophatidyl choline *J Neurol Sci* vol. 54, pp 13+

No attenuation constant or phase constant was introduced into their equations. Bostock has presented additional data[132,133] but a similar caution applies. Most of his voltage waveforms were computer-generated.

Figure 9.4.2-4 is from Smith et al. It is reproduced here with a series of dashed lines and a heavy vertical arrow added by this author. The specimen was a rat spinal root axon *in-vivo*. (A) was obtained by launching a pulse along an axon using the test configuration of Rasminsky & Sears[134] and measuring the voltage profile at 0.1 mm intervals using an (intercellular) probe next to the outside of the Schwann cell surrounding the axon. Usually, the detected signal was due to displacement currents. The leakage current component of the interneuron where it is myelinated is exceedingly low. It is possible the waveforms contained a conductive component for the probe positioned in the perinodal space. The signal levels were so low that considerable data processing was used to obtain these waveforms, typically averaging 128 individual traces at each location. (B) was obtained by taking the trace-to-trace differences after averaging. This process emphasizes the major changes occurring in the areas of the Nodes of Ranvier. These waveforms were then used to construct the contour map in (C).

The focus of each contour group represents the best estimate of the location of the Node of Ranvier (along the horizontal axis). It also represents the time of occurrence of the peak amplitude of the signal at that location relative to the signal at the previous measurement point. Note that the best estimate of the node position is in fractions of a millimeter in this presentation whereas the actual axial node dimension is in microns. The probes used had a nominal diameter of 100 microns. The contour map is a particularly compact form for interpreting the information obtained. However, it obscures some features of the raw data. The grouping of the waveforms in (A) is very important. In (C), overlaying a sloping line through the peaks of the contours to obtain an average velocity for the neural signal over a distance of several nodes is possible. The overlay shown corresponds to an average velocity of 44 meters/sec., a number consistent with the literature for a myelinated axon of about eight microns overall diameter. The peaks of the contours represent the peak of the newly regenerated action potential at each node. A second dashed line can be drawn slightly below this line and with the same slope. This second line is shown as intersecting the skirt of the contour at approximately the 10% amplitude point. It is meant to represent the average velocity line measured at the point where the threshold level of the regenerator circuit is exceeded. This is the point where the integrated current from the transmission line of the previous axon segment has resulted in a voltage exceeding the threshold voltage.

Looking again at (A), one sees a quite different picture. A similar dashed line drawn through the peaks of each of the individual groups of measurements is very nearly horizontal. At the scale shown, this overlay shows the phase velocity of the signal within a given axon segment is immensely faster than the average velocity. At the scale of the drawing, the phase velocity is clearly at least 30 times faster and probably 100 times faster than the average velocity in (C). The dashed lines in (A) represent the phase velocity of the signal energy. They are drawn at 1% of the slope passing through the nodes in (C), e. g. 4400 m/sec. Although these lines appear horizontal, they are not. Pending further experimentation, the phase velocity of the signal within an individual axon segment of a myelinated neuron of about eight microns overall diameter will be taken as 4,400 meters/sec. This measured value is at least a factor of 100 times the accepted average velocity associated with a myelinated neuron of this size. If dashed lines, again apparently horizontal, representing this phase velocity are introduced into (C) as the velocity between nodes, there is a considerable delay left unaccounted for at each node.

---

[132]Bostock, H. (1982) Conduction changes in mammalian axons following experimental demyelination, in Culp, W. & Ochoa, J. eds. Abnormal Nerves and Muscles as Impulse Generators. NY: Oxford University Press pp 236-252

[133]Bostock, H. (1993) Impulse propagation in experimental neuropathy. In Peripheral Neuropathy, 3rd. Dyck, P. & Thomas, P. eds. Philadelphia: W. B. Saunders pp. 109-120

[134]Rasminsky, M. & Sears, T. (1972) Internodal conduction in undissected demyelinated nerve fibres. J. Physiol. (London), vol. 227, pp 323-350

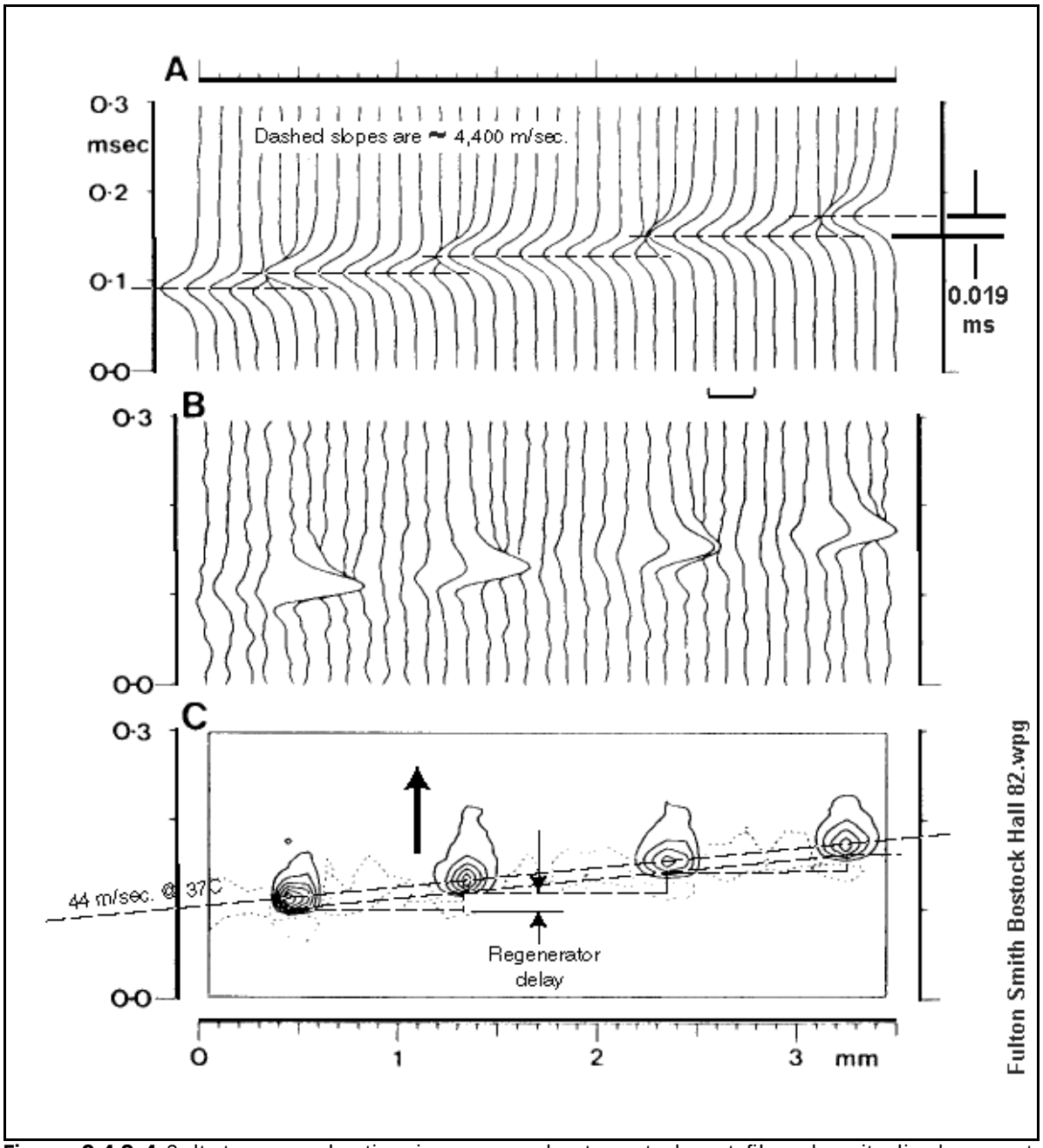

Figure 9.4.2-4 Saltatory conduction in a normal rat ventral root fiber: longitudinal current, derived membrane currents and membrane current contour map, plotted to same distance and time scales, with dashed lines and arrowheads added by this author. A, Averaged longitudinal currents (n=128) recorded at 100 micron intervals along the root (calibration bar: 4 microamps.). B, Membrane current records calculated by subtracting adjacent records of (A). C, Membrane currents re-plotted as a contour map. Inward currents are indicated by continuous lines, outward currents by dotted lines. Contour interval: 0.5 nA/100 micron electrode displacement, 37C. Dashed lines relate to signal velocities in the neuron, see text. Modified from Smith et al. (1982)

This delay is the pulse regenerator delay associated with the charging time of the regenerator conexus that reproduces the action potential. The delay derived from the graph is approximately 0.019 msec. (19 microseconds) at each node.

As shown in [**Figure 9.1.2-2**], the phase velocity of the signal propagating along an axon segment is inversely proportional to the diameter of the lemma. While this variation is substantial, it is not the dominant factor in the average velocity in a long axon containing more than one NoR. Using the relationships shown in the above figure, it is possible to calculate the average velocity of a stage 3 signal along a myelinated neuron with multiple Nodes of Ranvier. The average velocity is given by the expression;

avg. vel = distance signal traveled / total time of travel

avg. vel = phase vel. / (1 + (NoR delay x phase vel) / avg distance between NoR))

The second term in the denominator is usually much greater than 1. Therefore,

avg. vel. ≈ avg. distance between NoR / NoR delay.

avg. vel ≈ 0.9 mm / 0.019 msec ≈ 47 m/sec or 47 mm/msec at 37 Kelvin.

This relationship is contrary to early assertions attributed primarily to Rushton, but adopted by many lecturers, the **average velocity in a myelinated neuron is not strongly related** to the phase velocity within the axon segments. More importantly, **the average velocity is totally independent of the diameter of the axon**, whether measured at the lemma or at the exterior of the myelination. The delay associated with the phase velocity within each axon segment is negligible. The average velocity is calculated from the average axon segment length divided by the pulse regenerator delay at the associated Node of Ranvier. Taking the phase velocity of the signal as 4400 meters/sec, the calculated average projection velocity is 47 meters/sec, very near the 44 meters/sec obtained graphically. The delay associated with each NoR is remarkably constant. The difference in average velocity among stage 3 neurons is dominated by their differences in average axon segment length.

As noted in **Section 2.6.1**, the average velocity of signal propagation is a direct function of temperature.

Both Huxley & Stampfli and Smith et al. calculated an average velocity for their data but neither group addressed the obviously much higher phase velocity in their data or the NoR delay at each node.

9.4.2.2.1 The <u>average propagation velocity</u> of a neuron

Waxman[135] produced a paper in 1978 that included a wide variety of information related to the axon, the Node of Ranvier and other features (See **Section 5.1.2.5.2**). Much of the data assumes the chemical theory of the neuron with many identified ionic currents flowing by diffusion. It reproduces a graph from Brill et al[136]. with indicated data points. However the points shown are all calculated, using numerical integration rather than closed form solutions of the equations of Huxley and Hodgkin, and with additional smoothing to get stable solutions.

---

[135]Waxman, S. (1978) Variations in axonal morphology and their functional significance. *In* Physiology and Pathobiology, Waxman, S. *Ed*. NY: Raven Press, pp 169-190

[136]Brill, M. Waxman, S. Moore, J. & Joyner, R. (1977) Conduction velocity in myelinated fibers: Computed dependence on internode distance *J Neurol Neurosurg Psychiatry* vol 40, pp 769-774 (in ref. papers folder)

They provided no theoretical foundation for their mathematical models, other than a loose conformation with the H&H model of the neuron. Unfortunately, Brill et al. does not recognize the Node of Ranvier as a signal regenerator and predicts "As L becomes large, the conduction velocity falls and finally propagation is blocked." They did not quantify the value of L when conduction ceased but showed it becoming asymptotic near L = 10 millimeters (Fig. 1C) for an axon of 10 micron diameter. Their assertion clearly falsifies their empirical model and significantly undermines the Waxman paper. It also conflicts with the fact that neurons with lengths measured in meters remain quite functional in large animals (at least 2 meters in the author's personal case).

As noted previously, the theory of this work **(Sections 9.1.2)** predicts, and the available experimental data of Smith (**Section 9.4.2.2**) confirms a constant average propagation velocity of 44 m/sec for any neuron length that includes at least one NoR. At distances of less than one mm and not including a NoR, the instantaneous phase velocity of propagation is approximately 4400 m/sec (a paltry 1.5×10^{-5} the speed of light in vacuum). The low phase velocity relative to the speed of light is due primarily to the very high impedance of the axons and axon segments.

Linden, a neuro-scientist at Johns Hopkins, provided a book in 2015[137] in a paper for a popular audience, described the average velocity of three types of neurons: The Aβ-fibers traveled at about 70 m/s (250 kmh or 150 mph) while the Aα-fibers traveled at about 110 m/s (400 kmh or 250 mp). These *average propagation* velocities over myelinated fibers (**Section 8.7.5.1**) are similar to the value shown above based on Smith et al. Linden indicated signals traveled along non-myelinated neurons (C-fibers),via diffusion through the axoplasm, at the more leisurely *average diffusion* velocity of ~0.8 m/s (3 kmh or 2 mph). These values are very compatible with the ranges of signal velocity shown in the following figure.

9.4.2.3 Survey of reported stage 3 average signal velocities

Borenstein et al[138]. have provided data on a variety of somatosensory neurons in **Figure 9.4.2-5** based on clinical evidence. The difference in velocity of propagation in myelinated (stage 3) neurons versus the velocity of conduction in non-myelinated (other stage, and typically analog) neurons is significant. Borenstein describe the unmyelinated neurons, C fibers, as transmitting nociceptive impulses. This appears an inappropriate label on its merits. These unmyelinated neurons do not transmit pulses. They connect to, and are encoded by, stage 3 neurons that are designed to propagate nociceptor signals at high velocity to the CNS. Their designation of their neural fibers by letter and Greek alphabet extension are of largely historical origin within the clinical environment. Their further description of the purpose of these types is also largely anecdotal. As shown in this chapter, the velocity of propagation is only indirectly related to the diameter of the axon, and this relationship has to do with the thickness of the overlying myelin.

---

[137] Linden, D. (2015) Touch: The Science of Hand, Heart and Mind. NY: Viking.

[138] Borenstein, D. Wiesel, S. & Boden, S. (1995) Low Back Pain, 2nd Ed. London: WB Saunders pg 29

	MYELINATION	RECEPTOR TYPE	TRANSMISSION (m/sec)	THRESHOLD	DISTRIBUTION	MODALITY
A-alpha	+	Mechanoreceptor	Rapid (70–120)	Low	Local	Vibration (proprioception) Pain (prick)
A-beta	+	Mechanoreceptor	Rapid (40–70)	Low	Local	Vibration (proprioception) Reflex withdrawal
A-gamma	+	Mechanoreceptor	Rapid (20–40)	Low	Local	Muscle spindle
A-delta	+	Mechanonociceptor	Slow (5–15)	High	Local	Damaging pressure
A-delta	+	Thermal mechanonociceptor	Slow (5–15)	High	Local	Noxious Temperature (sharp)
B	+	Autonomic	Slow (10–15)	High	Diffuse	Preganglionic fibers
C	–	Mechanonociceptor	Slow (0.2–1.5)	High	Diffuse	Noxious
C	–	Polymodal nociceptor	Slow (0.2–1.5)	High	Diffuse	Pressure (sharp) Any noxious stimulus (dull)

Figure 9.4.2-5 Peripheral nerve fiber characteristics. Note the limited range of velocities for propagation in myelinated neurons, and the much slower velocity of conduction in non-myelinated neurons. No reason for the difference between A-alpha & A-beta velocities is apparent in this figure. From Borenstein et al., 1995

Redburn & Dahl have provided an average velocity distribution, **Figure 9.4.2-6**, showing what they describe as compound action potentials but without citation[139]. They assert a small subset of signals traveling along a large (sciatic) mixed nerve (not an individual neuron) of the human leg average a velocity of 120 m/s over distances of 120 mm (1.2 meters). The scale of their figure does not support an average velocity significantly faster than 44 m/s for an A-alpha neuron. Other neurons are reported to travel as slowly as one m/s on average. Their notation is similar to, but conflicts with, that of Borenstein (A-alpha is an afferent path in Borenstein but by definition an efferent path in Redburn & Dahl). They did not explain the low amplitude of the compound action potentials from their slower "compound action potentials."

[139]Redburn, D. & Dahl, N. (1998) Organization of the nervous system *In* Johnson, L. *ed.* (1998) Essential Medical Physiology, 2nd Ed. NY: Lippincott-Raven page 687

Krassioukov[140], writing in Ramachandran has provided additional data but without citations. It appears to be a summary of clinical data from different investigators. As a result, his Tables III & IV present a jumbled picture without rational structure.

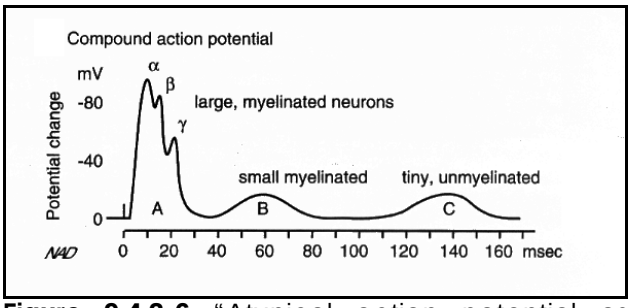

Figure 9.4.2-6 "Atypical action potential as recorded with external electrodes". Details were not provided on how the signals were recorded from the large sciatic nerve of the human leg. See text. From Redburn & Dahl, 1998.

9.4.2.4 The transmission of signals in a demyelinated axon

When a normally myelinated or otherwise electrically isolated neuron is stripped of its electrical isolation, its capacitance per unit length increases drastically. This causes the characteristic impedance of the axon to also change drastically. The result is an abrupt change in the impedance level as a function of position along the axon. This results in a significant reflection of the energy at the location of the change and a much lower transmission efficiency. It is also likely that a significant change in the phase constant of the circuit will be introduced.

The material reviewed in **Section 9.1.1**, particularly that of Kaplan & Trujillo, can be readdressed using different parametric values to determine the signal velocity along an unmyelinated axon. The parameters of such an axon can cause it to exhibit signal transmission by conduction (at a greatly reduced speed) rather than propagation. Alternately, the changes can result in propagation but under conditions of significant phase (and therefore pulse) distortion.

Rasminsky and Sears have provided similar data for a demyelinated ventral root nerve. Even in this condition, their data shows propagation with phase velocities of 500 to 600 meters/sec or higher (in some cases, much higher by scaling).

Nusbaum et al. have discussed "white matter" from a clinical perspective[141]. The material sheds light on the role of myelination in the new born as well as in the diseases of later life. They make the general statement that, "Because myelination of the CNS is essentially a postnatal process. . . ." but then go on to describe the order of myelination as well as the degree of myelination of different regions of the neural system at birth and at subsequent monthly intervals. Their findings generally support the idea that the infant does not perceive significant pain at the time of birth because of limited signal propagation within the neural system. Atlas has provided very detailed information suggesting the infant can feel little sensation from its extremities during the first months of life[142]. This is understandable if the neurons have not yet been myelinated. His text has also provided considerable material on the appearance of stage 3 neurons in MRI imaging.

Clinically, the loss of myelination is a very serious medical problem. It is typically described as a peripheral neuropathy (that may include neurons within the spinal cord). The most common name for diseases of the myelination are muscular sclerosis. The most common of these is Charcot-Marie-Tooth disease type 1. It is characterized by weakness in the legs and, to a lesser degree, the arms -- symptoms that usually appear between mid-childhood and age 30 (WebMD). Guillain Barr Syndrome is another group of symptoms frequently associated with

---

[140]Krassioukov, A. (2002) Peripheral nervous system *In* Ramachandran, V. *ed*. (2002) Encyclopedia of the Human Brain. San Diegeo, CA: Academic Press pp 825-827

[141]Nusbaum, A. Rapalino, O. Fung, K-M & Atlas, S. (2009) White matter diseases and inheritied metabolic disorders *In* Atlas, S. *ed*. Magnetic Resonance Imaging of the Brain and Spine. NY: Wolters Kluwer Chap 10

[142]Atlas, S. *ed*. (2009) Magnetic Resonance Imaging of the Brain and Spine, Vol 1. NY: Wolters Kluwer pg 346

demyelination of the peripheral nerves.

9.4.3 The unique physiological features of the *axon segment* (internode)

[xxx note features reminiscent of both an axon and a neurite]
[xxx the DC potentials involved would seriously impact the ionic conduction of signals along an axon segment]
[xxx rewrite; include separation of DC and AC signaling functions.]
Although the previous discussion has defined the plasmas on each side of a Node of Ranvier, it must be recognized that the postsynaptic plasma of one node is the pre-synaptic plasma of the next node. The conclusion is that an axon segment is a conduit within a closed lemma that is functionally the same whether considered an axon or a dendrite. A single reticulum extends from the postsynaptic end to the pre-synaptic end of the axon segment. The concentration of various particles may vary with location along the axon segment but this is functionally irrelevant. From a signaling perspective and in the first order, an axon and a dendrite are the same. From an electrical perspective, they are also functionally the same. In the case of a chain of non-bifurcating projection neurons, the axons and dendrites are essentially interchangeable. The only way to distinguish them is by associated structures, i.e., topologically or by morphological variation. Placing the subject in a historical context, a dendrite delivers its signal current to an Activa located within, or near, the soma of the cell. An axon delivers its signal current to an Activa located external to the cell body, within a synapse or a Node of Ranvier.

[xxx check following words
As discussed in the previous section, the power supply source associated with the pre nodal terminal of an axon segment is not required to provide power to the circuit within the node. Its primary purpose is to insure that the emitter of the Activa within the node is biased to insure cutoff of the Activa. The two ends of the axon segment are normally at different voltages. The post nodal terminal is at V_{cc} and the pre-nodal terminal is typically at V_{ee}. Here again, the potential difference is such as to charge the battery V_{ee}. The battery V_{ee} is called upon to maintain a fixed voltage. However, it is never called upon to provide power. This electrolytic battery is always in a charging mode. The battery, located within the manifold of the nodal gap is a supplier of higher energy bioenergetic material, typically GABA at the expense of a lower energy material, typically a glutamate. These materials can be transported by diffusion from the pre-nodal recess to the post nodal recess within the nodal gap where it can be used to power the collector battery, V_{cc}. This process does not involve any thermally dissipative loss, does not involve a Carnot Cycle and is not limited by the Second Law of Thermodynamics applicable to dissipative processes.
]

In signal processing, the axon and dendrite play a slightly different role. An axon is tailored to carry a single current from the Activa within the soma to the pedicle where a voltage is created that can be sensed by many dendrites without degradation. To avoid degradation, the terminal electrical impedance of the axon circuit must be low. On the other hand, the dendrite (and the podite) are designed to operate at a higher electrical input impedance and receive a small current from each of many pedicles without causing a degradation in the voltage of individual pedicles.

At the cytological level, considerable effort has been expended mapping the particles within the axon segment and other conduits within the neural system. It appears that most of these particles are not actively involved in the electrical functioning of the neural system. Some of them may play a structural role in forming Activa.

The Activa is shown surrounded by the podite space extending vertically to the cylindrical podite portion of the nodal lemma surface indicated by the dark horizontal bars. The podite portion of the nodal lemma, along with its external bioenergetic coating forms the power supply connection marked **P** in the lower figure. The bioenergetic coating and the nodal lemma participate in an electrostenolytic process. The bioenergetic material is provided to the nodal lemma by diffusion via the nodal gap. The overall path, diffusion through the nodal gap

and charge transfer through the lemma, may exhibit a resistive component.

Beyond the nodal lemma to the right, is the post nodal region, an unmyelinated portion of the axolemma. This region is dominated by a specialized portion of the axolemma providing an electrical power source, labeled **C**, for the Activa. The coating on the outside of this cylindrical portion of the axolemma participates with the axolemma in an electrostenolytic process. The coating is found in the "nodal recesses" of the nodal gap. The overall path, diffusion through the nodal gap and charge transfer through the lemma, may exhibit a resistive component. However, the most important feature of this topography is the large lemma area that is in direct electrical contact with the interneural matrix. The electrical capacitance of this area is much greater than all of the remainder of the internode.

The combination of the Activa, the resistive component in its base lead and the large capacitance in its collector, and/or emitter, lead constitute a regenerative, single shot, oscillator. This oscillator can respond to any excursion of the electrical potential between its emitter and base that exceeds a threshold. The result is the generation of a new action potential pulse with characteristics determined by these resistive and capacitive values. Since these values are typically the same for each internode and Node of Ranvier, it appears that the same action potential is regenerated at each node. This similarity is deceptive. The pulses at each node need not be similar, especially during experiments involving the connection of electrical probes to one or more neuron circuit elements.

Robertson[143] has noted that the area of the conseg exposed to the interneural matrix at the nodal gap is essentially independent of the diameter of the axon. In fact, "it is a striking fact that the total exposed area of the nodal axon membrane in many large fibers is actually smaller than in many small fibres." Assuming the electrical capacitance of the Node is proportional to this area, an explanation is available why all action potential waveforms appear to exhibit a similar time constant.

After (re-)generation of the action potential, the signal propagates along the internode via the reticulum until it reaches the next pre-nodal region. Its propagation velocity and attenuation characteristics are determined by the properties of the transmission line. In the pre-nodal region, a region of the axolemma is found that is very similar to that in the post nodal area. It is unmyelinated and coated on the outside by a bioenergetic material that can participate in an electrostenolytic process. The result is a second power source, labeled **E**, shunted by a large capacitance. The bioenergetic material occupies a second recesses similar to the earlier one. Bioenergetic material also reaches this area by diffusion through the nodal gap. The reticulum is also converging on the location of the next active device on the horizontal axis at the extreme right in this figure. Both the topography and the electrical configuration are the same as on the far left but the signal is applied to the emitter of the Activa. The large capacitance associated with the power supply labeled **E** is in shunt with the similar capacitance in the collector circuit of the second Activa.

Note that the shape of the action potential applied to the emitter of the second Activa is unimportant. As long as the amplitude of the signal exceeds the threshold level of the second Activa, that circuit will generate a new pulse that will look much like the original pulse as generated at the previous node. A Node of Ranvier does not amplify the signal received from the previous node. It generates a new "action potential" waveform.

The electrical relationship among the three power supplies, **P, C** & **E** is important. The values of **C** & **P** must be such as to ensure the collector of each Activa is reverse biased. Similarly, the values of **E** & **P** must be such that the emitter of the Activa is reverse biased except in the presence of the signal pulse from the previous node. Lacking an input signal, the Activa is cutoff and its collector is at the supply voltage **C**. This "quiescent voltage" is much more negative than that found in signal processing neurons that must handle a bi-phase electrical signal. When this signal arrives, the total voltage on the emitter compared with the base must

---

[143]Robertson, J. (1959) Preliminary observations on the ultrastructure of Nodes of Ranvier, Zeit. fur Zellforsch. vol. 50, pp. 553-560

forward bias the Activa momentarily. If this occurs, the regenerative cycle will begin and a new action potential will appear at the collector terminal of the Activa. This action potential may have a positive amplitude slightly larger than the absolute value of the quiescent voltage of the axon segment (the cutoff voltage) because of the capacitive overshoot found in some regenerative amplifiers.

The topography of the each power supply connection need not occupy the entire circumference of the axon. Rydmark & Berthold have examined the circumference of at least on nodal lemma in detail. About 30% of the circumference was covered with a coating, the putative area of the electrostenolytic process associated with the power supply. This external coating is usually reported as an electron opaque material.

The physical relationship of the three power supplies is also important. The walls of the nodal gap form a constricting channel between the grounding terminals of these power supplies and the surrounding perinodal interneural matrix. If an experimenter places a probe in the perinodal space, the potential detected by that probe can be very complicated. It can be due to both displacement and conductive currents flowing in the impedance of the nodal gap fluid. The conductive current is the sum of the currents flowing from all of these power supply connections to the perinodal space. The displacement currents are due to both the pre-nodal and post nodal signals being capacitively coupled to the perinodal fluid via the material in the nodal gap.

It is important to note that the illustrated circuit topography of the Node of Ranvier is the same as that predicted for the retinal ganglion cells based entirely on measured external waveforms, Section 9.5.

Figure 9.4.3-1 EMPTY Comparison of currents generating the action potential in the switching Node of Ranvier (or the conexus within a ganglion cell). See text.

9.5 A functional synapse as the electrolytic connection, a *type 3* conexus, between neurons EDIT

Shepherd has summarized considerable material related to the synapse[144]. The 3rd edition of this textbook (1994) is basically a reprinting of the 1st edition. Some of the drawings are unrelated to any functional framework related to the operation of the neurons. While the material is interpreted in terms of the Dual Alkali-ion Theory, the dimensional details are useful.

A more recent summary of the synapse has been provided by Pannese[145].

Currently, the biological community has become divided over their chemically based concept of a synapse. Most of the documentation suggests that a wide variety of neurotransmitters are released at the presynaptic terminal, traverse the synaptic gap and stereochemically unite with the surface of the postsynaptic terminal. Other literature treat the "neurotransmitters" as intermediaries. In this concept, the neurotransmitters are catalysts controlling the movement of ions between the presynaptic and postsynaptic terminals. These two concepts of the chemically-based synapse are intrinsically incompatible. This leaves understanding of the synapse in a state of limbo as noted by Messenger, et. al. in **Section 9.5.4**. Lack of an operational mechanism for the neurotransmitter as an active participant has led to three difficult situations:

1. a proliferation of putative neurotransmitters satisfying different proposed synaptic scenarios.

2. a proliferation of putative neurotransmitter receptors to accommodate the putative chemical neurotransmitters.

3. Virtually no definitive explanation of how these neurotransmitters are released from the presynaptic tissue.

The synapse plays a crucial role in the connection between elements of the neural system. This role is an electrolytic one as opposed to a chemical one. The synapse is fundamentally an active electrolytic junction between two neural conduits that is external to a neuron. It can be used to transmit electrotonic or phasic signals. The multitude of caricatures in the literature attempting to describe the chemical events taking place within the synapse, such as figure 4.8 of Shepherd, should be ignored. Most of the activity described in these caricatures relate to the electrostenolytic processes associated with the synapse and not the transmission of signal information across the "gap."

Defining the synapse from a gross morphological perspective is difficult because of the variety of morphologies encountered. At a cytological level, it appears that the smallest active area that can be considered an Activa is about 100 Angstrom in diameter. This "unit Activa" is frequently formed into two-dimensional arrays to form a practical Activa. These practical Activas appear in conexuses of three different styles.

Style 1. The structurally simplest synapse is the in-line conexus found between two stage 3 propagation neurons. The Activa array is unitary, planar, perpendicular to the axes of the adjacent neurons and two-dimensional. The dendrites typically connect to only one axon.

Style 2. The next simplest synapse is frequently found at the interface between photoreceptor cells and subsequent signal processing neurons. In this case, multiple dendrites from a single stage 2 signal processing neuron may converge on a single pedicle. The result is a synaptic structure containing multiple small Activa arrays. The total area of the Activa arrays determines the total current carrying capacity of the multi-terminal synapse.

Style 3. The most difficult synaptic configuration to define appears between signal processing neurons and the dendritic structures of ganglion cells (Purkinje cells within the CNS). This configuration involves dendritic extensions containing a large number of spines that contact similar axonal extensions over a significant distance. The analogy is two octopuses making love by extending two arms in parallel with the suckers of those arms paired. The total synaptic area consists of the area of the paired conexuses. This style synapse configuration may also be used extensively within the CNS to form "memories."

---

[144]Shepherd, G. (1994) Op. Cit. pp 69-86

[145]Pannese, E. (1994) Neurocytology. NY: Thieme Medical Publishers, Inc, pp 108-116

The specific electrophysiology of the synapse can vary significantly due to differences in the electrical parameters of the elements associated with it.

The Activa of a synapse is operated in the common base configuration. In this configuration, it provides a very low impedance connection between two neural conduits in the orthodromic direction if it is properly biased. To be properly biased the emitter-to-base potential must be positive and the collector-to-base potential must be negative. The base is normally connected by a high impedance, formed by a confined region of electrolyte, to the local INM. There is no voltage source associated with a membrane between the base and the local INM. The collector-to-base potential is normally negative due to the electrostenolytic potential of the postsynaptic dendroplasm. The origin of the emitter-to-base potential is frequently more complex.

In electrotonic cases such as the synapse between the photoreceptor cells and the bipolar cells, the photoreceptor cell axoplasm potential must be expressed in terms of the local INM of the synapse. This reference point is different than that normally used to describe the distribution amplifier of the photoreceptor cell. The common emitter circuit of the photoreceptor cell is connected through its poda terminal to the IPM. It is also probable that the base connection of the distribution amplifier is also connected to the IPM instead of the INM. Therefore, it is necessary to consider the potential difference between the local INM and the IPM.

In many phasic cases, the signal at the presynaptic terminal of an axon segment is a positive going waveform impressed on a very low negative quiescent DC potential of the axon segment plasma. Such a signal can result in a positively biased emitter-to-base potential at the synapse after the signal has overcome the quiescent DC potential. This quiescent DC potential forms at least a part of the threshold associated with the transfer of phasic signals through a synapse or a Node of Ranvier. As in the electrotonic case, the collector-to-base potential of the Activa forming the synapse is normally biased negatively by the dendroplasm of the following neuron or the plasma at the antidromic end of the axon segment.

Further detailed investigation will be required to determine whether some phasic synapses are able to operate as a monopulse action potential regenerators based on the amount of capacitance provided by the postsynaptic connection.

> In the general case, under normal operating conditions, the synapse should not be considered a “rectifier.” In most electrotonic cases, it is not used to change the shape of the signal being transmitted. However, it does prevent the flow of both quiescent and signal related electrical currents in the antidromic direction.

In the following discussion of the morphological styles of synapses, only the electrophysiology of the style 1 synapse will be explored in detail. The characteristics of the other styles are highly application specific and involve difficult modeling procedures to evaluate their overall electrical characteristics.

xxx Typical active circuits between and within neurons MERGE with above

One of the primary premises of this work is that **all** connections between morphologically identifiable neurons in animals involve active electrical circuits. This is obviously a controversial position. However, the fundamental circuit discussed above, and explored in depth for the Node of Ranvier, is easily configured to satisfy all of the requirements of the neural system. Furthermore, the bioenergetic requirements of the electrical system can be satisfied by a variety of readily available bioenergetic materials. While these materials may consist of those materials frequently named in the literature as neurotransmitters or neuroreceptors, GABA, glutamate, etc., other materials can also be used. The primary requirement is that they participate in reversible reactions that typically furnish electrons through electrostenolysis when they proceed toward the lower energy state. This lower energy state normally involves glutamine combined in any of a variety of chemical forms.

Chemically based neuron interconnections will not be discussed, or debated, in this work. If desired, the reader can consider the relevant parts of this section as the electrical equivalent circuit for his conception of a chemically based interconnection.

There are two primary forms of active circuits between sections of conduit within the animal neural system, external terminations and internal processing circuits.

9.5.1 The *style* 1 synapse typical of stage 3 connections EMPTY

9.5.1.1 The in-line characteristics of the style 1 synapse

[xxx change title to in-line characteristics of the style 1 synapse and expand to include both delay and impedance.]
The literature contains a number of estimates of the in-line impedance of a synapse based on the assumption that it can be considered a simple passive resistance. A number of estimates of the time delay between the input signal and the output signal also appear based on a different assumption, that the synapse is a diffusion controlled chemical pathway. These conceptual estimates should not be relied upon. When biased for *in-vivo* operation, the synapse is an active conexus containing an Activa. The in-line impedance of such a circuit must consider both the performance of the Activa and the associated circuit elements.

Looking at the Activa alone, its in-line impedance depends on its bias conditions. If the collector terminal is not biased negatively with respect to the base, the Activa exhibits an infinite resistive impedance between these two terminals in both directions. If the collector terminal is biased negatively with respect to the base, the resistive impedance between the emitter and the collector is asymmetrical and depends on the emitter to base potential. No current will flow from the collector to the emitter under any circumstances under these conditions since the collector diode is reverse biased. The current that flows from the emitter to the collector does not depend on the voltage between these two terminals. Because of this fact, the apparent impedance cannot be described as a resistance. The current that flows, by transistor action, is controlled by the emitter to base voltage and is exponential. Thus, the forward impedance of an Activa within a synapse is defined as a *transimpedance*. The transimpedance is the apparent current flow from the emitter to the collector of the Activa as a function of the emitter to base voltage. This function is shown in [**Figure 8.5.1-1(c)**]. At zero voltage, the transimpedance is very high. For positive voltages, the current increases rapidly. As noted in [**Section 8.3.2.1.1**], the transimpedance can be described by either the static transimpedance or the dynamic transimpedance as appropriate. The forward dynamic transimpedance of a typical synapse is very low under operational conditions. This impedance is frequently lower than the series impedance associated with the conductive currents within the plasmas of the circuit. The precise measurement of the Activa transimpedance requires the Ussing chamber approach to impedance measurement in order to eliminate the plasma impedances.

9.5.2 The *style* 2 synapse typical of stages 1, 2 & 4 connections EMPTY

Shepherd has described this style two synapse as a divergent synapse, a single pedicle interfacing with multiple neurites[146].

9.5.2.1 The synapse at a pedicel

Because of the great variability in topography available within the neural system to make interconnections in the most functionally efficient manner, selecting a prototype configuration for further analysis is very difficult. From the perspective of a functional termination, whether the post junction structure is myelinated or not is irrelevant. All of the external terminations are exposed to the surrounding INM--by gaps in the myelin for myelinated conduits. The important functional characteristic is the total capacitance placed in shunt with the input and output circuitry of the termination. This parameter plays a major role in determining the functional mode of the junction. The two primary roles of external terminations are acting as an electrotonic connection or acting to regenerate action potentials. The electrotonic connection is the most common and of primary interest in vision.

The description of a specific external axon termination is straight forward. It is primarily a matter of describing the morphology in the context of the Node of Ranvier with ramifications. Probably the simplest ramification is the spherule. A spherule is usually described in vision as the

---

[146]Shepherd, G. (1998) The Synaptic Organization of the Brain, 4th ed. NY: Oxford University Press pg 8

termination of a photoreceptor cell that connects to only one orthodromic neuron. A spherule is a paranode of an axon segment that happens to be at the terminal end of a photoreceptor axon. These axons are short enough that they do not require myelination. The spherule performs as part of a low impedance electrotonic interconnection just as in the Node of Ranvier. The spherule does not produce an action potential unless excessive capacitance is connected to the circuit by an investigator.

A more complicated termination for a photoreceptor cell is required to interconnect with several orthodromic neurons. This more general morphological structure is the pedicle. In all other functional respects, it is just like a spherule. Shichi provides a caricature of the spherule and pedicle that are nearly identical[147]. In a more general context, pedicles are found at the termination of photoreceptor cells and any other signal processing neuron interconnecting with multiple orthodromic neurons. The photoreceptor pedicles are found in the outer lateral layer of the retina shared with the horizontal cells between the outer fiber layer and the outer plexiform layer. The bipolar cell pedicles are found in the inner lateral layer of the retina shared with the amercine cells between the inner fiber layer and the inner plexiform layer.

The morphology of pedicles is three dimensional and difficult to illustrate adequately on paper. In addition, there are interconnections on the terminal surface of the pedicle, described as basal contacts, and interconnections folded more deeply into the pedicle, described as invaginating contacts. It is also important to note there is no requirement that every dendritic structure passing near a specific pedicle make contact with that pedicle.

Recently, the work reported in the literature related to this area has begun to merge with the electrophysiological studies of the same structures. The recent papers describing a pedicle by Osborne[148], Froelich[149], Vardi[150] are useful and include references to earlier work. There are minor morphological and major electrophysiological differences between this work and that presented by those authors. The underlying differences are three. This work defines a manifold within the pedicle morphology in which all neural elements at that location can share bioenergetic materials. Second, this work defines the contacts between neurons as fundamentally electronic and unidirectional. Third, the likelihood that one or more of the contacts within the pedicle geometry will be to a lateral cell, with a poditic terminal and an axon sharing a common plasma sheath, must be considered. It is also appropriate to consider how areas of different apparent electron density are shown in this type of figure.

Figure 9.5.3-1 presents the details of a pedicle based on this theory. The artwork is modeled after a figure appearing in Vardi. However, this figure;

---

[147]Shichi, H. (1983) Biochemistry of vision. NY: Academic Press pg. 18

[148]Osborne, M. (1977) Role of vesicles with some observations on vertebrate sensory cells. *In* Synapses, Cottrell, G. & Usherwood, P. *Ed*. London: Blackie, Chapter four

[149]Frohlich, A. (1985) Freeze-fracture study of an invertebrate multiple-contact synapse: The fly photoreceptor tetrad. J. Comp. Neurol. vol. 241, pp. 311-326

[150]Vardi, N. Morigiwa, K.Wang, T-L, Shi, Y-J, & Sterling, P. (1998) Neurochemistry of the mammalian cone 'synaptic complex' *Vision Res* vol. 38, pp 1359-1369

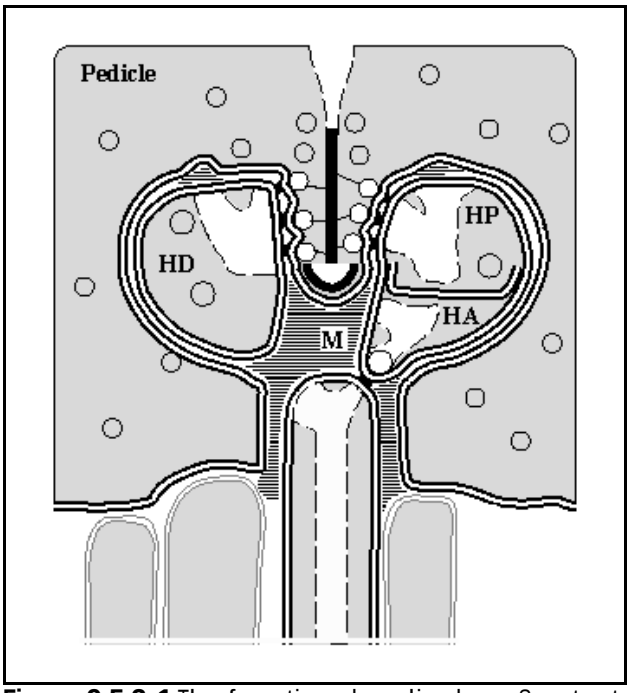

Figure 9.5.3-1 The functional pedicel. xxx See text. Modified from Vardi, et. al., 1998.

1. does not maintain the symmetry of neuronal structures of Vardi. The invaginating structure on the left is a common dendrite. It may be associated with a bipolar cell or as labeled here, a simple horizontal cell dendrite (HD). The invaginating structure on the right is taken to be a lateral cell. The upper half represents the poditic structure of a horizontal cell (HP). The lower half (HA) represents the axon of the same horizontal cell. Notice the single bilayer membrane separating these two halves. It is proposed that this internal bilayer membrane is non-specialized and turns to make a tight lap joint at each surface of the cell plasma membrane.

2. shows two separate classes of vesicles. Those shown scattered throughout the drawing are not directly relatable to the signal transmission function. Those shown connected to the ribbon of the pedicel are associated with the transmission function. They are in electrical communications with the reticulum of the photoreceptor cell on one side and with the specialized axolemma on the other. They may also play a structural role. There are references in the literature to vesicles that are embedded in the axolemma. These references appear in papers supporting the assumption that the vesicles are the source of a chemical neuro-tranmitter used to excite the nearby neurite structure. Such vesicles are difficult to photograph explicitly and adequately. They are not required in this work. The figure by deBlas of a synapse in brain tissue presented in Matthews[151] does not appear to show any vesicles opening into the inter-conduit space. Neither does it show the hydronium liquid crystal found in part of this space. The spacing between the two bilayer membranes is within 80-100 Angstrom as expected.

3. shows all bilayer membranes at their conventional thickness. Any additional thickness associated with these membranes is an artifact (potentially useful) of the observation technique. In Vardi, these thicker regions are described as electron dense.

4. shows a manifold occupying a central location where it can support the bioenergetic needs of all neurons. The manifold is not limited to a specific area. However, it is excluded by the laws of diffusion and probability theory from the very narrow spaces between the cells occupied by the Activas. The manifold reaches the top of the two invaginated structures by passages that are out of the plane of the paper, extends down between the lower neurons, and is in contact with the INM between the inner and outer limiting membranes of the retina.

5. adds several reticuli associated with the signal carrying axoplasm of each cell. These are shown as the space between the dashed lines. For purposes of convention, the reticulum of the pedicle is shown as containing two black areas of specific interest, the vertical bar known as the ribbon and the arciform structure at the lower end of the ribbon. A reticulum is also shown in the dendrite of a horizontal cell (HD) on the left. This reticulum contacts the specialized dendrite membrane where it most closely approaches the pedicle and at an area at the top where it is contact with the manifold. The reticulum then goes into the paper to contact the internal Activa of the cell. Two reticuli are shown on the right invagination. The

[151]Matthews, G. (1991) Op. Cit. pg. 9

upper one is in the poditic neurite of a horizontal cell. It is shown contacting the specialized podalemma in both the area closest to the pedicel and in an area at the top where it is in electrical communication with the manifold. This reticulum also goes into the paper to contact the internal Activa of the horizontal cell. The lower reticulum is returning to the plane of the paper from the collector terminal of the internal Activa and contacting the specialized areas of the axolemma. One area of contact is associated with the manifold and the second is associated with the orthodromic neuron, probably of the bipolar morphological type.

6. Shows electrical signal communication between the pedicle and the two horizontal cells, and between the right-hand horizontal cell and the orthodromic neuron at the bottom of the page, by means of active electrolytic semiconductor devices (Activas). These Activas may consist of one device at each location or a small group of devices in parallel, as shown here, where more power handling capability is required.

7. Shows several other structures associated with neurons at the bottom of the figure. However, lacking direct contact with the reticulum of the pedicle, it is doubtful that they are in signal communications with that neuron.

Figure 9.5.3-2 reproduces figure 5B of Vardi et al. at 42,000X. It overlays the above caricature and shows the concentration of electrical charge in appropriate regions supporting the above analyses. As Vardi et al. note, the opaque areas are areas of high electron density in electron-microscopic imagery.

The photoreceptor cells and all of the neurons interfacing with them process electrotonic signals. Therefore the binary concept of ON and OFF cells is of limited utility. As shown elsewhere, what is known is that the polarity of the signal emanating from the axon of a lateral cell is opposite to that of the input signal on the poditic neurite and of the same polarity as the input signal on the dendritic neurite.

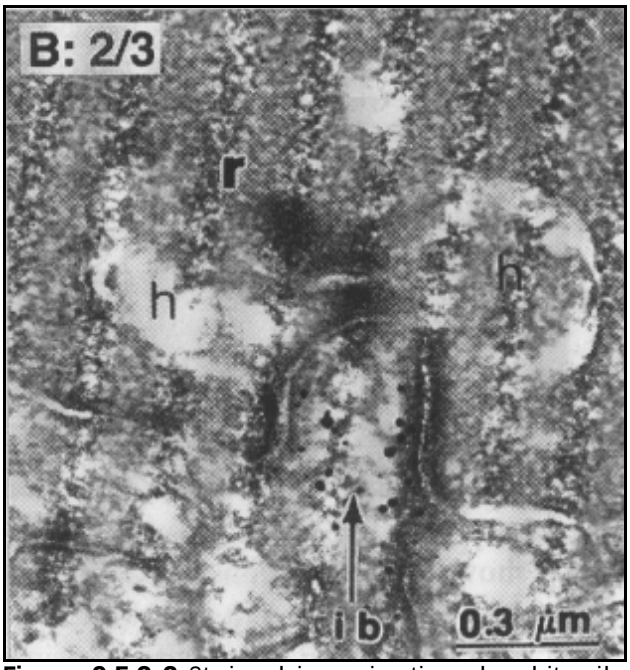

Figure 9.5.3-2 Stained invaginating dendrite, ib, between two horizontal neurons at 42,000X using electron-microscopy. The region between the axon ribbon central to the axon, r, and the dendrite, ib, shows an electron density asymmetry associated with the Activa at this location. The symmetrical electron density between the two horizontal neurons, h, and the dendrite, ib, suggests the presence of an electrostenolytic process at these two locations. The large opaque area within the axon, r, suggests the location of an out-of-plane electrostenolytic process at this location. From Vardi et al., 1998.

9.5.2.1.1 The electrical circuit at the *style* 2 synapse EMPTY

9.5.2.1.2 The bioenergetic circuit at the *style* 2 synapse

Although the paper by Vardi, et. al. assumes signal transmission at the synapse based on chemistry and assumes the signals are treated in a binary manner, the data regarding the location of the various materials they investigated can be extremely useful in developing a more general theory.

Their preparation protocol employed glutaraldehyde for most experiments, a close relative of the glutamates. It may be a solvent for the glutamates and possibly GABA as well. Much of their imagery was at less than x42000 and did not show membrane bilayers distinctly.

Two details: this work assumes the cone synaptic complex of Vardi,

et. al. corresponds to the photoreceptor pedicle of this work. Words below that within wiggly brackets were added by this author for context.

Some significant preconceptions were introduced into their paper:

Their abstract begins with a fundamental preconception: "The cone 'synaptic complex' is a unique structure in which a single presynaptic axon secretes glutamate onto processes of bipolar cells (both ON and OFF) and horizontal cells."

Their results included the statement: "To identify the ON cells we first looked at peripheral cone terminals in the monkey because here, all invaginating dendrites are ON, and quite likely all dendrites forming basal contacts are OFF. In other mammalian retinas, this segregation into invaginating/ON, basal/OFF, is true for most cell types, but not all."

It is unusual to find a "unique structure" of a cell, that secretes a non-protein material of the complexity of a glutamate. It is equally unexpected to find the molecular identity of the postsynaptic receptors of this putative secretion remains largely unknown and unlocalized at this date.

They provide two important datum in their abstract:

+ Invagination (probably ON) bipolar dendrites in the monkey and rat express the metabotropic glutamate receptro, mGluR6. The stain is intense on the dendritic membrane where it first enters the invagination, and weak at the tip nearest to the ribbon. The cone membrane is electron-dense where it apposes the intense stain for mGluR6.

+ The 'cone' membrane is electron-dense opposite to the receptor sites on both ON and OFF bipolar cells.

They provided a range of pertinent data in their results section:

+ The metabotropic glutamate receptor mGluR6 was identified in the rat retina and localized to the dendritic tips of the rod bipolar cell.

+ Close observation of serial sections revealed that a given dendrite may form a contact at the cone base in one section, and occupy the central element position in another.

+ At peripheral cone terminals of the monkey, all invaginating dendrites were stained, and all dendrites forming basal contacts were unstained.

+ 70% (28/41) of the stained dendrites terminated as central elements of the triad

+ At cone terminals of the rat, about half of all dendritic tips contacting the cone (41/79) stained for mGluR6, suggesting that about half of the bipolar cell types expressed this receptor.

+ Many of the stained dendrites contacted the cone at basal-like junctions. The cone membrane apposing these stained dendrites was often electron-dense or simply dark due to the immunostain was not clear.

+ When staining intensity in the invagination dendrites (both the monkey and rat) was relatively weak, it did not concentrate at the apex, i.e. at the region nearest the site of vesicular release. It concentrated near the base of the invaginating dendritic tips, particularly at the region apposed to the cone. Just beneath the cone membrane at this site is a layer of fluffy electron-dense material.

+ When stain was observed in the horizontal cell terminals, it appeared at the electron-dense membrane, subjacent to the presynaptic ribbon.

+ The stain was distributed along the electron dense horizontal cell membrane, facing the other horizontal cell terminal. Apparently, the ionotropic glutamate receptor is on a narrow strip of

horizontal cell membrane along the synaptic ridge.

The relevant findings presented in their discussion include:

+ all of the {chemical} receptors that they localized were present in apposition to an electron-dense membrane.

+ the glutamate and GABA receptors localized to the cone synaptic complex by immunocytochemistry correspond to junctions previously identified by morphology.

+ the glutamate receptors on bipolar dendrites are all located at relatively large distances from the {putative} site of vesicular release.

+ mGluR6 localizes not to the apex, but to the base of the invagination dendritic tip (monkey) or to the basal-like junction (rat).

+ the cone membrane in apposition to both types of glutamate receptor bears a noticeable layer of fluffy electron-dense material.

+ The horizontal cell membrane apposed to the $GABA_A$ receptor on bipolar dendrites bears a fluffy, submembranous electron-dense material.

+GABA receptors **[xxx check context and add words]** might reside in apposition to this electron-dense region at the unspecialized cone membrane.

+They "expected a synapse from the horizontal cell to the cone, because of evidence that the mammalian cone has an inhibitory surround. However, none of the $GABA_A$ subunits localized to cone membrane."

Some questions left unanswered involved;

+ "All these observations suggest that the monkey horizontal cell terminals release GABA onto both OFF and ON bipolar dendrites. This is puzzling."

+ "The questions of which subunits are expressed by photoreceptors and whether horizontal cell feedback to mammalian cone is exerted by GABA or a different neurotransmitter remain unsettled."

Their Figure 8 was described, with credit for the underlying schematic to Raviola and Gilula[152], as a tentative match of receptor localization to specialized junctions at the cone synaptic complex. Correlating their Figure 8 with the electrical circuit performance presented above, **Figure 9.5.3-3** results. [This figure ---]

9.5.3 The reported *style 3* synapse EMPTY

9.5.4 The "giant synapse" of squid as a hybrid style synapse

Messenger, et. al. have provided a discussion of the giant axon of squid[153]. The relevant figures are based on hand drawn sketches by Young dating from 1939 and 1973. Their opening quote is interesting. "Despite all the work on squid giant fibres since their rediscovery 60 years ago we still know nothing about how they innervate the mantel muscles and do not really understand how they are themselves activated. In particular we do not know the nature of the transmitters(s) at the largest synapse in the animal kingdom: the 'giant synapse' between

---

[152]Raviola, E. & Gilula, N. (1975) Op. Cit.

[153]Messenger, J. De Santis, A. & Ogden, D. (1995) Chemical transmission at the squid giant synapse *Chapter 19 in* Abbott, N. Williamson, R. & Maddock, L. *ed*. Cephalopod Neurobiology NY: Oxford University Press

second- and third-order fibres in the squid stellate ganglion." This is quite a statement for a book first published in 1995! Much of their discussion concerns the role of glutamate as a possible neurotransmitter. This work redefines the role of glutamate as that of primary neuro-facilitator, the fundamental fuel in the electrostenolytic process.

The primary feature and unusual form of the total synapse is evident in the sketches of J. Z. Young and of Martin and Miledi. It can be considered a hybrid of the *style 2* and *style 3* synapse. Multiple collaterals extend from the postsynaptic fibre to the presynaptic fibre. Martin and Miledi have provided a statistical analysis of the geometry of the squid giant synapse[154]. They estimated that 15,000 synaptic contacts (boutons) supporting a single synapse (with a total area of 16,312 square microns). The size of the boutons varied from 0.6 to 4 microns in diameter (with a mean of just over one micron). They also found a nominal synaptic gap dimension of 12 nm (120 Angstrom).

9.6 The fundamental neural signal decoding (stellite) neuron

The term stellite (with an i) is used as the functional description of the decoding neurons of stage 3. It describes a large number of the morphologically defined stellate neurons and includes a majority of the large neurons of layer IV of the cerebral tissue.

> Function is used here in the context of the underlying process of a given neural structure, and not as frequently found in neuroscience texts to describe the purpose of the structure.

The following material also appears on the authors website at;
http://neuronresearch.net/neuron/files/neuralcoderecovery.htm

9.6.1 The morphology and electrophysiology of the stellite cell

The typical stellite neuron is typically found at the orthodromic terminal of a long neuron that is contained within a nerve or commissure over a majority of its length. However, it may also be found at the orthodromic end of any stage 3 signal projection neuron. In these situations, the stellite neuron has a very simple dendritic tree (potentially synapsing with only a single pedicle. Its poditic tree is similarly simple or degenerate. Conversely, its axon may interface with a broad array of stage 4, 5 or 6 neurons. No standardized symbology has been found for the stellite neurons within the neuroscience literature.

9.6.2 The topology of the fundamental neural code recovery circuit

Figure 9.6.3-1 shows the fundamental neural configuration found in all stellite (signal recovery) neurons in Frame A. This configuration is the same as that used in virtually all neural circuits. However, the parameter values are different.

- The impedance in the base (poditic) circuit is so low, the internal feedback due to that impedance is not sufficient to support overall circuit oscillation.
- The capacitor shown at the lower right is so large relative to the axon impedance shown at upper right that the output circuit acts as a low pass filter. As such, it integrates the currents generated by the applied action potentials.
- The applied signal is a phasic signal but the output at G is its time integral, an analog signal.

9.6.3 The recovery of an electrolytically monopolar pulse train

Frame B shows the signals at the axon of the stellite neuron in the absence of the large capacitor. The waveforms are duplicates of the input action potentials. The 1-2 ms wide

---

[154]Martin, R. & Miledi, R.(1986) The form and dimensions of the giant synapse of squids *Phil Trans R Soc Lond B* vol 312, pp 355-377

waveforms are shown widened for pedagogical purposes.

Frame C shows the signals recovered at G for the condition where the input action potential stream is discontinuous. It consists of one or more individual monopulses from an electrolytically monopolar signal channel. The shape of the recovered signal depends on the time-delay between the pulses. At low time-delay, high pulse rates, the signal rapidly reproduces the nominal amplitude of the analog stimulus applied to the ganglion neuron generating the pulses.

The last statement is consistent with the proposal that no computation occurs within the fundamental circuits of stage 3. In the fundamental stellite circuit, the recovered analog signal is a copy of the analog signal applied to a single ganglion neuron.

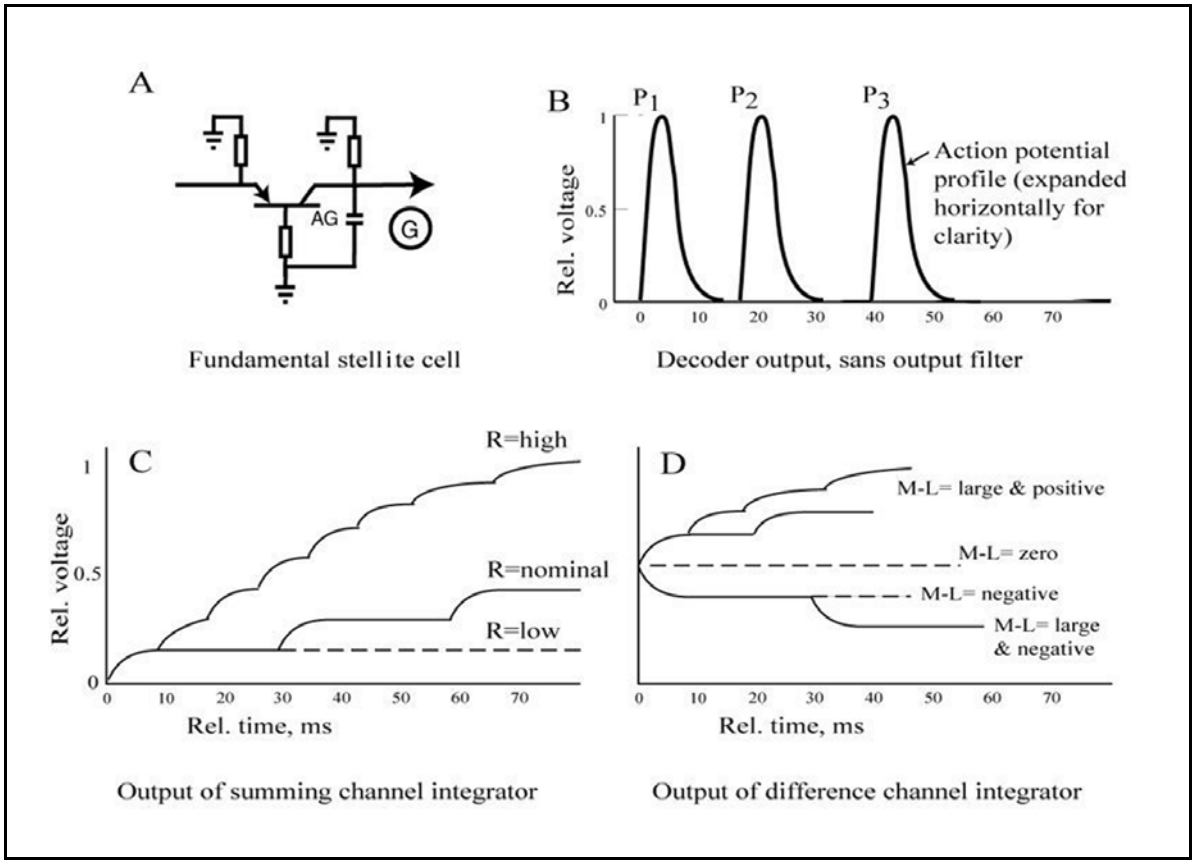

Figure 9.6.4-1 The decoding stellite neuron and representative waveforms ADD. (C); output waveform amplitude and quality vary with the rate of pulse stimulation to the stellite neuron. (D); A difference channel integrator following one or more stellite neurons can produce a bipolar signal output. See text.

Frame D shows the signals recovered at G for the condition where the input action potential stream is continuous. The output at G achieves an average potential (shown here as 0.5) in the absence of any stimulus to the associated ganglion neuron, which operates in a free-running pulse mode. For a bipolar analog signal causing a reduction in the time delay between pulses, the output rises (with a temporal profile that reflects the time delay interval between the pulses). The ultimate height reflects the amplitude of the original analog signal.

Note the long time required to recover the amplitude of a highly negative modulation of the ganglion neuron (resulting in long time intervals between the action potentials. Meaningful output is delayed considerably. This condition is commonly recognized in the visual system where the difference between the green and red signaling channels (commonly described as the Mid-wavelength minus the Long-wavelength signal. The condition is memorialized in the "mixed highs" form of color television transmission.

Berry & Pentreath recorded a great variety of neural signals (generally in pairs) among lower species such as the large air-breathing fresh water ramshorn snail, *Planorbis corneus*. They prepared multiple papers reporting their exploratory research. **Figure 9.6.4-2** shows several examples of signal recovery by stellite neurons from the applied stimulation *in-vivo* or using large neural masses removed with minimal disturbance. They described the stage 3 neuron propagating the action potentials as the giant dopamine-containing neuron (GDN) of that species. However, their discussion indicates this neuron was not an interface neuron dispensing dopamine to the glandular or CNS systems, but was delivering its signals via a synapse to an orthodromic stellite neuron for analog waveform recovery.

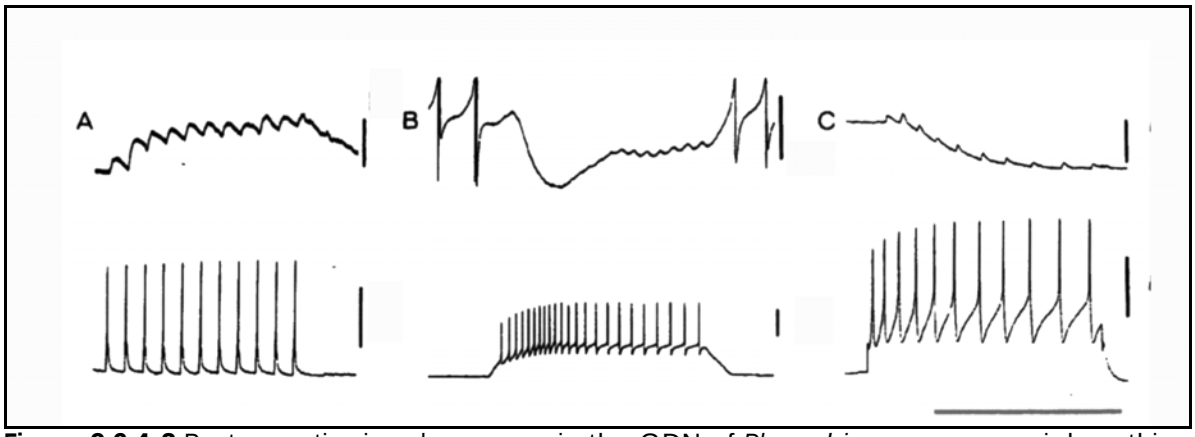

Figure 9.6.4-2 Postsynaptic signal recovery in the GDN of *Planorbis corneus*, an air-breathing fresh water ramshorn snail. Waveforms in vertical pairs; bottom is stimulation, top is the signal recovered from the orthodromic neuron acting as a signal recovery (decoding) stellite neuron. Pairs are from different preparations. Calibration bars are 10 mV in top row and 40 mV in bottom row. Time scales are 10 sec in (A) and (B); 2 sec in (C). See text. From Berry & Pentreath, 1987.

The left most pair (A) shows the action potential pulse stream generated by a stage 3 neuron (below) in response to a square wave stimulus with the recovered shape of the square wave (above) from an orthodromic stellite neuron (producing a positive going representation. (B); A negative-going representation (top) from an original stimulation by a square pulse with an additional prominence near the start of the pulse (several extraneous pulses are shown with this waveform). The lower waveform shows the encoded action potentials with the higher density pulses resulting from the higher amplitude portion of the original stimulation. (C); waveform pair similar to that in (A) but with a negative-going recovered pulse. The action potential pulse stream in (B) and (C) show the encoding neuron was subject to different bias conditions than in (A). The pulse rate in (A) is nearly constant at about 1 pps. The pulse rate of about 4 pps in (C) is indicative of a higher stimulus amplitude and leads to a more faithful representation in the recovered waveform. Note also the somewhat higher pulse rate during the initial pulses leading to a more rapid fall in the recovered waveform. The scale used in (C) makes the delay between the start of the action potentials and the beginning of the recovered waveform more obvious.

All of the waveforms of Berry & Pentreath are in excellent agreement with those predicted by the Electrolytic Theory of the Neuron presented above and in Chapter 2.

9.6.4 The recovery of additional information from more complex neural code

The previous discussion related to the fundamental stellite decoding circuit. By changing the impedance values of the fundamental circuit only slightly, additional information can be extracted from the ganglion neuron signal stream. **Figure 9.6.5-1** shows four of these modified circuits and their output.

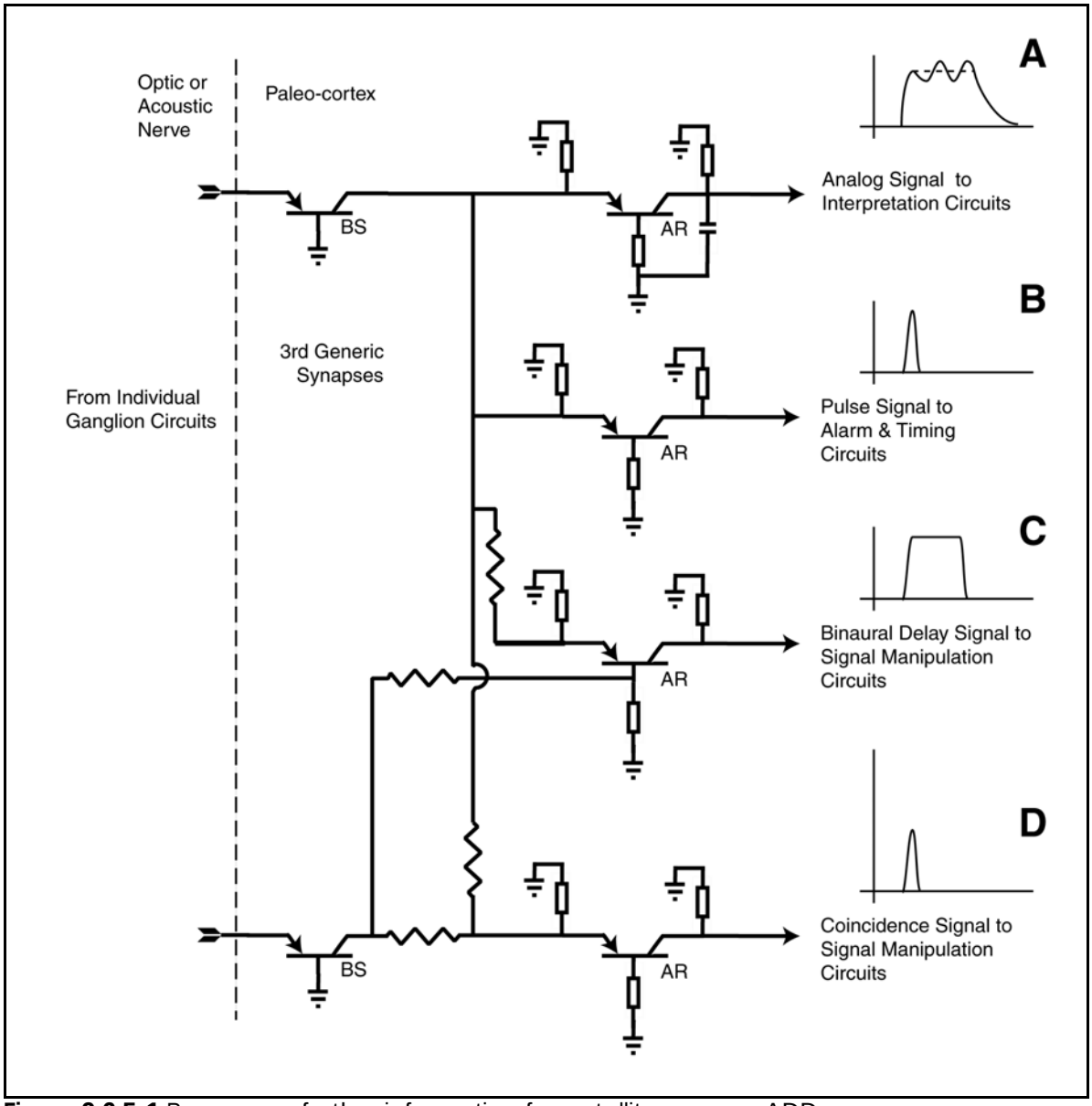

Figure 9.6.5-1 Recovery of other information from stellite neurons ADD.

- Frame A shows the fundamental circuit regenerating the analog signal applied to the

ganglion neuron.
• Frame B shows the circuit outputing only the initial pulse for use in alarm and timing circuits
• Frame C shows the circuit modified for two inputs. The resulting output is a pulse width proportional to the difference in timing between the two inputs, particularly useful in auditory source location.
• Frame D shows the circuit used as a coincidence circuit comparing two inputs.

All of these output signals are obtained using the same basic stellite circuit with simple impedance value and bias changes.

References xxx
Fulton, J. (2010) Neuron and Neural System Processes. Signal Projection Chapter. http://neuronresearch.net/neuron/document.htm

9.7 Parameters of modality specific stage 3 neurons

This section relies upon the earlier analyses of section 9.1establishing the various mechanism found in stage 3 neurons and later sections discussing the detailed features of each element of a stage 3 neuron.

The ganglion cells of the retina are prototypical encoding neurons used to encode an electrotonic signal received from a stage 2 signal processing neuron into a phasic signal prior to transmission over a stage 3 projection circuit to a stage 4 signal processing neuron. The Purkinje cells of the cerebellum and the pyramid cells of other CNS engines are other cell types performing the same function. The typical projection neuron has been uniquely optimized to transmit information over distances measured in tens of millimeters to meters. To accomplish this feat economically with regard to energy consumption, the typical projection neuron includes multiple functional units in series. Each of these units after the first and before the last contains a Node of Ranvier and an axon segment. The last functional unit consists of a pedicle electrically matched to the last axon segment. The first functional unit consists of an Activa embedded in the soma of the cell that is hybridized. It accepts electrotonic signals like a type 1 Activa (Section xxx) and generates action potentials like a type 2 Activa (Section xxx). The action potentials are delivered to an axon segment that is specialized more than most and is labeled an initial segment.

The ganglion cells take on two distinct electrophysiological roles using the identical physical morphology and cytology. In the first case, the Activa within the soma of the cell operates much like a Node of Ranvier. It does not generate an action potential in the absence of an input signal. However, in the case of this type of ganglion cell, the input is a unipolar electrotonic signal. The cells output, the distance between its action potentials, becomes a function of the amplitude of that electrotonic signal. This type of ganglion cell is known as a parasol ganglion cell within the visual modality. In the second case, the Activa within the soma operates as a free-running oscillator. It generates a series of equally-spaced action potentials in the absence of any input signal. This type of ganglion cell receives a bipolar or differential electrotonic excitation signal. The cells output, the distance between its action potentials, becomes a function of the amplitude and polarity of the input signal(s). This type of ganglion cell is known as a midget ganglion cell. The character of the output of the neurons in these two cases is dependent on the bias voltage to the Activa provided primarily by the podite impedance, labeled variously as P or R_B in this work or merely shown as an impedance between the podite (base terminal of the Activa) and the local matrix acting as a common electrical ground terminal.

9.7.1 Parameters of the stage 3A encoding neurons, variously named

Over the decades, and lacking an adequate block diagram, schematic and/or signal flow diagram, different investigators have adopted different names for the stage 3 decoding

neurons. These names have frequently been honorary (Purkinje neurons in a variety of cases), cytologically oriented (pyramid neurons) or histologically oriented (ganglion neurons).

All of the stage 3A encoding neurons deliver their signals to stage 3B stellite neuron, see below as you note the alternate spelling of this term.

9.7.1.1 Purkinje neurons of the cerebellum ala Stuart & colleagues

Williams, Christensen, Stuart et al. provided a 2002 paper containing a large amount of performance data on their "Purkinje neurons of the cerebellum." Unfortunately, they provided little context for how these neurons were employed other than to say, "Purkinje neurons are the sole output neurons of the cerebellum In-vivo they fire action potentials tonically at high rates (based on several old citations)." They attempt to explain their observations based on the chemical theory of the neuron with questionable results. The primary problem is the chemical theory does not recognize the differential input structure of many stage 3A encoding neurons compared to their similarly appearing unitary input structure companions. The Electrolytic Theory of the Neuron accounts for these two operational modes to be achieved without a change in cytological structure without difficulty. Their paper lacks any circuit diagram or flow diagram related to the Purkinje neuron. Without a more extensive circuit model, the above authors struggle to be clear concerning the use of the term tonic (typically reserved to describe analog as opposed to phasic neural signals). In their case, they appear to use the term tonic to describe the slowly changing envelope of various monopulse streams (typically described as action potentials). They also attempt to adopt a largely conceptual current proposed in the earlier work of this team. "We investigated the role of the hyperpolarization-activated mixed cation current, I_H, in the control of spontaneous action potential firing." They did not define the constituents of this cation current further or detail the origin and mechanism of the hyperpolarization-activation. Neither did they describe where the constituents of I_H occur relative to the envelope of the neuron.

[xxx rationalize these words with those in the Glossary]
Reviewing, the nature of currents passing through the lemma of a neuron differs substantially between the Electrolytic Theory of the Neuron and the conventional, largely conceptual, chemical theory. **Figure 9.7.1-1** illustrates the two situations

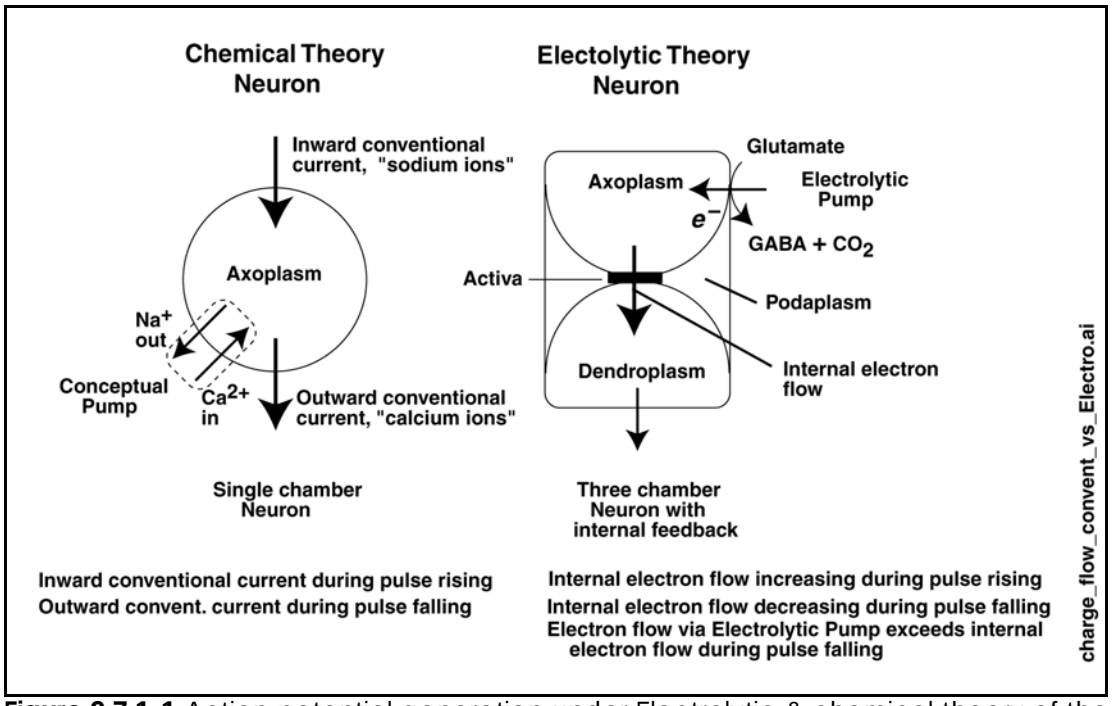

Figure 9.7.1-1 Action potential generation under Electrolytic & chemical theory of the neuron. The three-compartments of the neuron under the Electrolytic Theory offers much simpler explanation of current flow during pulse (Action Potential) generation than the single compartment neuron of the chemical theory. See text.

The neuron of the archaic chemical theory is shown on the left. It involves two distinct currents plus a largely conceptual ion pump. The **inward conventional current** was described euphemistically as a sodium current by Hodgkin & Huxley without any experimental verification. Since then, the putatively sodium ions have been associated with the rising portion of an action potential. When in solution, each sodium ion is coordinately bound to a surround of water molecules, $Na^+:6H_2O$. The complex is larger than any putative pore or gate in the cell lemma.

Section 8.5.4.4 shows the coordinate complex of the sodium ion and water is significantly larger in diameter (9 Angstrom) than the putative internal diameter of the pores in the axolemma typically proposed in the literature (about 2 Angstrom).

The ***outward conventional current*** was also described euphemistically as a calcium current by Hodgkin & Huxley without any experimental verification. Since then, the putative calcium ions have been associated with the falling portion of the action potential. When in solution, each calcium ion, Ca^{2+}, is coordinately bound to a surround of water molecules, $Ca^{2+}:6H_2O$. The complex is even larger than the sodium complex, and larger than any putative pore or gate. The ***putative ion pump***, whether two pumps or one dual action pump remains conceptual to this day (after more than 70 years since suggested by Hodgkin & Huxley in 1945). Any specialized character of the lemma has not been determined.

The three compartment neuron of the Electrolytic Theory of the Neuron is shown on the right. It involves ***only one "real internal current"*** *consisting of electrons flowing out of the axon compartment* via the Activa into the dendritic compartment under the control of the potential difference between the podoplasm and the dendroplasm. The impedance associated with the podite terminal introduces positive internal feedback whenever, the dendroplasm potential is more positive than the podoplasm potential threshold by more than a 12-15 millivolts depending on other parameters. While the axon compartment becomes more positive, the dendritic compartment becomes more negative until the $V_{den} - V_{pod}$ potential reaches zero when the current through the Activa is cut-off (at the peak of the positive action potential. The potential of the axon compartment then recharges exponentially back to a nominal –154 mV via the electron flow through the electrostenolytic process at a type 2 region of the lemma acting as a receptor for glutamic acid (glutamate). The electron flow is caused by the conversion of glutamate to GABA + CO_2 and the release of an electron into the axon compartment (**Section xxx**). Some of the *real internal current* flows through the dendritic compartment into the stimulating entity as shown. This entity may be an axon of an antidromic neuron via a synapse, or an electrical probe associated with a test set.

The stated goal of Williams, Christensen, Stuart et al. was, "to explore the role of [the putative] I_H in the control of tonic action potential firing in Purkinje neurons maintained in brain slice preparations." They compare the operation of their Purkinje neurons with their observations of pyramid neurons of layer V of the cerebrum (discussed in **Section xxx**).

The use of neurons still embedded in a slice of brain tissue provides some solace that the neuron is still provided with adequate nutrition and waste disposal to operate as if *in-vivo* for a reasonable period. However, it also leaves the neuron under test subject to uncontrolled stimulation by nearby neurons.

Their use of the term "whole–cell voltage–clamp" suggests they are not familiar with the separate compartments in a typical neuron formed by internal lemma and identifiable through careful electron microscopy. What compartment did they actually contact with their probe?

Their figure 1B and figure 1C provide the clearest differentiation between operation of their stage 3A Purkinje neurons of the cerebellum and their stage 3A pyramid neurons of layer V of the cerebrum. The differential input structure associated with the free-running Purkinje neurons leads to a nominal action potential pulse rate of about 80 PPS in the absence of stimulation (ramp slope of zero). The single ended input structure associated with the driven pyramid neurons has an action potential pulse rate of nominally zero PPS in the absence of stimulation (ramp slope of zero). Their figure 1A makes it abundantly clear, to a trained observer, that it is not the slope of the stimulating ramp but the absolute amplitude of the ramp that is controlling the instantaneous action potential pulse-to-pulse interval. Their Purkinje neuron of figure 1 is clearly being driven at the non-inverting differential input resulting in a higher action potential pulse rate with positive going stimulation. A positive going stimulation at the inverting differential input would have driven the action potential pulse rate lower. A positive going stimulation at the unitary non-inverting input to the pyramid neuron always causes a higher action potential pulse rate with stimulation amplitude.

Their initial sub-title under "Results" is supported here; "Action potential firing is independent of dI/dt in Purkinje neurons." This is the general case in the absence of any stage 2 signal processing associated with the input to the stage 3A neuron. Purkinje neurons, like most neurons are voltage controlled devices. Their next assertion is not supported; Purkinje neurons can support differential input signals and whether they generate voltage driven monopulse oscillation ***or*** free-running streams of monopulses depends on their bias conditions and stimulation as noted above with regard to the data in their figure 1C. Also, the last line under this sub-title is not supported. They assert that the "Purkinje neurons display hallmarks of a bistable system, . . . indicates that action potential firing is a quantitatively stable state with a high minimum value." This is a misinterpretation of the data in their figures where the horizontal time scale is so compressed, all of their action potentials merge together suggesting a stable state at the level of maximum hyperpolarization. Their figure 4 does not suggest a bistable state

near hyperpolarization, only the collapse of the pulse due to the high internal positive feedback forcing the rapid depolarization to the baseline.

Most of their paper subsequent to the above sub-title involves attempts to define the putative current, I_H, and the investigation of operating conditions not relevant to normal operations of a Purkinje neuron. Their subtitle, "Properties of I_H in Purkinje neurons," does not arrive at any conclusion as to the conceptually based inward and/or outward currents of the chemical model ***or*** the internal current of the electrolytic model of the neuron. The data in their figure 3 relates to Purkinje neurons operating under parametric condition (bias points) that do not occur in the normal role of these devices acting as output stages of the cerebellum. The stimulation conditions and the bias points were changed to elicit output signals consistent with stage 2 signal processing rather than stage 3A, signal projection. These output signals had durations measured in fractions of a second instead of the typical millisecond or two of an action potential. The remainder of their paper explores their claimed bistability of the Purkinje neuron that is not supported elsewhere in the literature relating to the normal operation of these neurons.

9.7.1.1.1 Unitary and differential input circuits of stage 3A encoders

Figure 9.7.1-2 shows the input structures employed by unitary and differential input stage 3A encoders. The top frame shows the basic morphology (cytology) of these neurons schematically. When both the dendrite and the podite are arborized, the configuration has frequently be described as a "bi-stratified dendritic tree." As shown in **Section xxx** and in the lower frame of this figure, the poditic terminal is totally distinct from the dendritic terminal. As noted, stimulation applied to the dendritic arborization results in an output signal at the axon of the same polarity while stimulation applied to the poditic arborization results in an output signal of opposite polarization. This is described in the engineering literature as a differential input circuit.

In the absence of poditic arborization, the neuron operates as a unitary input non-inverting device. Although not identified in the academic neuron literature, it is possible that the dendrite would not be arborized (and difficult to synapse with) while the podite was arborized. In this case, the neuron would operate as a unitary input inverting device. In fact, this is the normal configuration of the first of two Activa in the typical sensory receptor neuron of virtually all sensory modalities.

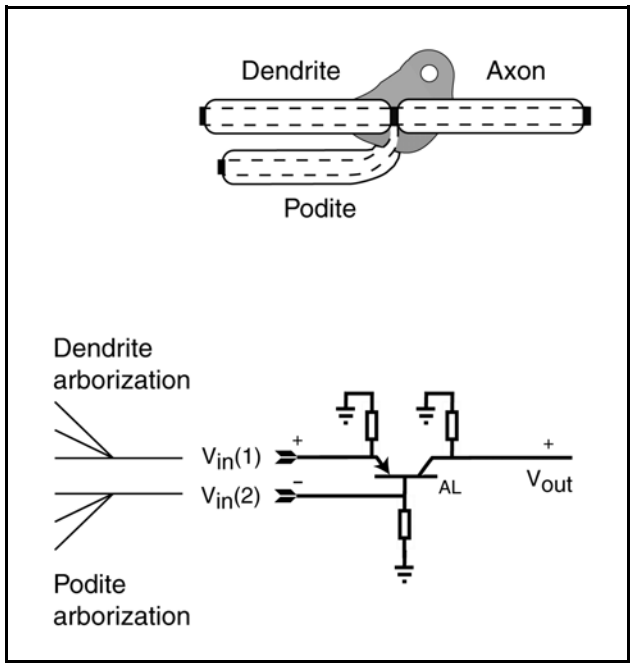

Figure 9.7.1-2 Unitary and differential input stage 3A encoding neurons. Top: the morphology (cytology) of the typical differential input neuron. Bottom: the circuit schematic of the typical differential input stage 3A (when the axon is myelinated). See text. This configuration is known as a Purkinje neuron, a pyramid neuron or a ganglion neuron depending of the sensory modality involved. When the axon is unmyelinated, the configuration is commonly used in stage 2 circuits and frequently described as a lateral neuron.

9.7.1.1.2 Output elements of Unitary and differential stage 3A encoders

The axon of the neuron illustrated can be myelinated or not myelinated. If it is not myelinated, the output signal is conveyed to the pedicle of the axon by *conduction* through the axoplasm (by the semiconductor mechanism of hole transport and not by ionic transport). If the axon is myelinated, the method of transport is changed at the beginning of

myelination to *propagation* based on Maxwell's mechanism conforming to his General Wave Equation, GWE (**Sections 9.1.1** & **9.4.2**). In the case of a long axon, it is formed into multiple couplet sections combining an axon segment and a Node of Ranvier as also illuminated in **Section 9.4.2**.

Section 9.4.2 provides a broad review of the operation of each axon segment, each Node of Ranvier and the cumulative performance of the entire axon from the Hillock to the pedicle of the neuron.

Figure 9.7.1-3 combines all of the principles discussed earlier into the morphological and electrolytic description of an axon. The signal, V_e is delivered to the Activa within the soma of the neuron by diffusion. The signal is used to cause the generation of an action potential at the output terminal of the Activa. The Activa circuit consists of a group of morphological and electrical components extending over a distance shown by the dimension x. These are called lumped components. Signals are transported by diffusion in this area at a velocity of less than 0.01 meters per second. Within the myelinated portion of the axon (labeled y), the electrical properties of the axon are described using distributed components described by their inductance, capacitance, etc. per unit length. The myelination of the axon greatly reduces its capacitance per unit length. As a result the propagation velocity is greatly increased. The signal is propagated by electromagnetic means at a nominal 4400 meters per sec. Attenuation of the signal is quite low in this region. The signal can be transmitted centimeters without being reduced below 10% of its original amplitude. At the termination of the myelination, the signal is returned to transport by diffusion. When it reaches the Node of Ranvier, it causes the Node to regenerate the action potential to its nominal amplitude. The process is repeated. The signal is returned to electromagnetic propagation until it approaches the next Node or a synapse.

The drawback to the mixed mode of operation just described is the finite delay (0.6 ms for endothermic animals) introduced at each regeneration point. This delay becomes the tradeoff point between diffusion and electromagnetic propagation of neural signals.

Once the electromagnetic propagation mode is adopted, it becomes important to minimize the distance related to the diffusion mode within the overall neuron. This is the reason why the myelination extends into the Node of Ranvier space so significantly. Any electrostenolytic and metabolic activity must occur as close to the junction of the Node as possible to minimize overall circuit delay.

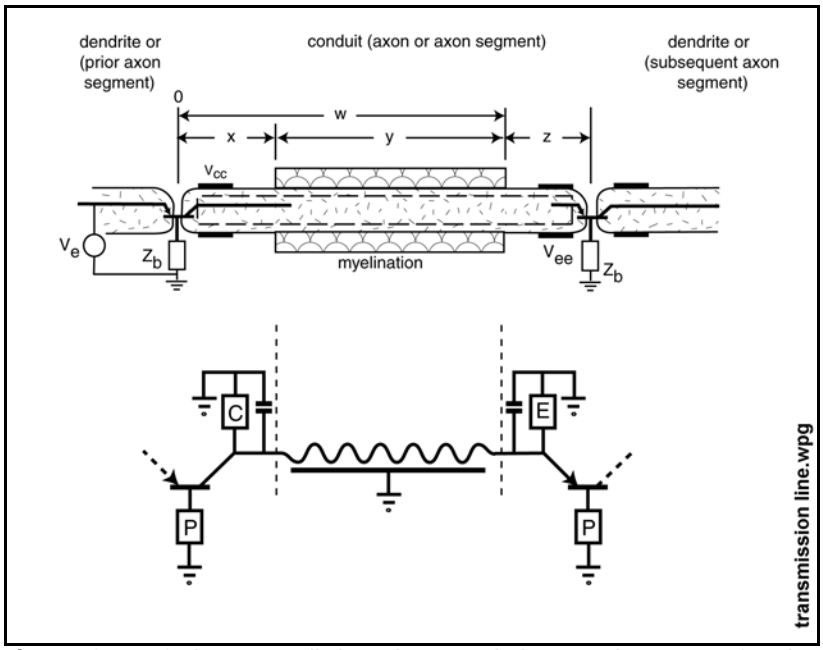

Figure 9.7.1-3 The overall signal transmission environment for the propagation of action potentials. Top; the morphological situation with electrolytic symbols as an overlay. Bottom; the electrolytic situation stressing the relevant lumped components and the distributed nature of the myelinated portion of the axon. Resistance plays no role in the operation of the interaxon (over the distance y). The letters in the boxes refer to the complex impedances of the electrostenolytic supplies. P = podite or base. C = collector. E = emitter.

[xxx move more of the following material into the early parts of this chapter]

Chapter 7 of PBH and **Chapter 14 of PBV** develop the

mechanisms of signal propagation along all stage 3 neurons in detail in accordance with the Electrolytic Theory of the Neuron. The mechanisms rely upon the electrostatic and electrodynamic laws of physics, the reliance on the hole transport theory of semiconductor physics rather than ionic transport, and Maxwell's General Wave Equations, GWE, to explain the precise data reported in the literature.

There is no satisfactory equivalent explanation of these mechanisms within the current chemical theory of the neuron.

9.7.1.1.3 The character of the signals generated by the Purkinje neurons of the cerebellum

After studying the Purkinje neurons of the cerebellum intensely, and asserting that they are the only output signal generators of the cerebellum, Stuart and colleagues did not address the purpose of the cerebellum *in toto*, or the information content of those output signals.

Section 7.1.3 shows the role of the cerebellum clearly with regard to its principle assigned functions. This role is expanded upon in **Section 19.6.3**. It plays a major role in non conscious storage of information in local memory and the comparison of new sensory inputs with the stored information. In the absence of a satisfactory comparison, it appears the system goes into a learning mode as discussed in that section.

Stuart and colleagues cited Lang et al. with regard to additional Purkinje neurons generating inter-engine action potentials representing the outputs of individual stage 4 information extraction engines within the cerebellum.

Lang et al[155]. have reported on the possibility that the inferior olive of the cerebellum may act as a source of synchronizing pulses at a clock rate of between one and ten Hertz may support the correlation tasks performed within the cerebellum. The suggested rates are relatively low compared to the fusion rate associated with signals from the visual modality.

> The terminology in their abstract seems to differ from that in the introduction. Their abstract speaks of "Spontaneous complex spikes occurred at an average firing rate of 1 Hz and a clear ~10 Hz rhythmiticity." while the introduction speaks of "Indeed it has been argued that because of its low average single-cell firing rate of ~1 Hz and maximum rate of ≈10 Hz," Can the rythmicity be at a higher rate than the underlying pulse rate?

Lang et al. failed to include any cytological model of their neurons except in a cartoon coarsely defining where they placed their multiprobe array. Their figure 1B and their histograms show a 5 x 9 array probing the left sector of area Crus 2a of the cerebellum with probes at a spacing of 250 microns. Their only reference to the array in the text refers to "a master cell (M) and the 28 other Purkinje cells" adequately accessed by the probes (rather than the total possible 44 "other Purkinje cells"). The long dimension of the array parallels a parasagittal plane. The highest synchronicity between neural action potentials is found for neurons perpendicular to the parasagittal plane. Figure 1C shows the high degree of synchronicity among these neurons. This synchronicity would be of major value if these neurons were generating messages in word serial/bit parallel form using three bit wide words. The cross-correlograms of complex spike ,CS, activity in their figure 1C(b) shows a synchronicity on the order of one millisecond for the neurons arranged perpendicular to the parasagittal plane. Their figure 2B and 2C describe the mean and dispersion in cross-correlation values they obtained as a function of probe spacing. Figure 3 shows similar data as a function of time over up to 4 hours. Their figure 5 shows autocorrelograms indicating an average frequency of 10.27 ± 2.89 Hz for their level of synchronization, with large variation among individual animals.

---

[155]Lang, E. Sugihara, I. Welsh, J. & Llinas, R. (1999) Patterns of Spontaneous Purkinje Cell Complex Spike Activity in the Awake Rat *J Neurosci* vol 19(7), pp 2728–2739

It is possible the clock-like signals of Lang et al. could be used in synchronizing the parallel bit streams associated with the possible word serial/bit parallel form of signal encoding between the stage 4A, stage 5 and stage 6B activity related to the saliency map, cognition and instruction generation related to these elements. It is also possible that there is an additional clocking function, at about 30 PPS, generated within the cerebellum for purposes of input signal comparison with stored signals in memory within the cerebellum.

9.7.1.2 Pyramid (Purkinje) neurons of the neocortex ala Williams & Stuart colleagues

In 2002, Williams & Stuart presented a paper clearly concerned with the stage 3A neurons of the cerebrum[156]. To accommodate the jargon of the community investigating the cerebrum, they labeled these neurons morphologically as pyramid neurons of the neocortex. They also changed their definition of sEPSP to spontaneous EPSP from simulated EPSP used in their 2000 paper[157] on the same neurons. Both papers rely upon the RC cable concept of Rall, that applies poorly, but better, to the dendritic and poditic structures than the axon structures of the neuron. Their putative mixed ionic current was labeled I_h in the earlier paper and I_H in their 2002 paper as well as that of Williams, Christensen, Stuart et al. The 2000 paper was labeled a "Rapid Communications" and is replete with the indefinite terms, "however," "should" and "or."

[156]Williams, S. & Stuart, G. (2002) Dependence of EPSP Efficacy on Synapse Location in Neocortical Pyramidal Neurons *Science* vol 295, pp 1907-1910

[157]Williams, S. & Stuart, G. (2000) Site Independence of EPSP Time Course Is Mediated by Dendritic I_h in Neocortical Pyramidal Neurons

In the 2002 paper of Williams and Stuart, there was additional fucus on unitary excitatory postsynaptic potentials, uESPS and less reliance on indefinite terms. They did not provide any internal circuit of their neurons. They did describe their use of Wistar rats and the fluid content of their probes in endnote 10. Many of their endnotes contain significant material and even conclusions. They primarily discussed dendritic spikes of subthreshold amplitude (less than 1.0 mV) in their figure 1 and noted in their Abstract, "Despite marked attenuation (>40-fold), when *coactivated* within a narrow time window (~10 milliseconds), distal EPSPs could directly influence action potential output following dendritic spike generation. These findings reveal that distal EPSPs are ineffective sources of background somatic excitation, but through coincidence detection have a powerful transient signaling role." [italic emphasis added] These comments appear poorly expressed in the absence of a creditable circuit description. Where, and what mechanism, was the source of their dendritic spikes? Were they generated within their target neuron or were they generated in nearby neurons within their brain slice. Their figure 1A suggests multiple action potentials generated by adjacent neurons were summated by their distal and proximal probes. Note the shape and low amplitude of these signals. The soma trace in the same figure shows much lower amplitude signals probably because of a lower impedance level, particularly if their probe actually accessed the podaplasm within the soma. *They apparently did not use patch-clamp technique to access the internal plasmas of the neurons associated with figure 1*. The character of the soma recording is much closer to random noise than in the distal and proximal recordings. The three waveforms do not exhibit a lot of coincident signals, even when allowing for the shift in time related to the velocity of signal travel toward the soma. The term "peri-somatic" does not appear in the paper except within figure 1B. Frame 1B may have originated in a different paper, based on the uniqueness of its terminology. Note the labeling of the non-distal traces in the "distal apical" inset. They assert they used current injection, via a separate probe, later in the paper in connection with their *artificial* EPSP's, a EPSP's, in figure 2. This assertion implies they did use the patch-clamp techniques in connection with this separate dendritic probe. The caption for figure 2 appears erroneous based on the notation in the paper. It should probably read "Comparison of artificial and spontaneous EPSP" since the term "simulated" was not used elsewhere in this paper.

Figure 9.7.1-4 reproduces their figure 4, the only figure in the paper related to action potential generation. *The individual frames of the figure are all as expected based on the Electrolytic Theory of the Neuron*. The labels at the top of the figure indicate where current was injected into the neural plasma to generate the data frames below in that column. Frame A lower left and right show the expected soma responses (with some reduction in action potential amplitude pulse-to-pulse due either to a limited power supply for the neuron or poor probe compensation. Frame A upper left and right show lower amplitude signals, much of it subthreshold amplitude activity, in the absence of somatic current injection. Frame B illustrates the requirement for th summing of the artificial spikes in the dendroplasm potential to generate an action potential. Frame C shows the expected subthreshold and combined threshold and supra threshold action potentials. The curves show the that any signal even marginally above threshold drives the action potential to saturation due to the positive internal feedback of the Activa circuit. An expanded horizontal scale and greater measurement precision would show a better overlap between the threshold and 1.5 x threshold curves.

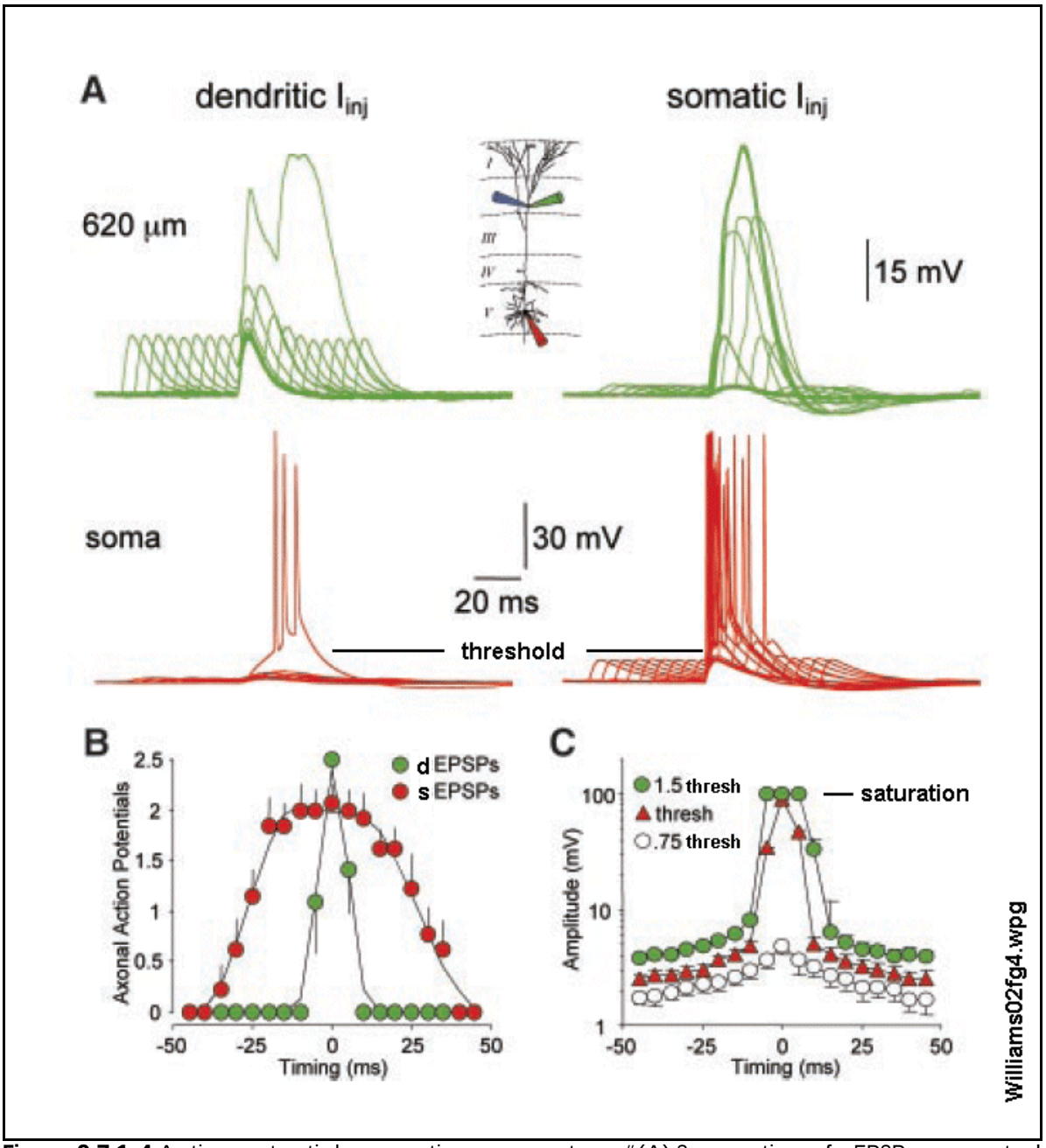

Figure 9.7.1-4 Action potential generation parameters. "(A) Summation of aEPSPs generated at distal dendritic (left) and somatic (right) sites in response to pairs of identical aEPSPs separated in time by 0 to 45 ms. Dendritic aEPSPs evoke action potential firing only when activated simultaneously. (B) Average (± SEM; n = 14) number of somatic action potentials initiated by dendritic (green) and somatic (red) aEPSPs separated by different times. Lines are Gaussian fits. (C) Somatic amplitude of the response to dendritic aEPSPs of different amplitude (0.75 times threshold, open circles; threshold, red triangles; and 1.5 times threshold, green circles). Threshold is defined as the aEPSP amplitude required for dendritic spike generation during coincident activation." From Williams & Stuart, 2002.

The two Williams & Stuart papers are analyzed in detail in **Section 2.10.2.1**of this work because of their focus on multiple simultaneous probe techniques applicable to any neuron. The high attenuation along the dendrite of either 40:1 or 100:1, discussed in their text, are not well supported by their data.

9.7.xxx Parameters of the stage 3B decoding neurons, the stellite neurons

The literature has presented many papers describing a star-like shaped neuron when represented in two dimensions. Such neurons can perform a variety of functions. To more clearly define stage 3B decoding neurons with a star-like shape, this work uses a more specific name, a stellite neuron.

[xxx change stellate to stellite in the remainder of this chapter]
The stellate cell is topologically similar to the pyramid cell discussed in **Section 10.4**. However, it typically receives phasic signals and outputs an electrotonic signal. The stellate cell accomplishes this conversion by acting as an integrator. To perform this function, its internal conexus operates exactly like the conexus of a pyramid cell. However, this conexus has a large capacitor attached to the collector terminal of its Activa. The electrotonic signal produced is passed to signal processing neurons through a synapse as discussed in **Section 10.8**.

9.8 Special topics–

9.8.1 Signaling properties of stage 3 neurons on specific paths

Several research teams have explored specific neural paths, generally within the CNS of lower species of *Chordata* and some primates. **Section 11.7.2** reviews the work of Cleland, Dubin & Levick involving the waveforms of the visual modality between the retina and the LGN of the cat. It also reviews the work of Usrey, Reppas & Reid concerning the same path and its extension to the occipital lobe (visual cortex).

9.8.2 The giant axon of squid as a timing mechanism–locomotion generator

The giant axon of the squid is not a stage 3 projection neuron. It is a special purpose stage 6 signal distribution neuron with other properties found in analog neurons. Like other members of the mollusc family, this neuron is not myelinated. However, to achieve its operating characteristics, it does depend on the arrangement of a large number of ancillary neuron surrounding it to provide effective capacitive isolation from the fluid matrix surrounding it (but not to the degree achieved through myelination in *Chordata*).

The main function of the giant axon is to provide a “tapped delay line” using a diffusion-based signaling mode. As a result, the dendrites of subsidiary stage 6 neurons (also diffusion-based in the mollusc) access the electrical potential associated with the diffusing signal at equally spaced delay intervals. The result is a rhythmic contraction of the set of targeted muscles and thereby implementation of a swimming motion.

The octopus uses a similar set of locomotion generators at two distinct neurological levels. The lower level provides stimulation to a set of muscles performing a ripple-like motion that is typically used to cause a single tentacle to encircle (and thereby grab and hold an object). Alternately, a higher level locomotion neuron can coordinate the activity of multiple lower level locomotion neurons to implement the frequently observed motion of the octopus over terrain. The octopus does not normally use its locomotion generators to support swimming. Instead, it relies on jet-propulsion to move it rapidly through the water with its tentacles trailing behind its body.

It is not clear whether fish (members of *Chordata*) employ a locomotion generator of the type found in *Mollusca* or rely upon lookup tables associated with their stage 6 neurons. Similarly, reptiles and amphibians may rely upon either locomotion generators or lookup tables (or both). Mammals that have returned to the maritime environment almost certainly rely upon

sophisticated lookup tables developed from their original terrestrial evolution.

9.8.3 The delay associated with Activa and related circuits in *Chordata*

There appear to be three major types of circuits employing Activa in different ways within the chordate neural system. Type 1 will be assigned to Activa found within the soma and neuritic structures of a neuron. Type 2 will be assigned to the Activa employed within a Node of Ranvier interfacing between two axon segments. Type 3 will be assigned to the Activa employed as interfaces between separately identifiable neurons.

It is useful to review the delays introduced by the various types of circuits used in the neural system. In general, it is the overall circuit that determines the total delay associated with a specific neuron. The Activa alone being a very small feature (with gap dimension between the two lemma on the order of tens of Angstrom) introduces a very small circuit delay associated with the transfer of charge between its emitter or base terminals and its collector terminal. The delay is difficult to measure in the laboratory because of the very much larger delays associated with ionic conduction within the various associated plasmas. However, best estimates by investigators, and the theoretical values based on modeling the junction of a liquid crystalline semiconductor device, suggest the delay within the Activa is on the order of microseconds to tens of microseconds.

The local circuit containing an Activa exhibits a delay largely controlled by the circuit. In the case of an Activa configured to generate an action potential within the soma (typically within the hillock) of a neuron,

• the delay associated with the switching associated with the Activa is typically described as less than tens of microseconds.
• the delay associated with the discharging of the axoplasm potential is dominated by the capacitance of the axolemma, the resistance of the collector to base circuit through the Activa and the difference between the threshold voltage and the saturation voltage of the axon to ground circuit. This total axon circuit delay is typically in the 0.5 msec range.
• The delay associated with the dendritic circuit prior to the dendrite reaching the threshold is a variable when measured *in-vitro* because of the artificial stimulus used. In-vivo under natural stimulation, this delay tends to be much shorter than the 0.5 msec associated with the axon discharge delay, but may under special conditions approach an additional 0.5 msec delay.
    • Dendritic circuits containing band pass filters will exhibit a delay characteristic of the filter.
    • Long dendrites frequently found in correlators may introduce significant delays on the order of 0.5 msec.

9.8.3.2 The delay associated with signaling within stage 3 neurons

9.8.3.2.1 The delay associated with a single type 1 conexus within a soma of stage 3

[xxx address analog versus pulse situations]
Several investigators have attempted to measure the delay between the emitter of an Activa and its collector. However, the experiment is extremely difficult under either *in-vivo* or *in-vitro* conditions. The primary task is to avoid including the delay associated with a finite amount of the electrolyte associated with the input and output plasmas. Alternately, the measurements that have been made suggest the delay within an Activa is less than 10^{-8} seconds. This small delay is trivial in any calculation regarding the overall operation of even the smallest neuron.

9.8.3.2.2 The transmission delay of a *type* 2 conexus, within a Node of Ranvier

[xxx delay is due to the charging process, not the Activa]
The conexus within a Node of Ranvier operates in the same manner as the conexus within the soma of a stage 3 neuron. The delay between a point on the leading edge of the incoming phasic signal and the similar point on the leading edge of the outgoing signal is typically [xxx check with other sections] one millisecond in warm-blooded chordates.

9.8.3.2.3 The transmission delay of a *type* 3 conexus, a synapse, of stage 3

[xxx The delay associated with a synapse within stage 3 that is not acting as a regenerative oscillator, is a few microseconds or less and can be ignored when discussing physiology.

9.8.4 The type 4 conexus of stage 7 as the interface with the glandular and muscular systems

See **Chapter 16. xxx**

Table of Contents 15 January 2018

Chapter 9 List of Figures 1/15/18

(Active) SUBJECT INDEX (using advanced indexing option)